SPLANCHNIC METABOLISM AND BLOOD FLOW IN MAN

PET Studies with Reference to Obesity and Diabetes

by

Henri Honka

ACADEMIC DISSERTATION

To be presented, with the permission of the Faculty of Medicine of the University of Turku, for public examination in the Osmo Järvi Auditorium, Kiinamyllynkatu 10, Turku, on December 16th 2016, at 12 o'clock noon.

TURUN YLIOPISTO
UNIVERSITY OF TURKU
Turku 2016

University of Turku

Faculty of Medicine
Institute of Clinical Medicine
Department of Internal Medicine
Doctoral Programme of Clinical Investigation
Turku PET Centre

Supervised by

Professor Pirjo Nuutila, MD, PhD
Turku PET Centre, University of Turku
Department of Endocrinology, Turku University Hospital
Turku, Finland

Docent Patricia Iozzo, MD, PhD
Institute of Clinical Physiology, National Research Council
Pisa, Italy

Docent Jarna C. Hannukainen, MSc, PhD
Turku PET Centre, University of Turku
Turku, Finland

Reviewed by

Docent Kirsi Timonen, MD, PhD
Department of Clinical Physiology and Nuclear Medicine, Central Hospital of Central Finland
Jyväskylä, Finland

Docent Veikko Koivisto, MD, PhD
Helsinki, Finland

Disseration opponent

Professor Filip K. Knop
Center of Diabetes Research, Gentofte Hospital
Hellerup, Denmark

The art of the front cover is modified from *de Humani corporis facriba Libri septem* by Andreas Vesalius (1543). Courtesy: U.S. National Library of Medicine.

The originality of this thesis has been checked in accordance with the University of Turku quality assurance system using the Turnitin OriginalityCheck service.

ISBN 978-951-29-6640-0 (Print)
ISBN 978-951-29-6641-7 (PDF)
Painosalama Oy – Turku, Finland 2016

These are the days of miracle and wonder
This is the long distance call
They way the camera follows us in slo-mo
The way we look to us all

The way we look to a distant constellation
That's dying in the corner of the sky
These are the day of miracle and wonder
And don't cry baby, don't cry
Don't cry

-Paul Simon

To my parents, Anu and Risto

ABSTRACT

Henri Honka

SPLANCHNIC METABOLISM AND BLOOD FLOW IN MAN
PET Studies with Reference to Obesity and Diabetes

From University of Turku, Faculty of Medicine, Institute of Clinical Medicine, Department Internal Medicine, Doctoral Programme of Clinical Investigation and Turku PET Centre, Turku, Finland

Splanchnic region comprises the interaction of multiple organs, hormones and neural factors and is a critical regulator of glucose homeostasis during both postabsorptive and absorptive states. While splanchnic functions deteriorate during long-standing obesity predisposing to impaired glucose regulation and type 2 diabetes, many of the aspects of splanchnic metabolism and blood flow (BF) in health and disease are still unknown.

In the present work, validation of positron emission tomography (PET) for the measurement of pancreatic and intestinal metabolism and BF *in vivo* was carried out and thereafter the method was applied to a total of 62 morbidly obese and 40 healthy individuals. In a set of cross-sectional and longitudinal studies glycemic control and β-cell function, splanchnic glucose and lipid metabolism, and splanchnic vascular responses to a mixed-meal, incretin infusions and glucose loading were explored before and after bariatric surgery and weight loss.

Compared to healthy controls, pancreatic fatty acid (FA) uptake and steatosis were markedly increased in obese patients whereas pancreatic glucose uptake (GU) and BF were impaired. Elevated pancreatic steatosis and inadequate BF were associated with poor insulin secretion rate. In the small intestine, insulin upregulated GU nearly three-fold over the fasting values in healthy controls whereas normally glucose tolerant obese patients were unresponsive to the stimulatory effect of insulin. In lean controls and patients with type 2 diabetes, mixed-meal increased both pancreatic and intestinal BF, whereas GIP infusion decreased and increased pancreatic and intestinal BF, respectively. Bariatric surgery was followed by a prominent weight loss, increase in insulin sensitivity and β-cell function, and decrease in pancreatic FA uptake, rate of steatosis and BF. While the vascular responses of GIP were essentially similar at post-surgery when compared to pre-surgery, splanchnic vascular responses during mixed-meal were enchanced, likely as a result of rapid gastric emptying.

In conclusion, pancreatic and small intestinal metabolism and BF respond to obesity and type 2 diabetes, and to metabolic changes elicited by bariatric surgery. The adequacy of pancreatic BF responses and insulin-dependence of intestinal GU are pivotal concepts in the regulation of glucose homeostasis in humans. Obesity influences both of these physiological concepts, whereas altered gastrointestinal anatomy, incretins responses and weight loss after bariatric surgery are able to reverse these obesity-induced perturbations leading to improved glucose homeostasis.

Keywords: pancreatic blood flow, pancreatic steatosis, intestinal glucose uptake, bariatric surgery, β-cell function, GIP, mixed-meal, positron emission tomography

TIIVISTELMÄ

Henri Honka

MAHA-SUOLIKANAVAN AINEENVAIHDUNTA IHMISELLÄ
PET-tutkimuksia lihavilla ja diabetesta sairastavilla potilailla

Turun yliopisto, lääketieteellinen tiedekunta, kliininen laitos, sisätautien oppiaine, Turun yliopiston kliininen tohtoriohjelma ja Valtakunnallinen PET-keskus, Turku, Suomi

Maha-suolikanavan alue käsittää lukuisten elinten, hormonien ja hermostollisten tekijöiden välisen vuorovaikutuksen ja se on keskeinen veren glukoositasapainoa säätelevä kokonaisuus niin paastossa kuin aterianjälkeisessä tilanteessa. Vaikka lihavuuden on osoitettu muuttavan maha-suolikanavan toimintaa altistaen heikentyneelle glukoosinsiedolle ja tyypin 2 diabetekselle, monia tämän alueen aineenvaihdunnallisia ja verenvirtaukseen liittyviä tekijöitä ei tunneta terveessä elimistössä eikä sairaustiloissa.

Väitöskirjatyössäni osoitin että positroniemissiotomografia eli PET-kuvaus soveltuu haiman ja suoliston glukoosi- ja rasvahappoaineenvaihdunnan ja verenvirtauksen mittaamiseen ihmisillä kajoamattomasti. Tämän jälkeen hyödynsin PET-menetelmää erilaisissa tutkimusasetelmissa 62 lihavalla ja 40 terveellä koehenkilöllä. Lisäksi tutkimuksissa tarkasteltiin lihavuusleikkauksen vaikutusta koko kehon glukoosiaineenvaihduntaan ja haiman beetasolujen toimintaan.

Tutkimuksessa todettiin että lihavilla koehenkilöillä oli suurentunut haiman rasvahappoaineenvaihdunta ja heidän haimansa olivat rasvoittuneempia kuin terveillä verrokeilla. Lihavien koehenkilöiden haiman glukoosiaineenvaihdunta ja verenvirtaus oli heikentynyt. Terveillä verrokeilla insuliini lisäsi suoliston glukoosinottokykyä lähes kolminkertaisesti paastonaikaiseen tilanteeseen verrattuna. Sen sijaan lihavilla koehenkilöillä insuliinin anto ei vaikuttanut suoliston glukoosinottokykyyn. Terveillä verrokeilla ruokailu lisäsi sekä haiman että suoliston verenvirtausta, kun taas GIP-hormonin annon aikana haiman verenvirtaus laski ja suoliston nousi. Lihavuusleikkauksen myötä haiman rasva-aineenvaihdunta ja verenvirtaus laskivat merkitsevästi. GIP-hormonin vaikutukset maha-suolikanavan verenvirtaukseen olivat samanlaisia sekä ennen leikkausta että sen jälkeen. Sen sijaan leikkauksenjälkeisessä tilanteessa ruokailun aiheuttamat maha-suolikanavan verenvirtausvasteet kiihtyivät johtuen todennäköisesti suurentuneesta mahalaukun tyhjenemisnopeudesta.

Tutkimuksen perusteella maha-suolikanavan alueen elimissä tapahtuu lukuisia muutoksia lihavuuden, tyypin 2 diabeteksen ja lihavuusleikkauksen myötä. Haiman verenvirtausvasteet ja suoliston insuliinista riippuvainen glukoosinottokyky ovat merkittäviä koko kehon aineenvaihduntaa sääteleviä ilmiöitä. Vaikka lihavuus näyttää muuttavan näitä ilmiöitä, lihavuusleikkaus ja sen vaikutukset maha-suolikanavan anatomiaan, suolisto-hormonien eritykseen ja painoon kykenevät palauttamaan haitalliset muutokset johtaen parempaan glukoositasapainoon.

Avainsanat: haiman verenvirtaus, haiman rasvoittuminen, suoliston glukoosinottokyky, lihavuusleikkaus, β-solutoiminta, GIP, ruoka-aineen anto, positroniemissiotomografia

TABLE OF CONTENTS

ABBREVIATIONS

2h OGIS	2-hour oral glucose insulin sensitivity index
ANOVA	analysis of variance
ADP	adenosine diphosphate
A-P	arterio-portal
ATP	adenosine triphosphate
AUC	area under the curve
A-V	arterio-venous
BF	blood flow
β-GS	beta cell glucose sensitivity
BMI	body-mass index
BSA	body-surface area
CA	celiac artery
BTFE	balanced turbo field echo
cAMP	cyclic adenosine monophosphate
CN	controls
[^{15}O]CO	^{15}O-labelled carbon monoxide
CT	computed tomography
DIF	dual input function
DPP-IV	dipeptidyl peptidase IV
EGP	endogenous glucose production
F_P	pancreatic fat percentage (steatosis)
FA	fatty acid
FABP	fatty acid binding protein
FATP	fatty acid transport protein
FE	fractional extraction
[^{18}F]FDG	2-[^{18}F]fluoro-2-deoxy-*D*-glucose
[^{18}F]FDG-6-P	[^{18}F]FDG-6-phosphate
FFA	free fatty acids
FI_P	pancreatic fat index
FPG	fasting plasma glucose
FSI	fasting serum insulin
[^{18}F]FTHA	14(R,S)-[^{18}F]fluoro-6-thia-heptadecanoic acid
FUR	fractional uptake rate
FWHM	full-width at half maximum
GF	germ-free
GI	gastrointestinal
GIP	glucose-dependent insulinotropic polypeptide
GIPR	GIP receptor
Glc6Pase	glucose-6-phosphatase
GLP-1	glucagon-like peptide 1

GLP-1R	GLP-1 receptor
GLP-1 RA	glucagon-like peptide 1 receptor agonist
GLP-2	glucagon-like peptide 2
GLUT	glucose transporter
GSIS	glucose-stimulated insulin secretion
GU/MR_{Gluc}	glucose uptake, metabolic rate of glucose
$[^{15}O]H_2O$	^{15}O-labelled radiowater
HAPF	hepatic arterial plasma flow
HbA1c	glycated hemoglobin
HCV	hepatic vein catheterization
HDL	high-density lipoprotein
HFD	high-fat diet
HGP	hepatic glucose production
HGU	hepatic glucose uptake
$HOMA_{IR}$	homeostatic model assessement for insulin resistance
HU	Hounsfield Unit
ICG	indocyanide green
ID-IF	image-derived input function
IGI	insulinogenic index
IIGI	isoglycemic intravenous glucose infusion
IL-6	interleukin 6
IMA	inferior mesenteric artery
IRS	insulin receptor substrate
ISR	insulin secretion rate
i.v.	intravenous
IVGTT	intravenous glucose tolerance test
K_i	influx rate constant
LADA	latent autoimmune diabetes of adulthood
LC	lumped constant
LDL	low-density lipoprotein
LEADER	Liraglutide Effect and Action in Diabetes: Evaluation of Cardiovascular Outcome Results study
LPS	lipopolysaccharide
M/F	male/female
M-value	whole-body glucose uptake
MCP-1	monocyte chemoattractant protein 1
MetS	metabolic syndrome
min	minutes
mRNA	messenger RNA
MRS	magnetic resonance spectroscopy
ND	non-diabetic
NGT	normal glucose tolerance

NIDDM	non-insulin dependent diabetes mellitus
NMRI	nuclear magnetic resonance imaging
NS	not significant
OB	obese
OGTT	oral glucose tolerance test
p.o.	peroral
PEPCK	phosphoenolpyruvate carboxykinase
PET	positron emission tomography
PSL	photon-stimulated luminescence
PVPF	portal vein plasma flow
ROI	region-of-interest
RYGB	Roux-én-Y gastric bypass
sec	seconds
SD	standard deviation
SGLT	sodium-glucose cotransporter
SGU	splanchnic glucose uptake
SMA	superior mesenteric artery
T1D	type 1 diabetes mellitus
T2D	type 2 diabetes mellitus
TAC	time-activity curve
TAG	triacylglyserol
TNF-α	tumor necrosis factor α
V_d	distribution volume
VLCD	very-low calorie diet
VLDL	very low-density lipoprotein
VSG	vertical sleeve gastrectomy

LIST OF ORIGINAL COMMUNICATIONS

This thesis is based on the following original publications, which are referred to in the text by the Roman numerals I-V.

I Honka H., Hannukainen J.C., Tarkia M., Karlsson H., Saunavaara V., Salminen P., Soinio M., Mikkola K., Kudomi N., Oikonen V., Haaparanta-Solin M., Roivainen A., Parkkola R., Iozzo P., Nuutila P. 2014 Pancreatic metabolism, blood flow, and beta-cell function in obese humans. J Clin Endocrinol Metab 99:E981-90.

II Honka H., Koffert J., Hannukainen J.C., Tuulari J.J., Karlsson H.K., Immonen H., Oikonen V., Tolvanen T., Soinio M., Salminen P., Kudomi N., Mari A., Iozzo P., Nuutila P. 2015 The effects of bariatric surgery on pancreatic lipid metabolism and blood flow. J Clin Endocrinol Metab 100:2015-2023.

III Honka H., Makinen J., Hannukainen J.C., Tarkia M., Oikonen V., Teras M., Fagerholm V., Ishizu T., Saraste A., Stark C., Vahasilta T., Salminen P., Kirjavainen A., Soinio M., Gastaldelli A., Knuuti J., Iozzo P., Nuutila P. 2013 Validation of [18F]fluorodeoxyglucose and positron emission tomography (PET) for the measurement of intestinal metabolism in pigs, and evidence of intestinal insulin resistance in patients with morbid obesity. Diabetologia 56:893-900.

IV Koffert J.*, Honka H.*, Teuho J., Kauhanen S., Hurme S., Parkkola R., Oikonen V., Mari A., Lindqvist A., Wierup N., Groop L., Nuutila P. 2016 Effects of meal and incretins in the regulation of splanchnic blood flow. Manuscript submitted for publication.

V Honka H.*, Koffert J.*, Kauhanen S., Teuho J., Hurme S., Mari A., Lindqvist A., Wierup N., Groop L., Nuutila P. 2016 Bariatric surgery enhances splanchnic vascular responses in patients with type 2 diabetes. Manuscript submitted for publication.

*Equal contribution

1 INTRODUCTION

Intermediary and energy metabolism entails all inter- and intracellular processes required for a homeostatic control of bodily functions. Humans have developed a number of sophisticated mechanisms to reassure energy supply to organs at any given physiological state. After food ingestion these homeostatic mechanisms ensure that excessive glucose and other nutrients in bloodstream are diverted into cells' metabolic needs whereas during periods of fast and starvation, liver, kidneys, adipose tissue and skeletal muscle are able to increase their output of glucose, fatty acids and amino acid from tissue cytoplasm to the circulation in order to maintain plasma glucose at a constant level and to satisfy brain's constant need for glucose. The regulation of intermediary and energy metabolism during these intermittent feed/fast cycles is based on the molar balance of anabolic and catabolic factors, favoring storage and cleavage of energy substrates, respectively. These factors are secreted from the designated endocrine organs in response to altering substrate levels in the circulation and exert their action in various organs in order to reverse the disruption in substrate homeostasis, after which their secretion is downregulated in a feedback manner.

In addition to adipose tissue and skeletal muscle, the splanchnic region comprising the interaction of liver, pancreas, small intestine, hormones and neural factors is a crucial regulator of nutrient and glucose metabolism and is responsible for a plethora of essential homeostatic functions: first, pancreatic islets of Langerhans secrete insulin and glucagon in appropriate molar ratio to divert glucose balance from positive (net uptake) to negative (net release) after meal ingestion and during fasting, respectively; second, while the most crucial function of the small intestine is the absorption of nutrients, the mucosal layer of the gut wall interacts with luminal bacteria, secretes gut hormones and utilizes glucose and free fatty acids, and regulates whole-body metabolism, insulin action and adiposity; third, liver contributes to glucose metabolism by extracting as much as one third of the ingested glucose and serving as a glucose reservoir to be utilized when food is not accessible. Because of the vast amount of crucial physiological functions, disruption of normal splanchnic functions has detrimental effects in whole-body metabolism and general health. Many studies have shown that the synergy of genes and environmental stressors such as overweight and obesity leads to disturbances in function of these splanchnic organs predisposing to impaired glucose regulation, lipid disorders and type 2 diabetes.

During the last two decades, the preponderance of western-style high-fat, high-carbohydrate diet and the decrease in physical activity has inflated the global prevalence of obesity and type 2 diabetes into epidemic proportions causing a marked social and economic burden for societies. In Finland, for instance, the total cost of diabetes is roughly 1.3 billion *per annum* equating nearly 9 % of the total health care budget. The main pathogenic mechanisms underlying impaired glucose

regulation and type 2 diabetes are the decreased sensitivity to the action of insulin to promote cellular glucose uptake (GU) and inadequate insulin output from the pancreatic β-cells to compensate for the greater metabolic needs. These typical diabetic interferences can be quantified also in the splanchnic region as a decrease in overall (net) splanchnic metabolic rate. However, it is not currently known to what extent the metabolism and vascular properties of individual splanchnic organs such as pancreas and small intestine are altered in response to obesity. The combination of insulin resistance and dysfunctional β-cells leads to the hallmark of the disease, i.e. fasting and postprandial hyperglycemia multiplying the risk for cardiovascular disease, chronic kidney disease, and retino- and neuropathy. In clinical practice, type 2 diabetes is a heterogeneous syndrome characterized by a combination of varying degrees of insulin resistance, diminished gut hormone effect and poor insulin secretion stipulating for individualized therapy. Today, management of obesity and type 2 diabetes include diet and lifestyle modifications, pharmacotherapy and invasive procedures, notably bariatric surgery. Many studies have shown the unique ability of the latter to produce sustained weight loss accompanied with marked increase in insulin sensitivity and nearly 80 % remission rate of diabetes. While it is commonly thought that many of the anti-diabetogenic properties of bariatric surgery are related to the mechanical caloric restriction and oversecretion of gut hormone GLP-1, it is largely unexplored whether splanchnic region adapts to surgical manipulation of the GI tract with alteration in metabolic rate and blood flow (BF) kinetics, and whether these plausible adaptations are related to favorable surgical outcome. While the bariatric surgery is undoubtedly effective treatment method for morbid obesity with and without type 2 diabetes, the cost of the operation and surgery-associated risks reduce its usefulness in a routine management of this large patient group. Thus, research is urgently needed to clarify the early pathogenic disturbancies in obesity and type 2 diabetes in order to identify novel targets for pharmacological, behavioral and other conservative therapies.

Splanchnic organs are positioned deep in the abdominal cavity. This and the unique vascular anatomy from abdominal aorta to hepatic artery and portal vein, and thereafter to hepatic vein render the quantification of splanchnic metabolism and BF particularly cumbersome. In humans, studies quantitating splanchnic functions so far have been performed with hepatic vein catheterization technique, double tracer technique with stabile isotopes and with dilution techniques. Although the knowledge derived from studies utilizing these techniques have been essential for our current understanding of the diabetic pathogenesis, they are not suitable for routine practice. During the recent years, multimodal imaging techniques have become a golden standard in the investigation of diseases in cardiology, endocrinology, neurology and oncology. Positron emission tomography (PET) is a molecular imaging modality exploiting the use of labile positron-emitting isotopes attached to the natural molecule which biological distribution and behavior during steady- or non-steady states is desired to be studied. For example,

the quantification of tissue GU, fatty acid (FA) uptake, BF, and blood volume can be performed by using the specific radiotracers. The main advantages of PET methodology is the non-invasiveness of the technique and the ability to isolate single organ functions from the surroundings in contrast to techniques presented earlier which are able to provide information only from the net splanchnic area. Measurement of single organ function in PET requires tissue data derived from computerized analysis of PET image and so-called input function derived either from image or from frequent peripheral blood sampling. In the recent years the PET scanner performance and spatial resolution has evolved considerably, and a combination of molecular imaging and anatomical reference imaging such as computed tomography and nuclear magnetic resonance has become a clinical routine.

Previous studies have shown the ability of PET to reliably quantitate metabolism and BF in skeletal and heart muscle, liver and adipose tissue whereas to the best of this author's knowledge PET has not been utilized nor validated for the measurement of pancreatic and intestinal functions. In this work, multimodal imaging approach was utilized to clarify splanchnic functions in health and disease. In the preclinical part performed in animals, a validation of the use of PET for the non-invasive measurement of pancreatic and intestinal functions was carried out. Thereafter the PET methodology was applied in a number of human data sets. The clinical study was divided into two distinct entities: 1) in the cross-sectional part the primary hypothesis was that obesity *per se* causes distrubances in the metabolic milieu and vascular kinetics in the intrasplanchnic organs contributing to impaired glucose regulation and insulin secretory defect in genetically predisposed individuals, whereas 2) in the longitudinal part it was rationalized that bariatric surgery and concomitant weight loss are able to fully of partly normalize the obesity-induced alterations in the intrasplanchnic organs mediating the favorable outcome of surgery on glycemic control and remission of diabetes.

2 REVIEW OF THE LITERATURE

2.1 An overview of intermediary metabolism

Humans and other vertebrates have a constant need for energy yet consume food only intermittently. Thus, a set of sophisticated intra- and interorganeous mechanisms have evolved to reassure the energy allocation for tissues during both fed (absorptive) state, and at fast (postabsorptive state). Intermediary metabolism entails all the chemical processes within and between the cells to maintain function and homeostasis of the organs. After a meal ingestion, body's regulatory orchestra favor *anabolic* storage of energy substrates as fuel reservoirs (glycogen, and triacylglyserols) and proteins, and at fast and early starvation, respectively, the fuel reservoirs are *catabolically* cleaved into readily-consumable energy substrates (glucose, lactate, amino acids, and free fatty acids). In the following discussion, I detail the metabolism of the two common intermediary products, carbohydrates and lipids, review the hormonal/fuel milieu of metabolic regulation during absorptive and postabsorptive state, and further these concepts into current knowledge on the pathogenesis of metabolic derangement in obesity and type 2 diabetes, as well as to their treatment perspectives. The protein metabolism is only scarcely addressed.

2.1.1 Glucose metabolism

Carbohydrates are abundant substrates for the body's energy metabolism. After food ingestion, gastrointestinal enzymes hydrolyze polysaccharides into monomer structures, most importantly glucose, which are thereafter absorbed into systemic circulation via brush-border membrane. Unlike insulin-sensitive tissues, the brain relies on a constant supply of glucose and other monosaccharides at any given time, and therefore it is crucial that glucose concentration in bloodstream does not fall below normoglycemic (i.e. 4-6 mM, **Fig. 1**) range at varying physiological states.

Glucose is a readily-consumable hydrophilic energy substrate for all cells of the human body. After internalization by the specific transporters (glucose transporters, GLUTs), glucose is phosphorylated by an enzyme called *hexo/glucokinase* to yield glucose-6-phosphase. Thereafter, depending on a nutritional state, glucose-6-phosphate participates in either energy production via *glycolysis* and Krebs cycle or energy storage via *glycogenesis*. During glycolysis, glucose-6-phosphate is enzymatically transformed into pyruvate, which then is transported into the mitochondria for tricarboxylic acid (Krebs) cycle. Full aerobic glycolysis of one glucose molecule yields a total of 38 adenosine triphosphates (ATP) which are utilized for cell's immediate metabolic needs. Alternatively, during exercise and other stressful events (trauma, hypoventilation, vascular distress) the oxidative

capacity of the cell is exceeded, in which case pyruvate is reduced into lactate by an enzyme called *lactate dehydrogenase*. Anaerobic glycolysis of one glucose molecule yields a total of 2 ATPs, equating 5 % of glucose's energy potential. Lactate in turn is mostly diffused into the bloodstream for reconversion to glucose via *gluconeogenesis* (in a phenomenon called the Cori cycle, see below) (Waterhouse & Keilson 1969).

Glycogen is a branched-chain homopolysaccharide composed exclusively from α-D-glucose in myo– and hepatocytes and acts as a fuel reserve from which glucose can be rapidly mobilized. During the absorptive state, insulin stimulates the action of *glycogen synthase* which then adds glucose-6-phosphate metabolites into an existing glycogen polymer. After the first hours of meal ingestion, muscle and hepatic glycogen reservoir, 400 and 100 grams respectively, are fully built (Champe & Harvey 2008). In contrast, during a prolonged fasting and early starvation, hepatic and muscle glycogen reservoirs are mobilized to produce glucose for themselves (muscle, liver) and to be released into the bloodstream (liver), with hepatic glycogenolysis being responsible for most of the endogenous glucose production (EGP) during postabsorptive state and early starvation (Rothman et al. 1991).

Whether fast persists beyond the postabsorptive state and early starvation (16-24 hours), hepatic and muscle glycogen reservoirs are depleted. In order to maintain euglycemia during times of prolonged fasting, body can neosynthetize glucose from circulating precursors such as lactate, amino acids, and glycerol in a process called *gluconeogenesis*. The main gluconeogenetic organ is liver, producing 30-65 % of EGP via gluconeogenesis after an overnight fast, whereas renal and intestinal gluconeogenesis account for a greater proportion of EGP when fast is prolonged for more than 48 hours (Kahn et al. 2005, Rothman et al. 1991, Rajas et al. 1999, Croset et al. 2001). If starvation is prolonged for more than a few days, net gluconeogenetic rate is lowered in response to decreased cerebral glucose consumption and amino acid precursor appearance in bloodstream. The rate-limiting enzymes in the gluconeogenic pathway (phosphoenolpyruvate carboxykinase, PEPCK; and glucose-6-phosphatase, Glc6Pase; respectively) are under strict control of the hormonal milieu, with glucagon and substrate availability being the main stimuli for the induction of enzyme synthesis and their transformation into active forms (Champe & Harvey 2008). Conversely, during absorptive state insulin is a powerful repressor of gluconeogenesis.

2.1.2 Lipid metabolism

In addition to glucose and other carbohydrates, lipids serve as a principal circulating metabolic fuel for tissues, rich in energy (9 kcal per gram) and hydrophobic in nature. During the absorptive state, the anabolic hormonal milieu (i.e. insulin excess and counter-regulatory hormone depletion) favor lipid storage as

Figure 1. Glucose kinetics during absorptive (1-4 hours), postabsorptive (4-16 hours) states, and during starvation. Immediately after meal ingestion, glucose is rapidly taken up by the cells for metabolic needs and for glycogen storage. With progression to postabsorptive state and starvation, glycogen is rapidly mobilized and thereafter hepatic, renal and intestinal gluconeogenesis is responsible for the majority of EGP production into the bloodstream. From Kahn et al. (2005).

triacylglyserols in the adipose tissue, and during postabsorptive state and starvation, this lipid reservoir is mobilized into the bloodstream for major source of fuel (Kahn et al. 2005, Ganong 2005). However, unlike other tissues, brain is unable to utilize lipids directly as an energy substrate and therefore, during

prolonged fasting, is dependent on ketone body formation from free fatty acids (FFA) in the liver (Owen et al. 1967).

Dietary lipids primarily consists of triacylglyserols (TAG), cholesterol esters and phospholipids (Champe & Harvey 2008). During the absorptive state, lipids are degraded by lingual, gastric and pancreatic *lipases* and bile to yield 2-monoacylglyserol, cholesterol, glycerylphosphoryl base, and FFAs, respectively, which are thereafter internalized by specific transport proteins (FABP family) into brush-border membrane of the enterocytes. Afterwards, enterocytes pack the hydrophobic substrates as lipid droplets within the lipoprotein complexes (chylomicrons) that enter the circulation via the lymphatic ducts. Alternatively, FFAs can be transported in the bloodstream bound to albumin. Ingestion of fatty meal stimulates insulin secretion of the pancreatic β-cells (Montague & Taylor 1968). Insulin, thereafter, increases the activity of the intravascular enzyme *lipoprotein lipase*, which cleaves FFAs and glycerol from TAGs inside chylomicrons (Kiens et al. 1989). These newly-released lipids enter the adipocytes and are thereafter re-esterified as TAG molecules contributing to as a long-acting energy reservoir in a process called *lipogenesis*. Moreover, adipocytes are able to store surplus glucose and amino acids in excess of the body's needs as TAGs via *de novo* formation of FFAs. After the cleavage of the majority of lipids by lipoprotein lipase, the chylomicron remnants are effectively internalized by the liver to produce very low-density lipoproteins (VLDL), which in turn are returned into the bloodstream. VLDLs serve a similar purpose as chylomicrons, i.e. the transport of diet- and liver–derived lipids into peripheral tissues with the aid of insulin-stimulated lipoprotein lipase postprandially. After complex circulatory apolipoprotein and TAG exchange reactions, VLDLs are converted as low-density lipoproteins (LDL) which are responsible for cholesterol-transport to peripheral tissues and/or the liver, the latter regulating LDL elimination from the bloodstream.

After an overnight fast and early starvation, metabolic regulation shifts from energy storage (anabolism) to energy utilization (catabolism). In the adipose tissue, the decreasing levels of serum insulin activates an enzyme *hormone-sensitive lipase* which stimulates the breakdown of TAGs into FFAs and glycerol, respectively. Immediately after *lipolysis*, these readily-consumable energy substrates are mobilized into the bloodstream for immediate utilization, mostly in the liver and muscle (Kahn et al. 2005). Eukaryotic cells can consume fatty acids via mitochondrial β-oxidation, producing high amounts of energy; for example, the oxidation of long-chained fatty acid palmitate can yield a total of 129 ATPs, equating 3.4-times the glucose's energy potential during aerobic glycolysis. In turn, the released glycerol is used as a precursor for gluconeogenesis. In contrast, during prolonged fasting and corresponding insulinopenic states, hepatic *ketogenesis* takes place. Here, plasma FFAs are internalized by the liver, oxidized to acetyl coenzyme A (CoA), and thereafter synthesized to ketones bodies, namely acetoacetate, β-hydroxybutyrate and acetone. Water-soluble and acid, ketone bodies are the

primary energy substrates by both peripheral tissues (expect liver) as well as the brain at times when glucose production is decreased and FFA mobilization and transhepatic flux is abundant (Cahill 1976). The main stimuli for rerouting of acetyl CoA into ketone body formation gateway are 1) the scarcity of mitochondrial oxaloacetate readily-utilizable for Krebs cycle due to catabolic hormonal milieu, and 2) fatty acid excess encountered by the liver during prolonged fasting state.

Circulating plasma FFA pool serves as an important energy fuel for all tissues expect brain during fasting and starvation. Given the intravascular lipolysis and internalization of fatty acids inside the adipocytes (see above), how it is possible that there are measurable amounts of plasma FFAs postprandially even in healthy individuals? Recent studies have suggested that a part of the newly-released FFAs from chylomicrons is not internalized but instead stay in the circulation and are diffused in other tissues, such as muscle (Miles et al. 2003). This 'fatty acid spillover' is thought to reflect subclinical impairment in dietary lipid storage capacity and/or inefficient lipolytic activity of lipoprotein lipase (Almandoz et al. 2013). More than 50 years ago, Randle et al. (1963) proposed a concept of 'substrate inhibition', whereby increased FFA oxidation results in increased amounts of intracellular acetyl CoA which further lowers the gluco/hexokinase activity leading to a decreased glycolytic rate. Later on, this Randle cycle has been validated in healthy individuals in several studies (Thiébaud et al. 1982, Ferrannini et al. 1983, Nuutila et al. 1992). Thus, while plasma FFA pool has a crucial function as an energy substrate, the abundance poses several detrimental effects on the regulation of intermediary metabolism.

2.1.3 Actions of the regulatory hormones during the feed/fast cycle

In fasted human, meal ingestion leads to a positive energy balance that elicits complex metabolic alterations that aim in the storage of ingested macronutrients – carbohydrates, lipids, and amino acids – to be again utilized during the postabsorptive state, where energy balance is considered to be negative. The "metabolic switch" from catabolic to anabolic energy pathways is regulated by a variety of hormones and other factors, the main stimuli for meal-induced hormonal response being the increase in nutrient – mainly glucose – concentration in the bloodstream. Increases in hormone secretion essentially aim at restoring the altered nutrient homeostasis, the restoration in turn inhibiting the secretion of regulatory hormone, therefore establishing a classical endocrine feedback loop. Briefly, the balance between plasma levels of insulin *versus* counter-regulatory hormones is the main determinant of whether the target organ metabolism favors energy storage: glycolysis, glycogenesis and TAG synthesis; or mobilization: glycogenolysis, gluconeogenesis, lipolysis, and ketone body formation.

2.1.3.1 Insulin

Insulin is the pivotal anabolic hormone of the mammalian body. Consisting of 51 amino acids arranged in two polypeptide chains and weighting 5808 Da, insulin is secreted by the β-cells clustered in the core of pancreatic islets of Langerhans in response to hyperglycemia and gastrointestinal hormones after a meal ingestion (for a detailed review, see 2.2.2.2). In glucose-tolerant individuals, serum insulin levels are low (1-10 mU L^{-1}) during fasting state but rise rapidly after a meal ingestion. Insulin exerts its effects by binding to specific receptors located on the cell membrane of various tissue types such as hepatocytes, myocytes, adipocytes and endothelial cells. After receptor binding, the tyrosine kinase activity within the receptor itself phosphorylates intracellular substrates (insulin receptor substrate, IRS) which in turn mediate the biological actions of insulin (White & Yenush 1998). While insulin has many biological actions controlled by delicate and complex downstream signaling pathways, the core actions are related to regulation of glucose and lipid metabolism.

In regards to glucose metabolism, insulin stimulates the translocation of vesicular GLUT4 to the cell surface of insulin-sensitive tissues leading to an increase in whole-body glucose disposal from the bloodstream (Yki-Järvinen & Utriainen 1998, Iozzo et al. 2006). Moreover, insulin is able to promote and stimulate key enzymes in the glycolytic pathway including hexo/glucokinase, phosphofructokinase and pyruvate kinase (Nouspikel & Iynedjian 1992, Dunaway 1983, Blair et al. 1976), increasing the amount of glucose-6-phosphate and the rate of oxidative glycolysis. The abundance of glucose-6-phosphate allosterically activates glycogen synthase and inhibit glycogen phosphorylase leading to increased glycogen storage in liver and muscle cells. In addition to increased glucose uptake (GU), insulin acts as a powerful repressor of hepatic gluconeogenesis thus decreasing EGP. Mechanistically, insulin inhibits the transcription of the key gluconeogenetic enzymes (PEPCK and Glc6Pase) (Kahn et al. 2005) and decreases circulating gluconeogenetic substrate availability from muscle and adipose tissue thereby influencing the rate of EGP. After insulin secretory burst, the combination of stimulated peripheral and splanchnic GU and inhibited EGP leads a rapid yet transient drop in blood glucose levels ensuring normoglycemia.

In adipose tissue, insulin promotes TAG storage and decreases the rate of lipolysis by three routes. First, the insulin-induced activation of endothelial lipoprotein lipase and membranous translocations of fatty acid transporters 1 and 4 (FATP1, FATP4) (Stahl et al. 2002) increases the uptake of nutrient-derived fatty acids into the adipocytes. Secondly, increases in GLUT4-mediated glucose internalization and glycolysis provide an excess of acetyl CoA to be utilized in *de novo* lipogenesis (Virtanen et al. 2002). Lastly, insulin is a powerful inhibitor of hormone-sensitive lipase, a key enzyme in the lipolysis.

While having a crucial role in the regulation of intermediary metabolism, multiple clamp studies have shown that insulin is able to dilate tissue nutrient arterioles in an endothelium-dependent mechanism. In a thorough review by Baron (1994), it is hypothesized that the insulin-dependent vasodilatation is functionally coupled to insulin effect in the metabolic regulation (i.e. glucose disposal). In fact, after an oral glucose load, Baron et al. (1990) observed largely blunted and delayed femoral mucle GU in obese insulin-resistant patients when compared with lean controls while the femoral muscle AV glucose difference was similar between the groups. As the femoral muscle blood flow (BF) was increased by 37 % only in lean controls and not in obese patients, the investigators hypothesized that tissue BF contributes to the disposal of oral glucose load and that the derangements in BF regulation may predispose to defective peripheral GU. Subclinical insulin resistance in endothelial cells may also explain the observed link between glucose-intolerance and hypertension. However, due conflicting results in later studies the pathophysiological relevance of the interaction between BF and metabolism is currently unsettled (Utriainen et al. 1995, Yki-Järvinen & Utriainen 1998, Guiducci et al. 2011).

Lastly, insulin is able to cross the blood-brain barrier and act as a satiety (anorexigenic) signal resulting to reduced eating habit and body weight (Benoit et al. 2002).

2.1.3.2 Counter-regulatory hormones

During postabsorptive and fasting states insulin secretion is largely blunted and without adequate counter-regulation, potentially fatal hypoglycemia would intervene. Thus a variety of hormones act as insulin antagonists leading to mobilization of the energy storages which were built during the absorptive state. Glucagon, a 29-amino acid polypeptide secreted by the pancreatic α-cells in response to drop in blood glucose levels and adrenergic stimulation ensures an immediate rise in blood glucose levels when administered exogenously (Sutherland & De Duve 1948). Later on, studies have shown that the hyperglycemic mechanism of glucagon resides in its ability to stimulate glycogenolysis (liver and muscle), hepatic gluconeogenesis and lipolysis (Cahill et al. 1957, Kalant 1956, Steinberg et al. 1959). These processes result in rise in glucose and the abundance of gluconeogenetic FFAs in the bloodstream.

Other hyperglycemic agents include catecholamines, mainly epinephrine and norepinephrine, which release from synaptic endings and suprarenal medullae is stimulated by hypoglycemia, excitement, or fear (Ganong 2005). Catecholamines increase the rate of glycogenolysis, hepatic gluconeogenesis and lipolysis. Moreover, corticosteroids released from suprarenal cortex act as permissive regulators in concert with glucagon in stimulation of hepatic gluconeogenesis. Endogenous and exogenous supplementary corticosteroid weaken insulin effect

(anti-insulin action) on peripheral GU resulting in impaired glucose tolerance (Jenkins et al. 1964). Finally, growth hormone antagonizes insulin action and worsens hyperglycemia by mobilizing FFA from adipose tissue, increasing hepatic glucose output and decreasing glucose disposal in peripheral tissues.

2.1.3.3 Incretins

Almost 50 years ago, Perley and Kipnis (1967) observed that both normally glucose-tolerant and diabetic individuals had considerably (60 – 70 %) larger insulin secretion rate (ISR) after oral glucose administration *versus* when identical plasma glucose excursion was reproduced with an isoglycemic intravenous glucose infusion. Moreover, the maximal insulin levels were reached earlier during oral than during intravenous glucose loading. The authors concluded that innate "alimentary insulinogenic mechanism" (**Fig. 2**) resides within the intestine and has a crucial function in the first-order hepatic metabolism of glucose after a meal ingestion, preventing a large proportion of meal-derived glucose to enter systemic circulation. Later on, studies by Perley & Kipnis and alike led to a discovery and identification of gut hormones, or incretins, most importantly glucagon-like peptide 1 (GLP-1) and glucose-dependent insulinotropic polypeptide (GIP) that play a significant role in the regulation of intermediary metabolism during the absorptive and postabsorptive states, and in the appetite control. For further details regarding gut hormone secretion, see 2.2.3.2.2.

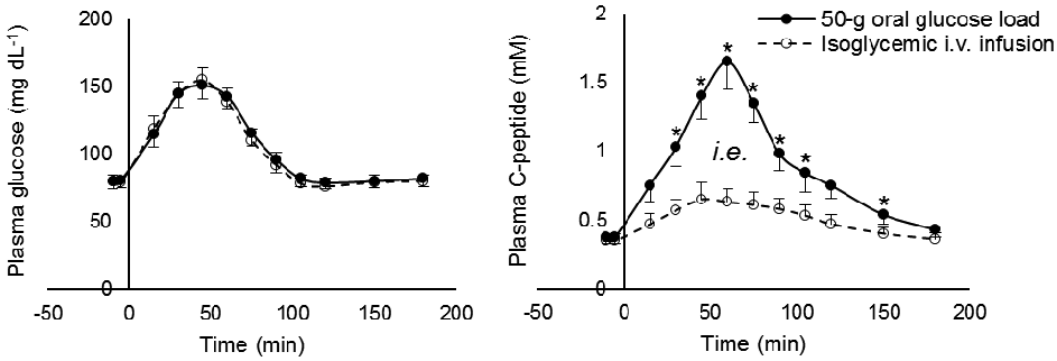

Figure 2. Plasma glucose and C-peptide responses after 50-gram oral glucose load and isoglycemic intravenous glucose infusion (IIGI) in six healthy individuals. The alimentary route of glucose administration elicits markedly larger insulin and C-peptide secretory responses when compared with similar dose given intravenously. This difference (*i.e.* on the right graph) is due to insulinogenic action of intestinal secretagogues and termed "the incretin effect". *$P < 0.05$ between modalities. Modified from Nauck et al. (1986).

Biologically active GLP-1 is a 30-amino acid polypeptide secreted by the enteroendocrine L-cells of the distal ileum in response to ingested carbohydrates, lipids and protein. After secretion into portal vein, GLP-1 is rapidly cleaved by the protease *dipeptidyl peptidase IV* (DPP-IV, originally discovered by Hopsu-Havu & Glenner [1966] and further studied by Heymann & Mentlein [1978]), resulting in only 2-minute half-life. GLP-1's most main anabolic function is the potentiation of glucose-stimulated insulin secretion (GSIS) from pancreatic β-cells, especially after meal ingestion but even at the fasting glucose values (Vilsboll et al. 2003). In addition to its short-term reflex action on insulin secretion, GLP-1 serves as trophic factor for mammalian β-cell mass by inhibiting β-cell apoptosis and stimulating proliferation and transdifferentation of pancreatic progenitor/duct cells into endocrine pancreatic cells (Xu et al. 1999, Zhou et al. 1999). GLP-1 also inhibits glucagon secretion, act as a satiety signal to reduce appetite, and dampen the GI mobility in order to alleviate excessive glucose excursion after a meal. GLP-1 receptors are present in the endothelial cells and exogenously administered GLP-1 receptor agonist (GLP-1 RA), liraglutide, induces nitric oxide synthesis in the endothelial cells which may protect against endothelial dysfunction (Hattori et al. 2012). Indeed, rodent and human studies have shown that GLP-1 increases coronary BF and decreases superior mesenteric arterial BF (Ban et al. 2008, Trahair et al. 2015). Due to GLP-1's beneficial metabolic and cardiac effects, GLP-1 RAs are widely used for the treatment of clinical diabetes and obesity (for a detailed review, see 2.1.6.3 and 2.1.6.4).

Biologically active GIP is a 42-amino acid polypeptide secreted by the K-cells of the proximal intestine in response to intraluminal contents. It possesses similar pharmacokinetics as GLP-1 as it is subject to enzymatic cleavage by DPP-IV with resulting half-life of five minutes. After meal ingestion, GIP shares similar insulinotropic and glucagonostatic properties as GLP-1 and it is widely appreciated that GLP-1 and GIP have impact on postprandial insulin secretion. However, a recent study by Christensen et al. (2011) showed that during fasting and hypoglycemic clamp exogenous GIP caused greater glucagon rises when compared with saline infusion. Thus, GIP seems to be a bifunctional glucose stabilizer during different physiological states. In the 1980's, Kogire et al. (1988) showed in a dog model that GIP has specific vascular effects in the splanchnic region. However, no human study has been conducted to validate these findings and their metabolic consequences in humans.

2.1.4 Overweight and obesity

Overweight and obesity (defined as body-mass index being greater than 25 and 30 kg/m^2, respectively) is a major burden for health care systems and societies worldwide. Obesity is a causal factor for diabetes, hypertension and heart disease, dyslipidemia, obstructive sleep apnea, arthrosis and certain types of cancer (Kelly

et al. 2008). In Finland, the prevalence of obesity has worryingly grown in the past two decades and today approximately 13 % of the adult population are classified as obese (Prättälä et al. 2012). While certain diseases (hypothyroidism and hypercortisolism, monogenic forms of obesity) and medications can provoke obesity by themselves, by far the most fundamental causes of obesity epidemic are the change in diet favoring high-fat, high-carbohydrate nutrients and the decrease in physical activity and labor in the past 100 years in conjunction with predisposing genetic background. Hence, overweight and obesity can be regarded as a disease of multifactorial etiology.

Humans and other vertebrates have developed elegant homeostatic mechanisms that prevent large variations in body weight, resulting in an extremely stable weight over both short and long periods of time. The long-term control of body weight is regulated by a coordinated feedback from adipose tissue, gastrointestinal tract and peripheral and central nervous system, and the afferent data is integrated in the arcuate and paraventricular nuclei of the ventromedial hypothalamus to adjust for energy intake and expenditure (Corbett & Keesey 1982). Therefore, any perturbation to this homeostatic state will induce compensatory mechanisms that aim to restore the body weight back to baseline; elevation in body weight is followed by an increase in resting metabolic rate, energy expenditure during physical activity, and sympathetic tone (Landsberg & Young 1984, Leibel et al. 1995) whereas loss in body weight results in a decreased resting metabolic rate and increased parasympathetic tone. The key humoral anorexigenic signals contributing to the metabolic responses following weight gain include leptin secreted by the adipose tissue, insulin, GLP-1, and glucagon (Abraham & Lam 2016).

Somewhat surprisingly, these metabolic and neural counter-regulatory responses to change in body weight are identical in both lean and obese individual who are at their "set-point" i.e. usual weight making it unlike that unhealthy eating habits and other behavioral traits are the sole contributors to obesity. In fact, many studies have shown that as much as 80 % of the inter-individual variation in body weight can be attributed to genetic factors (Bouchard 1994). The mechanisms by which genetic profile can affect the phenotype include adipose tissue distribution (visceral/subcutaneous), adipose tissue storage capacity, resting metabolic rate, eating behavior, and food preferences. Recent understanding on the evolution of obesity indicates that in our ancestors' time some thousand years back, genotypes optimized for food storage during famine and feast –cycles would have given a positive selection pressure for today's human population (Sellayah et al. 2014). As the genetic profile has not changed in the past centuries to compensate for the overwhelming supply of today's nourishment, resulting in overeating and storage of excess energy in the adipose tissue.

In addition to the environmental and social factors, and genes, individual phenotype and susceptibility to obesity are modified by the epigenetic factors irrespective of the genetic background *per se*. This is evidenced by cohort studies

showing that the maternal BMI at the time of pregnancy is associated with future health outcome, especially for cardiovascular disease and type 2 diabetes, in the offspring (Eriksson et al. 2014). In addition, a recent study by Ost et al. (2014) in *Drosophila melanogaster* observed that the features of obesity and metabolic state can be transmitted also from the paternal line via the conformational change to chromatin structure of the deoxyribonucleic acid. In the future, the epigenetic signatures of obesity ("intergenerational metabolic reprogramming") may offer potential in the clinical setting, especially predicting the disease risk and for diagnostic purposes.

2.1.5 Type 2 diabetes

Diabetes (latin. *dia bainein*, "to go through") equates to a disease state of excessive urination of undetermined etiology. While clinical diabetes can arise from numerous disease states and agents, the most common forms are type 1 and type 2 diabetes mellitus, of which only latter is detailed in the forthcoming chapters. Type 2 diabetes mellitus (T2D, formerly known as non-insulin dependent diabetes mellitus, NIDDM) is progressive, yet preventable disease that results from an imbalance between insulin effect on peripheral tissues and insulin secretion from pancreatic β-cells resulting in hyperglycemia and disturbance in intermediary lipid handling (DeFronzo et al. 1992). According to Finnish Social Insurance Institution (Kela), roughly 286 136 patients (5.2 % of the total population) received medication for diabetes (both type 1 and type 2) in 2013. However, recent national report estimates the prevalence of diabetes to be nearly 10 % of the Finnish population (Dehko 2000-2010) as many of the affected individuals are unaware of the their disease. Poorly controlled T2D is a significant contributor to non-traumatic amputation of lower extremity, coronary artery disease, end-stage renal disease with dialysis, and blindness in working adult population (for a detailed review, see 2.1.5.2). The annual medical cost of diabetes (of all etiologies) is approximately 1.3 billion euros (equating 8.9 % of the whole health care budget), and when combined with the reduced labor supply, the total cost of diabetes for the Finnish economic system is over 2 billion euros rendering 1 % decrease in gross domestic product (Jarvala et al. 2010). In summary, while being a severe cause of morbidity for individual, T2D poses as a major threat to the Finnish health care system and society as a whole.

2.1.5.1 The pathogenesis of type 2 diabetes

The occurrence of T2D is largely dependent on excess weight with 50-80 fold increase in relative diabetes risk when BMI exceeds 35 kg/m^2 when compared with normal-weight individuals (Chan et al. 1994). However, due to the multifactorial (i.e. genes and environment) nature of the disease, approximately 10 % of type 2

diabetic patients are normal-weight. In the lack of established criteria for T2D, hyperglycemic patients who do not meet the diagnostic criteria of other variants of the diabetes spectrum (T1D, latent autoimmune diabetes of adulthood [LADA], monogenic forms of diabetes or secondary diabetes) are conventionally considered to have T2D.

The progression from normal to impaired glucose tolerance (IGT) to T2D is associated with the development of severe insensitivity, or resistance, to the effects of insulin in peripheral tissues leading to decreased rate of insulin-stimulated GU and impaired insulin-mediated inhibition of hepatic gluconeogenesis (Kolterman et al. 1981, Ferrannini et al. 1988, Golay et al. 1988, DeFronzo et al. 1992). Numerous preclinical and clinical studies have been adapted to locate the exact cellular mechanism responsible for the decreased insulin effect. The main intracellular defects in impaired insulin-dependent GU include a reduction in insulin receptor tyrosine kinase activity (Freidenberg et al. 1988), a decrease in GLUT4 and mRNA levels (Zierath et al. 1996), and a delayed and decreased glycogen storage capacity (Shulman et al. 1990). Further, the intracellular mechanisms that bring about the diminished insulin-inhibitory function on hepatic EGP include increased levels of gluconeogenetic precursors, hepatic insulin resistance and increased activity of the key enzymes involved in the gluconeogenetic pathway (DeFronzo et al. 1992). In early stages of glucose intolerance, the result of impaired insulin-stimulated GU and inadequate EGP inhibition (hepatic "glucostat" function) can be clinically seen after a meal or oral glucose load, whereby postprandial glucose levels rise above the levels observed in healthy individuals (greater than 7.8 mM) yet fasting normoglycemia prevails.

Current evidence suggests that the earliest manifestation of diabetic pathogenesis with ensuing obesity is the inability of subcutaneous adipose tissue to sufficiently store surplus energy as TAG resulting in FFA spillover (Sattar & Gill 2014). The leaked fatty acids are thus accumulated to more metabolically active visceral adipose tissue (Virtanen et al. 2002), and other organs. Augmented fatty acid utilization and ectopic fat storage in liver and muscle activate Randle cycle and impair insulin-dependent and –independent glucose disposal (Shulman 2014). Similarly, using euglycemic clamp in concert with the double tracer technique (for a detailed review of the methodology, see 2.3.2) in 10 patients with T2D, Bajaj et al. (2002) found nearly 10 % decrease in net splanchnic GU (SGU) after an oral glucose load when plasma FFA levels were experimentally elevated into 2.5 mM by means of 20 % Intralipid-infusion when compared with saline infusion. Alongside with weight gain, a low-grade systemic inflammation ensues, clinically detected by simple assays to measure acute phase proteins. In the enlarged visceral adipose tissue, this inflammatory response is characterized by macrophage infiltration and the secretion of pro-inflammatory cytokines and chemokines TNF-α, IL-6, and MCP-1 (Tilg & Moschen 2006). In addition to storage capacity, it is now evident that adipose tissue functions as an endocrine organ, with multiple so-

called adipo(cyto)kines regulating intermediary metabolism and immune system. In obesity states, the secretion pattern of adipokines is dramatically altered, with increases in pro-inflammatory leptin and resistin and decrease in anti-inflammatory adiponectin. This altered adipokine milieu has been shown to be associated with observed peripheral insulin resistance in several animal and human studies (Fantuzzi 2005, Kusminski et al. 2005, Yamauchi et al. 2003). Lastly, acute hyperglycemia *per se* has been shown to downregulate glucose-transport system and induce insulin resistance (Yki-Järvinen et al. 1987).

With ensuing insulin resistance with impaired GU and hyperactive EGP, pancreatic β-cells respond to the increases in plasma glucose levels by augmenting their insulin secretory capacity. Therefore, it is not surprise that fasting and postprandial hyperinsulinemia is observed in individuals that later on develop IGT or T2D (Saad et al. 1989). For a few years, this compensatory increase in insulin secretion can warrant normoglycemia. However, during long-standing insulin-resistant states, in time, β-cells are subject to apoptosis and resultant defect in insulin secretory capacity fail to compensate for the increased peripheral need in genetically-susceptible and –predisposed individuals (Voight et al. 2010). The impairment in β-cell function can be visualized in post-mortem studies, where diabetic patients have 30-50 % less β-cell mass than normally glucose-tolerant individuals. Decrease in insulin secretory capacity antedates the full-blown T2D with both fasting and postprandial hyperglycemia. UK Prospective Diabetes Study (UKPDS) revealed that after T2D diagnosis loss in β-cell function progressed despite pharmacological intervention. By extrapolating this data it is suggestive that the decline in β-cell function takes place, in fact, relatively early in the pathogenesis of T2D and occur largely in parallel with ensuing insulin resistance years before clinical diabetes with fasting hyperglycemia is present (**Fig. 3**) (Holman 1998). For further discussion regarding insulin secretory defect in T2D, see 2.2.2.2.1.

While the ability of insulin to stimulate GU is largely blunted in patients with T2D when assessed in euglycemic clamp, the dose-response relationship between insulin levels and glucose disposal rate does not differ from non-diabetic controls when diabetic patients are clamped to the their basal hyperglycemic levels (Revers et al. 1984). This suggests that in full-blown T2D with fasting hyperglycemia, insulin-independent (i.e. mass action effect and GLUT1 –mediated [Ebeling et al. 1998]) mechanisms have a crucial contribution to the overall glucose disposal during insulin-resistant and hyperglycemic states.

Patients with T2D often have higher α– to β-cell ratio due to a decrease of the latter, and thus exhibit relative hyperglucagonemia in response to meal ingestion (Henquin & Rahier 2011). The α-cell dysfunction with impaired glucagonostasis, thought to result from perturbations in paracrine islet interaction, is the main causative factor for insufficient suppression of hepatic EGP postprandially (Consoli

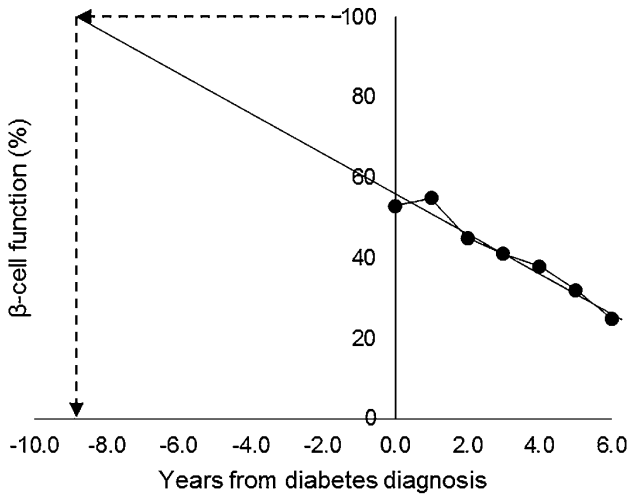

Figure 3. Extrapolation of the UKPDS data suggests that insulin secretory defect is a relatively early phenomenon in the pathogenesis of T2D. Modified from Holman (1998).

et al. 1989, Unger & Orci 2010). In contrast, during fasting state relatively higher glucagon-to-insulin ratio increase the basal EGP by 2.8 μmol kg^{-1} min^{-1}, equating to 72 grams of surplus glucose produced daily in 100-kg subject.

Nauck et al. (1986) first presented that the incretin effect is largely absent in diabetic patients. Further studies have shown that the primary defects behind this phenomenon are the reduced secretion but preserved action of GLP-1 and preserved secretion but decreased action of GIP (Muscelli et al. 2008, Holst et al. 2009). In the lack of longitudinal studies, it remains controversial whether the diminished incretin effect precedes or ensues T2D. However, a few studies designed to address this dilemma show that GLP-1 secretion is preserved in first-degree relatives and metabolically healthy identical twins of diabetic patients suggesting that the reduced GLP-1 secretion is a consequence rather than a cause of glucose intolerance (Vaag et al. 1996, Nyholm et al. 1999). In contrast, discordant results have been obtained for GIP. Vilsboll et al. (2003) investigated patients with pancreatitis and found that the reduced insulinotropic action of GIP was present only in patients with secondary diabetes suggesting that GIP resistance follows glucose intolerance. However, nearly 50 % of first-degree relatives of patients with T2D have impaired GIP effect on insulin secretion suggesting a primary or genetic defect (Meier et al. 2001). Recent genome-wide association studies have identified a common genetic GIP receptor (GIPR) variant rs10423928, associated with impaired glucose– and GIP-stimulated insulin secretion, and incretin effect (Lyssenko et al. 2011). Surprisingly, further associations between A allele of GIPR rs10423928 and lower BMI, lean body-mass and waist circumference obliterated the diabetogenic effects of impaired incretin effect emphasizing the complexity of GIP effects on the intermediary metabolism.

2.1.5.2 Natural course of type 2 diabetes

Multiple well-designed studies have shown that the progressive increase in peripheral and hepatic insulin resistance despite the lack of distinguishable insulin secretory failure initiates glucose intolerance (Lillioja et al. 1988, Saad et al. 1989). The resulting transient hyperglycemic episodes due to decreased insulin action upregulate insulin granule exocytosis and gene transcription leading to fasting and postprandial hyperinsulinemia which essentially can normalize plasma glucose levels for varying periods of time. However, in individuals that are genetically-susceptible to β-cell dysfunction (i.e. diabetes-prone), this compensatory mechanism fails to operate leading to hyperglycemia (DeFronzo et al. 1992). Not surprisingly, one obvious explanation behind β-cell dysfunction is a worsened degree of insulin resistance; obese patients with glucose intolerance and diabetes have more pronounced insulin resistance than the patients with normal glucose tolerance (Ferrannini 1998, Weyer et al. 1999) leading to a rationale that nearly all individuals can develop glucose intolerance if insulin action severely blocked. While a minority of patients with T2D are of normal-weight, still a considerable obese population do not develop glucose intolerance and concomitant metabolic abnormalities due to protective genetic and environmental background. These patients are often described as 'metabolically-healthy obese' (Phillips 2013). Early in the pathogenesis of glucose intolerance, fasting plasma glucose levels are generally within the normal range whereas postprandial hyperglycemia is present and clinically noticeable during oral glucose tolerance test. With worsening insulin resistance, progressive increase in fasting plasma glucose levels is also observed.

Longstanding T2D is associated with various acute and chronic complications. In contrast to type 1 diabetes, which is characterized by a nearly total loss of insulin-secreting β-cells due to autoimmune destruction, overt and potentially fatal ketoacidosis is not usually present in T2D as even minute insulin action can inhibit ketone-body formation. During acute illness or stress, however, the transiently provoked insulin resistance can lead to clinically-relevant dehydration, marked hyperglycemia (> 25 mM) and, at worst, coma (termed hyperosmolar nonketotic coma). Another feared acute complication with considerable mortality in diabetic patients is hypoglycemia due to excessive exogenous insulin administration, exercise, alcohol consumption, or insufficient diet. Although insulin resistance is present in T2D, insulin-independent mass action effect of glucose (Del Prato et al. 1997) during hyperglycemia mediates increases in peripheral GU. Of note, distinct cell lines (namely, capillary endothelial cells of the retina, mesangial cell of the glomeruli, and peripheral neurons and Schwann cells) are more prone to hyperglycemia- and diabes –induced toxic effects than other cell lines of the body. Thus, chronic hyperglycemia severely increases the risk of retinopathy, nephropathy, and neuropathy; the diabetic microvascular complication triad (Turner & Holman 1995). The exact pathogenesis of these late complications are

beyond the scope of this work but include the nonenzymatic formation of advanced glycation end-products (AGE), polyol accumulation and oxidative stress (Fowler 2008, Giacco & Brownlee 2010). Furthermore, insulin resistance with varying-degree of lipid abnormality and hypertension, renal failure, and the production of circulating advanced glycation end-products during long-standing hyperglycemia increase the risk of macroangiopathy, manifested as coronary artery disease, peripheral artery disease, and cerebrovascular disease. Lastly, the combination of sensory neuropathy and poor circulation in the lower extremity may lead to foot complications such as calluses, ulcerations, gangrene and infections often difficult to treat.

The combination of hyperglycemia, microvascular complications and macroangiopathy results in severe disease burden for an individual with T2D. The results of UKPDS indicated that T2D is a major cause of dialysis-requiring end-stage renal disease, blindness and foot amputation (Turner & Holman 1995). Moreover, the risk of developing cardiovascular disease – responsible for over 50 % of all-cause mortality in type 2 diabetic patients – is three-fold when compared with non-diabetic age– and BMI-matched controls (Garcia et al. 1974). In fact, Finnish East-West study showed that the type 2 diabetic patients without previous myocardial infarction were at greater risk (20.2 %) of developing myocardial infarction than non-diabetic patients with previous myocardial infarction (18.8 %) during the 7-year follow-up (Haffner et al. 1998). In patients that present T2D in their 40's or early 50's, the mortality rate is 2-fold when compared with control population.

2.1.6 Treatment strategies for obesity epidemic and type 2 diabetes

According to World Health Organization (Global Strategy on Diet, Physical Activity and Health 2004), the high global prevalence of obesity and the comorbid diseases can be attributed to radical change in the environment – including industrialization, sedentary lifestyle and the consumption of energy-dense foods – during the past decades. Therefore, the prerequisite for the management of the obesity epidemic at the population level is a change towards an environment that is supporting easier access to healthy food choices and physical activity. The responsibility of this environmental change cannot be left solely for the healthcare providers and rather warrant for a collaboration between healthcare, food and drug industry and policy makers. At the individual level, research during the 20th and early 21st century has provided a multiple treatment options available for patients with obesity, insulin resistance and glucose intolerance. In the following discussion, I will briefly review these different methods to decrease the burden of obesity and T2D in the clinical setting. The treatment of childhood obesity and diabetes are not discussed.

2.1.6.1 Diet treatment and exercise

The basis of the clinical treatment of obesity is healthy diet, aiming to reduce body weight (in the initiation period) and thereafter to maintain the achieved "new" weight (in the maintenance period). However, manny studies have shown that the efficacy of short-term diet is largely ineffective as up to 90-95 % of patients who have once lost weight will subsequently regain it (Wadden 1993). As previously discussed (for a detailed review, see 2.1.4), decrease in a "set-point" body weight is followed by a decreased resting metabolic rate and energy expenditure during physical activity, and increased parasympathetic tone meaning that patients who have once lost weight need 10-15 % fewer calories in order to maintain the new "normal" body weight. Leibel and Hirsch (1984) observed that this reduction in energy requirement in reduced-obese patients persists at least three to five years when weight is forced to maintain in the new "normal" level. Conversely, formerly obese patients require less caloric intake when compared to individuals of the same body weight who have never been obese (Leibel et al. 1995).

National Nutrition Council and Finnish Diabetes Association suggest that the diet in patients with obesity and uncomplicated T2D should consist of 40-60 % carbohydrates, 25-35 % lipids, and 10-20 % protein, respectively (Virtanen et al. 2008). The avoidance of oligosaccharides, table salt, and saturated fatty acids is recommended, whereas dietary fiber, fresh vegetables and fruits should be consumed abundantly. The diet treatment is initiated with a hypocaloric period aiming to achieve approximately 0.5-1 kg reduction in body weight per week, whereas during the maintenance period the caloric intake should equate to the energy consumption, which, in the new "normal" level, is less than that was prior to diet., as previously discussed. In patients with T2D, as little as 5 % reduction in body weight significantly improves insulin sensitivity, β-cell function and dyslipidemia, and decreases blood pressure (Franz et al. 2015). While the detailed pacing of weight-loss permitting diet is highly arguable, in a recent well-designed study by Kahleova et al. (2014), eating only two large meals during a hypoenergetic diet regimen resulted in a superior insulin sensitivity and glycemic control when compared to the equicaloric diet of six meals.

In addition to healthy and weight reducing diet, regular aerobic exercise (two and half hours on most days of the week) has been shown to result in a modest reduction in body weight and waist circumference (Thorogood et al. 2011), and may improve the durability of weight loss (Fogelholm & Kukkonen-Harjula 2000). Resistance training (at least two times per week) in turn leads to change body composition, and is shown to be beneficial especially for the obese patients with dysglycemia and T2D even in the absence of significant weight loss (Thomas et al. 2006). Moreover, during a 15-year follow-up (Srikanthan et al. 2016), high muscle-to-fat ratio led to lower cardiovascular and total mortality rate in patients with cardiovascular disease.

2.1.6.2 Behavioral perspectives

Achieving permanent weight loss requires substantial lifestyle modifications in terms of dieting and exercise. Therefore it is important that the individual has the motivation to lose weight and is able to pin-point the unhealthy and obesogenic habits. Recently, Karlsson et al. (2015) observed lowered μ-opioid receptor bioavailability in morbidly obese patients compared to lean controls suggesting that obese patients may compensate for the decreased hedonic responses of the opioidergic system with overeating. Consequently, better understanding of the psychopathology behind overeating is crucial for novel behavioral and drug therapies for obesity management.

2.1.6.3 Anti-obesity drugs

The lipase inhibitor orlistat prevents the absorption of diet-derived lipids and has been shown to improve weight loss and reduce weight regain (Sjöström et al. 1998). In addition, GLP-1 receptor agonist liraglutide 3.0 mg *o.d.* (Saxenda®, Novo Nordisk, Bagsværd, Denmark) led to additional 5.6 kg weight loss during the 1-year follow-up when compared to placebo in non-diabetic patients with BMI over 30 kg m^{-2} (Pi-Sunyer et al. 2015) supporting it's use as an anti-obesity drug even in the absence of T2D.

2.1.6.4 Anti-diabetic drugs

In early diabetes with either fasting or postprandial hyperglycemia, diet and exercise regimens may be sufficient to cease the disease progression. In many occasions, however, pharmacological treatment is necessary. In Finland, the cornerstone of drug therapy in newly-diagnosed T2D is biguanidine-class metformin. Via multiple cellular mechanisms including the activation of *adenosine-monophosphate activated protein kinase*, metformin significantly decreases hepatic EGP, acts as an insulin-sensitizer in peripheral tissues, and increases postprandial GLP-1 levels resulting in improved glucose control with low prevalence of treatment-related complications (Rena et al. 2013, Mannucci et al. 2001, UK Prospective Diabetes Study 1995). Sulphonylureas are another class of effective anti-diabetic compounds which lead to comparable glycemic control as metformin by triggering β-cell insulin secretion independent of glucose. However, the hypoglycemic tendency frequently associated with this class of drugs have largely reduced their use in Finland.

While insulin therapy (either basal or basal/bolus) is only occasionally needed in newly-diagnosed T2D, they are valid drug choice for overt diabetes with significant insulinopenia and hyperglycemia, and during various stresses where glycemic control is temporarily worsened. However, long-term exogenous insulin therapy is

often associated with weight-gain and considerable risk of hypoglycemia. Importantly, recent studies have clarified that insulin therapy is associated with increased risk of all-cause mortality (Currie et al. 2013) when compared treatment with oral anti-diabetic drugs.

During the last 10-15 years novel anti-diabetic compounds have been manufactured avidly. The three commonly prescribed drug classes include DPP-IV –inhibitors, GLP-1 RAs, and *sodium-glucose cotransporter* 2 (SGLT2) –inhibitors. The first two compound groups are based on increased GLP-1 –action resulting in upregulated GSIS and insulin sensitivity, and decreased appetite control and GI motility. For example, 5-year treatment with GLP-1 RA exenatide lead to significant improvements in glycemic control, weight loss, and cardiovascular risk markers and was well tolerated (Wysham et al. 2015). In addition, Liraglutide Effect and Action in Diabetes: Evaluation of Cardiovascular Outcome Results (LEADER) study has shown that, during the median follow-up of 3.8 years, treatment with GLP-1 RA liraglutide resulted in lower cardiovascular mortality rate than the placebo (Marso et al. 2016). In contrast, SGLT2-inhibition in the renal tubules decrease urinary glucose reabsorption rate by 30-50 % leading to glucosuria, decrease in plasma glucose levels and, via attenuation of glucose toxicity, improved ISR (Liu et al. 2012, Tahrani et al. 2013). Other metabolic consequences of SGLT-2 inhibition include increase in glucagon secretion and EGP (Bonner et al. 2014, Ferrannini et al. 2014), accelerated ketone body formation (Ferrannini, unpublished data), and lower cardiovascular mortality rate when compared to placebo (Zinman et al. 2015). In addition to monotherapy, recent trend in the clinical treatment of T2D include the use of combination therapy – for example, DPP-IV inhibitor, GLP-1 RA or SGLT-2 inhibitor as an add-on to metformin – tailored to target the variable aspects (fasting and/or postprandial) of hyperglycemia of the individual patient.

2.1.6.5 Bariatric procedures for morbid obesity and type 2 diabetes

Nearly 50 years ago Mason and Ito (1967) observed that patients who had undergone a partial gastrectomy exhibited a significant weight loss. Since then, surgical procedures targeting obesity and its comorbid diseases have gained remarkable interest. In Finland, the amount of bariatric surgical procedures *per annum* is nearly 900, estimated to increase over the next years. Swedish Obese Subjects (SOS) study concluded that bariatric surgery produces a rapid (less than 6 months) 20-30 % decrease in weight that – unlike non-pharmacological and drug treatment – sustained during the 15-year follow-up (Sjöström et al. 2007). However, a decrease in energy expenditure similar to that is observed after a low-calorie diet also follows bariatric surgery procedures (Tam et al. 2016).

More importantly, the prominent weight loss following bariatric surgery in patients with T2D is associated with 80-90 % full or partial diabetes remission rate

(Sjöström et al. 2004, Vella 2013), and similar results have been observed also in a Finnish patient cohort (Helmiö et al. 2012). The perioperative mortality rate of bariatric surgical procedures is less than during cholecystectomy and hysterectomy, and they can usually be performed by laparoscopic means.

Currently the most widely performed bariatric procedure is Roux-en-Y gastric bypass (RYGB, **Fig. 4A**). Here, the ventricle is divided into a proximal (20-30 mL) and a distal pouch. The proximal pouch is anastomosed into jejunum 50-100 cm distal to the pyloric sphincter creating a gastrojejunostomy. The, the distal gastric pouch, duodenum and proximal jejunum are bypassed and anastomosed 100-150 cm from this newly-constructed alimentary limb, creating a Y-shaped jejunoileostomy. The bypassed intestinal (secretory) limb transmits bile and pancreatic digestive secretions into the alimentary limb. Therefore, by excluding considerable portion of proximal intestine (foregut), the RYGB results in combination of malabsorption and restriction. Vertical sleeve gastrectomy (VSG, **Fig. 4B**) is another frequently performed bariatric procedure. Here, the majority of gastric pouch along the greater curvature is excised and removed, and the remaining tubular-shaped ventricle is sutured leaving the pyloric function and intestinal anatomy essentially unchanged creating solely restrictive gastrointestinal milieu without significant malabsorption.

Jackness et al. (2013) randomized patients with T2D into two study arms, one undergoing RYGB and another one receiving 500 kcal very-low calorie diet (VLCD) without surgery. During a follow-up of 3 weeks, the patients lost equal amounts of body weight, and had comparable increases in insulin sensitivity and ISR during an intravenous glucose tolerance test (IVGTT) suggesting that caloric restriction *per se* plays an important role in the early regulation of glycemic homeostasis after bariatric surgery. However, as many patients exhibit clinical resolution of diabetes before any significant weight loss has occurred, it is likely that surgery-specific GI alterations play a role in the maintenance of glycemic control. The hindgut-hypothesis based on animal experiments states that bariatric surgery allows nutrients to reach distal ileum (i.e. the hindgut) more rapidly and unprocessed increasing the secretion of insulinotropic alimentary factor. In fact, Nannipieri et al. (2013) observed a dramatic increase in postprandial levels of GLP-1, and this was associated with improved β-cell function, comparable between RYGB and VSG. In a pig model, RYGB-operated animals had doubled their β-cell mass and exhibited 3.8-fold increase in GLP-1R immunoreactivity at 20 days post-surgery when compared with sham-operated animals (Lindqvist et al. 2014). Taken together, it is now appreciated that the most evident causes of diabetes remission after bariatric surgery are increased peripheral and hepatic insulin sensitivity, improved β-cell function, and alterations in eating habits towards smaller portions and healthier diet preferences (le Roux & Bueter 2014). The aforementioned mechanisms may be consequences of both weight-loss and surgery-induced elevation of GLP-1. Unfortunately, there is a scarcity of evidence whether bariatric

surgery and concomitant weight loss has specific effects on pancreatic metabolism and ectopic fat accumulation.

In early 21st century GI Dynamics, Inc. introduced a novel minimally-invasive and reversible technique to manage obesity, diabetes and related metabolic diseases. The use of the duodeno-jejunal bypass liner, or Endobarrier®, is based on the foregut-hypothesis of bariatric surgery (Mingrone & Castagneto-Gissey 2009). The hypothesis holds that by excluding the duodenum and proximal jejunum (i.e. the foregut) from the transit of nutrients, a secretion of so-called *anti-incretin* promoting insulin resistance and β-cell dysfunction is downregulated accounting for the (weight-loss independent) beneficial effects of bariatric surgery. Deployed during esophagogastroduodenoscopy, the bypass liner is a 60 cm long plastic sleeve that is proximally anchored in the duodenal bulb and protrudes into duodenum and jejunum allowing the biliary and pancreatic secretions to flow in between liner and intestinal mucosa whereas ingested nutrients contact the intestinal brush-border membrane at mid-jejunum thereby mimicking the alimentary effects of RYGB. Recent studies have shown that the use of bypass liner was resulted in significant excess weight, loss and in patients with T2D, improvements in glycemic control (Patel et al. 2013). While still considered as an experimental therapeutic option legalized only in few European countries, the endoscopic bypass liner technique highlights the importance of foregut in the regulation of intermediary metabolism.

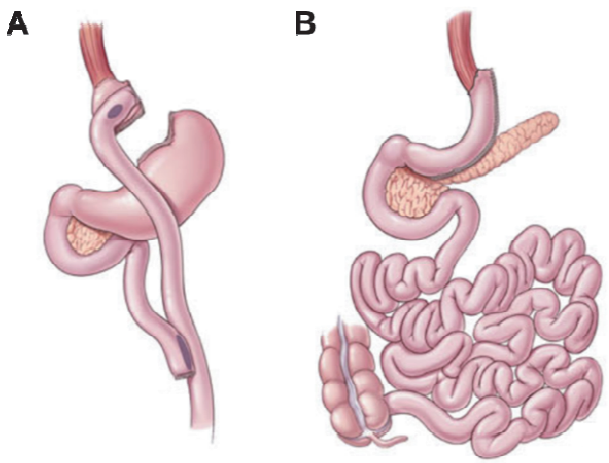

Figure 4. The outcomes of Roux-en-Y gastric bypass (A) and vertical sleeve gastrectomy (B).

2.2 Splanchnic functions and the metabolic regulation

Splanchnic (greek. *splanchna*, “organ”) region entails the complex system of organs, their vasculature, autonomic innervation and metabolism within the abdominal cavity. Traditionally splanchnic organs have been divided into liver and

as “extrahepatic”, the latter denoting pancreas, ventricle, intestine, spleen, and visceral adipose tissue. The splanchnic region has multiple coincidental functions during the feed/fast cycle, including nutrient absorption, insulin and glucagon secretion, glycogen and TAG storage, gluconeogenesis, and blood pooling, respectively. In regards to glucose metabolism, the simultaneous bifunctionality of the splanchnic region can be observed in an elegant series of studies by Barret et al. (1985) performed in dogs; at postabsoprtion the hepatic and extrahepatic splanchnic net glucose balances favor release and uptake, respectively, whereas rapidly after the start of the hyperglycemic insulin clamp or oral glucose administration, the hepatic GU is stimulated whereas the extrahepatic splanchnic glucose balance is dependent on the mode glucose is administered (*i.v. versus p.o.*). An overview of the splanchnic glucose metabolism during hyperglycemic insulin clamp and oral glucose administration is shown on **Figure 5**.

In humans, hyperglycemic hyperinsulinemia increases the net splanchnic glucose disposal to approximately 430 μmol min^{-1}, equating 5 to 20 % of whole-body GU (DeFronzo et al. 1978). Due to the critical role of splanchnic region in the intermediary metabolism, it is not surprising that the impairment in splanchnic organs’ function or their regulatory orchestra predispose to metabolic derangements and glucose intolerance. In the following discussion, current knowledge on splanchnic vasculature and extrahepatic splanchnic organ functions during feed/fast cycle is addressed, and further insight of pancreatic and intestinal dysfunction in the pathogenesis of dysglycemia is presented.

2.2.1 Macrovascular architecture and portal venous system

The arterial supply to the splanchnic region is derived from abdominal aorta via three main arteries, the celiac trunk, superior mesenteric artery, and inferior mesenteric artery, respectively. At fast, the splanchnic viscera receives approximately 30 % of the cardiac output, equating 1.5 liters per minute in a 70-kg man (Ganong 2005). The celiac trunk is the first subdiaphragmatic artery, and it divides soon into hepatic, gastroduodenal, and splenic artery delivering oxygenated blood into liver and extrahepatic splanchnic organs, respectively. The superior mesenteric artery supplies the majority of pancreas and small intestine, whereas inferior mesenteric artery supplies the colon. While liver receives arterial blood only via hepatic artery, extrahepatic splanchnic organs receive their arterial supply largely from parallel vascular circuits originated from the two superior arterial trunks.

Due to the crucial role of liver in the regulation of intermediary metabolism, a portal venous system is present in the splanchnic region. Here, the venules originating from the ventricle, the pancreas, small intestine, colon and spleen are united ultimately to form portal vein, which drains into hepatic parenchyma. After

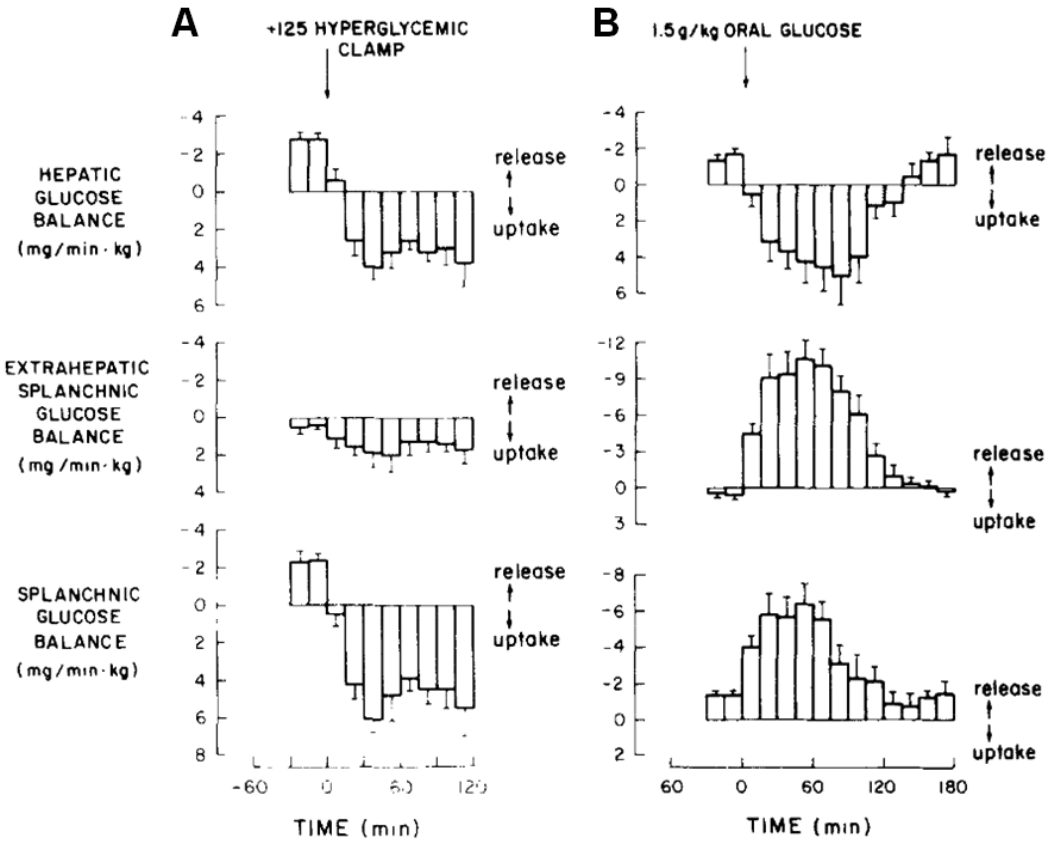

Figure 5. The effects of hyperglycemic insulin clamp and oral glucose administration on hepatic and extrahepatic splanchnic glucose handling in dogs. Combined hyperglycemia and hyperinsulinemia effectively inhibits hepatic EGP and increases hepatic GU (HGU). During intravenous glucose infusion, the gastrointestinal tissue glucose balance is positive (favor uptake), whereas after glucose ingestion intestinal glucose absorption and transcellular transport rate exceed the rate of extrasplanchnic basolateral GU. Modified from Barret et al. (1985).

a meal, portal vein is rich in glucose, amino acids, insulin, and gut hormones that exert their specific effects on hepatic energy homeostasis. Ultimately, the venous drainage from the splanchnic region are mediated by three hepatic veins which are merged into inferior vena cava. Due to the dual blood supply of the liver, it is extremely cumbersome to study splanchnic circulation on organ-specific basis (DeFronzo 1987). Traditionally, the portal vein BF represents the extrahepatic splanchnic BF, whereas the combination of portal vein and hepatic artery BF equates with total hepatic and thus splanchnic BF.

Based on several animal studies, at fasting state the liver receives approximately 25 % and 75 % of its BF from hepatic artery and portal vein, respectively (Kahn et al. 2005). However, after meal ingestion this ratio is rapidly changed to

accommodate the absorption of dietary nutrients and the endocrine and exocrine pancreatic secretions. Importantly, via regulation of substrate availability, portal vein BF is a strong determinant of glucose and insulin entry into and first-pass extraction of the liver and therefore of whole-body intermediary metabolism (Meier et al. 2005). Multiple human studies have shown that after a meal ingestion or intraduodenal glucose administration the superior mesenteric artery BF is rapidly doubled when compared with fasting flow values (Gentilcore et al. 2009), whereas contradictory results have been obtained for celiac trunk (Moneta et al. 1988, Someya et al. 2008, Hamada et al. 2014). The regulation of BF within the splanchnic region after a meal ingestion is mediated by a variety of factors, including autonomic nervous system, glucose, and vasoactive substances, such as adenosine and incretin hormones (Jansson 1994, Matheson et al. 2000). Unfortunately, the knowledge regarding the vasoactive role of various substances within the splanchnic region is derived from animal (rodents, dogs, pigs) data, and studies on humans are essentially lacking. Likewise, the possible alterations in splanchnic vascular functions in obesity and T2D have not been addressed to a great extent.

2.2.2 The pancreas and the islet organ

The pancreas plays a crucial role in the intermediary metabolism during both absorptive and postabsorptive states. After meal ingestion, the pancreatic islets respond to increases in plasma glucose levels by secreting insulin and thereby maintaining normal postprandial rise in plasma glucose levels. Moreover, decrease in β-cell mass and concomitant impairment in insulin secretion is required for the progression from NGT to IGT to T2D. In addition to endocrine (i.e. islet) function, exocrine pancreatic acinar cells secrete digestive enzymes including trypsinogen, lipase, and amylase which hydrolyze dietary proteins, lipids, and carbohydrates, respectively. The latter is not addressed in the forthcoming chapters.

2.2.2.1 Anatomy and histology

The pancreas is an elongated organ, weighting approximately 100 grams in a 70-kg man, located behind the lesser omentum deep in the retroperitoneal space at the level of first and second lumbar vertebrae. This anatomical location of pancreas makes it extremely difficult to study *in vivo.* Macroscopically, pancreas can be divided into functionally equivalent (with minor exceptions) head and uncinate process, body, and tail regions (**Fig. 6A**). The organ receives its arterial blood supply from anterior inferior pancreaticoduodenal, anterior superior pancreaticoduodenal, caudate pancreatic, dorsal pancreatic, gastroduodenal, great pancreatic, inferior pancreaticoduodenal, posterior inferior pancreaticoduodenal, posterior superior pancreaticoduodenal, and transverse pancreatic arteries

originated from celiac trunk (mainly) and superior mesenteric artery (to a lesser extent), with considerable inter-individual variability (Okahara et al. 2009). Conversely, pancreas is drained by multiple small veins merging to portal vein via superior mesenteric and splenic veins. Parasympathetic and sympathetic innervation is conducted from the branches of the vagus nerve and celiac plexus of the sympathetic trunk, respectively. The digestive enzymes are secreted into the main and accessory pancreatic ducts which exit the organ to join the common bile duct within the hepatoduodenal ligament. The digestive enzymes are cosecreted with bile through the ampulla of Vater inside the duodenum.

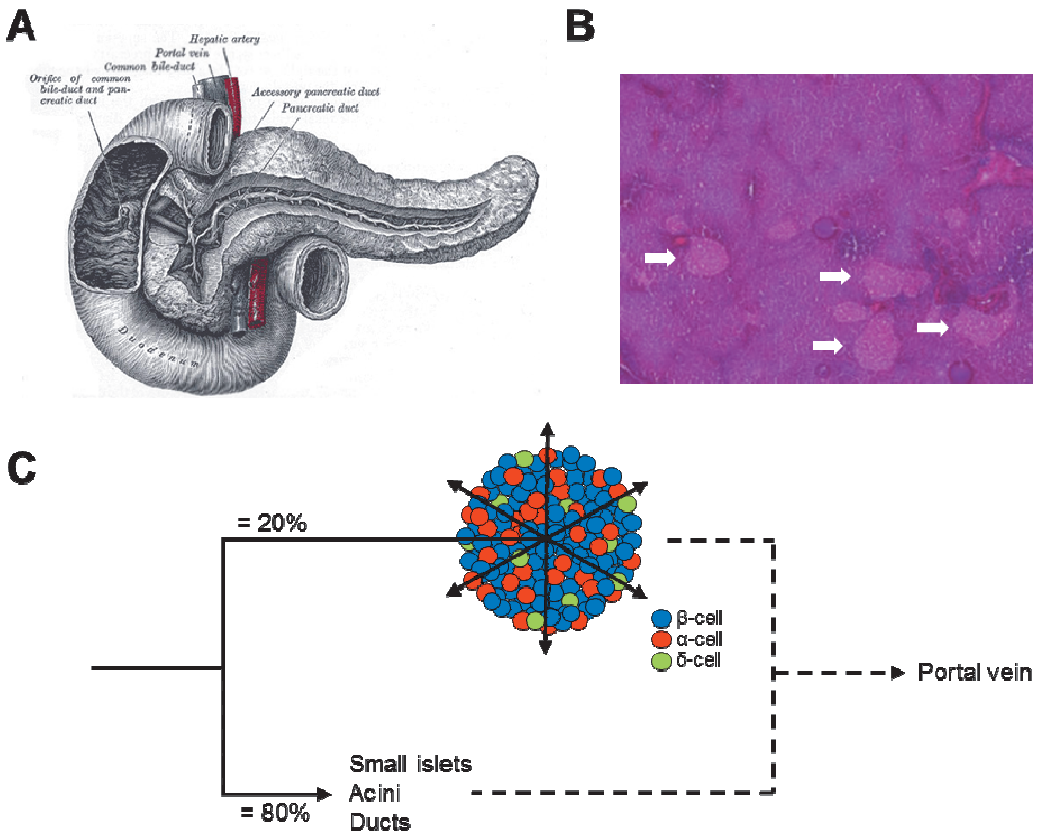

Figure 6. The pancreas is located retroperitoneally between the duodenum and great vessels of the abdominal cavity, adjacent to the hepatoduodenal ligament (A). Hematoxylin-eosin staining of rodent pancreas reveals the distinct exocrine and endocrine arrangement of the parenchyma. The pancreatic islets of Langerhans have been marked with white lines (B). While comprising only 2 % of pancreatic parenchyma, the large islets receive 10-20 % of whole pancreatic BF even during fasting state (C). Predominantly, arterioles perfuse the islet core and then proceed into periphery. Ultimately, blood from pancreas is drained into the portal vein. Modified from Jansson (1994) and Gray & Carter (2009).

Microscopically, pancreatic parenchyma has a pattern of exocrine acinar cells and pancreatic islets of Langerhans (**Fig. 6B**). Due to their different physiological functions, pancreas can be considered as a mixture of two separate organs, the exocrine secretory apparatus and the endocrine islet organ. In healthy, normally glucose-tolerant adult, the number of islets within the pancreas is approximately 1 million, with a total mass of 1-gram, tail-region having twice as much islets as the head or the body (Wang et al. 2013). Moreover, the islets *per se* can be divided as large islets (diameter >250 μm) clustered near the larger ducts and vessels, and small islets distributed evenly between the acinar cells (Kahn et al. 2005). Thus, all of the islets within the pancreas compose the 'islet organ' that has a significant role in energy metabolism yet comprise only 2 % of the whole pancreatic volume. Islets are composed of five different cell types (% of the total islet cells), namely insulin-secreting β-cells (40-70 %, approximately 1000 cells per islet), glucagon-secreting α-cells (15-20 %), somatostatin-secreting δ-cells (3-10 %), pancreatic polypeptide –secreting γ-cells (3-5 %), and ghrelin-secreting ε-cells, respectively. Immunohistochemical studies show that rodents have a distinct islet cytoarchitecture, with β-cell clustered in the core while non-β-cells are accumulated in the periphery of the islets (Attali et al. 2007) whereas in humans both β-cells and non-β-cells are distributed evenly throughout the islet to accommodate paracrine regulation between the different cell types (Hoang et al. 2014).

Although comprising only of 1-2 % of the total pancreatic volume, large islets consume nearly 20 % of pancreatic BF (Jansson 1994). Moreover, the arterioles in islets are more numerous and tortuous than in the surrounding exocrine tissue, due to high metabolic activity and to sensitively detect differences in blood glucose levels. Murine studies have shown that the nutrient artery preferentially perfuse β-cells in the islet core and then the perimeter (**Fig. 6C**) (Bonner-Weir & Orci 1982). By the aid of microsphere technique in a rodent model, Jansson et al. (2007) showed that during hyperglycemic and hypoglycemic clamp, islet BF was significantly higher and lower, respectively, when compared with normoglycemic conditions, while exocrine BF was unchanged. This has also been observed by means of radioactively-labelled red blood cells (Nyman et al. 2010). However, it is likely that glucose does not exert its vascular effects *per se*, but via a complex interaction of metabolic, such as adenosine, and nervous mediators (Carlsson et al. 2002). Previous rodent studies have also investigated the vascular effects of incretin hormones GLP-1 and GIP, and found that both of these hormones are able to regulate distribution of BF into the islets, leading to attenuation and augmentation of islet BF after GLP-1 and GIP injections, respectively (Svensson et al. 1997, Wu et al. 2012). While high islet perfusion rate has been associated with superior insulin secretory capacity in rats (Lau et al. 2012), human studies investigating the relation of pancreatic BF and glycemic control are lacking.

Nonetheless, these experimental results emphasize the distinct vascular patterns and regulations between the exocrine apparatus and the islet organ.

2.2.2.2 Insulin secretion *in vivo*, *in vitro*, and *in silico*

In β-cells, insulin precursor proinsulin is synthesized in the endoplasmic reticulum and is thereafter transported into membrane-bound granules. Within the granules, the two polypeptides of active human insulin are joined with connecting peptide (C-peptide). Glucose is the most potent stimulator of insulin secretion, with linear dose-response curve. After arriving to the islets, glucose is internalized to β-cells insulin-independently by GLUT2, and is metabolized in aerobic glycolysis. The resultant increase in intracellular ATP/ADP-ratio closes the ATP-sensitive calcium-channels leading to cell membrane depolarization and exocytosis of preformed insulin granules (Ganong 2005). During granule exocytosis, insulin and C-peptide are enzymatically-separated, and are thus secreted in equimolar amounts. Thereafter, insulin exits the pancreas via venules and drains into the portal vein and liver. In liver, a large proportion of insulin is extracted by the hepatocytes before ever reaching the systemic circulation. The hepatic extraction fraction of insulin under steady state conditions is approximately 50 % in dogs, and between 40 and 80 % in humans (Field 1973, Eaton et al. 1983, Polonsky et al. 1983). In fact, during fasting state the insulin concentration in healthy dogs in peripheral and portal vein are approximately 10 and 25 mU L^{-1}, respectively.

Normal-weight glucose tolerant individual secretes approximately 36 to 64 U of insulin per day. It is estimated that 50 % of this daily insulin load is secreted during basal state, and 50 % in response to meals (Kahn et al. 2005). During both postabsorptive and absorptive states, insulin is secreted in pulsatile fashion, and recent studies indicate that the secretory pulse amplitude in portal vein is a crucial mediator of hepatic insulin extraction rate leading to a nearly complete vanishment of this insulin pulsatility in peripheral circulation (Meier et al. 2005). Consequently, after meal ingestion the insulin burst mass and amplitude is increased to accommodate increases in plasma glucose level. In contrast to fasting state, wherein pulsatile ISR is stable, after glucose injection a biphasic pattern of insulin secretion is observed in normally glucose-tolerant individual. The first phase insulin secretion is rapid yet transient, and it is followed by a slowly increasing and modest peak. The first transient peak in insulin secretion following intravenous glucose administration is thought to reflect the exocytosis of preformed insulin granules, whereas the second phase secretion constitutes the insulin mRNA transcription and *de novo* synthesis of insulin by the β-cells whether the first phase insulin secretion would have not been sufficient to warrant normoglycemia, respectively (Grodsky 1972). Rodent studies indicate that pancreatic islets have a considerable functional heterogeneity; Lau et al. (2012) identified a sub-population (5 %) of islets characterized by a high perfusion rate and β-cell proliferation and

function which are responsible for the initial insulin supply after a glucose load. In contrast, 25-30 % of islets constitute the reservoir with minimal insulin secretion under normal physiological conditions, but which are thought to be recruited during greater metabolic needs, such as insulin resistance (Olsson & Carlsson 2011). However, in this respect it is worth emphasizing that the β-cell mass does not necessarily relate to β-cell function and that further studies are needed on this topic.

Amino acids are moderate stimulators of insulin secretion while lipids have only a modest effect on insulin secretion. Moreover, while cholinergic and adrenergic stimulation have been shown to augment and inhibit of insulin secretion *in vitro*, respectively, their significance in the regulation of glucose tolerance is unclear (Kahn 2005). In contrast, incretin hormones GLP-1 and GIP share similar extremely potent insulinotropic properties, and their effects on insulin secretion are additive (Dupre et al. 1973, Kreymann et al. 1987, Nauck et al. 1993). Once secreted to circulation in response to meal ingestion, GLP-1 and GIP bind to their respective receptors (GLP-1R, GIPR) on β-cell membrane leading to an increase in intracellular cyclic adenosine monophosphate (cAMP) level and which in turn activates cAMP-PKA and cAMP-Epac2 signaling pathways that mediate the insulinotropic actions of GLP-1 and GIP (Yabe & Seino 2011). By increasing the β-cell sensitivity to glucose, it is thought that the aforementioned hormones act primarily as permissive factors in the insulin secretion cascade, especially after meal ingestion where the incretin effect is estimated to account 50-70 % of the total insulin output.

In single perfused islets *in vitro*, ISR is easy to quantitate. As previously discussed, after leaving pancreatic islets a variable proportion of insulin is extracted by the liver and not streamed into peripheral circulation. As portal vein cannulation is not feasible in humans, it is particularly difficult to obtain the prehepatic insulin values and thus, quantitate ISR *in vivo*. Consequently, during recent decades multiple methods have been introduced to estimate insulin output during oral or intravenous glucose loads. Two commonly used methods, namely C-peptide deconvolution (Eaton et al. 1980, Van Cauter et al. 1992) and β-cell function model by Mari & Ferrannini (2008) are shortly introduced. The first of the mathematical methods is based on the different pharmacokinetic profiles between insulin and C-peptide; while insulin and C-peptide are secreted in equimolar amounts, hepatic extraction rate of C-peptide is negligible making it feasible to estimate ISR from peripheral C-peptide levels with a two-compartment model. In “Pisa-Padova” model (**Fig. 7**), β-cell function during OGTT is divided into three discrete components: 1) linear dose-response curve between plasma glucose and insulin secretion, signifying mean β-cell ability to sense increases in glucose levels, termed *glucose sensitivity*, 2) insulin secretory potentiation due to several factors (prolonged hyperglycemia, non-glucose insulin secretagogues, neural modulation),

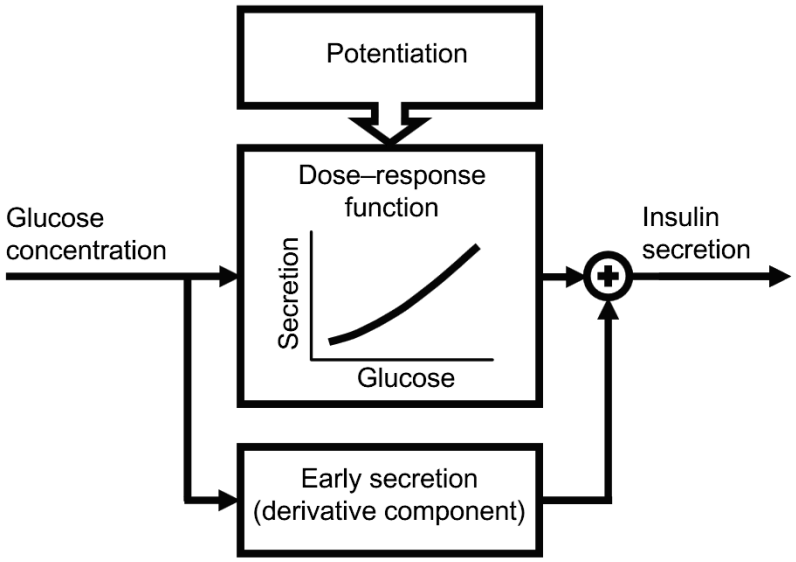

Figure 7. "Pisa-Padova" model of β-cell function. Modified from Mari & Ferrannini (2008).

termed *potentiation ratio*, and 3) the anticipatory component that affects insulin secretion as a function of change in glucose levels, typically during early phases after glucose loading, termed *rate sensitivity* (for a detailed review, see 5.5.6). In summary, when body-surface area (BSA), age, sex, and plasma levels of glucose, insulin and C-peptide during meal testing or glucose-loading are known, ISR can be accurately estimated by using the aforementioned mathematical models.

2.2.2.2.1 β-cell dysfunction in IGT and type 2 diabetes In normally glucose-tolerant obese patients with significant insulin resistance, fasting and postprandial levels of insulin are higher and their β-cell mass is larger than in age-matched lean controls (DeFronzo et al. 1992). However, the imbalance between ISR and peripheral insulin resistance leads to an inability to ensure normoglycemia. During IGT and thus prediabetic state, the hyperglycemic response is only seen after glucose loading, whereas during full-blown T2D, both fasting and postprandial hyperglycemia is present. Consequently, it has widely accepted that an intrinsic defect in the islet organ function and insulin secretion precedes the progression from normal glucose tolerance to IGT to T2D. Cadaver studies have shown that in long-standing non-insulin dependent diabetes, β-cell mass is greatly reduced when compared with weight-matched normoglycemic control (Deng et al. 2004). The intrinsic β-cell defect (increased apoptotic rate and decreased β-cell mass and function) is considered to be multifactorial in etiology, with non-genetic factors and genetic predisposition having an equal contribution in the pathogenic process. In clinical practice, after an intravenous glucose load, the first phase insulin secretion in blunted and virtually absent in patients with IGT and diabetes,

respectively (Ward et al. 1984, Byrne et al. 1996). Moreover, the second phase insulin secretion is severely reduced. The diabetic progression can be observed as a rightward shift in the glucose-ISR dose-response curve suggesting a decreased sensitivity of β-cells to increases in plasma glucose level. This has been validated in a large Italian cohort; patients with impaired glucose regulation had no defect in the compensatory ISR to insulin resistance, but their β-cell glucose sensitivity was reduced by 42 % (Mari et al. 2010). The relationship between fasting plasma glucose levels and fasting/postprandial insulin levels resembles an inverted "U". When fasting plasma glucose increases from 4.0 to 7.8 mM, a steep increase in fasting and postprandial insulin levels are observed. However, with further fasting glucose increases (i.e. from 7.8 to 11 mM), insulin levels drop to the level observed in normally glucose-tolerant individual (DeFronzo et al. 1989). This so-called Starling curve for insulin secretion prompts early and effective treatment of hyperglycemia in patients with established T2D, due to the progressive nature (**Fig. 3**) of β-cell dysfunction in untreated T2D.

Currently, it well-known that hyperglycemia *per se* impairs insulin secretory capacity, termed glucose toxicity. In an elegant study by Toschi et al. (2002), stepwise increase in glucose levels (2.8, 2.8 and 5.6 mM increments) by glucose bolus followed by glucose-insulin –clamp in normally glucose-tolerant individuals resulted in a large first phase insulin secretory response after the first hyperglycemic step whereas during the second hyperglycemic step insulin burst was clearly blunted and third hyperglycemic step failed to cause any increase in insulin secretion. Moreover, experimental 24-hour hyperglycemic clamp (5.4 mM above basal) in normally glucose-tolerant individuals resulted in 15 % and 24 % decreases in arginine-stimulated insulin release and disposition index, respectively (Solomon et al. 2012). It is prevalent that even minute increases in fasting plasma glucose (i.e. chronic hyperglycemia) impair the function of previously reduced β-cell mass and thus the glucose toxicity has been appreciated as a key perpetuating mechanism in T2D. In contrast, the causal link between lipids and β-cell dysfunction is not as clear. During obesity and insulin resistance, the adipose tissue capacity to store surplus lipids is impaired, and the resulting FFA spill-over results in lipid accumulation in various non-adipose tissues, such as liver, heart, and pancreas. Non-oxidative metabolism of these ectopic lipids is thought to commence organ dysfunction and programmed cell-death, apoptosis (Kusminski et al. 2009). When exteriorised islets were infused with palmitate mixture, short-term exposure lead to a powerful potentiation of GSIS thought to compensate lipid-induced decrease in insulin sensitivity, while long-term exposure lead to attenuated insulin secretion (Chen et al. 1994). Furthermore, experiments in healthy humans support these *in vitro* observations, as acute (90-min to 6-hour) and chronic (24 to 48-hour) Intralipid infusions had opposing effects on β-cell function (Paolisso et al. 1995, Carpentier et al. 1999). Moreover, in normally glucose-tolerant individuals with no family history or with positive family history of diabetes elevation of FFA levels to

those seen in patients with T2D (i.e. 0.5-0.6 mM) lead to an increase and a decrease in ISR, respectively (Kashyap et al. 2003). This latter result suggests an intrinsic, genetic vulnerability of β-cells to the increases in fatty acid levels and uptake as a consequence of obesity and insulin resistance. In contrast, Rebelos et al. (2015) investigated a large RISC cohort and failed to find any association between β-cell glucose sensitivity, acute insulin response and circulating FFA levels over wide range of subjects with variable glucose tolerance. Moreover, in subject with prediabetes (either IGT or increased fasting glucose), the plasma FFA levels did not predict the progression to T2D during the follow-up of 3 years. Thus the clinical relevance of the lipotoxicity-concept is unsettled. In addition to glucose- and lipotoxicity –concepts, β-cell resistance to the insulinotropic effects of GIP secondary to chronic hyperglycemia may perpetuate β-cell dysfunction and glucose tolerance (see 2.1.4.1) (Vaag et al. 1996, Nyholm et al. 1999).

The current evidence on the effects of chronic hyperglycemia and diabetes on islet BF has been derived from rodent studies with largerly contradictory results. In a study by Dai et al. (2013), researchers found that in three insulin-resistant strains of mice (*ob/ob*, GLUT4$^{+/-}$, HFD-fed *wt*) the capillaries in the islet β-core were dilated, likely due to increased nitric oxide synthase activity in response to high islet BF and cholinergic stimulus. The islet hyperperfusion and resultant hemodynamic stress has been observed in many animal models of diabetes (Wu et al. 2012), and may contribute to the toxic effects of glucose seen *in vivo*. In the light of this, the islet flow-attenuating effects of GLP-1 and GIP (see 2.2.2.1) during transient hyperglycemia – such as after meal ingestion – may in fact offer long-term β-cell protection. Hypothetically, the increase in islet BF after glucose loading serves to facilitate glucose supply to the β-cells and therefore increase the *glucose sensitivity*. However, Carlsson et al. (1996) compared islet BF in lean *wt* mice after 0.3 mg kg^{-1} glucose challenge with spontaneously hyperglycemic *ob/ob* mice and found that the islet BF was over 70% lower (1.8±0.3 *versus* 6.3±1.0 μL min^{-1} mg estimated islet wt^{-1}) in the latter. The authors concluded that the increased insulin demand during chronic hyperglycemia and obesity is dealt by increasing islet mass *per se* due to inherent inability to increase islet BF. Still others have concluded that vascular milieu and perfusion have negligible relevance in adult islets (Reinert et al. 2013). To date, no human studies have investigated pancreatic/islet BF and their relation to β-cell function and glucose tolerance.

Novel interesting concepts behind β-cell dysfunction including oxidative and endoplasmic reticulum stress (Kaneto et al. 2005) are not addressed in the present discussion.

From the pathophysiological perspective, it is clear that none of the previously discussed β-cell stressors can induce insulin secretory dysfunction *per se* without the predisposing genotype. The high heritability and familiality rates of T2D emphasize the genetic background of the disease (Kahn et al. 2005). The search for candidate genes responsible for vulnerable β-cells has been extensive and currently

the number of loci implicated in the pathogenesis of T2D is roughly 60, including the well-known candidate genes *TCF7L2*, *PPARG*, and *KCJN11* (Voight et al. 2010, Prasad & Groop 2015). The susceptibility genes responsible for diabetic risk increment can be clustered by their respective pathophysiological phenotype, associated with increased insulin resistance (IR cluster), decreased proinsulin (PI cluster), reduced insulin secretion and hyperglycemia (HG cluster), reduced insulin secretion in the presence of increased proinsulin (BC cluster). Moreover, a plethora of genes have been associated with diabetes risk yet they lack any common phenotypic traits, hence they are unclassified (UC cluster). While the individual genotype is a major determinant of impaired glucose regulation, the exact cellular mechanisms by which the candidate genes exert their diabetogenic effect remain largely obscure.

2.2.2.3 Pancreatic glucose and lipid metabolism

Glucose is the principal fuel for oxidative metabolism in both exocrine apparatus and in the islets. In β-cells, however, GU and further metabolic processing is crucial for the adjustment of insulin secretion accordingly. While the data for exocrine glucose utilization is essentially lacking, considerable amount of research has focused on cellular uptake and sensing of glucose in β-cells. Here, glucose is internalized insulin-independently by GLUT2, and is thereafter phosphorylated by glucokinase (Matschinsky et al. 1993). A study by Liang et al. (1994) concluded that the islet GU after intravenous glucose injection was significantly impaired in *db*/*db* mice and obese Zucker rats when compared with control mice, paralleled with a delayed or reduced insulin release. However, as similar defects in insulin release were observed in other diabetic and obese rodents (namely BHE rats, PX rats and H.ras transgenic rats) with normal *in situ* GU, it is likely that the defective GLUT2 activity, whether present in diabetic humans or not, has at most minute effect on impaired ISR. Rather, these results imply that the primary defect in glucose sensing in the diabetic state is accounted for either insufficient glucose supply to the islets, or derangements in post-phosphorylation steps in glucose metabolism. Human studies concentrating on pancreatic/islet GU and concurrent glycemic alterations are lacking.

Data derived from *in vitro* studies imply that pancreatic glucose and fatty acid metabolism are highly interrelated. Fatty acis (FA) uptake in exocrine and islet cells are mediated by either passive diffusion or facilitated transport, the latter consisting of fatty acid translocase (FAT/CD36), plasma membrane-bound fatty acid binding proteins (pm-FABP), and the fatty acid transporter protein family (FATPs). Moreover, the intracellular FA metabolism is guided by cytosolic FABPs. In experiments by Bazin & Lavaus (1982), the acinar cell glucose transport rate decreased by nearly 40 % in rats fed with high-fat diet when compared low-fat diet fed group. Conversely, doxycycline-induced facilitation of CD36 in rat INS-1

cells increased basal oleate uptake, inhibited the normal glucose-mediated inhibition of oleate oxidation, and markedly reduced GSIS (Wallin et al. 2010). Furthermore, Kim et al. (2012) observed that 12-hour incubation of rat INS-1 cells in high glucose (30 mM) media lead to increased CD36 and palmitate uptake in parallel with decreased GSIS. In the same study, siRNA-mediated inhibition of CD36 normalized impaired GSIS despite the hyperglycemic milieu. Similar interrelationships between glucose and FA metabolism in INS-1E cells have been observed for cytosolic FABP 3 and 5 (Hyder et al. 2010). These results imply that 1) Randle cycle, i.e. substrate inhibition, is operational in rodent exocrine/islet cells, 2) increased FA uptake and oxidation during chronic hyperglycemia inhibit glucose metabolism and sensing accounting for clinical glucose toxicity, and 3) interventions to decrease β-cell FA uptake improve GSIS by enabling adequate glucose oxidation and sensing. The previous implications support lipotoxicity-concept yet they are purely speculative. To verify these hypotheses, *in vivo* studies in humans are needed.

Based on the previous findings, obesity-induced lipid spill-over leads to an increase in FFA uptake. In addition, human autopsy studies have observed lipid deposition in pancreas with increasing age and body weight (Olsen 1978), and further investigations in rodents have detailed that this ectopic fat accumulation have different behavior between exocrine and islet cells; whereas in the former lipids are organized as large droplets with low rate of apoptosis, in the latter lipids droplets are few and apoptosis is far more common occurrence (Higa et al. 1999, Kusminski et al. 2009). While it is assumable that the rate of FA uptake and ectopic fat percentage within the pancreata are interrelated and associated, to date no study has addressed this question. Moreover, while pancreatic fat content have been associated with impaired β-cell function in cross-sectional imaging studies (Tushuizen et al. 2007, Heni et al. 2010), these do not prove the potential causality between the two parameters. Recently, Hannukainen et al. (2011), compared pancreatic fat content in identical twins with discordant physical activity and found that while in the pooled data the pancreatic fat content was associated with insulin resistance, the authors failed to find any significant link between pancreatic fat content and measures of β-cell function and glucose tolerance. In summary, the role of pancreatic ectopic fat accumulation on β-cell function and the potential reversibility of the former by weight-loss regimens is currently unsettled.

2.2.3 The small intestine

The most salient function of the small intestine is the enzymatic degradation and absorption of dietary carbohydrates, lipids and proteins. In addition to this absorptive function, small intestine contributes to the regulation of intermediary metabolism by secreting a number of alimentary hormones affecting insulin sensitivity, secretion and GU. Intestine is the first organ to filter ingested food, and

during the recent decade the potential role of small intestine in the pathogenesis of impaired glucose regulation and diabetes have gained considerable interest. However, due to the venous drainage into the portal vein and inherent mobility, direct measurement of intestinal metabolism is challenging.

2.2.3.1 Anatomy and histology

The small intestine is a 3-metre long (6-metres in autopsy) tubular organ originating from the pyloric sphincter in the ventricle, and extending into the cecum (**Fig. 8A**). The weight of the small intestine without contents is approximately 600 grams making it the largest organ in the extrahepatic splanchnic region. Functionally and macroscopically, small intestine is divided into three consecutive sections, namely duodenum, jejunum and ileum, respectively, without clear demarcations. While duodenum is a retroperitoneal organ, jejunum and ileum are anchored to the posterior wall of the abdominal cavity by the mesenterium, a fold of membranous connective tissue that conducts the arteries, veins and lymphatic vessels to the small intestine. Arterial blood supply of the small intestine is derived from the supraduodenal, gastroduodenal, and pancreaticoduodenal branches of celiac trunk and from the jejunal and ileal branches of superior mesenteric artery, whereas the duodenal, jejunal and ileal veins drain into superior mesenteric and portal vein, respectively (Matheson et al. 2000). The dual extrinsic innervation to the small intestine is accomplished by the respective branches of the vagus nerve and sympathetic trunk, respectively.

Throughout its course, small intestine is composed of four distinct layers (**Fig. 8B**). Innermost layer, the mucosa, is composed of multiple villus-like structures to increase the absorptive area of the small intestine, and form the characteristic brush-border membrane. The main cell type in the brush-border membrane is the enterocyte, which serves the absorptive function of the small intestine. In contrast, crypts protrude into the base of the villi, and contain the stem cells for regenerative purposes. While the enterocytes and stem cells constitute the majority of cells found in the mucosa, there is an abundance of other cell types as well (Ganong 2005). Mucous cells are found in the upper third of the villi, and discharge mucus to facilitate enzymatic degradation on the brush-border membrane. In contrast, hormone-secreting endocrine (such as K and L) cells and immunological Paneth cells can be found in depths of crypts. Located under the enterocyte layer in villi, the *lamina propria* offers structural integrity to the mucosa and is composed of connective tissue, small capillaries, nerves and lymphatic lacteals. Beneath the mucosa and a thin *muscularis mucosae* layer, the submucosa contains larger blood vessels, nerves and lymphatic ducts. Moreover, large lymphoid aggregates reside in the submucosa. The coordinated movement of the small intestine is accomplished by two layers of smooth muscle, arranged in circular and longitudinal fashion

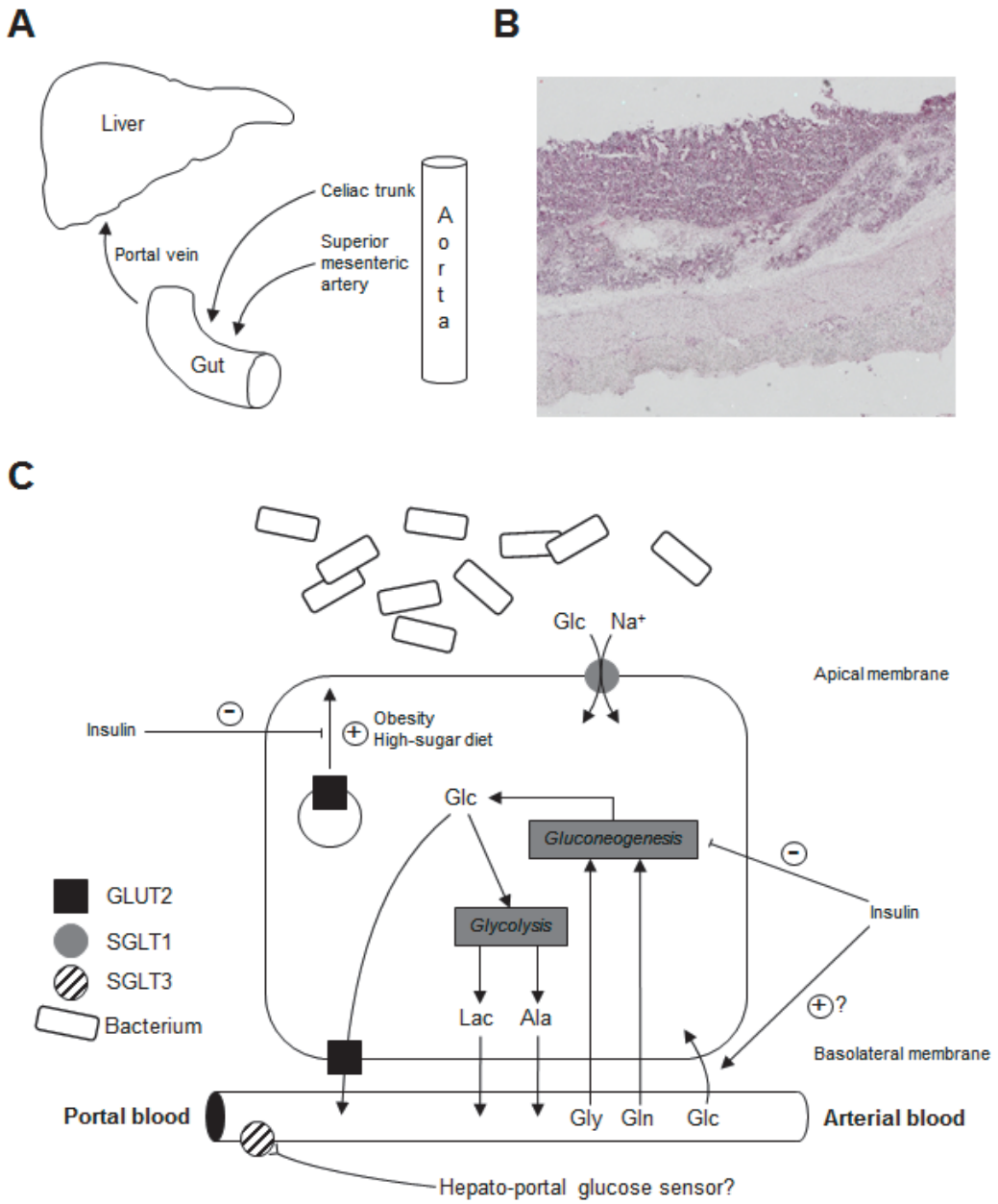

Figure 8. Macroscopic anatomy, vasculature and histological appearance of the small intestine (A-B). Current concepts on intestinal glucose handling including glucose entry to and from the enterocyte, oxidative metabolism and gluconeogenesis, insulin action, intrasplanchnic substrate cycle, and hepato-portal glucose sensor (C). GLUT2, glucose transporter 2; SGLT1 & 3, sodium-glucose cotransporter 1 & 3; Glc, glucose; Gly, glycerol; Gln, glutamine; Lac, lactate; Ala, alanine. Modified from Barret et al. (1985), Mithieux (2005), and Mithieux (2014).

beneath the submucosa (namely, *muscularis externa*). Lastly, the outermost layer of the small intestine is the serosa, composed of loose connective tissue to prevent friction damage with other gastrointestinal organs.

2.2.3.2 Intestinal metabolism in health and obesity

Enterocytes are the most crucial cells in the absorption of nutrients, water, vitamins and bile salts from the gut lumen, and are responsible for the glucose and lipid trafficking between the gut lumen and the circulation. The brush-border membrane located on top of the enterocyte layer contains the glycocalyx, a 0.3-micrometre thick layer of glycosaminoglycans and glycoproteins that bind the digestive enzymes thus and aid in the absorption of the ingested nutrients. Moreover, the peristaltic movement of the small intestine is thought to aid in the intraluminal degradation of ingested nutrients and absorption of the monomer structures (Ganong 2005). In fact, small intestine has two major networks, the Auerbach's and Meissner's plexuses located in between the circular and longitudinal muscle layers of the *muscularis externa* and within the submucosa, respectively. While the so-called enteric nervous system can function independently, it is connected to both parasympathetic and sympathetic nervous systems, with the former and latter increasing and decreasing the activity of intestinal smooth muscle, respectively. In general, the peristalsis occurs as a reflex response to the respective intestinal segment on which the luminal contents stretch the gut wall, and is thought to be mediated by serotonin and cholinergic neurons.

After meal ingestion, intestinal BF increases by 3-fold, stays elevated for 2-3 hours, and thereafter returns to baseline (Gentilcore et al. 2009). This postprandial hyperemia occurs in parallel with nutrient digestion and absorption, and compensates for the increased metabolic activity of the enterocyte layer. In response to meal-induced decrease in splanchnic vascular resistance, a subtle drop in blood pressure and a compensatory increase in heart rate is frequently observed (Gentilcore et al. 2008). The main stimuli for the postprandial hyperemia is the chyme passing through the intestine, and is thought to be mediated by a complex set of neural (mainly cholinergic), metabolic and non-metabolic factors, and gastrointestinal hormones. However, to date no study has addressed the solitary role of the various aforementioned factors on the regulation of intestinal BF in humans *in vivo*.

2.2.3.2.1 Apical and basolateral glucose fluxes During the absorptive state, the ingested glucose is transepithelially migrated into the portal blood by the *sodium-glucose cotransporter 1* (SGLT1) operating on the apical plasma membrane and GLUT2 providing the exit pathway for the intracellular glucose into the bloodstream (**Fig. 8C**) (Mithieux 2005). However, the regulation of glucose fluxes within the enterocytes is highly complex. Immediately after glucose ingestion a

transient GLUT2 translocation to the apical membrane can be visualized, thought to potentiate SGLT1-mediated lumen-to-blood glucose fluxes. In contrast, obese patients have been shown to permanently incorporate GLUT2s in the enterocyte apical membrane, creating a glucose exit pathway from bloodstream to gut lumen during fasting hyperglycemic states (Ait-Omar et al. 2011). Moreover, Tobin et al. (2008) showed that in human enterocytic colon carcinoma (Caco-2/TC7) cells, insulin treatment before glucose incubation period lead to apical GLUT2 internalization and decreased sugar absorption rate. Lastly, the translocation of GLUT2 is highly dependent on intestinal BF kinetics (Helliwell & Kellett 2002). Taken together, these results imply that obesity, macronutrient balance in diet, and splanchnic BF kinetics modulate the enterocyte glucose transporter localization leading to potentiation of either lumen-to-blood or blood-to-lumen net glucose flux rate depending on the metabolic state (i.e. normoglycemia and glucose ingestion *versus* chronic hyperglycemia) and glucose gradient between bloodstream, gut lumen and enterocyte cytoplasm.

It is not fully known whether insulin is operational in the regulation of basolateral GU during absorptive and postabsorptive states. In healthy anesthetized dogs, Barret et al. (1985) observed 3-fold increases in extrahepatic splanchnic glucose utilization rates during hyperglycemic hyperinsulinemia whereas no change was noticed during euglycemic hyperinsulinemia. This and the lack of change in glucose clearance and extraction rates suggest that the increase in extrahepatic SGU under hyperglycemic and hyperinsulinemic conditions is solely due to the increased mass action effect of glucose irrespective of the insulin action. However, the previous results were based on the arterio-portal differences in glucose levels, and thus represent net glucose balance (i.e. uptake and release) in the extrahepatic splanchnic region rather than unidirectional glucose fluxes across the enterocyte plasma membrane. Insulin-sensitizer metformin has been shown to greatly increase [^{18}F]fluorodeoxyglucose ([^{18}F]FDG) bowel uptake implying that insulin may indeed have an effect on basolateral gut GU (Gontier et al. 2008). No study has quantified insulin effect on gut GU in humans *in vivo.* Moreover, obesity-induced alterations in the former – if any – has not been studied.

2.2.3.2.2 Intestinal gluconeogenesis and portal sensor concept In healthy individuals, during prolonged fasting and early starvation, small intestine accounts for 20-25 % of the whole-body EGP in concert with liver and kidneys (Krebs 1972, Mithieux 2001). In fact, recent studies have shown that the enterocytes in the small intestine, but not in the colon, express the two rate-limiting enzymes in the gluconeogenetic pathway, PEPCK and Glc6Pase (Rajas et al. 1999, Rajas et al. 2000). In the previous studies, it was appreciated that the main gluconeogenetic precurcors in the gut are glutamine and glycerol, whereas the oxidative metabolism of glucose within the enterocyte yields lactate and alanine which in turn are substrates for hepatic gluconeogenesis, thus creating an intrasplanchnic substrate

cycle (**Fig. 8C**) (Barret et al. 1985). As the starvation is prolonged, the relative proportion of gut gluconeogenesis to total EGP is increased while hepatic EGP is decreased. This is thought to facilitate more pronounced hepatic glucose influx and rebound synthesis of glycogen during long-term food deprivation.

Moreover, Croset et al. (2001) observed that insulin infusion in 48-hours fasted rats lead to a complete inhibition of gut gluconeogenesis and decrease in portal vein glucose concentration measured by means of [^{3}H]glucose and arterio-portal balance technique. In contrast, gut gluconeogenesis is stimulated by prolonged insulinopenia such as during early starvation, as it is not until 48-hour of fasting before the GlC6Pase enzyme is sufficiently expressed to participate in gluconeogenesis. Studies in streptozotocin-treated diabetic rats mimic the similar glucose kinetics even at postabsorptive state as healthy rats with greatly prolonged (72-hours) fasting (Mithieux et al. 2004). These results suggest that insulinopenia is required for the adequate gluconeogenesis to take place in the gut; that serum insulin concentrations found in the postabsorptive state and early starvation are sufficient to inhibit any significant gut gluconeogenesis; and that deficiencies in insulin signaling and impaired gluconeogenetic inhibition (i.e. relative rather than absolute insulinopenia) may play a crucial role in the pathogenesis of T2D. However, to date no study has addressed whether insulin resistance exists in the small intestine in humans.

High porto-arterial glucose gradient and portal infusions of glucose have been suggested to play a direct and important role in the regulation whole-body metabolism. In 1960s Russek (1963) proposed that portal vein wall has neurons that can sense increases in portal vein glucose concentration insulin-independently by SGLT3 (Mithieux 2014). Thereafter, the information is transmitted to the central nervous system via vagal afferent fibers which modulate the orexigenic behavior leading to decreased food intake. In the recent decades, this hepatoportal glucose sensor concept have gained a considerable amount of interest and controversy. Rodent studies have shown that portal glucose infusion leads to an increased HGU, decreased insulin counter-regulation, and increase in GU in insulin-sensitive tissues, often leading to hypoglycemia without the rise in insulin levels in these experiments (Burcelin et al. 2000). Moreover, hepatic portal vein denervation in healthy dogs lead to significantly impaired glucose tolerance during OGTT whereas GLP-1 RA exenatide effects were essentially unchanged (Ionut et al. 2014). Troy et al. (2008) observed in a rodent study that the early beneficial effects of Roux-en-Y gastric bypass are due to bypassed foregut upregulating intestinal gluconeogenetic rate and triggering the hepatoportal sensor, whereas a latter study performed in humans has questioned this hypothesis (Hayes et al. 2011). Nevertheless, autonomic nervous system and vagal projections to the splanchnic region seem to be crucial in the regulation of intermediary metabolism during feed/fast cycle and warrant further research.

2.2.3.2.3 Gut hormone secretion Small intestine participates in glucose disposal after a meal not only by regulating glucose absorption and gluconeogenetic rate but also by secreting a number of alimentary hormones, namely incretins GLP-1 and GIP, GLP-2, peptide YY, cholecystokinin, secretin, motilin, and oxyntomodylin in response to nutrient load encountered by the specialized hormone-secreting cells. In addition to their β-cell mass promoting and insulinotropic effects (for a detailed review, see 2.1.3.3), gut hormones regulate appetite control, gastric emptying, GI motility and growth, bile secretion and gallbladder contraction, and possess cardio- and neuroprotective functions (Holst et al. 2009). The two most studied alimentary hormones, incretins GLP-1 and GIP, are secreted by the L cells in the distal small intestine and colon and K cells located in the duodenum and proximal jejunum, respectively. Moreover, GLP-2 has been shown to improve intestinal barrier function (Benjamin et al. 2000), thereby reducing the permeability of bacterial products and occurrence of low-grade inflammation (for a detailed review, see 2.2.3.2.4).

By far the most potent stimulator of incretin hormone secretion is ingested glucose (Lim & Brubaker 2006), but recent studies have also proposed the role of lipids in the secretion of both GLP-1 and GIP, especially after a fat-rich and carbohydrate-deficient meal (Edfalk et al. 2008, Iwasaki et al. 2015). Moreover, in an elegant study by Marathe et al. (2014), increase in intraduodenal glucose infusion rate from 2 to 4 kcal min^{-1} resulted in a more prominent and sustained incretin response and 40 % improvement in gastrointestinal glucose disposal rate suggesting that the rate of gastric emptying is a significant contributor to the gut hormone response after a meal. Due to the inhibitory action of GLP-1 on gastric emptying, the relationship between the two (i.e. gastric emptying and incretin response) is bidirectional. As the prevalence of abnormally delayed gastric emptying, gastroparesis, is 30-50 % in long-standing type 1 or type 2 diabetes, the role of gastric emptying on postprandial glycemic excursions and incretin response is emphasized in hyperglycemic states (Chang et al. 2010, Phillips et al. 2015). The GLP-1 secretion is impaired patients with T2D and this may at least partly result from impaired small intestinal glucose exposure. Moreover, a recent study performed in rodents revealed that after bariatric surgery gastric emptying was significantly accelerated and was mostly responsible for the dramatic increase in postprandial GLP-1 levels (Chambers et al. 2014). In the same study, bypassing the gastric digestion with direct glucose infusion to the duodenum resulted in three times as high GLP-1 levels in VSG operated mice as in sham-operated control mice. These results suggest that incretin hormone secretion is regulated not only by the rate of small intestinal glucose exposure but also via complex interactions at the level of intestine.

2.2.3.2.4 Microbiota, leaky gut hypothesis and endotoxemia Soon after birth, human gut is colonized by maternal and environmental bacteria, and approximately

10^{14} bacteria resides within the adult human gut constituting the microbiota (**Fig. 8C**). While over 1 000 bacterial species have been identified in human and rodent gut, the microbiota is dominated by only a few of these, including *Bacteroidetes*, *Firmicutes*, and *Actinobacteria* families. Generally, human microbiota serves a number of physiological functions, including fermentation of undigested carbohydrates and production of short-chain fatty acids, synthesis of vitamins B and K, immune modulation, and metabolism of bile acids, sterols and xenobiotics (Ganong 2005). During the recent years, it has become evident that microbiota composition is not stable but highly adaptive to changes in diet and innate diseases. Indeed, several studies have observed higher *Firmicutes*:*Bacteroidetes* ratio in obese humans and animals, reversible after weight-loss regiments (Turnbaugh et al. 2006, Ley et al. 2006). The latter observation clearly suggests that the alteration in microbiota composition is secondary to the obesity-rendering diet rather than being an innate pathology. Mice fed with high-fat, Western-style diet exhibit a considerable change in their microbiota with predominance of *Firmicutes* to that observed when the same mice were fed with standard chow (Delzenne et al. 2011). The role of gut microbiota in the pathogenesis of obesity and diabetes is highlighted by the fact that germ-free (GF) mice, lacking gut microbiota, are significantly leaner than their counterparts with intact microbiota despite consuming more energy (Bäckhed et al. 2004). Moreover, GF mice are very resistant to high-fat diet induced obesity (Rabot et al. 2010) suggesting that luminal bacteria participate in the regulation of intermediary metabolism.

Several hypotheses have been introduced to explain the causal link between high-fat diet, altered microbiota composition and obesity. Bäckhed et al. (2004) concluded that the increased body weight in mice with intact microbiota was associated with increased adiposity and fat storage capacity. Although intestinal bacteria are able to produce short-chain fatty acids from unfermented carbohydrates, this subtle increase in fatty acid absorption is not sufficient to explain the drastic increases in adipose tissue volume suggesting that additional, yet unidentified mechanisms contribute to this pathophysiological phenomenon.

One interesting concept between gut microbiota and glucose intolerance is the metabolic endotoxaemia: obesity is characterized by a systemic, low-grade inflammatory state manifested as slightly increased levels of C-reactive protein (Pickup et al. 1997, Delzenne et al. 2011). Originally Cani et al. (2007) observed that plasma levels of bacterial lipopolysaccharide (LPS) increased after meal ingestion when compared with postabsorptive state, and that mice fed with high-fat diet for 4-weeks experienced permanent, two- to threefold increase in LPS levels. Further studies have validated this metabolic endotoxemia –concept in humans as well (Pendyala et al. 2012). Furthermore, high plasma levels of LPS are positively associated with insulin and triglyceride levels, and negatively associated with high-density lipoprotein levels, respectively, implying that endotoxemia that is originated from the gut leads to glucose intolerance and poor lipid homeostasis

(Delzenne et al. 2011). As the increase in gram-negative bacteria in response to high-fat diet is not sufficient to explain increases in LPS levels, it is likely that the barrier function of the intestinal mucosa is disrupted to permit the entry (leak) of bacterial products into the systemic circulation (Brun et al. 2007). However, it must be emphasized that the present, so-called leaky gut –hypothesis, has gained considerable amount of both appreciation and criticism, and the reception of novel information on this subject must be handled with caution. The regulation of intestinal tight junctions and their integrity is out of the scope of the present discussion, but involves a complex set of cross-talk between various factors, including GLP-2 and the endocannabinoid system.

2.3 Established methods to measure splanchnic functions *in vivo*

In humans and other vertebrates, the splanchnic region – both hepatic and extrahepatic – is a significant contributor to both postabsorptive and absorptive glucose disposal, and impairment in splanchnic functions antecedes the progression from NGT to IGT to T2D (Bajaj et al. 2002, Kahn et al. 2005). In response to meal and glucose ingestion, splanchnic region is responsible for β-cell glucose sensing and insulin secretion, upregulation of GU and oxidative/non-oxidative glucose metabolism, and inhibition of hepatic and intestinal gluconeogenesis. Likewise, adaptive changes in BF within the splanchnic bed and between organs presumably aid in the efficient metabolism of glucose load encountered by the body. Due to complex anatomy, localization deep in the abdominal cavity and dual blood supply of the liver, the direct measurement of splanchnic function organ-specifically is extremely difficult. In the following discussion, a brief review of the established methods to quantitate splanchnic organ glucose/lipid metabolism and BF is presented.

2.3.1 The splanchnic/hepatic balance technique

The splanchnic net glucose balance entails three parallel phenomena, the hepatic and intestinal glucose production, total splanchnic (i.e. hepatic and extrahepatic) GU, and basal or stimulated insulin secretion. While earlier studies have shown that both hyperglycemia (Soskin & Levine 1952), hyperinsulinemia (Madison et al. 1960), and the combination of the two (Bergman 1977) are key triggers to switch the net splanchnic glucose balance from negative (release) to positive (uptake), the exact switch threshold on glucose handling is particularly cumbersome to detect. In humans, the net splanchnic glucose balance can be calculated using the arterio-venous balance technique. Here, cannulas are inserted into the femoral artery and vein, and the latter is advanced into one of the hepatic veins under fluoroscopic or x-ray surveillance. Total splanchnic plasma flow (SPF) is measured using dilution

technique, usually indocyanide green (ICG) (DeFronzo 1987). The net splanchnic glucose balance (NSGB) is calculated as

$$NSGB = (A\text{-}V)_{Gluc} \times SPF,$$

and provides valuable information concerning the contribution of splanchnic tissues on whole-body glucose metabolism. Unfortunately, while the above equation yields an estimate of total glucose balance in the splanchnic bed, it does not allow to separate to what extent this variable is dependent on 1) SGU, 2) EGP, or 3) the relative contribution of hepatic and extrahepatic (gastrointestinal) tissues on these parameters. While the administration of [^{3}H]glucose under steady state conditions in combination with arterio-venous balance technique can be used to estimate total EGP (for a detailed review, see 2.3.2) and total splanchnic GU in humans, it is not possible to differentiate hepatic and extrahepatic compartments by using these techniques. Moreover, the invasiveness of femoral artery and hepatic vein catheterization restricts its use in clinical practice.

The cannulation of portal vein can yield reliable estimates of extrahepatic splanchnic glucose kinetics, but it is not practical in humans. However, in pig and dog models the portal vein cannulation can be performed under general anesthesia. The use of portal balance technique yields estimates of glucose handling in the compartments of splanchnic region as

$$EHGB = (A\text{-}P)_{Gluc} \times PVPF$$
$$HGB = (P\text{-}V)_{Gluc} \times PVPF + (A\text{-}V)_{Gluc} \times HAPF,$$

where PVPF and HAPF denote portal vein and hepatic arterial plasma flow, respectively. The use of portal balance technique is challenged by the need for separate measurements of hepatic arterial plasma flow and portal vein plasma flow. These variables can be measured with either ultrasonographic probes inserted during surgery or with double dilution technique (ICG and bromosulfophthalein) (Ishida et al. 1983). The application of the splanchnic/hepatic balance technique in healthy dogs (Barret et al. 1985) revealed that during postabsorptive state hepatic glucose balance is negative favoring release of glucose whereas gastrointestinal tissues consume glucose. During euglycemic clamp study, HGP is decreased by 90 % but not completely inhibited whereas gastrointestinal GU remains similar. In contrast, during combined hyperglycemia and hyperinsulinemia, hepatic glucose balance is switched from negative to positive and gastrointestinal GU is increased by 75 %. The authors concluded that gastrointestinal tissues play an important role in the glucose disposal during both fasting and prandial conditions, and account for 20 % of the whole-body glucose disposal.

Last, while combined catheterization technique can be used to quantitate glucose kinetics during various physiological states, the calculations yield only net glucose

balance (i.e. uptake – release) rather than unidirectional measurements. Moreover, as the extrahepatic region constitutes a mixture of physiologically variable organs (intestine, pancreas, visceral adipose tissue, spleen) with varying BF rate and intracellular glucose pathways (see 2.2.2.3, 2.2.3.2.1, and 2.2.3.2.2 for comparison), the extrahepatic results derived from catheterization technique must be interpreted with caution.

2.3.2 The double tracer technique

While the splanchnic/hepatic balance technique gives reliable and robust estimates of glucose kinetics during various physiological states (postabsorptive and absorptive states, insulin clamp), it is highly invasive and not practical in humans. In contrast, the double tracer technique originally presented by Pilo et al. (1981), and many of its modifications, relies on the use of two separate glucose tracers ([^{3}H]glucose infused intravenously and [^{14}C]glucose administered orally) to investigate glucose metabolism during basal (fasting) state and after an oral glucose load non-invasively. During the steady-state conditions, the rate of EGP equates to whole-body glucose disposal and can be calculated as a ratio of [^{3}H]glucose infusion rate (decays per min) to plasma [^{3}H]glucose specific activity (decays per mg) in a rather straightforward fashion. During absorptive state, in contrast, plasma glucose concentration is dependent on gastric emptying, intestinal glucose absorption, EGP, net splanchnic glucose extraction and peripheral glucose disappearance (Vella & Rizza 2009) leading to decrease in accuracy to quantitate the glucose fluxes, more complex calculations and an array of potential pitfalls. When [^{14}C]glucose is mixed to oral glucose (or meal) solution, rate of total (RaT) and oral (RaO) glucose appearance and rate of disappearance (RaD) can be estimated to some accuracy. Here, SGU can be expressed as a substraction of RaO from the amount of glucose ingested (Cersosimo et al. 2011) equating with the amount of glucose metabolized within the splanchnic tissues and not reaching systemic circulation. While highly practical and widely assessed methods in humans, the double-tracer technique has the same drawback as the hepatic balance technique, i.e. its inability to distinguish hepatic from extrahepatic splanchnic glucose metabolism. Moreover, the innate calculations of the double-tracer methodology rely that the oral glucose load is entirely (100 %) absorbed, which is somewhat questionable.

2.3.3 Positron emission tomography (PET)

The clinical implementation of positron emission tomography (PET) and other nuclear imaging modalities in the 1980s circumvents many of the challenges associated with splanchnic/hepatic and double tracer techniques. PET is a nuclear imaging modality providing functional and quantitative information of the tissues

organ-specifically *in vivo*. Moreover, in addition to imaging during fasting state, PET methodology can be utilized in concert with various stimuli, including insulin clamp (Nuutila et al. 1992), exercise (Kemppainen et al. 2002), cold exposure (Virtanen et al. 2009), and meal testing (Vosselman et al. 2013). The PET methodology is based on the use of short-lived, positron-emitting radioactive isotopes (such as ^{18}F and ^{15}O), integrated into a natural compounds that behave similarly as the physiological counterparts. After administration (intravenous injection, ventilation, ingestion), the PET tracer is distributed and metabolized into body similarly as the physiological counterpart, such as glucose or fatty acids. In tissue, the nuclear imbalance, i.e. positron excess in the atomic nucleus, leads to β^+ decay and an emission of a positron and a neutrino. The positron traverses a short distance (0.35 mm) within the tissue gradually losing its energy until it collides with an electron. The resulting annihilation process generates two 511 k*e*V photons traveling in opposite directions. Ring-shaped detectors of the PET scanner around the subject are designed to detect these γ quants in a coincidental fashion (**Fig. 9**), and send the raw data to the processing unit for tomographic image reconstruction. Afterwards, the computerized PET quantitation (of the physiologic process) is performed using the designated software either manually or automatically: the modelling is based on the relative tracer kinetics between the input (usually blood) and the tissue chosen. The former can be obtained via frequent sampling of arterialized blood or directly from the PET image, whereas the latter is derived from the PET image by placing 3-dimensional volume-of-interest (for a detailed review, see 5.3.1) to the tissue parenchyma producing averaged time-activity curve of the tissue. Novel PET scanners are combined with a reference image modality, either computed tomography (Teräs et al. 2007) or magnetic resonance imaging (Zaidi et al. 2011) to allow correction for tissue attenuation and to obtain topographical landmark image for easier PET analysis.

PET has become a standard imaging modality in cardiology, neurology and oncology. Moreover, with the introduction of more advanced PET scanners with higher spatial resolution and increased number of detector rows, comprehensive metabolic research in the splanchnic region is now possible. Indeed, previous studies utilizing PET methodology in Turku PET Centre have validated the use of PET for the quantification of hepatic glucose and lipid metabolism (Iozzo et al. 2007, Iozzo et al. 2010), and have evidenced *in vivo* decreased insulin-stimulated hepatic GU in patients with T2D, and the operation of Randle cycle in the liver in healthy individuals (Iozzo et al. 2003, Iozzo et al. 2004). Studies by Virtanen et al. (2002) have clarified the role of visceral rather than subcutaneous adipose tissue in the regulation of whole-body glucose metabolism. To the best of this author's knowledge, PET methodology has not been implemented to investigate pancreatic and/or intestinal metabolism and BF. In addition, no PET validation for the measurement of these extrahepatic splanchnic organ function exists. The biological distribution of the natural compound between organs is largely dependent on the

specific PET tracer chosen, all of which have their benefits and limitations. Next, a brief introduction of PET tracers utilized in the present work is presented.

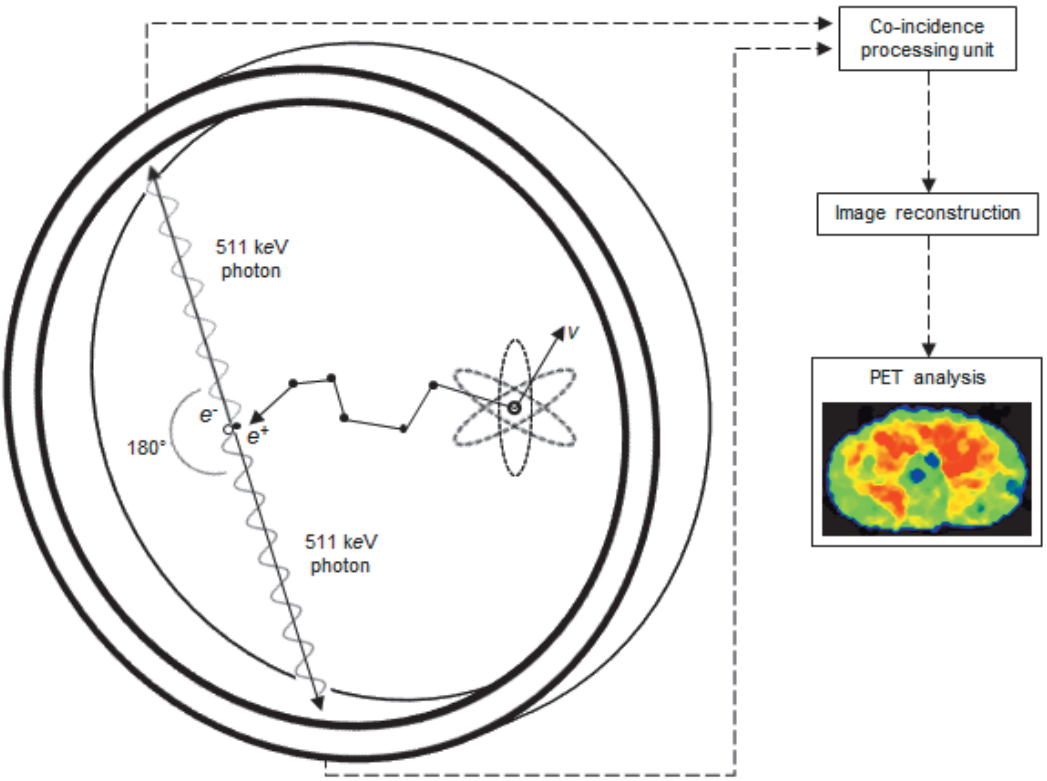

Figure 9. The principles of β^+ decay, positron emission and annihilation, co-incidental detection of opposing γ quants, and PET instrumentation in a clinical setting. The PET methodology is very computer intensive and results in functional and organ-specific imaging of body functions depending on the assigned PET tracer (see text). e^-, an electron; e^+, a positron; v, a neutrino.

2.3.3.1 2-[^{18}F]fluoro-2-deoxy-*D*-glucose ([^{18}F]FDG)

Estimation of metabolic rate of glucose by means of PET has most commonly been performed with 2-[^{18}F]fluoro-2-deoxy-*D*-glucose ([^{18}F]fluorodeoxyglucose, [^{18}F]FDG). The rationale for the use of the [^{18}F]FDG tracer is that both glucose and [^{18}F]FDG share the same transport proteins and hexo/glucokinase action in a competitive fashion and accumulate within the cell in proportion to each other. However, unlike glucose, after phosphorylation by the rate-limiting step by hexo/glucokinase, [^{18}F]FDG-6-phosphate ([^{18}F]FDG-6-P) is not a substrate for any known enzyme present in the mammalian cell and therefore cannot participate in either glycolysis, glycogen synthesis or gluconeogenesis (Lammerstma et al. 1987). As this assumption stands also for Glc6Pase, [^{18}F]FDG-6-P is essentially trapped

within the tissues and can be used to quantitate the unidirectional uptake of glucose. Given the irreversible pharmacokinetic profile of [^{18}F]FDG, the use of [^{18}F]FDG model results in optimal target-to-background ratio and PET images of high statistical quality for the measurement of metabolic rate (MR_{Gluc}) of glucose (GU). Another advantage of [^{18}F]FDG-PET is that it can be utilized in concert with insulin clamp (Nuutila et al. 1992) to mimic steady-state during absorption.

Originally, [^{18}F]FDG pharmacokinetics were quantified with Sokoloff's three-compartmental model, which describes tracer fluxes (rate constants) as a function of time between plasma and tissue unphosphorylated compartment (inflow K_1 and outflow k_2), and the phosphorylation (k_3) and dephosphorylation (k_4) of [^{18}F]FDG/[^{18}F]FDG-6P, respectively (Sokoloff et al. 1977, Phelps et al. 1979, **Fig. 10A**). Later on, Patlak graphical analysis (Patlak & Blasberg 1985, **Fig. 10B**) and fractional uptake concept (Ishizu et al. 1994) provided simplification to the three-compartment model by discarding pharmacokinetic constants k_4 (both models) and V_d (volume of distribution, only fractional uptake concept). Both of the later methods are based on multiple blood sampling and steady state conditions during the imaging session and result in the influx rate constant (K_i or fractional uptake rate, FUR) representing a mixture of multiple steps in the compartment model.

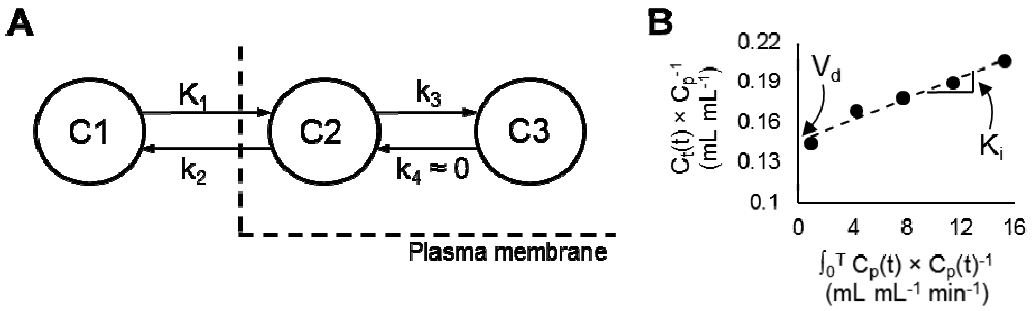

Figure 10. Three-compartmental pharmacokinetic model by Sokoloff et al. (1977) to quantitate local glucose utilization (A). An example of a plot in Patlak graphical analysis for HGU (B). For C1-C3, K_i, K_1-k_4 and V_d, see text.

2.3.3.2 14(R,S)-[^{18}F]fluoro-6-thia-heptadecanoic acid ([^{18}F]FTHA)

Free fatty acids derived from meal or from the adipose tissue via lipolysis circulate in blood bound to albumin, and enter the cells either passively (minority) or by facilitation (majority) by fatty-acid transport proteins. PET tracer 14(R,S)-[^{18}F]fluoro-6-thia-heptadecanoic acid ([^{18}F]FTHA) is a palmitate analogue that employs the same transportation and intracellular handling as naïve fatty acids in a competitive fashion. Within the mitochondria, [^{18}F]FTHA participates in the initial steps of β-oxidation, but is thereafter trapped as the sulfur heteroatom blocks the

further metabolic steps (DeGrado et al. 2000). This trapping phenomenon leads to optimal target-to-background ratio necessary for the adequate PET imaging data. Modelling *in vivo* FA uptake is similar to [^{18}F]FDG, and both Patlak graphical analysis and fractional uptake concept can be utilized (Guiducci et al. 2007). However, after tracer injection rapidly-produced label-carrying metabolites of [^{18}F]FTHA do not participate in the normal pharmacokinetics of fatty acids and, if not corrected, would lead to underestimation of FA uptake. In fact, 30 minutes after injection only around 20-30 % of blood radioactivity is due to parent tracer (Labbe et al. 2011). Therefore, metabolite-correction for blood time-activity curve using high-performance liquid chromatography (HPLC) is needed.

[^{18}F]FTHA coupled with PET offers a non-invasive method to investigate tissue-specific FA uptake *in vivo*. Previous study by Guiducci et al. (2007) observed nearly 5.5-fold increase in pancreatic FA accumulation during hyperinsulinemia *versus* fasting state suggesting that insulin-mediated increase in pancreatic FA uptake might function as a feedback inhibitory signal to downregulate insulin production. However, no study have addressed the effects of chronically elevated pancreatic FA uptake, probable in obesity and diabetes, on insulin secretion and β-cell function.

2.3.3.3 [^{15}O]water ([^{15}O]H_2O)

Determination of organ BF can be measured non-invasively using [^{15}O]water ([^{15}O]H_2O) coupled with PET. [^{15}O]H_2O is a chemically inert and freely diffusible tracer and as such an ideal option for estimation of tissue perfusion. The short half-life of ^{15}O (122 seconds) allows for a repeated measurements in dynamic experiments, such as meal testing or *i.v.* glucose loading. While [^{15}O]H_2O-PET has been a standard method for a quantification of myocardial and renal BF in a clinical setting, it has not been utilized to a great extent in the splanchnic region. In pancreas and small intestine, arterial blood is derived solely from the abdominal aorta and thus the kinetics of [^{15}O]H_2O are described with one-tissue compartmental model (Kety & Schmidt 1946). In contrast, liver receives a dual blood supply from portal vein and hepatic artery, and more complex models are needed for reliable flow measurements. Recent study by Kudomi et al. (2008) investigated the feasibility of [^{15}O]H_2O-PET to estimate portal/hepatic arterial BF under a steady state conditions (i.e. at fast) in healthy pigs and found that the PET-derived flow rates were in close agreement with the reference Doppler ultrasonography flow values. The input function for one-tissue compartmental analysis can be obtained from either continuous arterial sampling (blood pump) data, or directly from PET image (Germano et al. 1992); this latter image-derived input function (ID-IF) renders [^{15}O]H_2O methodology as a truly non-invasive technique to study tissue-specific BF.

The combination of one-tissue compartment model and the newly-validated "gut-compartment" model by Kudomi et al. (2008) offers a promising tool for the measurement of flow kinetics across the whole splanchnic region. Particularly, the question of whether [^{15}O]H_2O coupled with PET is able to estimate islet function *per se* has gained considerable interest. As previously discussed (for a detailed review, see 2.2.2.1), pancreatic islets constitute only 1-2 % of the whole pancreatic volume, but consume nearly 20 % (and even more during *i.v.* glucose stimulation) of the organ BF (Jansson 1994). Previous study performed in anesthetized rats applying the microsphere technique suggested that the hyperglycemia-induced increase in islet BF is reflected to as higher flow of the whole pancreas (Iwase et al. 2001). As the resolution of new-generation PET scanners is at best 25-times the size of an average islet (Teräs et al. 2007, Zaidi et al. 2011), direct measurement of islet flow with [^{15}O]H_2O-PET is currently infeasible.

2.3.3.4 [^{15}O]carbon monoxide ([^{15}O]CO)

Change in organ BF is rapidly reflected to as a change in organ blood volume, regarded as a more sensitive indicator of altered vascular milieu than flow *per se*. ^{15}O- or ^{11}C-labelled carbon monoxide coupled with PET acquisition has been a standard imaging modality for cerebral blood volume measurements, but recent studies indicate that it can be applied also in the analysis of hepatic blood volume (Kiss et al. 2009). [^{15}O]CO is usually administered by inhalation, and is assumed to be permanently bound to blood hemoglobin and distributed evenly throughout the body. The need for manual sampling of blood radioactivity multiple times during the scanning complicates [^{15}O]CO-PET study. While it is suggestive that the ID-IF approach from abdominal aorta or other large-bore vessel yields accurate input for blood volume analysis, validation on this respect is lacking.

2.3.4 Nuclear magnetic resonance imaging (NMRI)

Nuclear magnetic resonance imaging (NMRI) is based on the chemical shift of protons (hydrogen atoms in water molecules) in a strong magnetic field and consequent radiofrequency emission as the chemical excitation is normalized when magnetism is discontinued. Therefore, the resulting 3-dimensional image is an approximation of water content within the tissue-of-interest. When combined with functional imaging modality, such as positron emission tomography, NMRI provides an ideal background reference image for accurate analysis especially in the splanchnic region where the combined tomography fails to separate various soft-tissues. However, the NMRI technique can be solely applied to estimate numerous organ parameters *per se*, including the non-invasive estimation of organ fat content. The traditional [^{1}H] MR spectroscopy is regarded as the most sensitive imaging modality to estimate liver fat content (Borra et al. 2009), and it has also

been applied to investigate pancreatic fat content (Hannukainen et al. 2011). Moreover, the feasibility of measuring pancreatic fat content by novel and rapidly-obtainable In – and Out-of-Phase MR spectroscopy method has been recently validated against fat-selective spectral-spatial gradient-echo imaging (Schwenzer et al. 2008). While both of these methods offer promise in the non-invasive estimation of pancreatic fat content, they are not able to differentiate parenchymal fat compartments (intracellular, interlobular, intralobular) and require fairly large (10-millimetres) and homogeneous tissue sections for image analysis. This prerequisite hampers their reliability in pancreatic analysis. In addition, the small size and irregular morphology of pancreas and the surrounding layer of visceral fat may be subject for MR artefacts. Finally, as pancreas is inaccessible in healthy humans, no study has validated [^{1}H] MR spectroscopy or In- and Out-of-Phase method against histological samples.

2.3.5 Computed tomography (CT)

Computed tomography (CT) imaging is regarded as a standard imaging modality to investigate organ structure and (cardiac) BF in clinical practice. Coupled with PET or another functional imaging modality, it offers a rapid reference image for accurate analysis. However, the use of CT as an anatomical reference in the splanchnic region is weakened by the poor capability to differentiate soft-tissues, such as intestine, pancreas or blood vessels from each other. During recent years the ability of CT in the non-invasive estimation of organ fat content has been appreciated. CT-based method offers many of advantages lacking in the MRI-based approach, including small section thickness and short image acquisition time. This simple estimation is based on the decrease in tissue attenuation as a result of fatty infiltration and the values are conventionally normalized to splenic attenuation (presumed to be stable due to high blood content). The validation of the aforementioned methodology against histological samples has been published for both liver (Oliva et al. 2006) and pancreas (Kim et al. 2014). However, the cross-validation between MR spectroscopy and CT-based method in various organs has not been performed.

2.3.6 Duplex ultrasonography

B-type ultrasonography measurements combined with Doppler function can provide information concerning BF velocity in different vascular territories and vessels. The method is based on the use of piezoelectric crystals producing 20-kHz ultrasound penetrating soft-tissues and returning to the transducer from tissue demarcation lines. The ultrasonography measurement is easy to perform by an experienced operator, and the method is relatively inexpensive and do not cause

ionizing radiation for the study subject. Therefore, the Duplex ultrasonography has been growingly assessed to investigate vascular dynamics in the splanchnic region. In healthy humans, however, BF measurements can only be performed from the superior mesenteric artery and celiac artery equating total splanchnic BF (Gentilcore et al. 2009). In contrast, while during experimental studies in large animal models such as pigs, the ultrasonography probes can be inserted to the walls of portal vein and hepatic artery under general anesthesia (Slimani et al.. 2008), this methodology is not feasible in humans. After probe insertion, the Duplex ultrasonography can be applied to study dynamic changes in vessel BF using various stimuli, such as meal testing. The ultrasonography method is hampered by numerous challenges associated with the methodology, including air trapped within the bowel preventing adequate visual signal to be produced, and large inter-observer bias. Moreover, it is not possible to measure organ perfusion and redistribution of BF between multiple organs simultaneously.

2.3.7 Summary

The splanchnic regions has a crucial role in the regulation of intermediary metabolism during absorptive and postabsorptive conditions, and in the pathogenesis of T2D. This region is positioned deep in the abdominal cavity and is characterized by established intrasplanchnic substrate cycles and altering BF milieu dependent on organ metabolism at any given time and physiological condition. Therefore, the direct measurement of the change in substrate concentrations and BF dynamics between peripheral arteries and veins fails to capture the majority of metabolic exchange and flow redistribution unless more sophisticated methods are applied. The aforementioned techniques all have their typical advantages and shortcomings and, ideally, complement each other in the thorough investigation of splanchnic functions. To date, while numerous studies have been implemented to gain knowledge of the splanchnic regulations as a whole, organ-specific data in the splanchnic region is mostly lacking. Positron emission tomography coupled with reference imaging modalities is a non-invasive method to measure both organ glucose and fatty acid metabolism, and BF kinetics organ-specifically *in vivo*. The computerized PET-analysis is easy to perform and provides reliable, repeatable, and quantitate information on the particular dynamic parameter. When combined with empirical and model parameters of insulin sensitivity, β-cell function and plasma concentrations of intermediary metabolites, PET methodology has an outstanding potential in the investigation of splanchnic organ function and BF. However, on the verge of new-generation scanners with high resolution, limitations of PET are inherent to the novelty of this methodology and no proper validation studies for the estimation of pancreatic and intestinal function exist.

3 AIMS OF THE PRESENT STUDY

I. To test the feasibility of PET for the quantification of pancreatic and intestinal metabolism and BF in animal models (studies I, III).

II. To evaluate whether obesity and type 2 diabetes alter the metabolism and BF of the pancreas and, if so, whether these alterations occur parallel to β-cell dysfunction (study I).

III. To assess whether bariatric surgery and concomitant weight loss are able to reverse the detrimental effects of obesity on pancreatic lipid metabolism and BF in line with improved glycemic control in patients with and without T2D (study II).

IV. To quantitate the effects of insulin on intestinal GU in healthy individuals and to test whether intestine is subject to insulin resistance in obese non-diabetic patients (study III).

V. To clarify the role of glucose and incretins, and mixed-meal on the physiological BF redistribution within the splanchnic vasculature in healthy individuals (study IV).

VI. To investigate the early postoperative effects of bariatric surgery on splanchnic redistribution of BF during mixed-meal and GIP-infusion in morbidly obese patients with T2D (study V).

4 SUBJECTS AND STUDY DESIGN

4.1 Animal and subject characteristics

The current study was initiated to investigate splanchnic metabolism and BF in healthy controls (n = 40) and obese patients with (n = 30) and without (n = 32) diabetes a) during postabsorptive state, b) during insulin stimulation, c) after intravenous glucose loading, d) during mixed-meal, and e) during GIP- and GLP-1 –infusions by applying PET methodology. The validation of PET for the non-invasive estimation of splanchnic metabolism was carried out in pig and rodent models. The preclinical part composed of a total of 31 pigs (10 obese and streptozotocin-treated and 21 healthy pigs), and 12 adult mice (nine atherosclerotic and diabetic IGF-II/LDLR$^{-/-}$ApoB$^{100/100}$ and three healthy C57BL/6N mice). The study included data from three projects, namely SLEEVEPASS (ClinicalTrials.gov NCT00793143), SleevePET2 (ClinicalTrials.gov NCT01373892), and GIP-PET (ClinicalTrials.gov NCT01880827).

4.1.1 Animals (I, III)

The preclinical study consisted of a total of 31 Finnish landrace pigs and 12 mice and their details are given in **Table 1**. Ten of the studied pigs were rendered obese and hyperglycemic by administration of high-fat diet (HFD), consisting of either 1.5 % cholesterol + 15 % lard (n = 6), or 4 % cholesterol + 20 % lard + 1.5 % sodium cholate (n = 4) for six months. In addition, 50 mg/kg streptozotocin (Zanosar, Pharmacia & Upjohn, MI, United States) was injected to the ear vein on three consecutive days before the initiation of HFD. Healthy pigs received regular farm chow and water *ad libitum*. Nine of the studied mice represented IGF-II/LDLR$^{-/-}$ApoB$^{100/100}$ strain and were obese and hyperlipidemic when compared with healthy C57BL/6N mice. The animal experiments were performed at age 6-8 and 3-7 months in pigs and mice, respectively. Animal studies were carried out in the afternoons and food was deprived at 5 PM on the day before the study for pigs and for 4 hours prior to experiments for mice.

4.1.2 Humans (I-V)

Morbidly obese patients eligible for bariatric surgery were recruited to the study from endocrinology and gastrointestinal surgery outpatient clinics. Healthy controls were recruited from an occupational health service clinic and by internet

Table 1. Animal characteristics.

Study	Species	Group	n	Weight (kg or g)	FPG (mM)	FFA (mM)
I, III	Pig	CN	8	82 ± 9.7	6.0 ± 2.2	0.6 ± 0.3
		OB	10	126 ± 7.6[a]	12 ± 5.0[a]	1.0 ± 0.5
I	Mice	CN	3	22 ± 0.6	10 ± 2.5	1.3 ± 0.4
		OB	9	28 ± 5.1	10 ± 3.7	2.1 ± 0.8
III	Pigs	Fasting	6	30 ± 0.6	3.7 ± 4.0	0.5 ± 0.1
		Insulinemia	4	30 ± 0.5	5.0 ± 0.1[a]	0.1 ± 0.0[a]

Data are shown as mean ± SD. CN, healthy controls; OB, obese and diabetic animals; FPG, fasting plasma glucose; FFA, serum free fatty acids. Weight shown as kilograms for pigs and as grams for mice, respectively. Main comparison within the study: [a]$P < 0.05$ between groups.

Table 2. Human characteristics.

Study	Group	n	M/F	Age (y)	Weight (kg)	BMI (kg m^{-2})	MetS (n/%)
I	CN	25	2/23	46 ± 10	64.8 ± 7.7	23.0 ± 2.5	0/0
	T2D	20	3/17	49 ± 7.1	114 ± 12.3[a]	41.2 ± 4.2[a]	18/90
	ND	32	1/31	41 ± 10[b]	120 ± 14.4[a]	42.9 ± 3.6[a]	12/38
II	CN	15	0/15	45 ± 12	58.0 ± 7.1	22.6 ± 2.8	0/0
	T2D	10	0/10	41 ± 11	107 ± 11.0[a]	40.4 ± 4.6[a]	10/100
	ND	13	0/13	45 ± 7.1	116 ± 17.4[a]	41.7 ± 4.0[a]	7/54
III	CN	8	2/6	46 ± 5.8	70.3 ± 7.1	24.0 ± 1.8	0/0
	ND	8	0/8	41 ± 8.1	118 ± 12.8[a]	43.9 ± 4.1[a]	5/63
IV, V	CN	15	7/8	43 ± 9.4	69.7 ± 13.7	23.7 ± 2.4	1/7
	T2D	10	2/8	52 ± 7.0[a]	115 ± 18.9[a]	40.8 ± 5.9[a]	10/100

Data are shown as mean ± SD. CN, healthy controls; T2D, patients with type 2 diabetes; ND, obese patients without type 2 diabetes; n, number of subjects; M, male; F, female; BMI, body-mass index. Metabolic syndrome (MetS) was defined according to IDF Clinical Practice Guidelines. Main comparisons within the study: [a]$P < 0.05$ obese *versus* controls, [b]$P < 0.05$ T2D *versus* ND.

and newspaper announcements at University of Turku and Turku University Hospital. Clinical screening was performed for all subjects. The inclusion criteria for the patient population were identical to the current eligible criteria for bariatric surgery, i.e.age 18-60 years, body-mass index greater than 40 kg m^{-2} or greater than 35 kg m^{-2} and additional risk factor (diabetes, hypertension, dyslipidemia, obstructive sleep apnea), and failure of the past conservative treatment. Patients

with body-mass index greater than 60 kg m^{-2}, weight more than 170 kg, waist circumference greater than 150 cm, mental or eating disorder, excessive use of alcohol, active peptic ulcer or insulin dependence (in patients with diabetes) were excluded. The inclusion criteria for the healthy control population were age 18-60 years, body-mass index 18-27 kg m^{-2}, fasting and 2-hour plasma glucose less than 6.1 and 7.8 mM, respectively. Healthy controls with hypertension (blood pressure more than 140/90 mmHg or treatment) or any chronic disease, mental or eating disorder, pregnancy, or poor compliance were ultimately excluded. The experiments were performed after an overnight fast (12 hours), caffeine and nicotine were prohibited for 24 hours before the studies, alcohol consumption and fatty meals were prohibited for 72 hours before the studies, and recommendation to avoid strenuous exercise for 48 hours before the studies was given. Moreover, a washout period (24 hours for antihypertensives, 72 hours for anti-diabetic drugs excluding long-acting GLP-1 RAs, 10 weeks for long-acting GLP-1 RAs) was designated to terminate the effects of medication during the experiments. The anthropometric, biochemical and metabolic characteristics at baseline (i.e. before surgery for obese patients) are given in **Table 2** and **Table 3**.

In all of the studies control subjects were similar in terms of demographics, biochemical and metabolic profiles. None were taking any medication at the time of the study, and were classified as healthy based on medical history, physical examination, and laboratory assays. Age-matched obese patients in study I (n = 52) were gathered from two larger data sets, namely SLEEVEPASS and SleevePET2, describing a typical representation of patients undergoing bariatric surgery. In these two data collections, total number of patients with diagnosed T2D was 20 (38 % of the obese pool), and no diabetic complications. All of these patients received anti-diabetic medication (metformin n = 18, DPP-IV inhibitor n = 7, thiazolidinedione n = 2, sulphonylurea n = 1). 26 and 14 patients were taking antihypertensive and lipid-lowering medication, respectively. When compared with healthy controls, obese group was severely insulin resistant as depicted by $HOMA_{IR}$ and 2h OGIS indices and this reflected to as higher fasting serum insulin levels. In patients with T2D, measures of β-cell function were significantly lower when compared with both healthy control group and non-diabetic obese group.

Study II included part of the healthy controls (n = 15) and obese patients (n = 23) from study I, with 10 (43 %) having T2D and 13 with NGT or IGT (classified as non-diabetic obese group, respectively). Their anthropometrics, biochemical and metabolic profile were similar to as the larger groups in study I. Study III was a substudy of SLEEVEPASS trial, and included healthy controls (n = 8) and obese

Table 3. Baseline biochemical and anthropometric characteristics of the study groups.

Study	Group	n	FPG mM	FSI mU L^{-1}	HbA1c mmol mol^{-1}	FFA mM	$HOMA_{IR}$ fraction	2h OGIS mL min^{-1} m^{-2}	β-GS pmol min^{-1} m^{-2} mM^{-1}
I	CN	25	5.4 ± 0.5	5.8 ± 3.6	38 ± 3.0	0.5 ± 0.2	1.4 ± 0.9	427 ± 58.0	123 ± 43.8
	T2D	20	7.2 ± 1.4[a,b]	20 ± 14[a]	47 ± 7.5[a,b]	0.7 ± 0.2[a]	7.0 ± 7.4[a,b]	305 ± 41.1[a,b]	52.2 ± 34.4[a,b]
	ND	32	5.7 ± 0.5[a]	14 ± 9.2[a]	38 ± 3.7	0.7 ± 0.2[a]	3.5 ± 2.3[a]	341 ± 44.0[a]	133 ± 93.3
II	CN	15	5.3 ± 0.6	5.2 ± 3.5	38 ± 3.4	0.6 ± 0.2	1.3 ± 0.9	435 ± 68.5	139 ± 48.1
	T2D	10	7.0 ± 0.9[a,b]	18 ± 9.4[a,b]	46 ± 7.3[a,b]	0.8 ± 0.2[a]	5.7 ± 3.3[a,b]	315 ± 39.1[a,b]	52.4 ± 23.1[a,b]
	ND	13	5.5 ± 0.4	9.3 ± 5.4[a]	38 ± 4.6	0.8 ± 0.2[a]	2.3 ± 1.4[a]	368 ± 36.5[a]	136 ± 87.4
III	CN	8	5.6 ± 0.3	6.3 ± 2.9	38 ± 2.2	0.5 ± 0.2	1.6 ± 0.8	406 ± 33.0	95.2 ± 20.5
	ND	8	5.6 ± 0.3	16 ± 11[a]	37 ± 3.8	0.6 ± 0.2	3.9 ± 2.7[a]	328 ± 56.7[a]	176 ± 145
IV, V	CN	15	5.1 ± 0.4	4.6 ± 2.1	32 ± 3.7	0.7 ± 0.2	1.1 ± 0.5	450 ± 44.5	88.8 ± 33.8
	T2D	10	6.5 ± 1.1[a]	19 ± 9.3[a]	40 ± 4.0[a]	0.8 ± 0.2	5.9 ± 3.4[a]	313 ± 62.9[a]	55.6 ± 36.3[a]

Data are shown as mean ± SD. CN, healthy controls; T2D, patients with type 2 diabetes; ND, obese patients without type 2 diabetes; n, number of subjects; FPG, fasting plasma glucose; FSI, fasting serum insulin; HbA1c, glycated hemoglobin, FFA, serum free fatty acids; $HOMA_{IR}$, homeostatic model assessment for insulin resistance; 2h OGIS, oral glucose sensitivity index; β-GS, glucose sensitivity. Main comparisons within the study: [a]$P < 0.05$ obese *versus* controls, [b]$P < 0.05$ T2D *versus* ND.

patients (n = 8) from study I. The obese patients selected for study III were chosen to represent typical non-diabetic patients undergoing bariatric procedures. While the glycemic parameters and measures of β-cell function in these patients were similar to the ones in healthy controls, their systemic insulin sensitivity was significantly decreased and this reflected to as 2.5-fold increases in fasting serum insulin levels. Studies IV and V consisted of a 15 healthy controls, and 10 obese patients with T2D

undergoing bariatric surgery. Of the obese patients nine were receiving anti-diabetic medication (metformin n = 8, DPP IV inhibitor n = 3, long-acting GLP-1 RA n = 1), and one was on a diet treatment. Eight and five patients were taking antihypertensive and lipid-lowering medication, respectively. The control subjects in studies IV and V were assigned to two separate study arms, denoted as control group A (imaging studies during mixed-meal, GIP-infusion, and GLP-1 –infusion) and control group B (imaging studies during 75-gram oral and 0.3-gram kg $^{-1}$ intravenous glucose loading) (for a detailed review, see 4.3.3). When compared with healthy controls, the obese patients had severe insulin resistance and this reflected to as fasting hyperinsulinemia. Moreover, their measures of β-cell function were impaired, and hyperglycemia as perceived by fasting plasma glucose and glycated hemoglobin was evident.

4.2 Preclinical study designs

All of the experiments were performed at postabsorptive state. For 18 pigs in the "PET-validation" –protocol, anesthesia was induced with an i.m. midazolam 1.0 mg/kg (Midazolam Hameln 5 mg mL^{-1}, Hameln Pharmaceuticals GmbH, Hamelm, Germany) and xylazine 4 mg/kg (Rompun vet 20 mg mL^{-1}, Bayer Animal Health GmbH, Leverkusen, Germany) and maintained with a continuous infusion of propofol 10-50 mg kg^{-1} h^{-1} (Propofol Lipuro 20mg mL^{-1}, B. Braun Melsungen AG, Melsungen, Germany). For 13 pigs in the "lumped constant" –protocol, anesthesia was induced and maintained with ketamine 1.5 g and pancuronium 40 mg, respectively. Catheters were placed in the carotid artery and femoral vein for blood sampling (both protocols) and administration of [^{18}F]FDG (both protocols), [^{2}H]G ("lumped constant" –protocol), glucose ("lumped constant" –protocol), and insulin ("lumped constant" –protocol), respectively. For 10 pigs in the "lumped constant" –protocol, abdominal cavity was accessed with a subcostal incision and catheter was sutured into the portal vein (Iozzo et al. 2007). Pigs were intubated, connected to the respirator and ventilated with 40 % oxygen at the frequency of 16 breaths per minute. In mice, anesthesia was induced (3 %) and maintained (1.8 %) with isoflurane (Attane vet 1000 mg g^{-1}, Piramal Healthcare UK Limited, Northumberland, UK), and catheter was placed in the tail vein for blood sampling and [^{18}F]FTHA administration. Before the PET acquisition in pig data, a transmission scan was performed to measure photon attenuation.

4.2.1 Validation of the splanchnic functions *in vivo* using [^{18}F]FDG-PET (I, III)

4.2.1.1 PET-validation

The feasibility of PET in the non-invasive quantification of pancreatic and intestinal GU was addressed in eight healthy pigs and in 10 obese and streptozotocin-treated diabetic pigs during fasting state. After the induction of anesthesia and catheter placement, pigs were positioned on the scanner and an intravenous bolus of [^{18}F]FDG (890 ± 180 MBq) was administered. 40 minutes after the injection, a set of two dynamic 20-minute (frames 4 × 300 seconds) PET acquisitions of the upper and lower abdomen was obtained (**Fig. 11A**). During the scanning, blood was continuously drained to measure plasma glucose and ^{18}F-radioactivity. At 240 minutes post-injection, the pigs were sacrified with an intravenous bolus of potassium chloride, abdominal cavity was accessed and tissue samples from pancreas (head, body and tail regions) and intestine (duodenum, ileum, colon) were excised for *ex vivo* radioactivity measurement (for a detailed review, see 5.2) and autoradiography analysis. The validation was performed by a comparison between *in vivo* (PET) and *ex vivo* (tissue samples) –derived uptake rates.

4.2.1.2 Lumped constant (LC)

Splanchnic fractional extractions and lumped constant during fasting *vs.* insulin-stimulation was investigated in a total of 13 healthy pigs. After the induction anesthesia and catherer placement, n = 3, n = 4 and n = 6 pigs received either insulin (supraphysiological and physiological dose) or saline though the venous cannula for 240 minutes, respectively. In the hyperinsulinemic clamp study, a prime-continuous insulin infusion (either 5.0 or 1.0 mU kg^{-1} min^{-1}) was initiated and euglycemia was maintained by a variable 10 % glucose infusion accordingly. At 60 minutes from the start of the saline/insulin infusions, boluses of [^{18}F]FDG (247 ± 7.0 MBq) and [^{2}H]G (451 ± 9 and 1043 ± 26 µmol for fasting and clamp studies, respectively) were coinjected and 180-minute (31 frames) dynamic PET-acquisition of the abdomen was initiated (**Fig. 11B**). Arterial and portal blood was sampled at every time frame to measure ^{18}F-radioactivity and [^{2}H]G tracer-to-tracee ratios. The latter were multiplied by plasma glucose at steady state to obtain absolute [^{2}H]G concentrations. After the PET-acquisition, animals were sacrificed by an injection of potassium chloride.

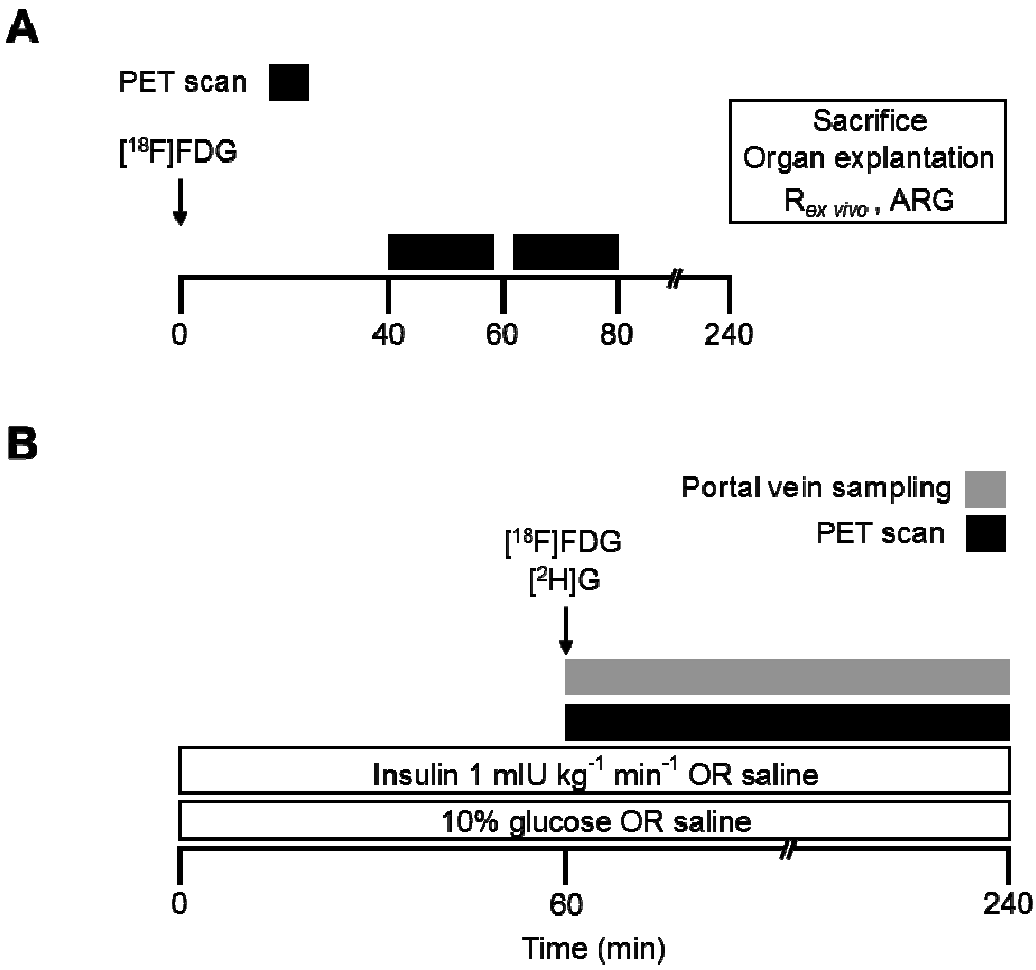

Figure 11. Animal experimentation in studies I (A) and III (A, B). Upper panel (A) denotes the "PET-validation" –protocol performed in 18 pigs, and lower panel (B) denotes "lumped constant" –protocol performed in 10 pigs (n = 6 during fasting state, n = 4 during insulin stimulation), respectively. $R_{ex\ vivo}$, tissue sample radioactivity; ARG, autoradiography analysis.

4.2.2 Pancreatic biodistribution of [^{18}F]FTHA in healthy and obese rodents (I)

To investigate the distribution of fatty acids within the pancreatic parenchyma (i.e. exocrine *vs.* endocrine), 15 MBq bolus of [^{18}F]FTHA was injected to three healthy and nine obese, diabetic and hyperlipidemic mice at postabsorptive state. 30 minutes post-injection, animal were sacrificed by neck dislocation, abdominal cavity was accessed and pancreas was excised for autoradiography analysis to

quantitate of the distribution of [^{18}F]FTHA between endocrine and exocrine parenchyma. This study did not involve molecular imaging assessment.

4.3 Clinical study designs

All imaging studies were performed after an overnight fast, in most cases in the morning. Peripheral catheters were placed on both antecubital veins, one for radiotracer (studies I-V), saline (studies I-V), insulin (studies I, III), glucose (studies I, III, IV), and/or incretin (studies IV, V) administration, and one for sampling of arterialized venous blood (studies I-V) throughout the scan. Studies were performed in the supine position, with the abdominal region placed within the scanner gantry. Euglycemic hyperinsulinemic clamp (studies I, III) was performed as previously described (DeFronzo et al. 1979). [^{15}O]carbon monoxide (studies IV, V) was administered by inhalation, and the face mask was removed after 2-minute inhalation period, as previously described (Kiss et al. 2009). For the obese patients before the bariatric surgery, the imaging studies were performed prior to the start of the 4-week very-low calorie diet (VLCD). Bariatric procedures (either Roux-en-Y gastric bypass or sleeve gastrectomy) were done laparoscopically as previously described (Helmiö et al. 2012), and no major complications including reoperation, more than 7 days of ward-stay, or more than 4 units of blood transfusion were observed. PET acquisitions were anteceded by a transmission scan to measure and correct for the photon attenuation.

4.3.1 Splanchnic glucose metabolism in healthy controls and obese patients (I, III)

Pancreatic and intestinal GU in postabsorptive state and during insulin clamp were measured in 25 obese patients (nine with T2D) eligible for bariatric surgery and 10 age-matched healthy controls on two separate days (**Fig. 12**). The study was cross-sectional, case-control study, and was performed using [^{18}F]FDG-PET. The anatomical reference image was obtained using separate MRI scanning. During clamp days, insulin (Actrapid®, Novo Nordisk, Bagsværd, Denmark) was infused at a steady rate of 1 mU kg^{-1} min^{-1}, and euglycemia (plasma glucose 5.0 ± 0.5 mM) was maintained by 10 % glucose infusion. After 90 minutes from the start of the clamp (i.e. when steady state condition is reached), or at fast on a separate day, a bolus of [^{18}F]FDG (187 ± 8.0 MBq) was injected to the peripheral vein. Seventy minutes after the injection, a 15-minute (frames 5 × 180 seconds) dynamic scanning of the abdomen was initiated. Arterialized venous blood was sampled throughout the experiments to measure plasma radioactivity, glucose, insulin, and FFA concentration. Plasma ^{18}F-radioactivity curve was used as an input function for the calculations (for a detailed review, see 5.3.1).

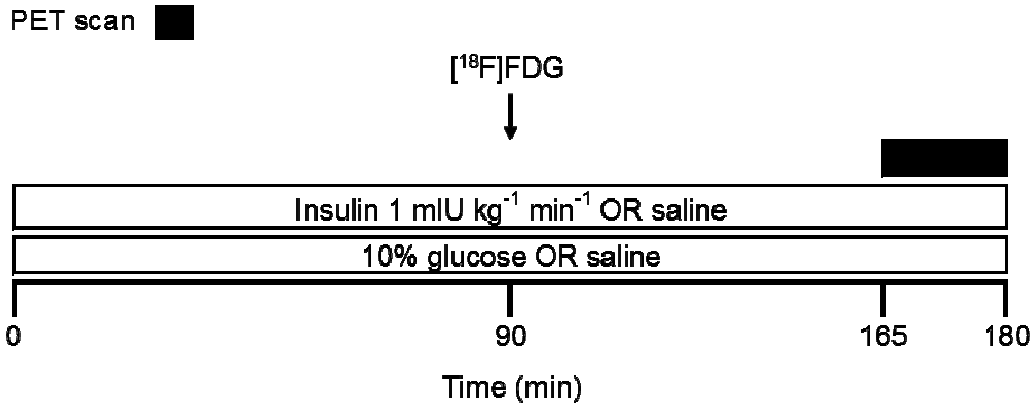

Figure 12. Experiments in studies I and III were done in two separate days, i.e. at postabsorptive state (saline infusion) and during insulin clamp. Time interval between the experiments for individual subjects ranged between 1 and 57 days. White boxes denote insulin, glucose or saline infusion, and black box denotes PET acquisition of abdominal region.

4.3.2 Pancreatic lipid metabolism and blood flow in healthy controls and obese patients, and the effects of bariatric surgery on pancreatic functions and on diabetes remission (I, II)

Pancreatic uptake of long-chain fatty acids and BF during postabsorptive state were measured in 27 obese patients (11 with T2D) before and 6 months after bariatric surgery, and in 15 age-matched healthy controls (**Fig. 13**). The design was cross-sectional, case-control study for the whole study population, and longitudinal in a total of 23 obese patients. The experiments were performed once for the healthy controls. For the obese patients, the experiments were repeated six months after bariatric surgery to observe the effects of surgery and concomitant weight loss on the pancreatic variables.

After an overnight fast, a CT-scan of the abdominal region was obtained for an anatomical reference image. An intravenous bolus (554 ± 124 MBq) of [^{15}O]H_2O was injected, and a 5-minute (26 frames) dynamic PET acquisition of the abdomen was initiated. This was followed by an [^{18}F]FTHA injection (185 ± 46 MBq). Seventy minutes after the injection, 15-minute (frames 5 × 180 seconds) PET acquisition was obtained (**Fig. 14**). Arterialized venous blood was sampled throughout the experiments to measure plasma radioactivity, glucose, insulin, and FFA concentration. For FA uptake and radiowater analyses, metabolite-corrected plasma ^{18}F-radioactivity curve and uncorrected ID-IF from abdominal aorta (for a detailed review, see 5.3.1), respectively, were used as previously described.

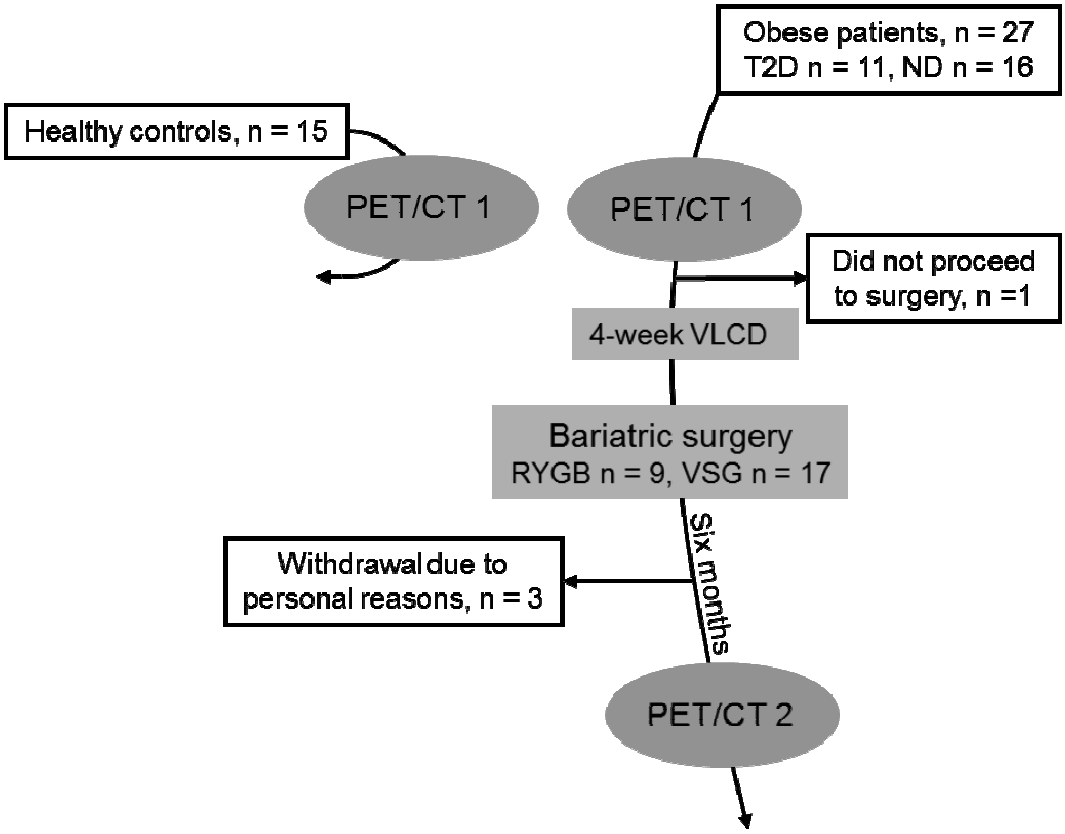

Figure 13. Flow chart for studies I and II. The experiments were performed once for the healthy controls, and twice (before and six months after bariatric surgery) for obese patients. T2D, patients with type 2 diabetes; ND, non-diabetic obese patients; VLCD, very-low calorie diet; RYGB, Roux-en-Y gastric bypass; VSG, vertical sleeve gastrectomy.

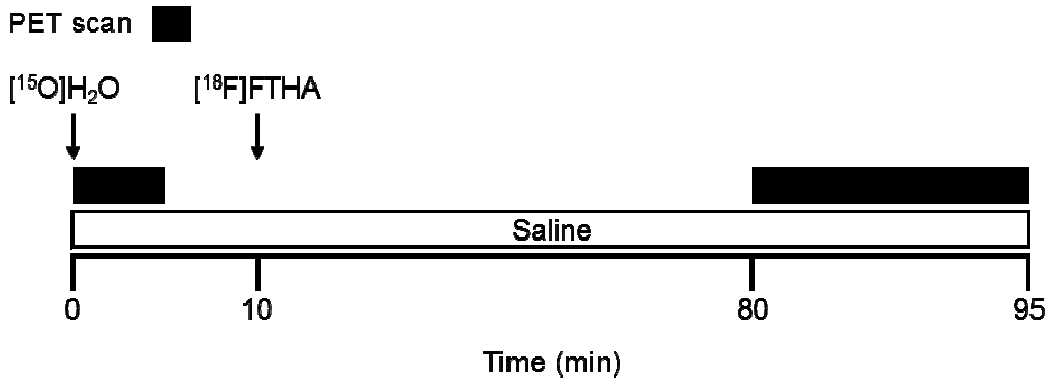

Figure 14. Experiments in studies I and II were performed at postabsoprtive state. Healthy controls were studied once, and obese patients twice, i.e. before and six months after bariatric surgery. White box denotes saline infusion, and black boxes denotes PET acquisition of the abdominal region.

4.3.3 Splanchnic vascular responses to mixed-meal, oral/intravenous glucose loading, incretin administration, and bariatric surgery in healthy controls and obese patients (IV, V)

Splanchnic (pancreatic, intestinal, hepatic) vascular responses to meal and glucose ingestion, *i.v.* glucose loading, and incretin administration were studied in a total of 10 obese patients with T2D eligible for bariatric surgery and 15 healthy controls (**Fig. 15**). The aim of the study was to determine 1) the physiology of BF and volume redistribution within the splanchnic region and 2) between splanchnic *versus* peripheral (i.e. extrasplanchnic) tissues 3) between normoglycemic and hyperglycemic subjects in response to various vasoactive stimuli by using the [^{15}O]H_2O-PET/MRI methodology. Moreover, in obese patients the experiments were repeated after bariatric surgery to gain insight to the GI factors (upregulation of GLP-1 secretion, downregulation of GIP secretion, changes in receptor affinity) responsible for vascular regulation. In these patients, the experiments were repeated early (6-8 weeks) after bariatric surgery to minimize the effects of sole weight loss over GI factors.

Subjects in control group A (n = 10, M/F = 2/8) underwent three separate experiments. First, abdominal MRI and baseline [^{15}O]H_2O-PET and [^{15}O]CO-PET acquisitions were obtained. This was followed by either 1) ingestion of a mixed meal of 300 kcal and containing 37 g carbohydrates, 11.6 g fat, and 12 g protein (Nutridrink, Nutricia Advanced Medical Nutrition, Amsterdam, Netherlands) over the course of 10 minutes, 2) 80-minute infusion of human GIP acetate (Bachem Holding AG, Bubendorf, Switzerland) at the rate of 4 pmol kg^{-1} min^{-1} for 15 minutes, and thereafter at the rate of 2 pmol kg^{-1} min^{-1}, respectively, and 3) 80-minute infusion of human GLP-1 (7-36) amide acetate (Bachem Holding AG, Bubendorf, Switzerland) at the rate of 0.75 pmol kg^{-1} min^{-1} throughout the experiment. Two consecutive image acquisitions were obtained at 20 and 50, and at 40 and 70 minutes (for [^{15}O]H_2O and [^{15}O]CO, respectively) from the start of the ingestion or infusion.

In addition, control group B (n = 5, M/F = 5/0) was established to further investigate the splanchnic vascular effects of *p.o.* and *i.v.* glucose. Herein, subjects ingested oral glucose (75-gram) solution over the course of two minutes or were administered with 0.3 g kg^{-1} *i.v.* glucose (50 % glucose, B. Braun Melsungen AG, Melsungen, Germany) over the course of two minutes. Before the ingestion/administration, abdominal MRI was obtained for an anatomical reference image and 5-minute (26 frames) baseline [^{15}O]H_2O-PET acquisition was performed. The ingestion/administration was followed by three consecutive [^{15}O]H_2O-PET acquisitions (time points 10, 20 and 40 minutes post-ingestion and 3, 15, and 25 minutes post-administration for oral and *i.v.* glucose loading, respectively) from the abdominal region. The activity of injected [^{15}O]H_2O-PET

and inhaled [^{15}O]CO-PET were 495 ± 54 and 743 ± 86 mBq, respectively. Arterialized venous blood was sampled throughout the experiments to measure plasma glucose, insulin, C-peptide, GIP, GLP-1 and FFA concentration. Background saline infusion was constant throughout the experiments. Uncorrected ID-IF from abdominal aorta was used for both [^{15}O]H_2O- and [^{15}O]CO-PET analyses, but arterialized venous blood after [^{15}O]CO inhalation was gathered in six subjects (controls and obese) for validation purposes. The experimental protocols are shown in **Fig. 16**.

Obese diabetic patients underwent a total of four experiments during the study, two before and two 6-8 weeks after bariatric surgery. The experimental design was similar to that in healthy control group B; however, due to radiation dosage the obese patients participated only in mixed-meal and GIP infusion experiments. No adverse effects were observed in response to meal ingestion or incretin administration.

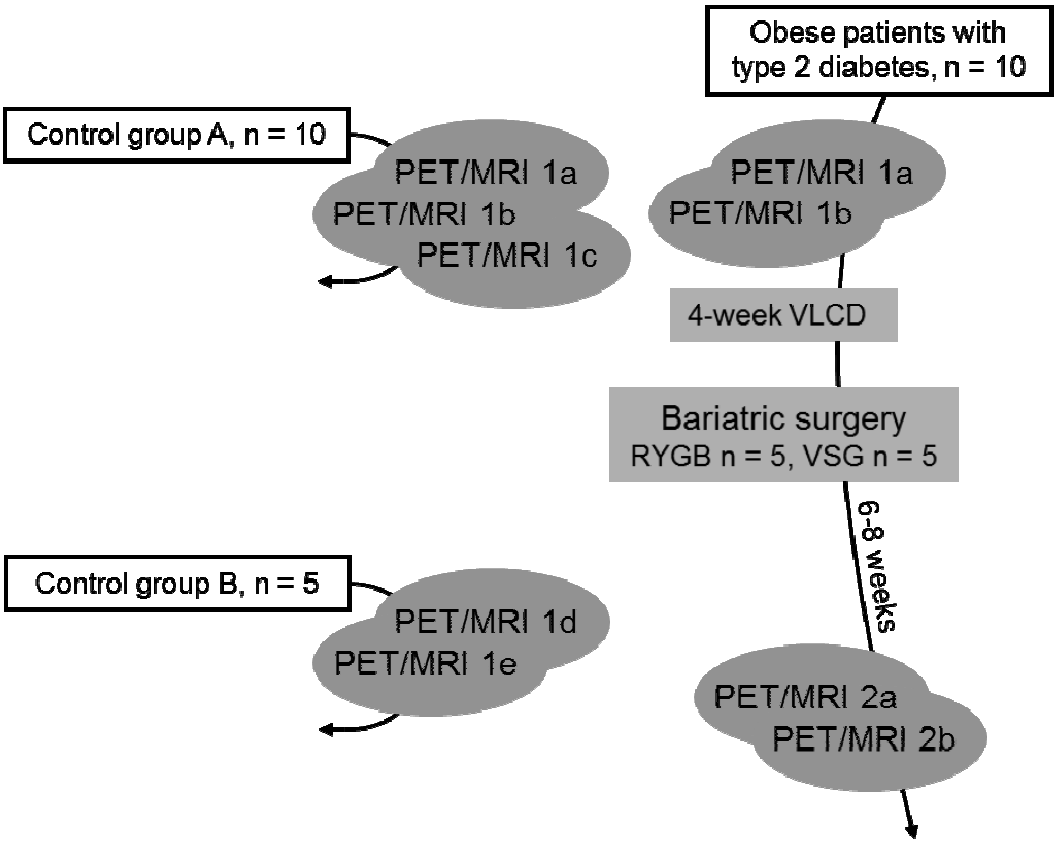

Figure 15. Flow chart in studies IV and V. Healthy controls were allocated to two experimental groups (A and B). The obese patients with T2D underwent identical experiments as control group B. RYGB, Roux-en-Y gastric bypass; VSG, vertical sleeve gastrectomy; PET/MRI a, mixed-meal; PET/MRI b, GIP infusion; PET/MRI c, GLP-1 infusion; PET/MRI d, oral glucose loading; PET/MRI e, *i.v.* glucose loading.

4.4 Ethical considerations

In regards to the preclinical studies, the principles of laboratory animal care were followed and permission for the study protocols were obtained from the State Provincial Office for Southern Finland. Prior to clinical enrollment, medical history was carefully assessed and physical examination with routine laboratory measurements was done by study physician. All subjects gave their written informed consent after the nature, purpose, and potential risks of the study were explained. After completion of the studies, a summary of the laboratory measurements and imaging findings were sent to participants. The Ethical Committee of the Hospital District of South-Western Finland approved the study protocols.

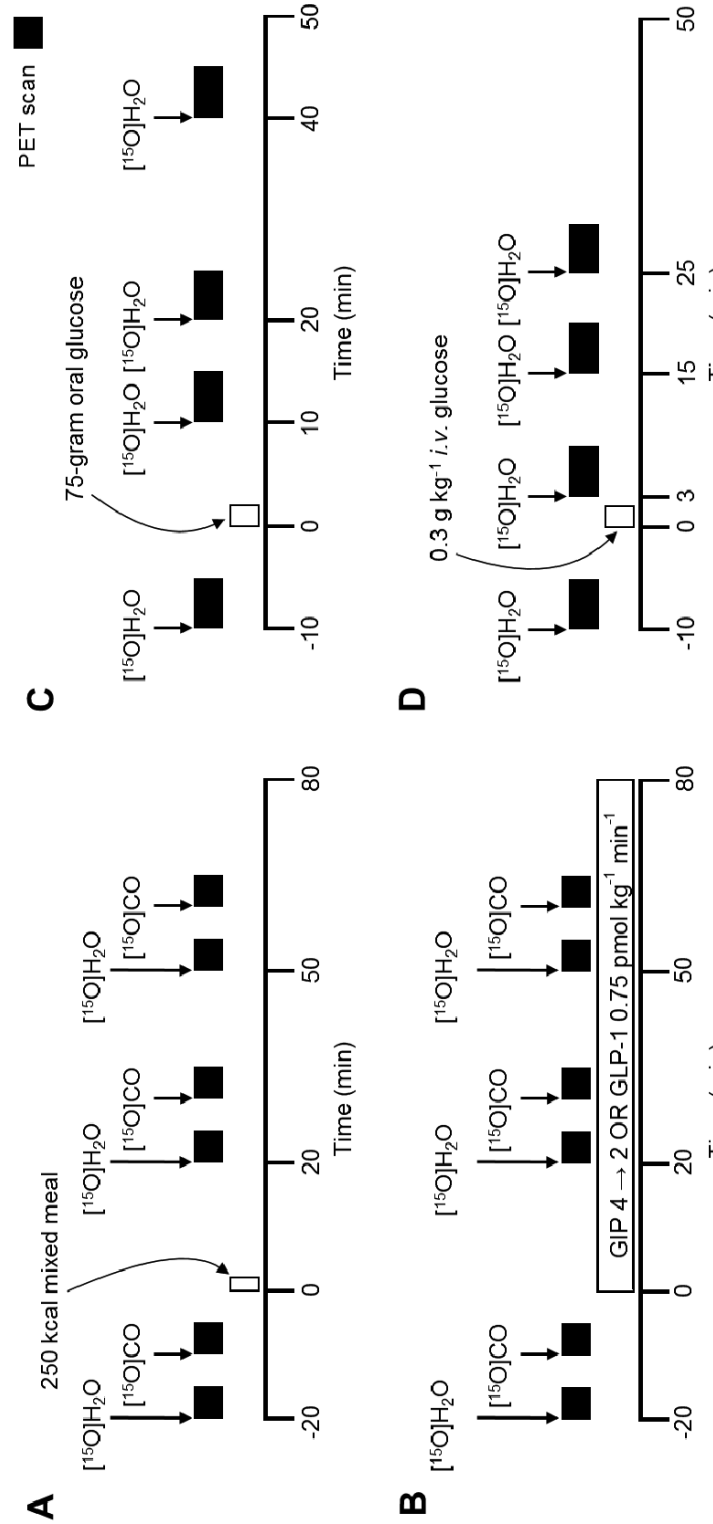

Figure 16. The experimental protocols in studies IV and V. White boxes denote incretin infusion, *p.o.* or *i.v.* glucose administration or meal ingestion, black boxes denote PET acquisition of the abdominal region. Radiotracer administration followed identical scheme during mixed-meal (A) and incretin infusion studies (B), whereas in *p.o.* (C) and *i.v.* (D) glucose administration studies radiotracer administration was designed to detect maximal glucose effect on splanchnic flow redistribution.

5 METHODS

5.1 Tracer production (I-V)

[^{18}F]FDG was synthesized with an automatic apparatus by a modified Hamacher method (Hamacher et al. 1986). [^{18}F]FTHA was synthesized by labelling 14(R,S)tosyloxy-6-thia-heptadecanoic acid with [^{18}F]fluoride and with HPLC, as described elsewhere (Takala et al. 2002). [^{15}O]H_2O and [^{15}O]CO were produced using the low-energy deuteron accelerator Cyclone 3 (IBA International, Louvain-La-Neuve, Belgium) and the diffusion-membrane technique. The radiochemical purity the tracers exceeded 92 % in all studies.

5.2 *Ex vivo* radioactivity (I, III)

After animal sacrifice and organ explantation, pancreatic and intestinal (duodenum and ileum) [^{18}F]FDG-6P radioactivity was measured with an automated γ-counter (Wizard 1480 3", Perkin-Elmer-Wallac, Turku, Finland), corrected for decay and normalized to the weight of the tissue specimen. *Ex vivo* influx rate constant was calculated as

$$\textit{Ex vivo}\ K_i = C_t(t) \times (\int_0^T C_p(t)dt)^{-1},$$

where $C_t(t)$ and the integral of $C_p(t)$ represent the measured tissue radioactivity and the area under the curve (AUC) of arterial plasma radioactivity from injection (0) to sacrifice (T), respectively (Haaparanta et al. 2003). *Ex vivo* K_i values were used as a golden standard against *in vivo* (PET) –derived values in the preclinical studies.

5.3 PET image acquisition and processing (I-V)

PET acquisitions were performed using the hybrid PET/CT scanners Discovery 690 and Discovery VCT (General Electric Medical Systems, Milwaukee, WI, USA) in studies I and II, PET scanner Advance (General Electric Medical Systems, Milwaukee, WI, USA) in studies I and III, and the hybrid PET/MRI scanner Philips Ingenuity (Philips Medical Systems, Nederland B.V., The Netherlands) in studies IV and V. The axial field of view (FOV) was 15.7, 15.2 and 15.7 cm for Discovery VCT, Advance and Ingenuity, respectively. The spatial resolutions (radial×tangential) of the scanners were as follows: 5.9×5.5 mm for Discovery VCT, 5.6×4.8 mm for Advance and 5.1×5.1 mm for Ingenuity full-width at half maximum (FWHM). After positioning the subject to the scanner gantry, a transmission scan was performed to measure photon tissue attenuation. After tracer

administration, a dynamic ([^{18}F]FDG, [^{18}F]FTHA and [^{15}O]H_2O) or static ([^{15}O]CO) PET acquisitions of the abdominal region were carried out. All sinograms were corrected for dead time, decay, and measured photon attenuation, and reconstructed in a 256×256 matrix. During [^{18}F]FDG and [^{18}F]FTHA scans, arterialized venous blood was frequently sampled to measure plasma radioactivity, and during [^{18}F]FTHA scans for label-carrying metabolites (Labbe et al. 2011).

5.3.1 Regions-of-interest (ROIs) and input functions (I-V)

To obtain time-activity curves (TACs) (dynamic acquisitions in studies I-V) and static organ data ([^{15}O]CO images in studies IV and V), 3-dimensional regions-of-interest were manually placed on pancreatic, intestinal and hepatic parenchyma using Carimas 2 software (freely downloadable at http://www.turkupetcentre.fi/carimas). Large free-hand ROIs were drawn in ten to 15 consecutive planes from tail to head region of pancreas carefully avoiding nearby organs and especially the splenic vein passing through the posterior margin of pancreas. Hollow tube-shaped ROI (**Fig. 17A**) was placed in the vertical regions of duodenum, jejunum, ileum and colon, and adjusted with vertex-function to approximate margins of gut wall. Horizontal regions of intestine were excluded from the analysis to minimize spill-over caused by diaphragmatic motion. For the hepatic BF analysis (for a detailed review, see 5.4.3), large ROI was placed in the right and left lobe of the hepatic parenchyma. The resulting TACs represent average organ radioactivity per volume of tissue as a function of time. Intestinal TAC was corrected for a delay between arterial and tissue radioactivity, whereas delay correction for pancreatic and hepatic TACs were not considered necessary.

For [^{18}F]FDG and [^{18}F]FTHA analyses, the input function was derived from arterialized blood radioactivity samples obtained frequently during the scanning. For ^{15}O-labelled tracers, the input function was derived directly from image (ID-IF), as described by Germano et al. (1992). In studies I, II, IV and V, ID-IF was extracted from the abdominal aorta, with ROIs placed four to ten image planes to obtain an estimate of laminar flow aortic TAC. The methodology is based on the following assumptions: 1) the aortic section must be circular i.e. perpendicular to the imaging axis, 2) zero spill-over from adjacent structures to aorta, 3) small ROIs (2-3mm) or less than 1/5 of aortic diameter centered on the pixel of maximum activity, 4) aorta must not move during the scanning. An example of such aortic ROI (single plane) is shown in **Fig. 17B**. For the hepatic BF measurements, a dual input function (DIF) was extracted, as described by Kudomi et al. (2008).

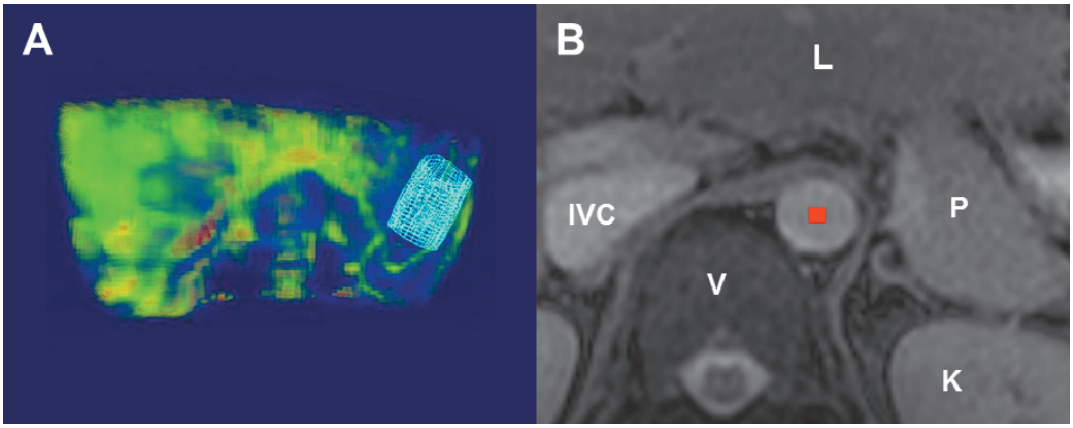

Figure 17. Hollow tube-shaped ROI placed on the descending colon in healthy control pig (part of study III) in [^{18}F]FDG-PET image (A). For [^{15}O]H_2O and [^{15}O]CO analyses, the input function was extracted directly from image by centering small ROIs (shown here in red) in an area of maximum activity in the abdominal aorta (B). Vertebral body (V), left kidney (K), pancreas (P), liver (L) and inferior vena cava (IVC) are positioned adjacent to the aorta.

5.4 PET data modelling (I-V)

5.4.1 Patlak graphical analysis and fractional uptake rate (I-III)

In the present work, models to quantitate tissue GU are based on the irreversible uptake of radiotracer [^{18}F]FDG from plasma to tissue unphosphorylated compartment to tissue phosphorylated compartment. As [^{18}F]FDG-6P is not a substrate for tissue Glc6Pase, the dephosphorylation rate constant k_4 is assumed to be 0 (**Fig. 10A**). In the Patlak graphical analysis, the graph is generated by plotting

$$C_t(t) \times C_p(t)^{-1} \textit{ vs. } \int_0^T C_p(t) \times C_p(t)^{-1},$$

where C_t and C_p represent measured tissue and plasma radioactivity at any given time point. When the tracer concentration in plasma (C1) and reversible tissue compartment (C2) reach equilibrium, the plot becomes linear (**Fig. 10B**). The slope of the linear phase of the plot is the net influx rate constant (K_i) of [^{18}F]FDG and represents a balanced combination of the constants utilized in the traditional three-compartmental model (Sokoloff et al. 1977) as follows

$$K_i = (K_1 \times k_3) \times (k_2 + k_3)^{-1}.$$

The approximation of Patlak graphical analysis, originally presented by Ishizu et al. (1994), lacks the apparent distribution volume constant (V_d), and can be presented as

$$FUR = C_t(t) \times (\int_0^T C_p(t)dt)^{-1}.$$

When mean plasma glucose during PET imaging is known, the metabolic rate of glucose (GU) can be expressed as follows

$$MR_{Gluc} = P_{Gluc} \times K_i \text{ or } FUR \times LC^{-1},$$

where P_{Gluc} and LC denote plasma glucose level and lumped constant, respectively. The latter parameter accounts for the differences in membrane transport and phosphorylation rates between glucose and [^{18}F]FDG due to competition of the two (Phelps et al. 1979, Iozzo et al. 2007. Based on the preclinical data (see 5.6.1 and 6.2), LC-values of 1.30 and 1.16 (at fast and during hyperinsulinemia, respectively) were used to derive intestinal GU, and LC-value of 1.0 was used to derive pancreatic GU.

5.4.2 One-tissue compartmental analysis (I, II, IV, V)

The measurement of pancreatic and intestinal BF is based on the on the principle of exchange of inert gas between blood and tissues, as described by Kety & Schmidt (1946), and on the Fick's principle. Briefly, the latter states that the BF to the desired organ can be calculated when 1) the amount of marker substance taken up by the organ per unit of time and 2) concentration of marker substance in arterial and venous blood are known. Due to single arterial input function, one-tissue compartmental (i.e. two-compartment model) analysis can be utilized. Here, tracer concentration in tissue as a function of time can be expressed as

$$dC_T(t)\, dt^{-1} = f \times C_A(t) - (f \times C_T(t))\, p^{-1},$$

where C_T and C_A denote [^{15}O]H_2O concentration in tissue and arterial blood, f denotes BF and p is the partition coefficient of water, respectively. PET-derived [^{15}O]H_2O-TAC is biased by the radioactivity originating from (stable) arterial blood pool within the tissue, and is expressed as

$$C_{PET}(t) = C_T(t) + V_A \times C_A(t),$$

where C_{PET} and V_A denote tissue [^{15}O]H_2O concentration measured by PET and arterial volume fraction in the tissue, respectively. In the present work, V_A was automatically estimated with a fixed upper limit of 25 %. BF is expressed as mL

mL^{-1} min^{-1}, whereas in studies IV and V pancreatic and intestinal BF rates were corrected for organ volume and thereby expressed as mL min^{-1}. For the aforementioned volume conversion, pancreatic volume was measured directly from MR derived data whereas conventional values of 60 grams (for both M/F) and 580/540 grams (M/F) were used for duodenum and jejunum, respectively (Snyder et al. 1975).

5.4.3 Gut compartment model (I, IV, V)

Unlike pancreas and other extrahepatic splanchnic organs, liver receives dual blood supply from hepatic artery (20-25 %) and portal vein (75-80 %). Therefore, one-tissue compartmental analysis cannot be assessed for the hepatic BF measurements, and dual input function (DIF) is required. The gut compartment model presented by Kudomi et al. (2008) assumes a single compartment between arterial blood and gut compartment that can be utilized to estimate portal vein BF. The model can be expressed as

$$C_T(t) = (f_a C_A(t) + f_p C_P(t)) \times e^{-k2 \times t},$$

where C_T, C_A and C_P denote $[^{15}O]H_2O$ concentration in tissue, arterial blood and portal vein blood, respectively, f_a and f_p denote hepatic arterial and portal vein BF, respectively. In the above equation, k_2 is defined as $(f_a+f_p)\ V_L^{-1}$, where V_L (mL g^{-1}) is the distribution volume of water between blood and tissue. Furthermore, PET-derived hepatic $[^{15}O]H_2O$-TAC is expressed as

$$C_{PET}(t) = (1 - V_0) \times (f_a C_A(t) + f_p C_P(t)) \times e^{-k2 \times t} + V_0 C_{input}(t), \text{ where}$$

$$C_{input}(t) = r_a C_A(t) + r_p C_P(t).$$

Here, r_a and r_p are hepatic arterial and portal vein BF ratios to total hepatic BF, respectively. Validation study performed in 14 healthy pigs during postabsorptive state revealed that the hepatic BF values (f_a and f_p) calculated using the gut compartment model were in close agreement ($r = 0.90$, $P < 0.001$) with the flow values measured using B-type ultrasonographic probes. While the validation of the gut compartment model is lacking in humans due to inaccessibility of hepatic artery and portal vein, it is likely that the aforementioned assumptions are not limited to preclinical models.

5.4.4 Tissue blood volume (IV, V)

Blood volume in splanchnic organs was measured using frequent [^{15}O]CO inhalations, and blood was sampled at 4, 6 and 8 minutes from the start of the inhalation. The calculation of blood volume follows simple arithmetic as

$$V_B\,(\text{mL } 100\text{g}^{-1}) = 100 \times C_{tissue} \times (C_{blood} \times \rho_{tissue} \times HCT_{SV}/HCT_{LV})^{-1},$$

where C_{tissue} and C_{blood} denote tissue (PET) and blood (manual sampling) radioactivity during the static scanning, respectively, and HCT_{SV}/HCT_{LV} denote tissue-specific small-to-large vessel hematocrit ratio.

5.5 Calculations and analyses (I-V)

5.5.1 A-P difference, LC, and extrahepatic SGU (III)

Extrahepatic splanchnic fractional extractions (FE) of [^{18}F]FDG and [^{2}H]G were estimated in a total of 10 healthy pigs, six during fasting state and four during physiologic hyperinsulinemia. Under steady state conditions, the concentration of these tracers in artery (C_A) and portal vein (C_P) are measured and the fractional extraction is calculated as

$$FE_{tracer} = \Sigma(C_A - C_P) \times \Sigma C_A^{-1},$$

where FE_{tracer} denotes the fractional extraction (i.e. the fraction trapped between two blood compartments) of [^{18}F]FDG or [^{2}H]G across the extrahepatic splanchnic region (Kelley et al. 1999). Extrahepatic splanchnic lumped constant (LC) for [^{18}F]FDG was defined as a ratio between $FE_{[18F]FDG}$ and $FE_{[2H]G}$. Due to the prominent weight of the intestine over pancreas, visceral adipose tissue and spleen, the extrahepatic splanchnic LC closely approximates sole intestinal LC. The unidirectional extrahepatic SGU from [^{18}F]FDG data was calculated as

$$\text{Extrahepatic SGU} = FE_{AP} \times f_p \times AP_{Gluc}.$$

In the above equation, FE_{AP} denotes [^{18}F]FDG fractional extraction between artery and portal vein, f_p is the portal vein BF (measured using ultrasonographic probes) and AP_{Gluc} is steady state glucose concentration in the arterial plasma.

5.5.2 Biochemical analyses (I-V)

During standard oral glucose tolerance test and scanning, blood was collected to lithium heparin and EDTA tubes and stored at -70°C until analyses. Arterial and venous plasma glucose was determined in duplicate by the glucose oxidase method (GM9 Analyser, Analox Instruments, London, UK). Plasma lactate and serum total cholesterol, triglyserides, and HDL cholesterol were measured using standard enzymatic methods (Roche Molecular Biochemicals and Boehringer Mannheim, Mannheim, Germany) with a fully automated analyzer (Hitachi 704, Hitachi, Tokyo, Japan). Serum LDL cholesterol was calculated using the Friedewald equation (Friedewald et al. 1972), and serum oxidized LDL (oxLDL) was assessed spectrophotometrically as the amount of diene conjugation of the extracted lipids (Ahotupa et al. 1998). Glycated hemoglobin was measured by fast protein liquid chromatography (MonoS, Pharmacia, Uppsala, Sweden). Serum FFA were determined by an enzymatic method (ACS-ACOD Method, Wako Chemicals, Neuss, Germany). Serum insulin and C-peptide concentrations were measured by a double-antibody fluoroimmunoassays (Autodelfia, Wallac, Turku, Finland and Bio-Plex 200, Bio-Rad Laboratories Inc., Hercules, California, United States). To measure plasma GIP, GLP-1 and glucagon (studies IV and V), 25 mg of DPP-IV – inhibitor (Diprotin-A, Sigma-Aldrich, St. Louis, Missouri, United States) and 2000 KIE of trypsin inhibitor (Trasylol, Bayer AG, Leverkusen, Germany) were added to chilled EDTA tubes before blood sampling. Thereafter, analyses were performed by an enzyme-linked immunosorbent assay (Millipore, Billerica, Massachusetts, United States).

5.5.3 Lipid accumulation: fat index and F_p (I, II)

The lipid accumulation of pancreas was non-invasively estimated from both MRI (study I) and CT (studies I and II) images. The former is based on the different chemical shifts of water and fat in In- and Out-of-phase NMR methodology, and has previously been proven to be a reliable method to rapidly detect excessive lipid accumulation in the liver (Borra et al. 2009). T_2-weighted images of the abdominal region (slice thickness 10 mm) were obtained using the 1.5 Tesla Intera scanner (Philips, Best, Netherlands) and unenhanced abdominal CT scans (slice thickness 3.3 mm) were obtained using the hybrid Discovery VCT scanner. ROIs were placed in the three parts of the pancreas (head, body, tail) on the In-Phase and Out-of-Phase MR images. The estimate for pancreatic lipid accumulation was thereafter calculated by the modified Kawamitsu (Kawamitsu et al. 2003) method as follows

$$FI_P = (SI_{in} - SI_{out}) \times SI_{in} \times 100,$$

where FI_P denotes pancreatic fat index (as arbitrary units) and SI_{in} and SI_{out} denote NMR signal intensity in In-Phase and Out-of-Phase images, respectively. While the In- and Out-of-Phase method provides a rapid adiposity estimate of pancreas, it is weakened by the lack of validation against histological samples. In contrast, the CT-based method presented by Kim et al. (2014) has been shown to correlate well with the values derived from tissue biopsies of human patients who had undergone a partial pancreatectomy for malignancy, cysts or focal pancreatitis, and who had underwent abdominal CT scan within one month of the operation. The method is based on the difference in Hounsfield Unit (HU) between pancreas and spleen: while the ectopic fat accumulation frequently takes place in pancreas resulting in a decrease in CT attenuation, splenic CT attenuation remains constant due to large venous sinuses and low amounts of fat. ROIs were placed on the homogeneous pancreatic and splenic parenchyma, and the pancreatic fat accumulation (in percentage) was calculated as

$$F_P = -60.86 \times P/S + 59.4,$$

where F_P and P/S denote pancreatic fat percentage and pancreas-to-spleen CT attenuation ratio, respectively (courtesy of Dr. So Yeon Kim). Cross-validation between the methods (In- and Out-of-Phase and CT-based methods) was performed in the present work.

5.5.4 Volume analysis (I, II, IV, V)

Pancreatic and hepatic (acquisition in studies I, II, IV and V: see above; acquisition in studies IV and V: T_2-weighted balanced turbo field echo (BTFE) images of the abdominal region [slice thickness 5.5 mm] were obtained using the 3.0 Tesla Ingenuity scanner) volumes were measured manually from the MR and CT images by placing ROI in plane-by-plane fashion to the margins of organs, carefully avoiding the inclusion of nearby organs, visceral adipose tissue and extra- and intraorgan blood vessels. The pancreatic and hepatic volumes were used to adjust the BF and volume results per 100-gram of tissue to total organ BF and volume (i.e. per organ), respectively.

5.5.5 Whole-body glucose uptake, and insulin sensitivity (I-V)

A prime-continuous insulin infusion of 1 mU kg^{-1} min^{-1} is administered to subjects, and a glucose infusion is initiated to maintain euglycemia (5.0 mM). The glucose infused over the rate of the experiment equates with the amount of glucose translocated out of the plasma glucose space (DeFronzo et al. 1979). Whole-body GU (i.e. glucose metabolized, *M*-value) was calculated after reaching the steady state conditions. The *M*-value is expressed per kg of lean body-mass.

The surrogate indices for insulin sensitivity were calculated in all studies. Homeostatic model assessment for insulin resistance ($HOMA_{IR}$) was calculated as previously described (Matthews et al. 1985), and represents an estimate of insulin resistance as a fraction to 1.0, a value found in lean individuals. While practical and easy to calculate, $HOMA_{IR}$ is based only on fasting glucose and insulin values and thus not regarded as the most accurate surrogate index. In contrast, model-derived estimate of insulin sensitivity (2h OGIS) by Mari et al. (2001) was calculated from the 2-hour OGTT data. The calculation is based on the established principles on glucose kinetics and insulin action and takes into account subject-specific factor such as age, sex and BMI and thus can be regarded as an accurate surrogate index for insulin sensitivity.

5.5.6 Empirical and model parameters of β-cell function (I, II, IV, V)

The main culprit behind the progression from NGT to IGT and to overt T2D is the decrease in β-cell function and insulin secretion rate against prevailing glucose levels. While fasting serum insulin level offers a robust estimate of insulin secretory capacity, it is a poor marker of β-cell function, due to notable and highly variable hepatic insulin extraction and whole-body sensitivity to insulin. Moreover, fasting serum insulin levels do not account for the changes in plasma glucose levels, the most potent insulin secretagogue. Thus, the estimation of the many aspects of β-cell function by more sophisticated methods is justified. The insulinogenic index (IGI) was calculated as a ratio of the change between 30-min and fasting values of insulin and glucose during OGTT, respectively.

Moreover, the "Pisa-Padova" model (**Fig. 7**) of β-cell function was assessed in studies I, II, IV, and V. The model, which is based on the observation in isolated perfused pancreata and clinical experience, depicts three distinct components of β-cell function. The first one is the linear dose-response relationship between absolute plasma glucose concentration and insulin secretion rate, and elucidates the extent of insulin secretion rate increment to the increases in plasma glucose. The slope of the dose-response curve is called *glucose sensitivity*, and is independent of peripheral insulin resistance. Moreover, recent cohort study revealed that the decrease in *glucose sensitivity* is the key defect in impaired glucose tolerance (Mari et al. 2010). The relationship between plasma glucose and ISR is modulated by a time-varying potentiation of insulin secretion by several factors (alimentary hormones, neural modulation, non-glucose secretagogues) during oral glucose and meal testing. This results in higher ISR during the descending phase of hyperglycemia than during the increasing phase with similar glucose concentrations. The ratio between 2-hour and baseline potentiation is called *potentiation factor ratio* and has been shown to be largely blunted in patients with T2D (Mari et al. 2002). Recent evidence suggests that the dissection of the potentiation phenomenon into *incretin potentiation* and *i.v. potentiation* can be

accomplished with isoglycemic glucose infusion test (Tura et al. 2014). However, this was not applied in the present studies. Lastly, the early ISR is dependent not only on the absolute glucose concentrations, but also on the rate of change in glucose. This derivative component is quantitated as *rate sensitivity*. The equations of the aspects of β-cell model from the "Pisa-Padova" –model are beyond the scope of this discussion and can be found in the references.

5.5.7 Total and incremental areas under the curve (IV, V)

To quantitate plasma excursions of glucose, insulin, C-peptide, glucagon, GIP and GLP-1 during meal testing, oral and intravenous glucose loading, and incretin infusions, total plasma areas under the curve (tAUCs) were calculated using the trapezoideal method. Incremental AUCs (iAUCs) were calculated by substracting baseline AUC from the tAUC, respectively.

5.6 Statistical analysis (I-V)

Statistical analysis was performed using SAS software for Windows, version 9.2 (SAS Institute, Cary, NC, United States). The results are expressed as mean ± SD and median (interquartile range) for normally and non-normally distributed data, respectively. Prior to analysis, tests to confirm equal variances and normality were performed. *Ln*-transformation was performed for skewed variables. Differences between groups and paired data were addressed by Student's *t*, paired *t*, Mann-Whitney *U* and Wilcoxon signed rank tests respectively. Bivariate analysis was performed using Pearson or Spearman correlation tests, as appropriate. To identify the independent factors affecting pancreatic, intestinal and hepatic BF, and β-cell function during postabsorptive (studies I and II) and absorptive state (studies IV and V), generalized linear models with and without adjustment for insulin sensitivity and weight were carried out. Analysis of changes over time, between interventions and study groups (studies IV and V) were performed using ANOVA for repeated measurements and Tukey-Kramer's *post-hoc* tests. A statistical significance was set at $P < 0.05$.

6 RESULTS

6.1 *In vivo vs. ex vivo* and splanchnic biodistribution of ^{18}F-labelled tracers in pig and rodent models (I, III)

The influx rate constant of glucose in pancreas and small intestine was calculated with Patlak graphical analysis (K_i) and fractional uptake rate (FUR) from the [^{18}F]FDG-PET images, and they exhibited a tight correlation with the values measured from tissue samples (ex vivo K_i) (**Fig. 18A-C**). In the Patlak graphical analysis, the linear fit of the measured data was always $r > 0.95$ for all measured tissues, indicating good performance of the model. Based on absolute values, need for recovery coefficients for *in vivo* (PET) derived values were not considered necessary. Patlak graphical analysis –derived K_i values were lower than the ones obtained with FUR or from tissue samples ($P < 0.05$ for Patlak *vs.* FUR/tissue sample), and the apparent distribution volumes (V_d) of [^{18}F]FDG in the graphical analysis were 0.31 ± 0.10 and 0.26 ± 0.22 mL mL^{-1} for pancreas and intestine, respectively. In the autoradiography analysis, both in normally glucose tolerant and streptozotocin-treated diabetic pigs the accumulation of [^{18}F]FDG was homogeneous in the pancreatic parenchyma with no hot-spots detectable in islets/exocrine parenchyma (**Fig. 18D)**. In contrast, while the accumulation of palmitate analogue [^{18}F]FTHA was homogeneous in pancreata of healthy mice, a substantial decrease in [^{18}F]FTHA accumulation was observed in the islets of the hyperlipidemic IGF-II/LDLR$^{-/-}$ApoB$^{100/100}$ mice (**Fig. 18E**). Here, the islet:exocrine photon-stimulated luminescence (PSL) ratio was 0.7:1. In the small intestine, the majority of gut wall [^{18}F]FDG accumulation took place in the mucosa with mucosa:non-mucosa PSL ratios ranging between 1.7 and 3.4, respectively (**Fig. 18F**). As the mucosa comprises a relative large proportion of the whole gut wall thickness, it is suggestive that at least 75-80 % of the whole gut glucose disposal during postabsroptive state occurs in the mucosa.

6.2 Insulin effect on extrahepatic SGU in a pig model (III)

Arterio-portal (AP) fractional extractions of [^{18}F]FDG and [^{2}H]G at postabsoprtive state were 0.28 and 0.23, respectively, and did not differ statistically between the two tracers (NS). During insulin stimulation, FE was 41-53 % higher than during fasting state (**Fig. 19A**). In the supraphysiological and physiological insulin infusion studies, the FE-values were overlapping (NS) and thus pooled for the statistical analysis. From this data, the extrahepatic (arterio-portal) splanchnic GU increased by 47 % (821 ± 360 *vs.* 1196 ± 217 μmol min^{-1}, $P < 0.05$) from baseline values during euglycemic clamp. Individual AP fractional extractions correlated

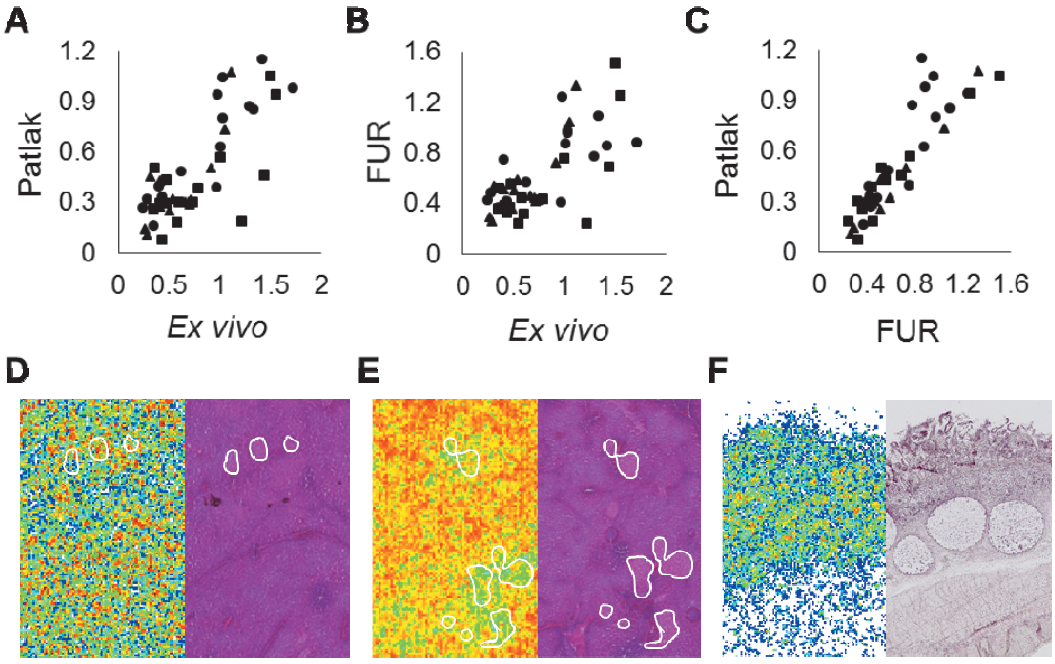

Figure 18. PET-validation of influx rate constants (in mL $100g^{-1}$ min^{-1}) against *ex vivo* data (A-C). All *r*-values ranged between 0.63-0.97 (*P*-range < 0.05 to < 0.0001). Balls, pancreas; triangles, duodenum; squares, ileum. Autoradiography analysis of pancreas (D-E). Islets are encircled in white. Gut wall accumulation of [^{18}F]FDG in a pig model (F).

tightly between the two tracers, and the slope of the AP fractional extractions (i.e. splanchnic lumped constant, **Fig. 19B**) were 1.30 ± 0.44 and 1.16 ± 0.23 for fasting and insulin-stimulated state, respectively, suggesting more avid [^{18}F]FDG uptake and phosphorylation over glucose.

6.3 Pancreatic metabolism, blood flow and β-cell function in obesity (I)

Baseline biochemical and anthropometric characteristics are shown on **Table 3**. In healthy controls, pancreatic GU did not change during euglycemic hyperinsulinemic clamp when compared with fasting values (**Fig. 20A**), whereas in obese patients pancreatic GU was *circa* 23 % lower during clamp than during fasting state ($P < 0.01$). The latter is likely due to insulin-independent mass action effect of glucose during fasting state, as no difference in influx rate constant (0.3 ± 0.1 *vs.* 0.3 ± 0.1 mL $100g^{-1}$ min^{-1}, NS) was seen between the two experiments. No change in fasting and insulin-stimulated GU rates was seen between obese patients with and without diabetes or impaired glucose regulation.

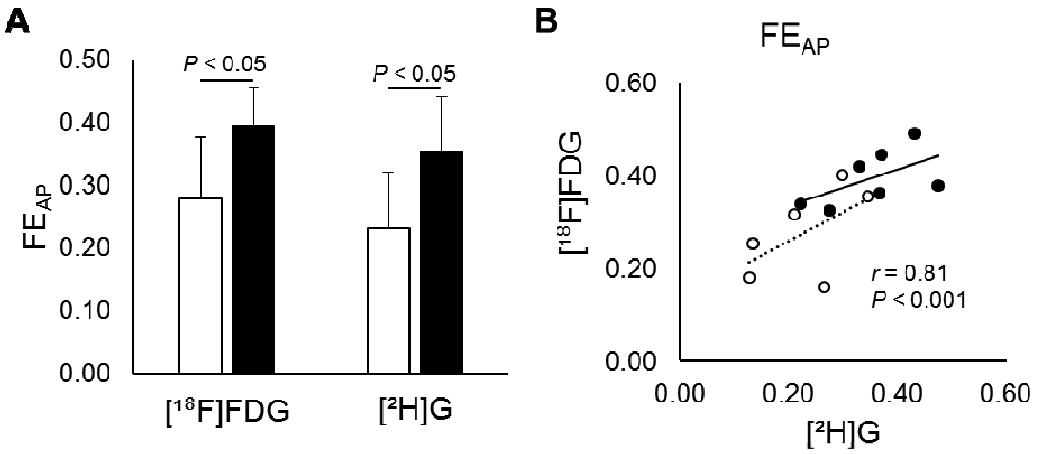

Figure 19. The effects of insulin infusion on arterio-portal fractional extractions (FE_{AP}) in the dual-tracer experiment (A). Individual FE-values correlated tightly between the radiotracers over the pooled data (B). White bars and balls, fasting state; black bars and balls, insulin-stimulation.

GU during hyperinsulinemia did not associate with mean plasma FFA concentration. In contrast, pancreatic FA uptake per organ during fasting state was *circa* 84 % higher in the obese patients *vs.* controls ($P < 0.001$) (**Fig. 20B**), without significant difference between patients with and without diabetes (data not shown). As the fractional fatty acid extraction did not differ between the groups (1.9 ± 0.5 *vs.* 1.6 ± 0.4 mL $100g^{-1}$ min^{-1}, $P = 0.07$), the difference in total FA uptake was mostly accounted for larger pool of circulating FFAs (see **Table 3**) in obese patients. In the pooled data, pancreatic FA uptake was inversely related to systemic insulin sensitivity (2h OGIS, $r = -0.49$, $P < 0.01$). Based on these observations, it is suggestive that the relative uptake of glucose and lipids is shifted during obesity with preferential uptake of lipids over glucose in obese patients (amino acid uptake for energetic metabolism is considered negligible in the aforementioned rationale). Combined molar influx of the two substrates (i.e. glucose and fatty acids) did not differ between healthy and obese subjects (2.9 ± 0.7 *vs.* 3.0 ± 0.4 μmol $100g^{-1}$ min^{-1}, NS). The measures of pancreatic steatosis, as obtained using the In- and Out-of-Phase and CT-based methods, revealed 5.1-7.2 ($P < 0.01$) higher values in obese patients than healthy controls (**Fig. 20C-D**). Data from the two methods were well correlated (**Fig. 20E**) whereas large inter-individual variation was present in values derived from both of the methods. Interestingly, measures of pancreatic steatosis did not associate with pancreatic FA uptake in any of the groups (i.e. controls, obese patients with and without diabetes), whereas FI_P was inversely related with pancreatic GU ($r = -0.38$, $P < 0.05$).

Pancreatic BF per 100 grams of tissue at fast was *circa* 30 % lower in the obese patients than in controls ($P < 0.01$) (**Fig. 21A**), and this persisted even though

volumes of the panreata were taken into account (126 ± 45 *vs.* 98 ± 45 mL min^{-1}, P = 0.08). In healthy but not in obese subjects, plasma glucose and insulin levels were associated with pancreatic BF (r = 0.60, P < 0.05 and r = 0.80, P < 0.01, respectively), whereas in pooled obese group pancreatic BF was inversely associated with visceral adipose tissue volume (r = -0.64, P < 0.001). In the pooled (controls+obese) data, pancreatic BF was inversely related with FI_P (r = -0.68, P < 0.01) and had a moderate association with portal vein BF (**Fig. 21B**). Still, portal vein BF did not differ in obese and controls (0.34 ± 0.11 *vs.* 0.30 ± 0.13 L 100g^{-1} min^{-1}, NS).

Total pancreatic fat volume (steatosis [%] × total volume) was inversely related with fasting insulin levels in obese but not in controls (**Fig. 22A**) and in pooled data FI_P had a positive association with mean glucose during OGTT (r = 0.32, P < 0.01). Interestingly, in the pooled data, pancreatic BF at fast was moderately associated with insulinogenic index (r = 0.38, P < 0.05) and β-cell glucose sensitivity (**Fig. 22B**). In contrast, neither glucose (at fast or during clamp) nor FA uptake were associated with measures of β-cell function and glycemic control.

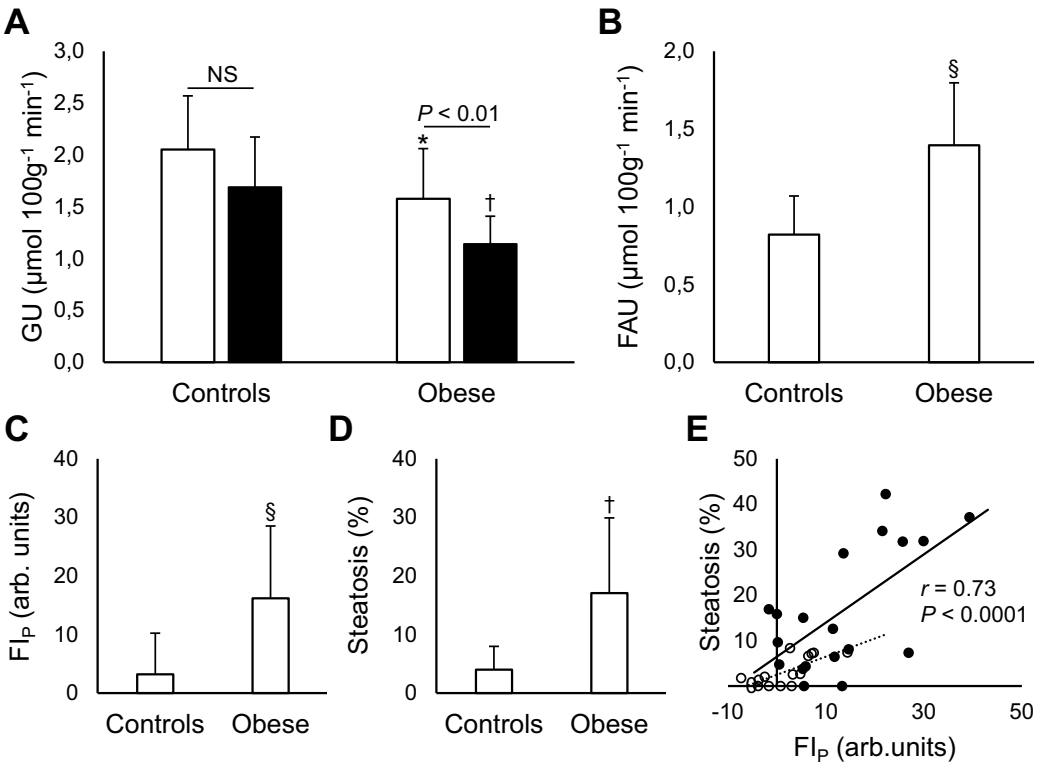

Figure 20. Pancreatic GU during fasting state (white bars) and insulin-stimulation (black bars) (A), FA uptake during fasting state (B) and measures of steatosis (In- and Out-of-Phase technique [FI_P] and CT-based method) (C-E) in healthy controls and obese patients. White balls, controls; black balls, obese. *P < 0.05, $^{\dagger}P$ < 0.01, $^{\S}P$ < 0.0001 for obese *vs.* controls. r in panel E represents correlation over the pooled data.

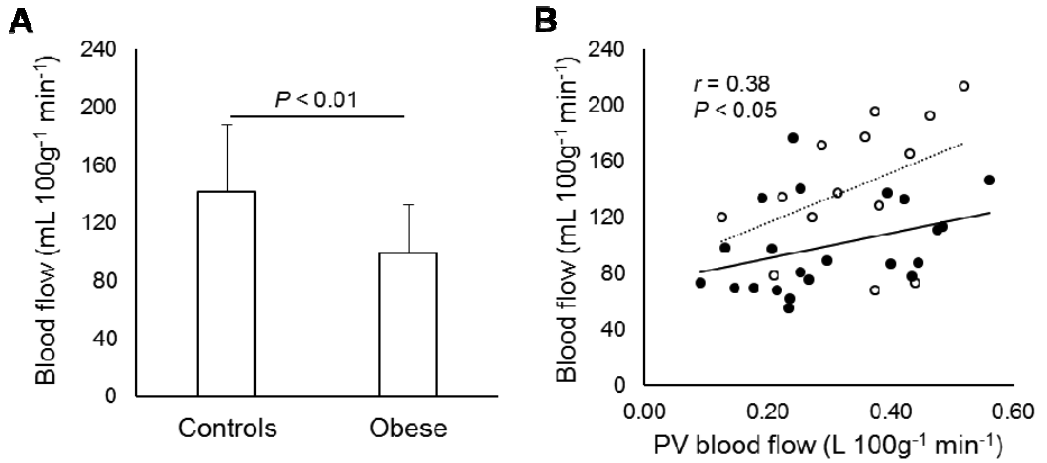

Figure 21. Pancreatic BF at fast (A), and the relation (over the pooled data) between pancreatic and portal vein (PV) BF (B). White balls, controls; black balls, obese.

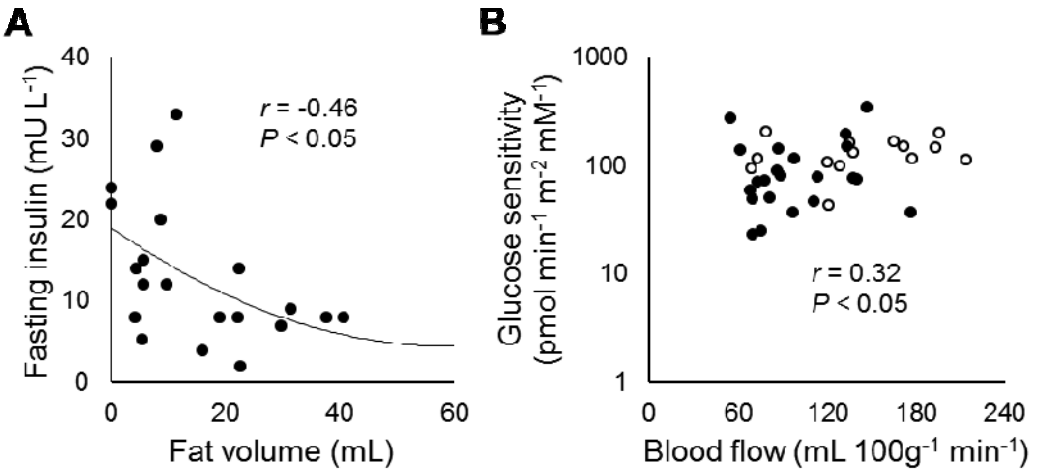

Figure 22. Scatter plots between serum insulin levels and β-cell glucose sensitivity against pancreatic fat accumulation (A) and BF at fast (B) White balls, controls; black balls, obese.

6.4 Early and late metabolic effects of bariatric surgery (II, V)

Bariatric surgeries (either Roux-én-Y gastric bypass or vertical sleeve gastrectomy) were performed laparoscopically as previously described (Helmiö et al. 2012), are were well tolerated. The drop-out rate (i.e. patients who did not underwent surgery) were 2/25, 4/27 and 0/10 for SLEEVEPASS, SleevePET2 and GIP-PET, respectively.

Detailed pre-surgery *vs.* post-surgery data are given on **Table 4**. Early (two months) and late (six months) after bariatric surgery, 14 and 23 % of weight loss

was observed, and this was accompanied with a progressive resolution of systemic insulin resistance at 2-mo ($P < 0.001$ *vs.* controls) to 6-mo (NS *vs.* controls) post-surgery near control values. Before bariatric surgical procedures, plasma glucose and C-peptide ($P < 0.05$) during OGTT were significantly higher in patients with diabetes *vs.* patients without diabetes, whereas no difference was observed in insulin levels. Six months after surgery, however, a notable decrease in glucose, insulin, and C-peptide levels during OGTT was observed both in ND and T2D groups (P range < 0.01 to < 0.0001 for all comparisons). Interestingly, identical results in terms of fasting and 2-hour glucose values were obtained in the T2D surgical group only two months after surgery suggesting a rapid alleviation of dysglycemia in patients with diabetes (**Fig. 23**). In concert with the previous observation, glucose sensitivity was upregulated already two months after surgery and persisted so six months after surgery in T2D patients. Groupwise, however, glucose sensitivity was still 25-28 % lower (P range 0.04 to 0.07) in the T2D post-surgical groups than in healthy controls. No change in potentiation factor ratio was observed at 2-mo and 6-mo post-surgery when compared with pre-surgical values (NS), and rate sensitivity was upregulated only at 6-mo post-surgery ($P < 0.05$).

Notable post-OGTT insulin response was seen two months post-surgery in the T2D group when compared with pre-surgery and six months post-surgery responses; however, it cannot be totally excluded that this transient upregulation in insulin secretion is due to differences in study populations at pre-surgery *vs.* early *vs.* late post-surgery. Active incretin hormones were measured in a sub-population of T2D patients at baseline, and at two months post-surgically. While fasting incretin levels were unchanged, two months post-surgery a dramatic increase in GLP-1 secretion during OGTT took place.

The total remission rate of diabetes in these three studies was 72.4 % (i.e. 21 out of 29 T2D patients that underwent surgery). Improved fasting and post-OGTT glycemic response resulted in a subtle 6.4 % (35.4 ± 3.9 *vs.* 37.7 ± 3.7 mmol mol^{-1}, $P < 0.0001$) decrease in HbA1c levels in the ND surgical group six months post-surgery and a more pronounced 9.6 % (35.9 ± 2.8 *vs.* 39.7 ± 4.0 mmol mol^{-1}, $P < 0.05$) and 16.5 % (38.7 ± 3.8 *vs.* 47.1 ± 7.3 mmol mol^{-1}, $P < 0.0001$) decrease in HbA1c levels in T2D surgical group two and six months post-surgery, respectively. In the pooled surgical data, change in BMI had a moderate correlation with a change in HbA1c (**Fig. 23**), whereas no direct association between weight loss and insulin sensitivity was observed.

Table 4. Anthropometrical and biochemical characteristics before and after bariatric surgery.

	ND			T2D				
	Pre-surgery	*P*	6 months	Pre-surgery	*P*	2 months	*P*	6 months
n	27		27	29		10		19
Anthropometrics								
Weight (kg)	120 ± 14.4	< 0.0001	91.2 ± 13.1	114 ± 14.4	< 0.0001	98.0 ± 16.2	< 0.0001	88.4 ± 14.2
Weight change (%)	-	-	23.0 ± 5.9	-	-	14.4 ± 4.9	-	22.6 ± 6.6
BMI (kg m^{-2})	42.9 ± 3.6	< 0.0001	32.9 ± 4.1	41.1 ± 4.8	< 0.0001	35.2 ± 6.3	< 0.0001	32.0 ± 4.8
Diabetes (n/%)	0/0.0	-	0/0.0	29/100	-	2/20	-	6/32
Biochemical data								
FPG (mM)	5.7 ± 0.5	< 0.0001	5.1 ± 0.5	7.0 ± 1.3[a]	< 0.01	5.7 ± 0.7	< 0.0001	5.7 ± 0.8[a]
FSI (mU L^{-1})	14.0 ± 9.2	< 0.001	6.2 ± 2.9	19.6 ± 12.4[a]	< 0.05	12.2 ± 7.1	< 0.01	9.3 ± 6.1[a]
HbA1c (mmol mol^{-1})	37.7 ± 3.7	< 0.0001	35.4 ± 3.9	44.4 ± 7.3[a]	< 0.05	35.9 ± 2.8	< 0.0001	38.9 ± 3.9[a]
Insulin resistance indices								
$HOMA_{IR}$ (fraction)	3.5 ± 2.3	< 0.0001	1.5 ± 0.8	5.9 ± 3.4[a]	< 0.05	3.1 ± 1.9	< 0.05	2.4 ± 1.6[a]
2h OGIS (mL min-1 m-2)	341 ± 44.0	< 0.0001	453 ± 44.1	308 ± 48.4[a]	< 0.05	361 ± 64.3	< 0.0001	410 ± 54.8[a]
β-cell function parameters								
IGI (mM U^{-1})	31.2 ± 28.4	NS	29.1 ± 19.8	10.6 ± 6.6[a]	NS	18.6 ± 11.1	< 0.05	13.4 ± 6.5[a]
β-GS (pmol min^{-1} m^{-2} mM^{-1})	133 ± 93.3	NS	160 ± 77.3	53.3 ± 34.5[a]	< 0.05	82.7 ± 41.5	< 0.01	79.0 ± 30.8[a]

Data are shown as mean ± SD. The table is a compilation of three data collections, whereby baseline characteristics represent data from all of the three studies, and postoperative data are is derived from either GIP-PET (2-mo post-surgery) or SLEEVEPASS and SleevePET2 (6-mo post-surgery). More details regarding study population and the abbreviations are given on Table 3. *P* column represent 2-mo or 6-mo post-surgery *vs.* pre-surgery, [a]$P < 0.05$ ND *vs.* T2D pre-surgery or 6-mo post-surgery.

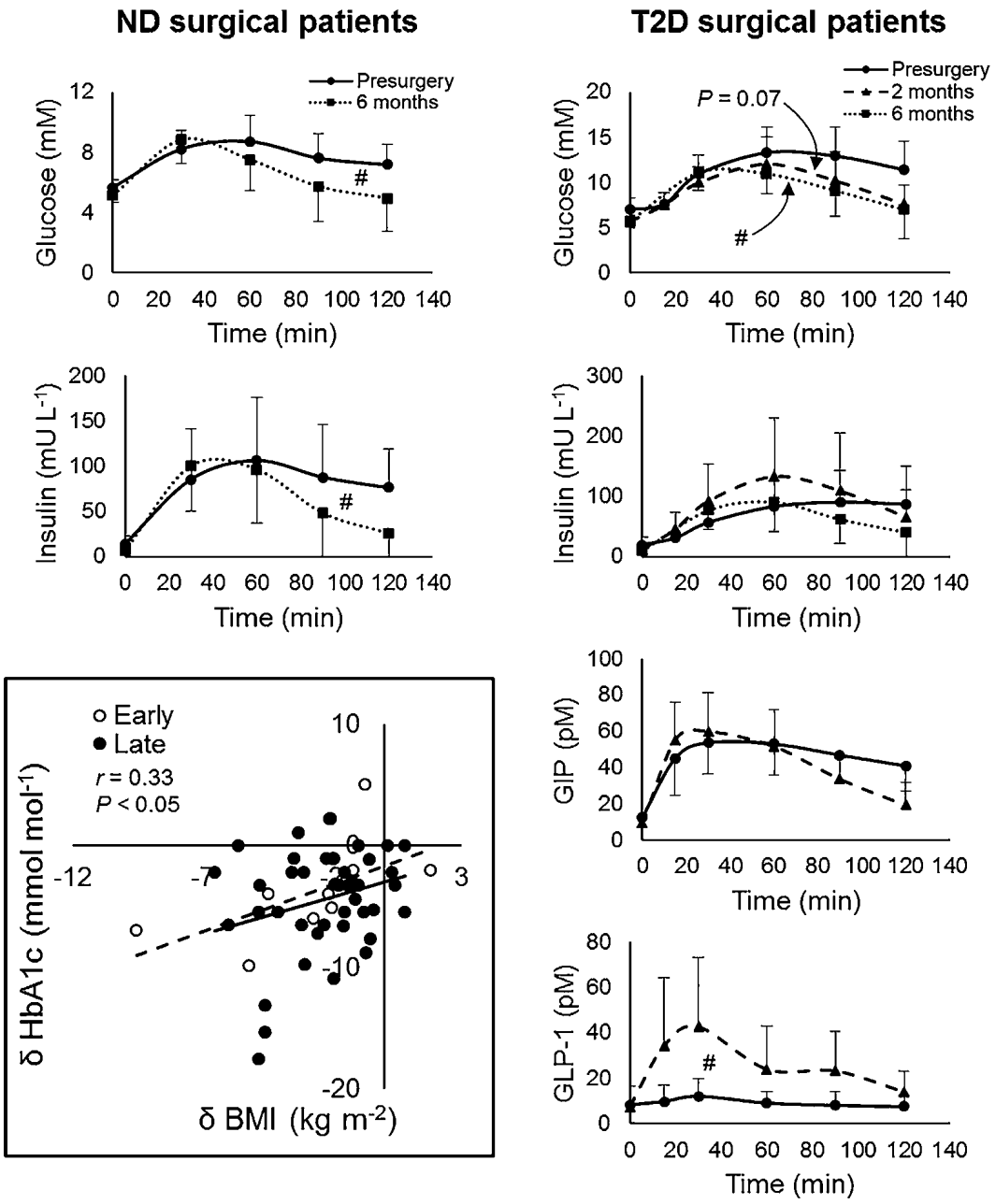

Figure 23. Plasma glucose, insulin, GIP and GLP-1 levels during OGTT in patients with and without diabetes before, two months (only T2D) and six months after bariatric surgery. $^{\#}P < 0.05$ in tAUC post-surgery *vs.* pre-surgery. In the pooled surgical data, change in BMI was associated with a favorable glycemic control.

6.5 The effects of bariatric surgery on pancreatic metabolism (II)

Six months after bariatric surgery, both pancreatic FA uptake (1.4 ± 0.4 *vs.* 1.2 ± 0.3 μmol $100g^{-1}$ min^{-1}, $P < 0.05$), total pancreatic volume (**Fig. 24A**), and fat accumulation (**Fig. 24B**) were significantly decreased. As plasma FFA levels were unchanged post-surgically (0.80 ± 0.23 *vs.* 0.76 ± 0.18 mM), the decrease in pancreatic FA uptake was due to attenuated extraction of fatty acids from the circulation (**Fig. 24C**). The parenchymal volume was unaltered (74 ± 28 *vs.* 72 ± 22 mL, NS). No difference in the aforementioned lipid variables was observed between patients with and without diabetes at baseline. Surprisingly, after bariatric surgery fasting pancreatic BF even further lowered (**Fig. 24D**) by *circa* 16 %, similarly in patients with and without diabetes at baseline.

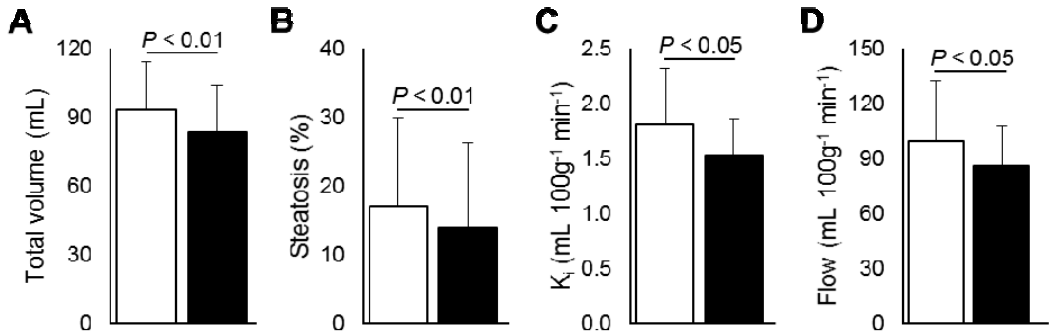

Figure 24. Pancreatic volume (A), fat percentage (B), fractional fatty acid extraction (C) and fasting state BF (D) in obese patients (ND+T2D pooled) before (white bars) and six months after (black bars) bariatric surgical procedure.

Pancreatic fat volume after surgery in the pooled obese group was inversely associated with fasting insulin levels, similarly as before surgery ($r = -0.54$, $P < 0.01$). Moreover, the change in pancreatic fat was inversely associated with change fasting insulin levels in patients with T2D at baseline but not in non-diabetic patients (**Fig. 25A**). Interestingly, decrease in fatty acid extraction or FA uptake was not associated with any measure of β-cell function or glycemic control, or with the decrease in pancreatic fat volume (NS). Furthermore, decrease in HbA1c did not have a significant correlation with pancreatic lipid variables. In the pooled data, change in weight and insulin resistance/sensitivity indices ($HOMA_{IR}$ or 2h OGIS) were not associated with changes in pancreatic steatosis and FA uptake.

In patients with T2D before surgery, seven out 10 was in remission six months after surgery. While the low number of patients in the remitter *vs.* non-remitter analysis failed to enable any statistical analysis, patients that did not proceed to diabetic remission had considerably lower rates of pancreatic fat decrease (-1.3 ± 2.9 *vs.* -9.8 ± 7.7 mL) and relatively larger decrease in fasting insulin levels, as

depicted by arrows in **Fig. 25A**. In multivariate analysis, the decrease in pancreatic fat independent predictor of the increase in insulinogenic index (β = -0.72, $P < 0.05$) in a pooled patient group, and of the increase in insulin secretion rate at fixed glucose (β = -0.20, $P < 0.01$) even after adjustment for weight loss and insulin sensitivity.

The groupwise decrease in pancreatic blood was not associated with a change in weight whereas a moderate association was found between BF and 2h OGIS (r = -0.48, $P < 0.05$). In patients without diabetes before surgery but not in the diabetic group, change in BF was associated with changes in rate sensitivity (r = 0.68, $P < 0.05$) and insulinogenic index (r = 0.63, $P < 0.05$), while in the diabetic but not in the non-diabetic group lesser decrease in BF was associated with improved fasting glucose levels (**Fig. 25B**). The latter relationship remained significant after adjustment for weight loss and insulin sensitivity (β = -0.019, $P < 0.001$; pancreatic BF as mL mL^{-1} min^{-1}).

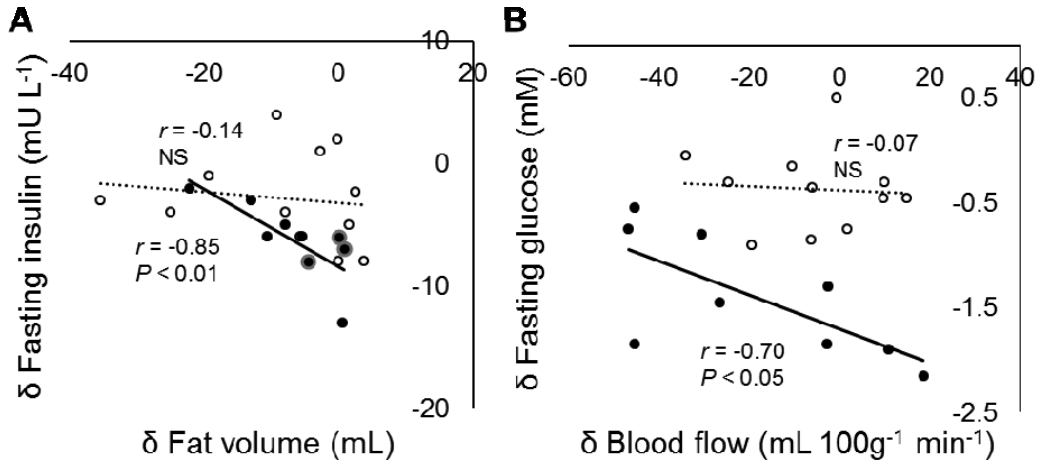

Figure 25. Scatter plots in between changes in pancreatic fat volume (A), BF (B) and glycemic variables after bariatric surgery (i.e. post-surgery minus pre-surgery) in patients with (black balls) and without diabetes (white balls) at pre-surgery. In the diabetic sub-population, three patients who did not proceed to diabetic remission are encircled in gray (only in panel A).

6.6 Intestinal glucose uptake in obese patients with normal glucose tolerance (III)

At postabsorptive state, GU in duodenum and jejunum was similar between obese non-diabetic patients and healthy age-matched controls (**Fig. 26A**). Moreover, no change in GU was observed between duodenum and jejunum in neither groups (1.3 ± 0.7 *vs.* 1.1 ± 0.7 μmol $100g^{-1}$ min^{-1}). During clamp, plasma glucose was 5.0 ± 0.5 mM, and 84-86 % decrease in plasma FFA levels was

observed in both groups. While the plasma FFA levels during PET-imaging period were slightly higher in obese patients (0.11 ± 0.06 *vs.* 0.07 ± 0.02 mM, $P = 0.07$), statistical significance was not reached. In healthy controls, euglycemic hyperinsulinemia increased GU by 274 and 385 % in duodenum and jejunum, respectively. In contrast, GU values during clamp were unchanged in obese patients (NS).

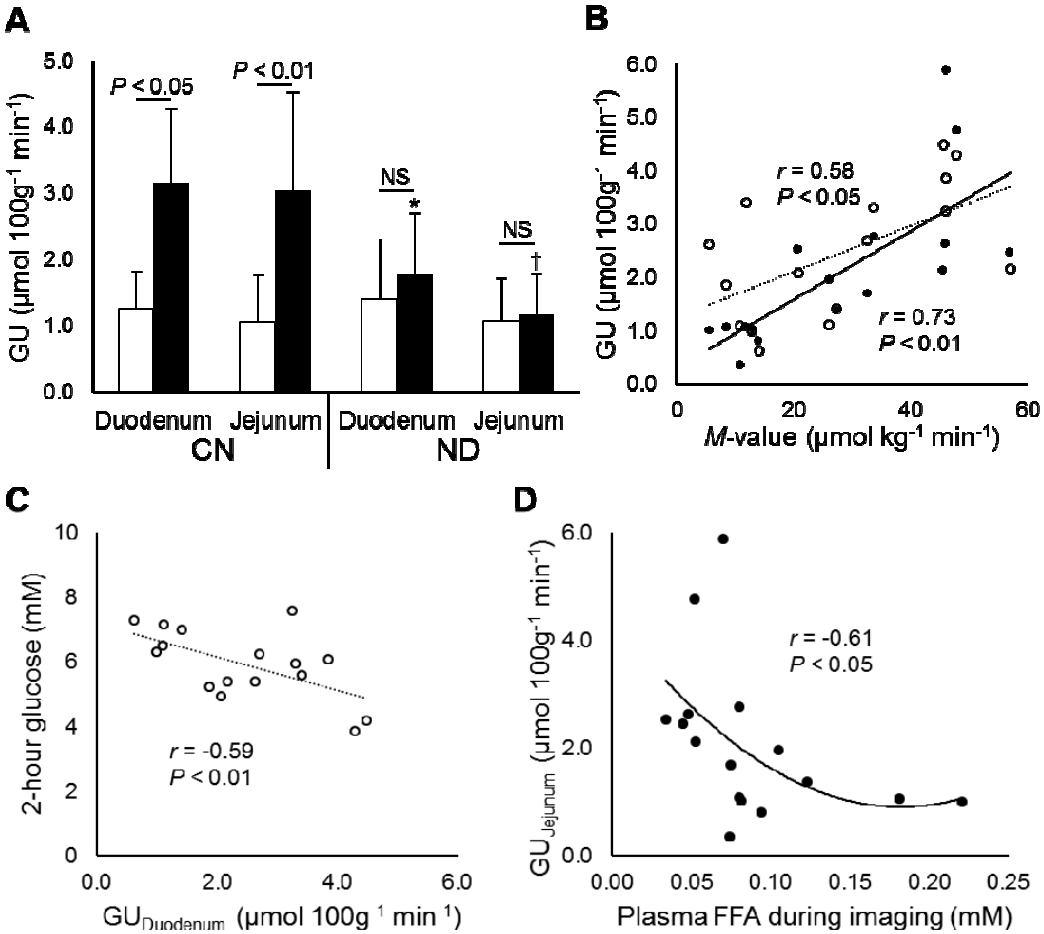

Figure 26. Intestinal GU in healthy controls and obese normally glucose tolerant obese patients at postabsorptive state (white bars) and during euglycemic hyerinsulinemia (black bars) (A). The relationship between whole-body insulin sensitivity (*M*-value) and intestinal GU during clamp (B). High insulin-stimulated duodenal GU was related to improved glycemic control (C) whereas plasma free fatty acids impaired insulin-stimulated GU in the jejunum (D). GU, glucose uptake; CN, controls; ND; non-diabetic obese patients; FFA, free fatty acids. White balls, duodenum; black balls, jejunum. *$P < 0.05$, †$P < 0.01$ obese *vs.* controls.

In the pooled data intestinal GU were tightly associated with whole-body insulin sensitivity (*M*-value, **Fig. 26B**). Moreover, insulin-stimulated duodenal GU values were inversely related with 2-hour glucose levels during OGTT (**Fig. 26C**), whereas this association was not seen in jejunum. Conversely, plasma levels of FFA were inversely related with jejunal but not with duodenal GU during clamp (**Fig. 26D**). Fasting intestinal GU were not associated with fasting plasma glucose or FFA levels.

6.7 Splanchnic redistribution of blood flow during mixed-meal (IV, V)

Prior to meal administration, plasma glucose was significantly higher in patients than in controls (6.9 ± 0.9 *vs.* 5.0 ± 0.4 mM, $P < 0.001$), Soon after the ingestion of a liquid meal, plasma levels of glucose, insulin secretion and GIP increased similarly in healthy controls and obese patients before surgery (**Fig. 27A-C**). No change in plasma GLP-1 levels were observed in these groups (**Fig. 27D**). Two months after bariatric surgery fasting glucose level was significantly decreased (5.8 ± 0.9, $P < 0.01$ *vs.* pre-surgery) yet still higher to that in controls ($P < 0.05$). At post-surgery glucose, insulin secretion, GIP and GLP-1 responses (as incremental area under the curve, iAUC) were considerably higher than in controls and in patients before surgery.

After meal ingestion, healthy controls and patients before surgery exhibited similar (NS for time × group interaction) pancreatic flow response after meal ingestion, with 18.2 ± 24.7 % increase in BF rate at 20-minutes post-ingestion ($P = < 0.001$ for time factor, **Fig. 28A**), normalized at 50-minutes post-ingestion. In these two groups, increment in pancreatic flow was associated with corresponding increments in plasma glucose (**Fig. 28B**), GIP ($r = 0.57$, $P = 0.01$) and GLP-1 ($r = 0.59$, $P = 0.01$). In contrast, pancreatic BF during mixed-meal was not directly associated with insulin secretion rate. Two months after bariatric surgery, basal BF rate of pancreas tended to be lower (76.8 [65.2-106]) than pre-surgically and in controls but no statistical significance (NS) was reached for these baseline values. In contrast, at post-surgery meal ingestion resulted in 49.8 ± 43.4 % ($P < 0.05$ and NS *vs.* controls and pre-surgery, respectively) increase in pancreatic BF at 20-minutes post-ingestion.

Meal ingestion did not affect duodenal BF in healthy controls and patients before surgery (NS for time factor and time × group interaction, **Fig. 28C**), whereas jejunal BF increased approximately 30.7 (9.3-118) and 86.1 (53.3-194) % ($P = < 0.0001$ for time factor, NS for time × group interaction) at 20-minutes post-ingestion and remained elevated during the 50-minute PET-experimentation (**Fig. 28D**). Bariatric surgery did not affect basal gut BF (39.5 [33.2-51.2] and 261 [248-297] mL min^{-1} for duodenum and jejunum, respectively, all NS *vs.* controls and

obese patients before surgery). Post-surgical meal-induced flow response in duodenum was preserved when compared with controls and patients before surgery. In contrast, after surgery meal ingestion resulted in a nearly 4-fold increase in jejunal BF ($P < 0.05$ and NS *vs.* controls and patients before surgery, respectively. In the pooled data (i.e. controls and patients before surgery) increment in plasma glucose was associated with corresponding increment in duodenual BF ($r = 0.63$, $P < 0.01$) but not with jejunal BF. Moreover, after surgery duodenal flow response was positively associated with GIP excursion ($r = 0.69$, $P < 0.05$) and negatively with GLP-1 excursion ($r = -0.74$, $P < 0.01$).

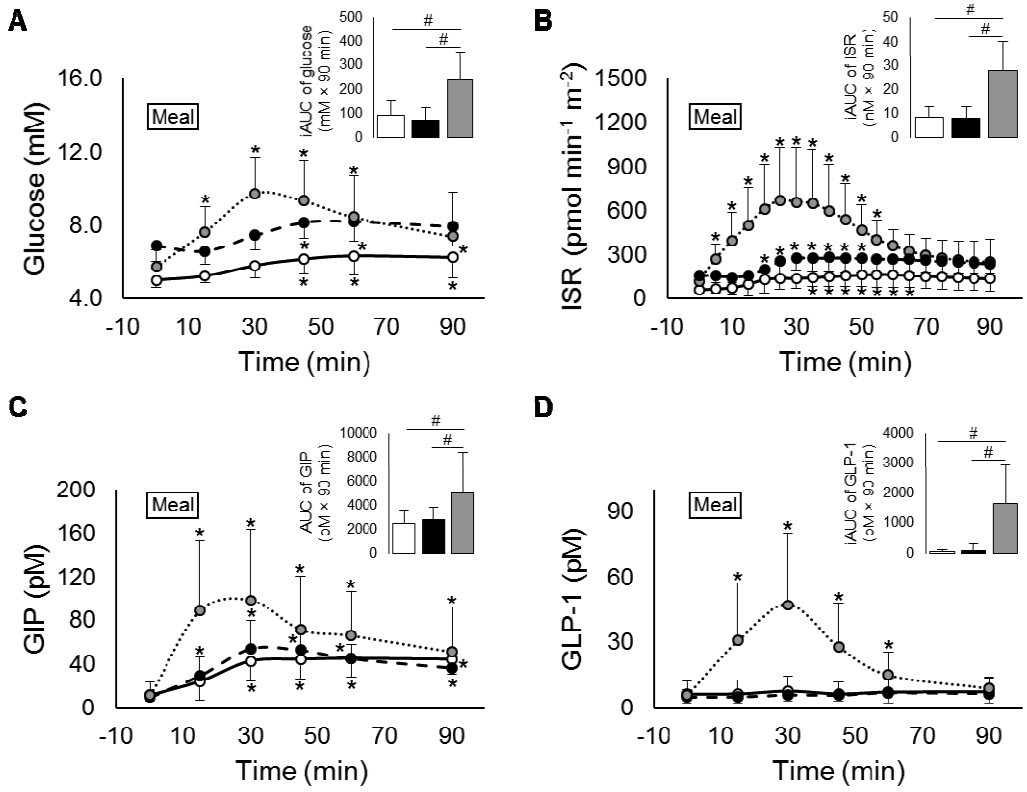

Figure 27. Plasma glucose (A), insulin secretion (derived by convolution of C-peptide concentration, B), GIP (C) and GLP-1 (D) responses during the 90-minute mixed-meal in healthy controls (white balls and bars) and patients before (black balls and bars) and two months after (gray balls and bars) bariatric surgery. Insets denote incremental areas under the respective plasma curve ($iAUC_{0\text{-}90min}$). *$P < 0.05$ *vs.* baseline in ANOVA with Tukey-Kramer's correction; $^{\#}P < 0.05$ for patients after surgery *vs.* healthy controls and patients before surgery in Student's and paired *t* test, respectively.

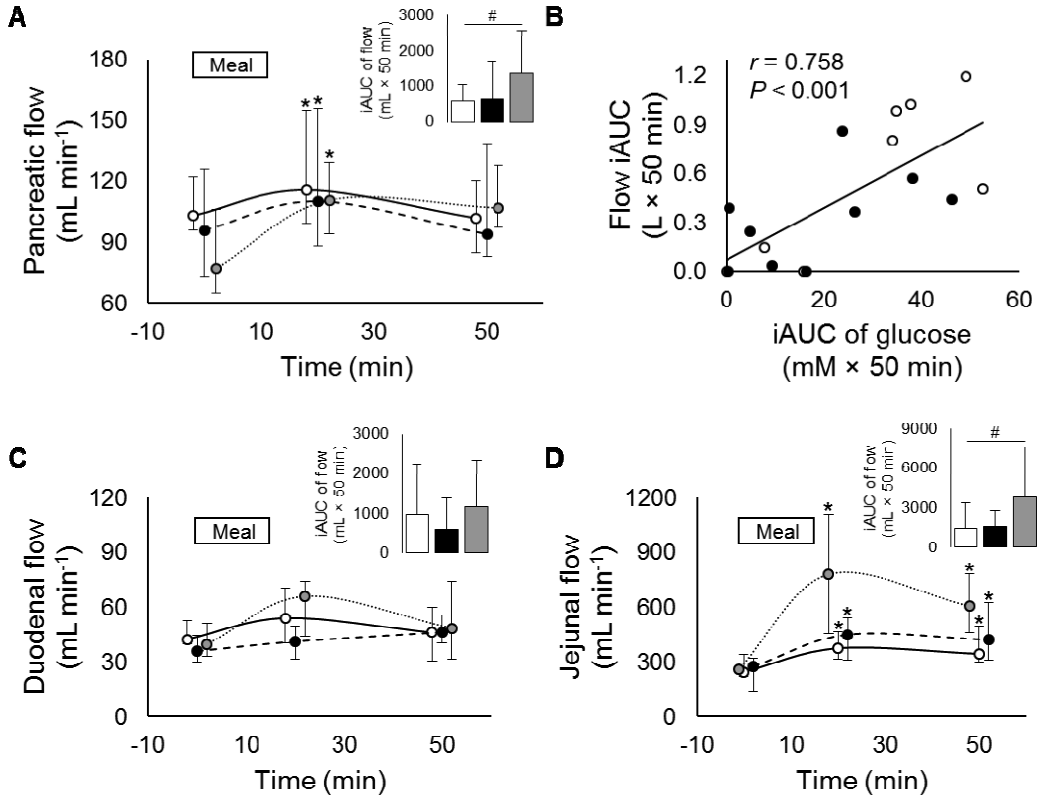

Figure 28. Pancreatic (A), duodenal (C) and jejunal (D) BF response during mixed-meal in controls (white balls and bars) and obese patients before (black balls and bars) and after (gray balls and bars) bariatric surgery. In the pooled (controls and patients before surgery) data increment in plasma glucose was a significant determinant of the magnitude of total pancreatic flow response (B). Insets denote incremental areas under the respective flow curve. *$P < 0.05$ *vs.* baseline in ANOVA with Tukey-Kramer's correction, $^{\#}P < 0.05$ in paired *t* test.

Patients allocated to different surgical procedures were similar in terms of anthropometrics, OGTT data, insulin sensitivity and β-cell function both before and after surgery. While glucose and insulin excursions were similar between the groups during mixed-meal, $iAUC_{0\text{-}90min}$ of GIP was higher in the VSG group (6.8 ± 3.8 *vs.* 3.5 ± 1.3 nM × 90 min, $P < 0.05$) than in the RYGB group, and $iAUC_{0\text{-}90min}$ of GLP-1 tended to be higher in the RYGB group (2.3 ±1.3 *vs.* 0.9 ± 0.6 nM × 90 min, $P = 0.056$), respectively. Pancreatic flow response was similar (NS for time × group interaction) between the surgical groups. Consistent with the surgical manipulation, duodenal flow response was markedly higher in the VSG group than in the RYGB group (1941 ± 902.7 *vs.* 405.2 ± 389.3 mL × 50 min, $P < 0.05$). In contrast, jejunal flow response was similar between the surgical groups (5447 ± 3972 *vs.* 2244 ± 2036 mL × 50 min, $P = 0.061$).

6.8 The effects of glucose, GIP and GLP-1 on splanchnic vasculature (IV, V)

6.8.1 Oral and intravenous glucose administration

A standard 75-gram and 0.3 g kg^{-1} *p.o.* and *i.v.* glucose tolerance tests were performed for a total of four and five healthy subjects, respectively. At baseline plasma glucose were 5.1 ± 0.4 and 4.9 ± 0.4 mM (NS between the experiments) whereas the peak glucose levels of 7.6 ± 1.6 and 12.1 ± 1.4 mM were observed at 60 and eight minutes post-ingestion/administration during OGTT and IVGTT, respectively (**Fig. 29A**). Increasing glucose levels were accompanied with an upregulation of insulin and C-peptide secretion (**Fig. 29B**). While a prominent increase in plasma GIP was observed after oral but not after intravenous glucose loading (**Fig. 29C**), plasma GLP-1 levels remained unchanged during both of the experiments (**Fig. 29D**). An initial rise and thereafter a decline in pancreatic BF was evident in both of the experiments, whereas statistical significance was reached only after *i.v.* glucose loading (**Fig. 29E**). Oral and *i.v.* glucose loading did not change BF in small intestine (**Fig. 29F-G**). After oral glucose loading, however, a tendency towards increase was observed in both of the studied intestinal segments with a peak value at 10 and 20 minutes post-ingestion for duodenum and jejunum, respectively, consistent with the passage of chyme through the small intestine.

6.8.2 GIP and GLP-1 infusion studies

Continuous 4.0 → 2.0 pmol kg^{-1} min^{-1} infusion of GIP was performed to a total of 10 healthy controls and 10 obese patients before and after bariatric surgery. Before the start of the GIP infusion, plasma levels of GIP were similar between the groups (NS) whereas plasma glucose was within the hyperglycemic range only in patients before surgery (7.0 ± 1.2 mM) but not in healthy controls (5.3 ± 0.4 mM) and patients after surgery (5.5 ± 0.8 mM). During the 60-minute infusion, supraphysiological GIP concentration was achieved (**Fig. 30A**) in all of the groups; however, incremental GIP excursion was 30-50 % higher in patients both before and after surgery than in healthy controls (P range 0.011 to < 0.001) due to the rapid weight loss in patient groups. On average, obese patients exhibited GIP excursion of a similar degree between the sessions (NS). Incremental insulin response during the infusion was considerably higher in patients before surgery than in controls (562 ± 441 *vs.* 91.3 ± 52.6 mU L^{-1} min^{-1}, $P < 0.01$), whereas after surgery mean insulin secretion (344 ± 259 mU L^{-1} min^{-1}) was lower than to that of before surgery ($P = 0.01$) but higher than in controls (both $P < 0.01$) (**Fig. 30B**). Plasma GLP-1 levels were unchanged in all of the studied groups. A stable hypoglycemic response was seen only patients before surgery (**Fig. 30C**), in whom

plasma glucose was decreased to 6.3 ± 1.1 mM ($P < 0.01$ *vs.* baseline). Pancreatic ($P = < 0.0001$ for time factor, NS for time × group interaction) BF decreased approximately 20 % and jejunal ($P = < 0.0001$ for time factor, NS for time × group interaction) BF increased approximately 100-130 % in all of the studied groups (**Fig. 30D-F**). In contrast, no change in duodenal BF was observed during GIP-infusion.

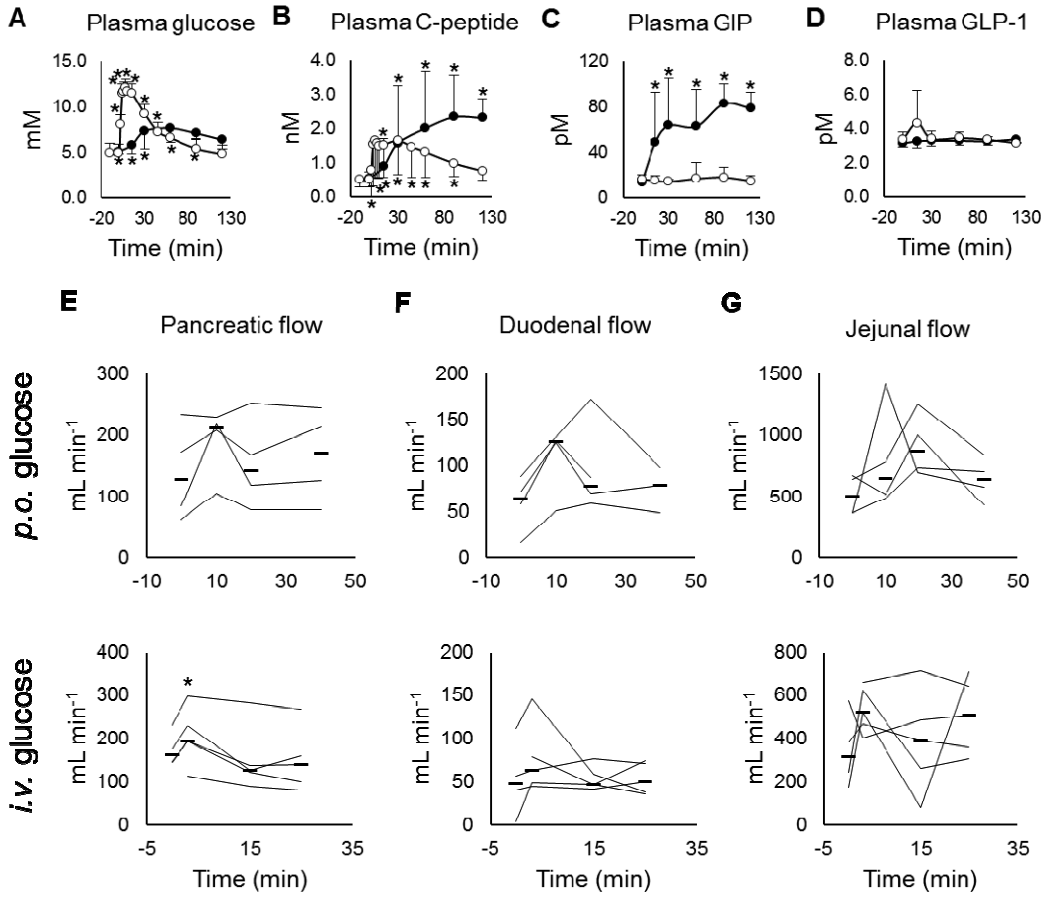

Figure 29. Plasma glucose, C-peptide, GIP and GLP-1 after oral (black balls) and intravenous (white balls) glucose loading (A-D) in a set of five healthy controls. Pancreatic (E), duodenal (F) and jejunal (G) BF after oral (upper panel) and intravenous (lower panel) glucose loading. BF data are presented as individual curves and median values. *$P < 0.05$ *vs.* baseline in ANOVA with Tukey-Kramer's correction.

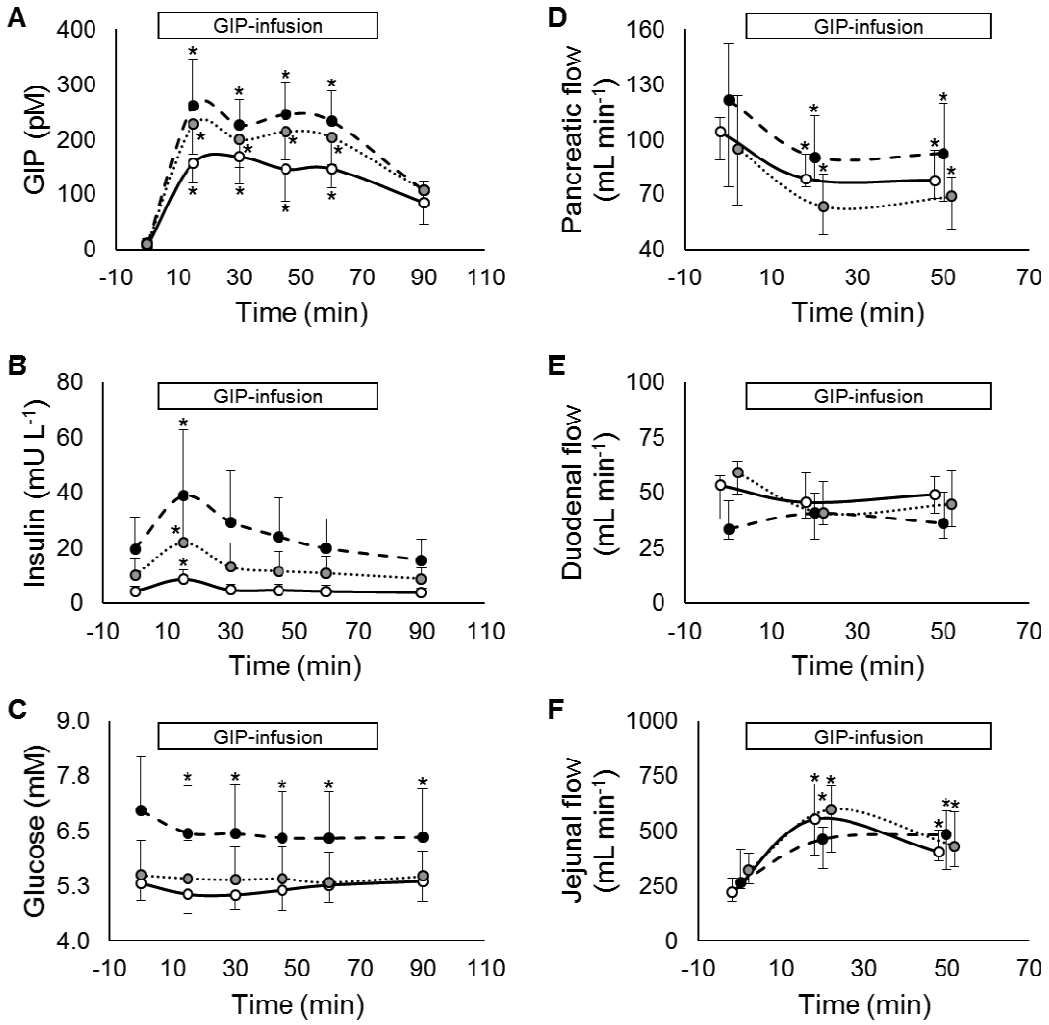

Figure 30. Plasma GIP (A), insulin (B) and glucose (C) during GIP infusion study in healthy controls (white balls and bars) and patients before (black balls and bars) and after (gray balls and bars) bariatric surgery. Plasma levels were of GLP-1 were unchanged in all groups (data not shown). Pancreatic (D), duodenal (E) and jejunal (F) BF during GIP infusion study. *$P < 0.05$ *vs.* baseline in ANOVA with Tukey-Kramer's correction.

Continuous 0.75 pmol kg^{-1} min^{-1} infusion of GLP-1 was performed to a total of 10 healthy controls. Before the start of the GLP-1 infusion, plasma glucose level was within the normoglycemic range (5.4 ± 0.5 mM, NS *vs.* baseline level before GIP infusion) in healthy controls. Throughout the infusion, supraphysiological levels of GLP-1 (50 pM, **Fig. 31A**) were achieved in all subjects. In contrast, plasma of levels of GIP did not change from basal levels. While insulin secretion was upregulated only at 15-minutes from the start of the infusion (**Fig. 31B**), a

stable hypoglycemic response to a nadir of 4.4 ± 0.3 mM ($P < 0.001$ *vs.* baseline) was observed until the discontinuation of the infusion at 60-minutes (**Fig. 31C**). Pancreatic BF (**Fig. 31D**) decreased approximately 18% (NS *vs.* GIP response) whereas no change in gut BF (**Fig. 31E-F**) was observed (NS and $P < 0.0001$ *vs.* GIP response for duodenum and jejunum, respectively).

During both of the incretin infusion studies, decrease in plasma glucose was not associated with corresponding flow responses in pancreas and intestine suggesting direct vascular regulation by incretins over a secondary response to hypoglycemia.

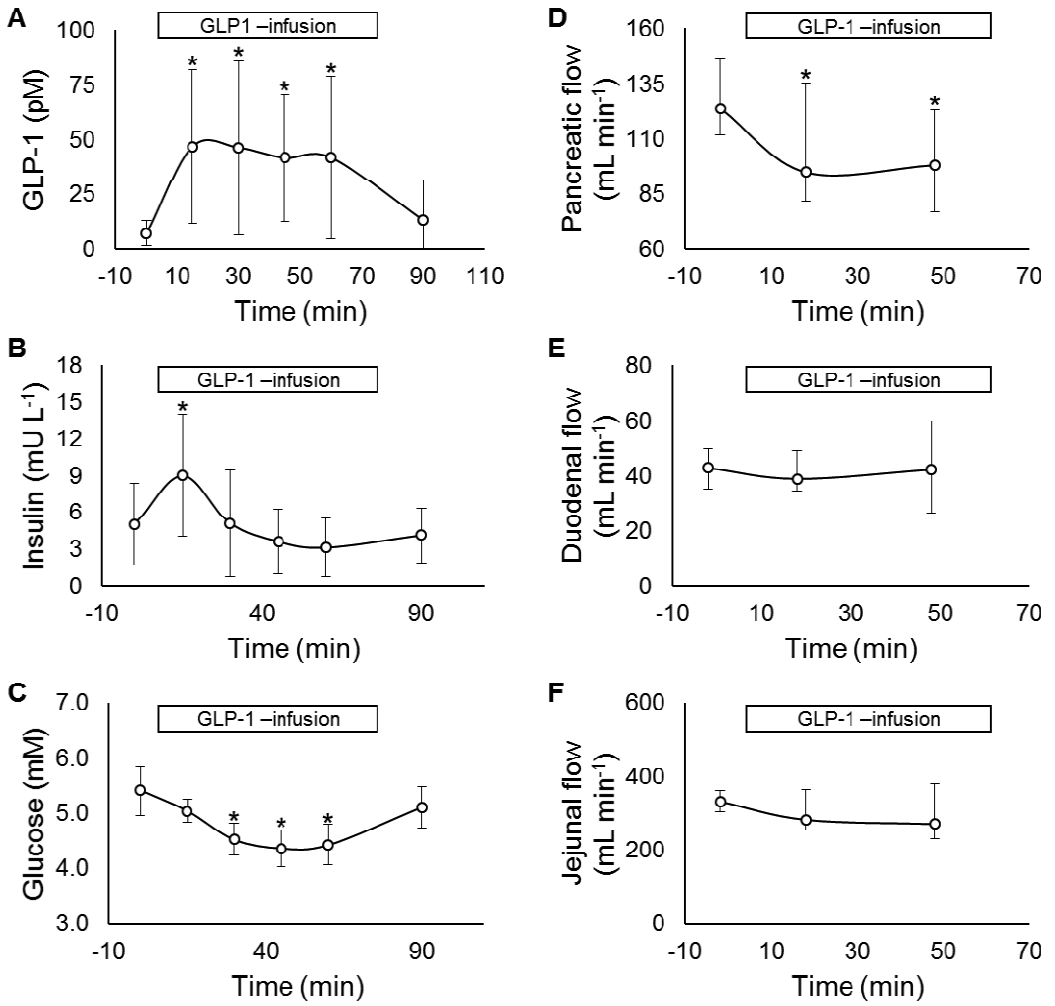

Figure 31. Plasma GLP-1 (A), insulin (B) and glucose (C) during GLP-1 infusion study in healthy controls. Plasma levels were of GIP were unchanged in the experiment (data not shown). Pancreatic (D), duodenal (E) and jejunal (F) BF during GIP infusion study. *$P <$ 0.05 *vs.* baseline in ANOVA with Tukey-Kramer's correction.

7 DISCUSSION

7.1 Study of splanchnic functions *in vivo* – framework

The methodological cornerstones of research in clinical endocrinology and metabolic diseases are the anthropometrics and clinical appearance of the patient, laboratory assays and histological samples. In the last three decades, the resolution and performance of the imaging modalities to investigate organ composition and function *in vivo* have taken giant leaps. Previous studies have introduced the use of PET for the non-invasive measurement of metabolism and BF in heart and skeletal muscle (Nuutila et al. 1992, Labbe et al. 2011, Labbe et al. 2012), subcutaneous and visceral adipose tissue (Virtanen et al. 2001, Oliveira et al. 2015), brown adipose tissue (Cohade et al. 2003, Virtanen et al. 2009), and in liver (Iozzo et al. 2003). In the present work, in studies I and III the measurement of the unidirectional [^{18}F]FDG influx of pancreas and small intestine by means of PET (*in vivo*) in healthy and obese diabetic pigs was carried out, and thereafter these values were compared to the ones obtained from tissue samples (*ex vivo*) and by using arterio-portal balance technique. This preclinical approach provided solid data that PET is a feasible and novel tool to investigate pancreatic and small intestinal metabolic rates of glucose and fatty acids and perfusion (in studies I, III and IV), the interaction of hormones and other substrates, and the effects bariatric surgery on splanchnic functions (in studies II and V) also in humans. While the splanchnic region contributes significantly to the regulation of glucose homeostasis at postabsorptive and absorptive, insulin-stimulated states (DeFronzo et al. 1992), previous methods to quantitate splanchnic metabolism including hepatic balance and double-tracer isotope technique, have proven somewhat limited or inaccessible in their ability to differentiate single organ metabolism from net substrate balance within the splanchnic region. Moreover, although the application of the ICG and thermodilution techniques provide accurate estimates of splanchnic and muscle BF, respectively (DeFronzo 1987, Baron et al. 1990), their use is limited to steady state conditions and cannot be used to estimate BF within a single intrasplanchnic organ, such as pancreas and small intestine. The application of PET, on the other hand, enables for a direct and non-invasive measurement of single organ metabolism and perfusion under various physiologic states (i.e. steady and non-steady) and experiments.

7.2 Critical evaluation of the study design and population

The present work was designed to explore the splanchnic metabolism and BF in healthy individuals, and to investigate the effects of obesity, type 2 diabetes and bariatric surgery on the former by means of multimodal imaging, especially PET.

The prerequisite for the application of novel methodology is careful validation. In studies I and III, we quantitated pancreatic and intestinal GU values *ex vivo* (tissue samples) and *in vivo* (PET data), and showed a tight correlation between the two methods. Moreover, biological distributions of ^{18}F-labelled tracers in the splanchnic region were determined with autoradiography analysis. Our preclinical data suggest that PET is a reliable tool to investigate human pancreatic and intestinal metabolism (GU, FA uptake) and BF *in vivo*.

Compared to multimodal imaging studies, our human study population was large in size, consisting of a total of 62 morbidly obese patients with (n = 30) and without T2D (n = 32), and 40 age-matched healthy controls. The anthropometric characteristics of obese patients in our study were in line with previous reports investigating the effects of bariatric surgery on whole-body metabolism (Buchwald et al. 2009, Camastra et al. 2013, Nannipieri et al. 2013, Vella et al. 2013, Bojsen-Moller et al. 2014) suggesting that our results can be generalized to larger population and also to clinical practise. However, as patients with T2D were generally well-treated (with mean HbA1c of 46 and 40 mmol mol^{-1} in studies II and V, respectively), patients with poorly controlled T2D may have different outcomes and therefore our results are not directly applicable to this patient group. Moreover, a limitation in study V is the lack of BMI-matched non-diabetic control group leading to inability to explore the relative contributions of obesity *vs.* diabetes status on the observed post-bariatric splanchnic BF responses.

Study IV was designed to investigate the physiological redistribution of BF in the splanchnic region after meal-ingestion in healthy individuals. In addition, splanchnic BF effects of intravenous glucose, GIP and GLP-1 were studied with similar PET-scan design to further clarify the role of different vasoactive mediators of the mixed-meal test. We concluded that glucose is a predominant regulator of pancreatic BF whereas GIP mainly regulates jejunal BF. In contrast, our results imply that the splanchnic vascular effects of GLP-1 are weak when compared to glucose and GIP. On the other hand, our approach had a few limitations: first, ideally the glucose profile during intravenous glucose challenge should have matched for glucose profile during mixed-meal with IIGI. Second, a more sophisticated way to determine the sole effect of GIP and GLP-1 on the splanchnic redistribution of BF is based on the administration of specific hormone antagonists together with mixed-meal, namely exendin$_{9\text{-}39}$ (Schirra et al. 1998) and Nω-nitro-L-arginine methyl ester (L-NAME, Rees et al. 1989) for GLP-1 and nitric oxide – mediated pathway of GIP, respectively. Appreciation of these limitations serve as a ground for further research.

Pancreatic GU, FA uptake, steatosis, BF at fast and during mixed-meal in obese patients were compared to control data in studies I, II, and V, respectively, and intestinal GU at fast and during euglycemic hyperinsulinemic clamp and BF during mixed-meal in obese patients were compared to control data in studies III and V, respectively. Differences in all of the measured imaging parameters were observed

between obese patients and controls, and in many cases these were associated with parameters of glycemic control, such as 2-hour glucose, fasting insulin and β-cell glucose sensitivity. Due to the cross-sectional nature of the these studies, however, causality between imaging parameters, metabolic homeostasis, and glycemic control in patients with obesity and type 2 diabetes at baseline cannot be drawn. This was in contrast to the longitudinal parts of studies II and V, where the effects of bariatric surgery on splanchnic metabolism and BF were investigated with repeated measurements, i.e. before and after surgery.

7.3 Pancreatic metabolism, fat accumulation, blood flow and glycemic control (I)

In study I, aim was set to quantitate the measures of pancreatic metabolism – namely GU, FA uptake, and extent of steatosis – and fasting BF with a combination of PET, NMRI and CT, and to relate these findings with β-cell function and insulin output rate to extent the knowledge on how obesity-induced metabolic and vascular alterations on pancreas and the islet organ contribute to the pathogenesis of T2D. *Hitherto*, pancreatic multimodal imaging studies have only focused on the differentiation, staging and aggressiveness of tumors and cysts (Komar et al. 2009, Kauhanen et al. 2015). Based on the current study it can be concluded that that obesity and insulin resistance substantially modulate pancreatic functions in parallel with changes in β-cell function in patients with T2D. Metabolic and vascular alterations in pancreas were identical in the obese subgroups (i.e. patients with and without T2D or impaired glucose regulation) suggesting that obesity and insulin resistance *per se* have an effect on pancreas whereas the intrinsic (genetic) vulnerability determines whether these alterations impair β-cell glucose responsiveness and insulin output.

In the cross-sectional study, pancreatic FA uptake at postabsoprtive state was higher whereas GU during clamp was lower in obese patients than in lean controls, irrespective of the diabetic status. While glucose toxicity, i.e. chronic hyperglycemia is regarded as one of the key pathogenic mechanisms behind impaired glucose regulation and β-cell function (DeFronzo et al. 1992, Toschi et al. 2002, Solomon et al. 2001), the concept of lipotoxicity has not been fully elucidated. In the present study, the fractional uptake rate (FUR) of long-chain fatty acids from the bloodstream did not differ between the study groups suggesting that the upregulation of pancreatic FA uptake is due to larger circulating pool of FFAs in the obese patients. Moreover, pancreatic FA uptake was inversely associated with systemic insulin sensitivity confirming the reciprocal relationship between insulin resistance and hyperlipidemia (Groop et al. 1991). So far the most convincing evidence regarding the effects of endogenous FFAs on β-cell function has been presented by Rebelos et al. (2015) who, by studying nearly 1300

individuals in the RISC-cohort, concluded that even though postabsorptive FFA levels were moderately associated with total insulin output, the high FFA levels neither associated with an impairment in β-cell glucose sensitivity at baseline nor predicted glucose intolerance in the follow-up of 3 years, and are in concert with the current results, as pancreatic FA uptake of was not associated with measures of β-cell function. However, by utilizing only single tracer measuring palmitate kinetics, the influxes of other long-chain fatty acids, oleate and linoleate, are discarded.

The preclinical data confirmed that during hyperlipidemic states (such as insulin resistance) the pancreatic islets are able to downregulate FA influx by nearly 30 % and this may partly be responsible as why high FFA levels do not lead to deterioration of β-cell function and glycemic control in the clinical setting. In contrast, GU was similar between islets and exocrine pancreas. As glucose has been shown to stimulate fatty acid transport system (pm-FATP, FABP family, CD36) (Kim et al. 2012), the decrease in pancreatic GU seen in the present clinical data may mediate the downregulated islet FA uptake and thus circumscribe the fatty acid –mediated toxicity, if any, to the β-cells.

During excessive caloric intake and obesity, the ability of subcutaneous adipose tissue to store surplus lipids is somewhat reduced and thereafter the FFAs "spilled over" from the subcutaneous fat are stored in visceral adipose tissue – contributing to insulin resistance – and parenchymal organs. Experimental rodent studies have shown that in pancreas the lipid moieties are stored as large droplets of neutral fat in the exocrine parenchyma posing no meaningful threat to the acinar cells, whereas in β-cells the FA oxidation capabilities are relatively constrained leading to low number of lipids storaged as TAGs and high apoptosis rate (Saisho et al. 2007, Kusminski et al. 2009). While the excess lipid accumulation is derived from circulating FFA pool and pancreatic FA uptake, any association between the two phenomena was not observed, possibly as the FA uptake is a dynamic phenomenon with altering rates during the feed/fast cycle whereas the rate of steatosis is relatively stable in long-term. Thus, it is justified to consider these phenomena as separate risk factors for glucose intolerance and β-cell dysfunction.

To confirm the former preclinical evidence between pancreatic lipid accumulation and β-cell dysfunction, insulin deficiency and impaired glycemic control, multiple cross-sectional studies with either CT, NMRI or ^{1}H-MRS have been executed in a clinical setting with largely opposite conclusions: while all of the studies have observed higher pancreatic fat content in the pancreata of obese and diabetic patients when compared age-matched controls, a direct negative association to measures of β-cell function and insulin secretion have been found in approximately half of the studies (Tushuizen et al. 2007, Heni et al. 2010, Lim et al. 2014), whereas in the rest of studies no clear relationship has been found (van der Zijl et al. 2011, Begovatz et al. 2015, Wicklow et al. 2015). The advantage of the present study was that the measure of pancreatic lipid accumulation was

performed both with In- and Out-of-Phase MR spectroscopy as well as with morphometrically validated CT-based method and revealed that the individual numbers were highly correlated between the methods. Moreover, while no association between pancreatic lipid accumulation and model parameters of β-cell function (i.e. glucose sensitivity, rate sensitivity, potentiation) was found, pancreatic fat was inversely related with fasting insulin levels and mean glucose during OGTT suggesting toxic effects of fat on endocrine pancreatic functions. In contrast, no difference between pancreatic steatosis rate between the diabetic *vs.* BMI- and body fat –matched non-diabetic group was found. It is of note that the high inter-individual variation in steatosis rate (min 0.0 %, max 42 %, median 16 %) and small number of participants in the diabetic group may have obliterated any potential differences.

Islets of Langerhans constitute a unique and complex organ dispersed within exocrine pancreas. Being exposed to vascular endothelial growth factor-A (VEGF-A) secreted from the β-cells during the developmental period, the endothelial cells and vascular milieu of the islets differs greatly from their surroundings (Brissova et al. 2006). Although extensive preclinical research has focused on the metabolic consequences of islet vascular function and dysfunction, it is not currently known whether pancreatic BF has an effect on glycemic homeostasis and insulin secretion. Adequate perfusion of the islets ensures the delivery of nutrients, oxygen and insulinotropic factors (such as incretins) to the vicinity of endocrine cells, and accommodates the drainage of secreted hormones into the portal vein and systemic circulation. Recent *in vitro* studies in rodents have shown that at resting (i.e. postabsorptive) state only a sub-population of islets characterized by higher perfusion rate and insulin secretory output is active whereas during times of greater metabolic needs, the rest of the "hibernating" islets are recruited (Lau et al. 2012). In the present study, a utilization of $[^{15}O]H_2O$-PET –methodology was done in a clinical setting and, while the present technology cannot fully differentiate exocrine (80 %) from islet (20 %) BF, it is likely that alterations in islet BF reflect to as a decrease or increase in whole pancreatic BF (Iwase et al. 2001). As a result, the quantification of pancreatic BF was carried out at fasting (i.e. unstimulated) state and the rate of 141 mL $100g^{-1}$ min^{-1} was detected in healthy controls, with only minute variation present between different parenchymal regions. These values are considerably higher as those reported in other GI organs (Virtanen et al. 2002, Koffert et al. 2015), and equal approximately 3.6 % of the total splanchnic (portal vein) BF. Moreover, in healthy controls pancreatic BF was associated with fasting plasma glucose levels implying a crucial role of glucose in regulating – either directly or indirectly – BF to the islet organ and exocrine pancreas.

Although the islet organ comprises only 1-2 % of the total pancreatic volume, it is characterized by a substantially higher BF rate than the exocrine pancreas, and thus it is estimated that nearly 15-20 % of the whole pancreatic BF is, in fact, diverted into the islets (Jansson 1994). In the light of this, even a minor

downregulation of pancreatic BF may have detrimental effects on β-cell function. A 30 % reduction in whole pancreatic BF in mordibly obese patients with and without diabetes was observed when compared with healthy, insulin-sensitive controls. These results are in line with preclinical evidence appreciating that during events of transient hyperglycemia an increase in islet BF is commonly seen in healthy rodents whereas in diabetic rodents a chronic islet hypoperfusion due to loss of islet capillaries is present (Li et al. 2006). Similar rates of pancreatic BF between patients with and without diabetes suggests that obesity *per se* without chronic hyperglycemia can impair pancreatic BF.

Regarding the relationship between islet BF and insulin secretory capacity, contradictory results have been presented by Reinert et al. (2013), reporting only minimal impairment in β-cell gene expression, mass and function in mice whose islet BF was reduced with VEGF-A inactivation at six months of age (i.e. at adulthood). In the pooled data pancreatic BF was linearly associated with β-cell glucose sensitivity and empirical insulinogenic index even after adjustment with insulin sensitivity and weight, suggesting that adequate pancreatic BF does have a role in the regulation of glucose homeostasis at postabsorption. Dai et al. (2013) reported that during insulin resistance states such as obesity, islet capillaries undergo vasodilatation to accommodate the greater metabolic needs of the islet organ. As the obese patients in the present study were highly insulin-resistant, a failure of such compensatory upregulation may have occurred predisposing to dysglycemia. All in all, supporting the observations in the majority of the animal studies, the study results imply that fasting pancreatic and islet BF regulates fasting glucose homeostasis by improving β-cell function and insulin secretion in healthy controls, whereas in obese patients with diabetes defects in pancreatic BF may contribute to the fasting hyperglycemia. Novel study by Hashimoto et al. (2015) suggests that this association lies behind inadequate dispersal of insulin to the efferent arterioles and portal vein rather than β-cell glucose unresponsiveness after glucose loading.

7.4 Bariatric surgery and pancreatic lipid metabolism and blood flow (II)

Bariatric surgery is regarded as the most efficient method to achieve permanent weight loss and, to those concerned, remission of type 2 diabetes and other comorbidities leading to a decrease in overall mortality (Sjöstrom et al. 2007). Despite obvious improvements in metabolic homeostasis, weight and quality-of-life, the exact mechanisms by which surgical manipulation of the GI tract mediates these outcomes are largely unknown. We hypothesized that pancreatic metabolism and BF kinetics undergo notable adaptations in response to bariatric surgery in parallel with recovery in insulin and glucose homeostasis, and thus measured the

aforementioned parameters before and six months after surgery by means of [^{18}F]FTHA- and [^{15}O]H_2O-PET and CT in a total of 23 obese patients, 10 with T2D at baseline. In the present data, bariatric surgery resulted to a striking 26 kg (23 %) decrease in weight and a notable increase in whole-body insulin sensitivity as measured with $HOMA_{IR}$ and 2h OGIS. In patients with type 2 diabetes at baseline, seven out of 10 patients was in remission at the postoperative screening visit to the research center. Moreover, the measures of β-cell function were significantly improved in both diabetic and non-diabetic subgroups. The anthropometrics, demographics and biochemical profile in the present study population were in line with previous well-designed studies investigating the effects of bariatric surgery on glucose homeostasis, incretin secretion and β-cell function (Buchwald et al. 2009, Camastra et al. 2013, Nannipieri et al. 2013, Vella et al. 2013, Bojsen-Moller et al. 2014). Thus, the imaging results can be applied to represent surgery-induced pancreatic adaptations in general population undergoing bariatric surgery.

Significant reductions in pancreatic FA uptake, steatosis and fat volume were observed at post-surgical state but still, the absolute numbers remained higher than in healthy controls (P range < 0.05 to < 0.01). In addition, while BF rate of pancreas was lower in obese patients undergoing surgery when compared with healthy controls, it decreased even further six months after bariatric procedure. The reductions in pancreatic lipid metabolic variables and BF were similar between the diabetic and non-diabetic groups, and the type of surgery did not affect these outcomes. In an elegant study by Nannipieri et al. (2013), both RYGB and VSG resulted in a similar degree of weight reduction and improvements in GLP-1 secretion, β-cell function and glycemic control suggesting that duodenal bypass offers only limited or no advantage over VSG, both of which has been shown to result in comparable rates of gastric emptying in both humans and rodents (Braghetto et al. 2009, Chambers et al. 2014).

Six months after bariatric surgery fasting plasma FFA levels were unchanged, confirming previous observations by Bojsen-Moller et al. (2014). Interestingly, despite the unchanged circulating FFA pool, pancreatic FA uptake was decreased due to smaller extraction rate, associated with the degree of weight loss. Still, no association between change in FA uptake and measures of β-cell function in the diabetic group was present implying, again, that the dynamic FFA influx may not pose a threat to the pancreatic endocrine functions. However, as Bojsen-Moller et al. observed a slight (0.13 mM) reduction in fasting FFA levels 1 year post-surgery, it is speculative whether further reductions in pancreatic FA uptake (due to combined effect of reduced FFA pool and extraction rate) may improve β-cell function after a longer follow-up. In contrast to FA uptake, however, the present sutdy provided solid evidence that the decrease in pancreatic (ectopic) fat volume after bariatric surgery and concomitant weight loss directly ameliorates glucose homeostasis. Previously, Gaborit et al. (2015) observed a 44% decrease in pancreatic TAG content six months after bariatric surgery, the results which are in

close agreement with the present data. Interestingly, in their data no change in $HOMA_{\beta}$ (despite 63% diabetes remission rate) was observed and thus the effect of reduced pancreatic TAG content on glycemic homeostasis was not evaluated. On the other hand, the present study provided an association between decreased pancreatic fat content and multiple measures of β-cell function that remained significant even after adjustment for change in weight loss and insulin sensitivity. Moreover, the three obese patients whose diabetes was not remitted exhibited almost no change in pancreatic fat volume whereas six out of seven remitters has considerable decrease in pancreatic volume. Together these data suggest that the one of the key mechanisms behind diabetes remission seen after bariatric surgery is due to resolution of pancreatic steatosis.

Interestingly, the decrease in pancreatic steatosis was not associated with the degree of weight loss suggesting that other factors in addition or irrespective of simple weight loss contribute to this phenomenon. Emerging evidence from rodent studies have suggested that gastrointestinal hormones, especially GIP (Miyawaki et al. 2002) can regulate adiposity. As incretin hormone levels were not measured in study II, the confirmation of this hypothesis cannot be made. Lastly, the current date does not exclude whether similar results can be obtained by other modes of weight-loss promoting interventions, such as exercise or diet treatment.

Before surgery, the pancreatic BF per 100 grams of parenchymal tissue at fast was 30% lower in obese patients than healthy age-matched controls. Initially, a hypothesis was made that bariatric surgery and the resulting weight loss would "normalize" i.e. increase the fasting state BF to the pancreas. Instead, even further reduction in perfusion rate not directly associated with the amount of weight loss was observed. As the increase in whole-body insulin sensitivity was inversely related with a change in pancreatic BF it is assumable that the resolution of the functional stress of the islets with lesser metabolic needs may reflect to also a decrease in whole pancreatic BF (Dai et al. 2013). However, recent report by Immonen et al. (2014) suggests that also hepatic and portal vein BF are decreased six months after bariatric surgery suggesting that the decrease in BF is not unique to pancreas and may at least partly be mediated by a decreased cardiac output (data not shown) and consequently decreased flow in celiac artery. Moreover, surgery-induced alterations in basal incretin levels may play a subtle role in the regulation of resting pancreatic arterial tone (studies IV and V, Kogire et al. 1988, Trahair et al. 2015). Despite pancreatic BF was downregulated in a group level, the additional analyses implied that the good preservation (smaller decrease) was associated with improved glycemic control irrespective of the change in weight loss and insulin sensitivity thereby supporting previous observation in study I that adequate BF to the pancreas and islet organ *in vivo* is essential for the satisfactory endocrine pancreatic functions at fasting state. In contrast, the vascular regulation of islet function (β-cell function, α-cell function) after a meal challenge is more extensively discussed in chapters 7.6 and 7.7.

7.5 Fasting and insulin-stimulated intestinal glucose uptake (III)

By means on arterio-portal balance technique and [^{18}F]FDG-PET methodology, the present study demonstrated *in vivo* that small intestine is an insulin-sensitive organ in terms of glucose disposal with nearly 3-4 –fold increases in GU during euglycemic hyperinsulinemic clamp experiment in both humans and pigs. From the autoradiography analysis performed in preclinical study, it is suggestive that most of the glucose taken up by the gut wall is actually accumulated in the mucosal (enterocyte) layer of the small intestine during postabsroptive stage. Whereas the former may not be true for the insulin-stimulated state, an additional gut wall autoradiography analysis was performed after 3-hours of 1 mU kg^{-1} min^{-1} insulin clamp for one healthy pig (data not shown) and identical results were received, i.e. 75-80 % of gut wall glucose disposal takes place in the mucosa whereas only minute amounts of glucose is taken up in the muscular layer of the gut wall. By using mean data from the human subjects (healthy and obese at postabsorptive state, healthy during clamp) and autopsy data regarding the volume of the small intestine (Snyder et al. 1975), one can calculate that the GU of the small intestine is approximately 5.6 µmol min^{-1} in the fasting state, and is increased up to 18 µmol min^{-1} during insulin stimulation. Based on previous literature (Iozzo et al. 2003), these values represent 24 % and 51 % of total liver GU at fast and during clamp, suggesting that small intestine may in fact be relatively more sensitive to insulin stimulation than liver.

Previously, the quantification of splanchnic glucose kinetics during postabsorptive and absorptive state and, during euglycemic clamp in humans has been possible with either hepatic vein catheterization (HVC) or double-tracer technique. However, these techniques are weakened by the following shortcomings: 1) at best they provide only net SGU, i.e. it is not possible to obtain estimates of hepatic GU *vs.* extrahepatic SGU, 2) in the HVC technique, the splanchnic glucose balance does allow to differentiate between unidirectional GU from endogenous (hepatic and intestinal) glucose production and 3) the HVC is cumbersome and has considerable risk for complications, such as heart arrhythmias. By applying the aforementioned techniques, well-designed studies in humans have shown that the splanchnic glucose balance/uptake is approximately 150 µmol min^{-1} and between 175-200 µmol min^{-1} at fast and during euglycemic hyperinsulinemic conditions, respectively (DeFronzo et al. 1983, Vella et al. 2001) and correspond to 24-29 % of the whole-body glucose disposal after oral glucose loading (DeFronzo et al. 1992). Using these numbers, the small intestine contributes with 3.7 and 9.0-9.3 % to the net SGU at fast and during insulinemia, respectively, and with 0.7 % to the whole-body glucose disposal during insulinemia. An overview of the splanchnic glucose metabolism at postabsorptive state and during insulin stimulation in a lean individuals can be seen on **Fig. 32.**

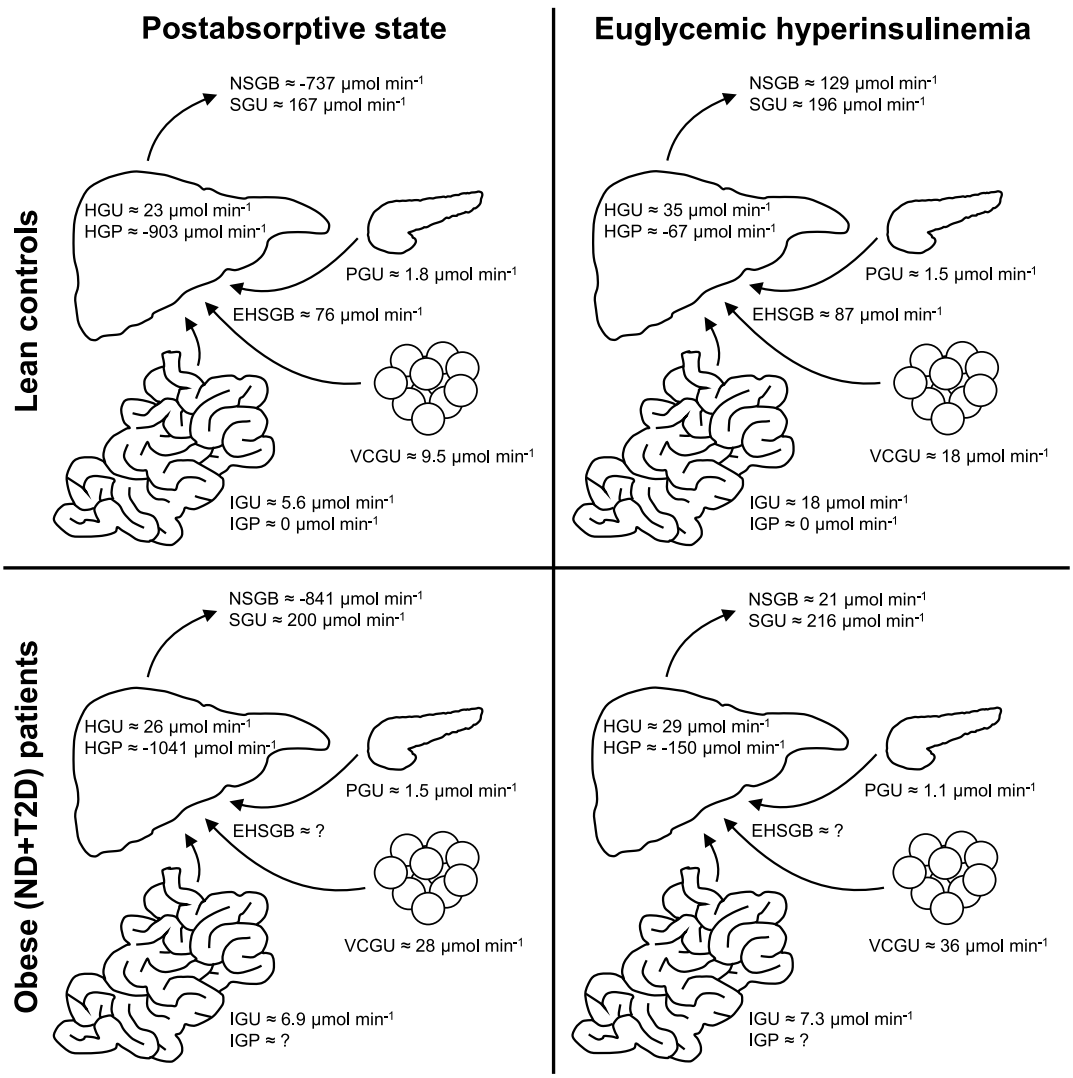

Figure 32. Glucose uptake (GU), glucose production (GP) and glucose balance (GB) in splanchnic, hepatic and extrahepatic (gastrointestinal tissues) splanchnic compartments at postabsorptive state and during 1.0-1.4 mU kg^{-1} min^{-1} euglycemic insulin clamp in healthy and obese humans. GU and GP are presented by positive and negative numbers, respectively, and expressed per depot (µmol min^{-1}). Based on research by DeFronzo et al. (1985), Barret et al. (1985), Croset et al. (2001), Iozzo et al. (2003), Honka et al. (2013 & 2014), Immonen et al. (2014), and Dadson et al. (2015). EHS, extrahepatic splanchnic; I, small intestinal; NS, net splanchnic; P, pancreatic; S, splanchnic; VC, visceral (intraperitoneal) fat.

Based on the evidence provided in the present study it is of no doubt that small intestine is a significant contributor to whole-body glucose disposal both at postabsorptive and absorptive state. The present study also provided evidence that

the extrahepatic splanchnic compartment is highly insulin-sensitive with nearly 50 % increment in extrahepatic SGU during euglycemic clamp. In the previous literature, Barret et al. (1985) measured GU in gastrointestinal tissues using the same method (portal vein balance technique) with [^{3}H]G in anesthetized dogs, inaccessible in humans. The authors concluded that the extrahepatic SGU does not change during euglycemic hyperinsulinemic clamp – although a tendency towards increase is seen after 60 minutes from the start of the clamp – whereas during combined hyperglycemia and hyperinsulinemia increases up to 300 % from baseline are observed. A few important differences in the study design and methodology between Barret's and current experiments may account for the disconcordant results. First, from the former values the contribution of small intestine to net extrahepatic SGU is only 8 and 26 % at fast and during euglycemic clamp, respectively, suggesting that most of the measured extrahepatic GU data is in fact derived from the remaining extrahepatic splanchnic organs. For instance, as shown in study I, pancreatic GU does not seem to respond to insulin during euglycemia whereas pancreatic GU was increased in obese patients with hyperglycemia (by insulin-independent mass action or GLUT1 –mediated effects). While recent study carried out in Turku PET Centre (Dadson et al. 2015) suggests that visceral adipose tissue GU responds to insulin stimulation, the net effect of insulin on extrahepatic SGU (small intestine [↑], adipose tissue [↑], pancreas [↔], ventricle [?], and spleen [?]) may be ± 0 μmol min^{-1}. Second, although 1.4 mU kg^{-1} min^{-1} continuous insulin infusion implemented by Barret et al. should completely suppress intestinal glucose production (Croset et al. 2001, Mithieux et al. 2004), the portal vein balance technique with stable isotopic tracer represents a bidirectional glucose kinetics across the extrahepatic splanchnic bed whereas [^{18}F]FDG measures the unidirectional uptake of glucose (k_4 is assumed zero, see **Fig. 10A**). The disconcordance due to glucose tracer used in the current experiments should be limited as the arterio-portal [^{2}H]G and [^{18}F]FDG differences were tightly coupled and exhibited similar results at fast *vs.* insulinemia in the preclinical study. Third, species-related differences cannot completely be ruled out. Nevertheless, future endeavors should be aimed at measuring intestinal glucose kinetics during mixed-meal, representing physiological combination of hyperinsulinemia, hyperglycemia, alimentary factors and neural regulation.

At fast, small intestinal GU was similar in healthy controls and obese non-diabetic patients. In contrast, during euglycemic clamp the intestinal GU was not upregulated in the obese patients as in healthy controls. In fact, the incremental GU (from baseline values) was decreased by striking 88 % from the values observed healthy controls during insulin stimulation. Moreover, in the pooled data intestinal GU values were in close agreement with *M*-values suggesting, again, the significant contribution of small intestinal glucose handling in the regulation of systemic glucose tolerance. Previous study by Iozzo et al. (2003) showed that insulin-stimulated GU in the liver is not impaired in patients with normal glucose

tolerance but low systemic insulin sensitivity (IS) when compared with normal- and high-IS groups. As the obese patients in the present study were normally glucose tolerant, it is likely that the defects in insulin action on small intestine occurs early in the pathogenesis of metabolic diseases and precedes any impairment in systemic glucose regulation. Unfortunately, PET technique does not allow to examine the molecular mechanisms behind impaired insulin-dependent GU in the enterocytes in obesity, resulting either from defective glucose internalization, the lack of suppression of glucose production, or the combination of the two. The latter scenario is strengthened by Gutierrez Repiso et al. (2015), who observed significant increases in PEPCK and Glc6Pase mRNA expression in intestinal cell excised during bariatric surgery in obese non-diabetic patients with high insulin resistance when compared with low insulin resistance group. While studies in rats have shown that after 6-h fast the rate of intestinal gluconeogenesis is virtually zero and is increased only after prolonged starvation (Croset et al. 2001), it cannot be excluded that during insulin resistance states the enterocytes contribute to upregulated hepatic glucose production by supplying more gluconeogenetic substrates such as lactate and alanine irrespective of the nutritional state (Mithieux et al. 2006). Saeidi et al. (2013) observed reprogramming of the jejunal Roux-limb in gastric bypass –treated rats leading to upregulation of GLUT1, enhanced basolateral GU and hypertrophy of the mucosa suggesting that the defective intestinal insulin signaling may be reversed by either drug intervention (metformin, rosiglitazone) or with bariatric surgery. Future humane studies are urgently needed to verify these observations.

7.6 Physiology of splanchnic circulation during meal and associated factors (IV)

The splanchnic vascular bed is perfused by the celiac (CA), and superior (SMA) and inferior mesenteric arteries. Perfusion to the ventricle and pancreas is supplied by the CA whereas small intestine receives it's BF via the mesenteric – primarily SMA – arteries. The distribution of BF within the gut wall is not uniform, and in the fasting state mucosal layer receives about 80 % of the total blood perfusing the bowel wall (Chou & Coatney 1994). Absorption of nutrients from intestinal lumen produces segment-specific hyperemia, persisting as long as the chyme remains in that bowel segment. The intestinal mucosa is the site of nutrient absoption and in general BF to bowel wall is autoregulated by metabolic factors such as pH, osmolarity, CO_2, and adenosine. Previous studies (Chou et al. 1972, Kvietys et al. 1980, Kvietys et al. 1981, Chou et al. 1985) have shown that lipids, fats and bile acids are the most potent inducers of BF followed by glucose and proteins.

Hypothetically and partly based on previous literature, meal ingestion alters the vascular milieu within the GI tract to accommodate nutrient absorption in the gut

(Matheson 2000), insulin secretion (Carlsson & Jansson 2015) and hepatic metabolism (Meier et al. 2005). The present study documented *in vivo* that jejunal and pancreatic BF are increased by *circa* 70 and 20 %, respectively, rapidly after meal ingestion. The vast difference in the magnitude of flow upregulation between small intestine and pancreas may derive from several aspects: first, pancreatic flow response is dependent only on the levels of circulating vasoactive substances and of neural factors (Jansson 1994), while postprandial hyperemic response of the gut described above is largely caused by a direct contact of chyme to the mucosal layer. Second, as a large proportion of the initial splanchnic GU after meal ingestion is occurring in the gut rather than in pancreas (see studies I and III), the stimulated gut perfusion may accommodate elevated metabolic rate and associated processes, such as waste removal (Chou et al. 1994). A schematic representation of the splanchnic vascular responses after meal is shown on **Fig. 33**.

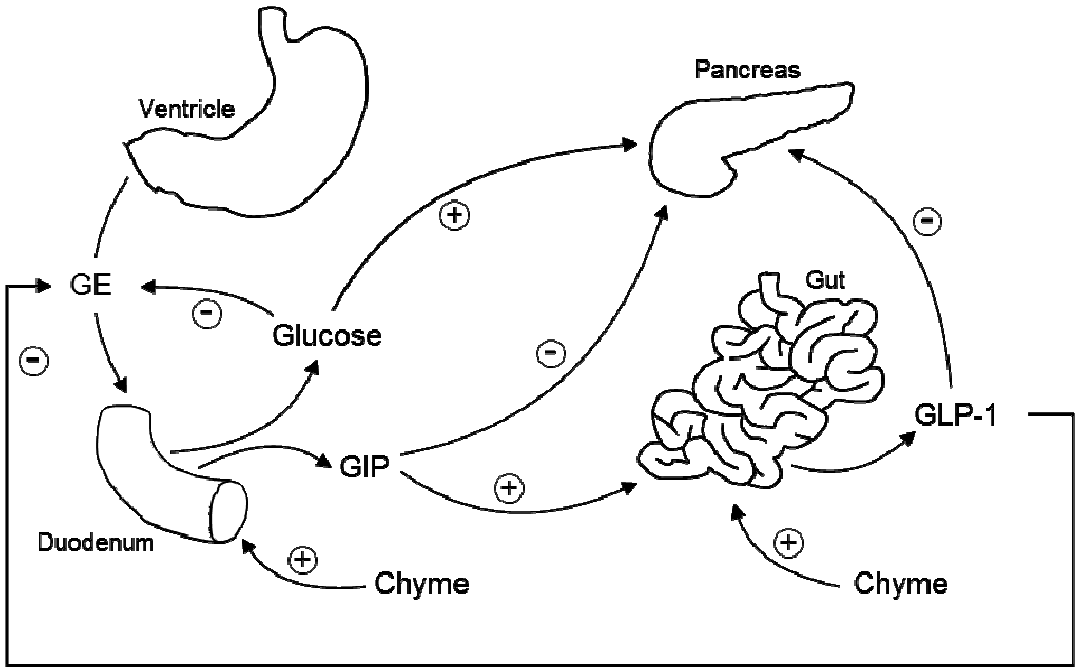

Figure. 33. The contribution of chyme:mucosa interaction, glucose and GIP on splanchnic vascular redistribution and on gastric emptying (GE) after a meal ingestion. Stimulation and inhibition are presented as plus and minus signs, respectively. The schematic representation is based on research by Nauck et al. (1997), Rayner et al. (2001), Koffert et al. (2016).

In contrast to jejunum, duodenal BF remained unchanged during mixed-meal. This suggests that the main physiological role of the proximal small intestine (i.e. the foregut) is, in fact, unrelated to its absorptive capabilities but in its role as nutrient-sensing (Carlsson et al. 1999, Gribble et al. 2012, Breen et al. 2012) organ.

Previous rodent studies have shown that pancreatic islets respond to alterations in plasma glucose levels by decreasing or increasing their perfusion rate (Jansson 1994, Jansson et al. 2007), while no change in total pancreatic and gut BF rate has been demonstrated during experimental hyperglycemia. However, the previous data have been obtained using the microsphere-technique and essentially lack the dynamic information of the splanchnic vasculature after glucose loading. On the other hand, the present study applied standard *i.v.* glucose tolerance test in a total of five healthy subjects with simultaneous quantification of splanchnic flow responses in a time-dependent fashion. This allowed to distinguish the solitary role of glucose on splanchnic circulation without the concomitant effects of incretins and chyme:mucosa interaction. After *i.v.* glucose bolus injection, an immediate increase in total pancreatic BF was observed, and this was accompanied with a significantly stimulated insulin and C-peptide secretion throughout the 2-hour experiment. Interestingly, already at 15-minutes post-injection the total pancreatic BF had returned to sub-basal levels despite considerable hyperglycemia. Based on the rodent data this rapid normalization is likely caused by decreased vagal stimulus whereas the methodology utilized in the present study fails to provide detailed information on the islet BF, which has been shown to stay upregulated for longer periods after glucose challenge (Carlsson et al. 2001). Nevertheless, based on the present study it is suggestive that in humans the glucose-stimulated insulin secretion (GSIS) is dependent on the early upregulation of the total organ BF, permitting nutrient entry to the islets and insulin drainage to the portal vein.

In accordance with the previous literature, the redistribution of blood into the gut seemed to be elicited by chyme and bile salt contact with the mucosal layer. After oral glucose load intestinal BF showed increasing tendency but lacked a promt rise in flow response due to a small number of study subjects. In contrast, gut BF remained unchanged after *i.v.* glucose challenge suggesting that hyperglycemia *per se* does not contribute to the increase in gut BF seen after meal ingestion.

In addition to their endocrine and metabolic effects, receptors for both GIP and GLP-1 (GIPR and GLP-1R) have been identified in the endothelial and smooth muscle cells of the arterioles and the vascular effects of incretins – especially that for GLP-1 – have been linked to cardioprotection and endothelium-dependent vasodilation (Zhong et al. 2000, Koska et al. 2015). While previous studies in cultured cells and canine *in vivo* have suggested that incretins may regulate splanchnic BF kinetics at absorptive state (Kogire et al. 1988, Hattori et al. 2010), their involvement in postprandial hyperemia is not clear because the levels of active incretin hormones measured from the systemic circulation are lower than the minimum doses required to produce vasodilatation (Chou et al. 1994). However, local tissue concentrations of these hormones, especially in the prehepatic vasculature, are high enough to exert their vasoactive properties (Lu et al. 2008). In the current study, the concentration of incretins were experimentally elevated to the

supraphysiological levels to mimic postprandial conditions and the effects of GIP and GLP-1 on splanchnic flow redistribution was verified *in vivo*. Interestingly, infusion of GIP provoked largely contradictory results, with prominent increase in jejunal BF and stable decrease in pancreatic BF. Both of the incretin infusions led to an upregulated yet transient insulin secretion, consistent with the previous literature (Meier et al. 2004). These results suggests that in humans GIP may "prepare" hindgut for the increases in metabolic demand, accompanied with parallel increase in insulin secretion. Previous rodent study (Svensson et al. 1997) implied that GIP may in contrast dilate the arterioles of the islets encouraging to assume that the GIP-induced decrease in total pancreatic BF seen in the present study may simply reflect a decrease in exocrine pancreatic flow instead of the islets. Since GIP does not affect directly the CA flow (Kogire et al. 1988), it is likely that the vascular effects of GIP on pancreatic parenchyma are direct in nature. Interestingly, during mixed-meal the total pancreatic BF was returned to baseline rather early (50 minutes) after meal ingestion despite increasing glucose levels. Therefore, we postulate that increases in plasma GIP levels (reaching a *plateau* at 30 minutes post-ingestion) optimize pancreatic vascular milieu by shunting the perfusion from the exocrine pancreas to the islets.

In contrast, the increase in jejunal BF elicited by GIP is in concert with studies documenting augmentation of SMA flow after GIP bolus administration (Kogire et al. 1988, Fara & Salazar 1978). Previous studies in conscious animals failed to show any vasodilatation in the gut wall arterioles in response to postprandial incretin levels indicating that the observed GIP-induced gut hyperemia is likely caused by the elevation in SMA flow (Chou et al. 1994).

Compared to GIP, the splanchnic vascular effects of GLP-1 were modest and constituted only of a decrease in pancreatic BF and unchanged gut BF. Previous studies in healthy Wistar rats support current observations that GLP-1 does not regulate intestinal BF at postabsorptive state (Svensson et al. 2007), whereas the authors managed to identify the GLP-1 –induced attenuation of pancreatic BF only after glucose administration but not during fasting conditions. The disconcordance in results may arise from differences in experimental protocols (bolus injection *vs.* constant infusion); moreover, species-related factors cannot be ruled out. If any, the vascular effects of GLP-1 are likely to be more potent during postprandial and hyperglycemic conditions and may serve partly in a similar way as GIP to simultaneously potentiate insulin secretion and shunt the blood away from pancreas/islets (and possibly from the gut) to the systemic circulation to accommodate peripheral metabolism.

7.7 Splanchnic circulation in obesity and early after bariatric surgery (V)

In previous study (II), a total of ten patients with T2D were subjected to undergo bariatric surgical procedure and, at post-surgical screening six months after the surgery, observed over 20 % decrease in body weight. This was accompanied with significant reductions in fasting and 2-hour plasma glucose, HbA1c, and increases in insulin sensitivity and measures of β-cell function. In contrast, study V was designed to investigate the metabolic and vascular outcomes of bariatric surgery early after the operation in a set of 10 patients with T2D. Interestingly, while the weight loss (14 %) was significantly minor in these patients studied at two months post-surgery when compared to patients studied at six months post-surgery ($P < 0.05$ *vs.* study II), their fasting plasma glucose were similarly improved. Moreover, the post-OGTT insulin and glucose response were markedly and similarly improved in both of these post-surgical (i.e. 2– and 6-mo) groups suggesting that the surgery-specific manipulation of the GI anatomy outweights the metabolic consequences of weight loss *per se*. These results are in concert with longitudinal studies by Nannipieri et al. (2013) and Bojsen-Moller et al. (2014) implying that while the improvement in insulin sensitivity is mainly determined by weight reduction, resolution of β-cell function is based on the stimulation of postprandial incretin effect. This hypothesis is further supported by an elegant study by Laferrère (2008), wherein bypass surgery resulted in a significantly increased incretin effect and decreased glucose when compared with matched patients who where subjected to diet-induced equivalent weight loss. In summary, our and others' results clearly suggest that the improvement in dysglycemia and remission of diabetes after bariatric surgery is mainly due to the altered GI anatomy and increased gastric emptying rather than weight loss or ventricular restriction.

After surgical manipulation of the GI tract, meal ingestion was followed by a rapid gastric emptying and small intestinal nutrient exposure, as indirectly indicated by preponed appearance of glucose and GIP into the bloodstream and, consequently, largely enhanced pancreatic and jejunal BF responses.

Circulating glucose is a significant regulator of total pancreatic BF *in vivo* after a meal ingestion (see study IV). While plasma glucose elevation above baseline was postponed in obese patients before surgery when compared with controls, the total pancreatic BF rose similarly in both of these groups at 20-minutes post-ingestion suggesting operational neural (cephalic) factors (Carlsson et al. 2002). In contrast, at post-surgery nearly 50% increase in total pancreatic BF was observed after meal-ingestion. While a prominent leftward shift of plasma glucose time course (with peak a value 3.9 and 2.3 mM higher at 30-minutes post-ingestion than in other groups) occurred in parallel with pancreatic BF increase, glucose was not directly associated with total pancreatic flow increment at post-surgery. These data

suggest that additional factors, such as intestinal glucoreceptors and jejunal nutrient sensing (Carlsson et al. 1999, Breen et al. 2012), are potential regulators of pancreatic BF at post-surgical state. In contrast to glucose and intestinal transit *per se*, the current study provided further evidence that incretins play a little role in the regulation of pancreatic flow at postprandial state. This is indicated in the post-surgical data, wherein pancreatic perfusion rose similarly in RYGB and VSG treated patients despite large differences in incretin milieu.

The findings that small intestinal BF responses – unchanged in duodenum and increased in jejunum - after a meal ingestion were identical in patients before surgery and in lean controls suggests that the gut vascular regulatory orchestra remains intact after the onset of morbid obesity and diabetic state. This was evident in the present data, as the glucose excursion (an indirect measure of gastric emptying, Marathe et al. 2013) and GIP response during the 90-minute mixed-meal were similar in both of the groups. In contrast, two months after bariatric surgery small intestinal BF, especially in jejunum, was markedly upregulated after meal ingestion. Based on the early peak in plasma glucose at 30-minutes post-ingestion, it is suggestive that much of the increase in small intestinal BF is related to rapid gastric emptying, observed both after Roux-en-Y gastric bypass (Marathe et al. 2013) but also after vertical sleeve gastrectomy (Chamber et al. 2014). However, the results of the present study imply that, in addition to the direct chyme and bile salt –mediated acceleration in perfusion, GIP and GLP-1 have notable roles in the redistribution of splanchnic BF at post-surgical state. This can be deduced from the differences in jejunal BF responses after meal ingestion between the two surgical groups: patients in the VSG and RYGB group exhibited 213 (155-331) and 61.5 (58.8-70.8) % increase in jejunal BF at 20-minutes post-ingestion *vs.* baseline, respectively. Based on the identical glucose appearance within the first 30 minutes post-ingestion, it is likely that the small intestinal nutrient exposure between these two surgical groups were of similar degree. In contrast, a major difference in the incretin levels during mixed-meal can be seen between the groups with mean GIP-to-GLP-1 concentration ratios being 12:1 and 2.2:1 for VSG and RYGB groups, respectively (data not shown). We postulate that a promt rise in glucose levels accompanied by GLP-1 burst at post-ingestion induces a vast increment in insulin secretion rate in RYGB group explaining better postprandial glucose control. Hypothetically, the inadequate pooling of blood within the splanchnic region may postpone the delivery of insulin and other glucoregulatory hormones into the peripheral vasculature (Baron et al. 1990), contributing to the lower diabetic remission rate in VSG than in RYGB. However, further studies are needed to validate these presumptions.

Multiple studies have shown that after the onset of diabetic state the secretion of GLP-1 during meal is impaired and the dose-response curve is preserved, whereas the secretion GIP is preserved but the insulinotropic activity is reduced (Holst et al. 2009, Nauck et al. 1993). It was hypothesized that this so-called “GIP resistance” is

present in the vascular smooth muscle cells in diabetic patients. However, the current study showed that the during the 60-minute GIP infusion, pancreatic BF decreased and jejunal BF increased to a similar extent in all groups. As the insulin secretion rate during the 60-minute experimentation was also similar between the groups (data not shown), the present data supports the observations by Meier et al. (2004) that a specific defect in the GIP receptor and postreceptor signaling in vascular smooth muscle and β-cells is unlike.

Taken together, the splanchnic vascular responses to meal ingestion are markedly increased early after bariatric surgery accommodating nutrient absorption and insulin secretion. While much of this increase is caused by the rapid gastric emptying and nutrient exposure to the small intestine, the contribution of GIP cannot be discarded especially in VSG treated patients. Furthermore, a conclusion is made that the splanchnic vascular effects of GIP are preserved in hyperglycemic patients.

8 SUMMARY OF THE FINDINGS

The results of the preclinical data support the notion that PET coupled with radiotracers [^{18}F]FDG, [^{18}F]FTHA and [^{15}O]H_2O is feasible and reliable method to non-invasively quantitate GU, FA uptake and BF in the splanchnic region, notably in pancreas and small intestine. Based on the arterio-portal balance technique the behavior of [^{18}F]FDG in the extrahepatic splanchnic compartment is similar to that of its radioactively stable counterpart [^{2}H]glucose. In contrast to previous studies, current work in a pig model showed that hyperinsulinemia upregulates extrahepatic SGU over 50 % despite normal glucose levels. However, from the preclinical data the exact location of this increased GU within the extrahepatic splanchnic (gastrointestinal) region could not be evaluated. While radiation dose introduced to patient and high cost reduce the assessment of PET in a routine practice, molecular imaging can be perceived as a complementary tool in the investigation of metabolic diseases affecting splanchnic region.

Exogenous insulin administration had only minute effect on pancreatic GU in healthy controls and obese patients, respectively. The latter is likely due to resolution of the mass-action effect of glucose during euglycemic clamp. In contrast, while GU in small intestine was increased 2-3 fold in healthy controls, insulin had no effect on intestinal GU in obese non-diabetic patients suggesting that intestinal insulin resistance is an early defect in the pathogenesis of impaired glucose regulation and type 2 diabetes. While the current data does not account whether the lack of insulin effect on GU of small intestine is either due to decreased internalization of glucose, incomplete suppression of intestinal gluconeogenesis, or a combination of the two, it is possible that disturbancies in gut glucose handling affect gut:microbiome interaction, incretin secretion and nutrient absorption warranting further research. Furthermore, disturbed insulin signaling in the gut wall may prove to be a reasonable target for pharmacotherapy with agents increasing insulin sensitivity, such as biguanides.

Obesity is associated with increased FA uptake and steatosis of pancreas irrespective of the glycemic status of the patients suggesting that overweight and obesity *per se* rather than hyperglycemia affect pancreatic lipid metabolism. Despite these findings, FA uptake was not associated with impaired insulin secretion or β-cell glucose sensitivity. Present rodent data suggested that pancreatic islets are in fact able to compensate for hyperlipidemia, evident in obesity and insulin resistance states, by downregulating FA uptake serving as a physiological explanation why we and others have failed to verify the lipotoxicity-consept in humans. In contrast, pancreatic steatosis was independently associated with impaired insulin secretion and glycemic homeostasis, suggesting that excessive lipid accumulation – rather than passive FA uptake from bloodstream to pancreas – leads to oxidative stress, toxic metabolic pathways and high apoptosis rate in the pancreatic β-cells. In concert with this cross-sectional data, bariatric surgery lead to

a marked decrease in steatosis rate without altering the non-fat (parenchymal) mass of the pancreata in parallel with upregulation of β-cell function. As the weight loss *per se* was not directly associated with the resolution of pancreatic steatosis, further research is implicated to clarify the role of weight loss –independent mechanisms (incretin secretion, neural factors) of surgical manipulation of the GI tract to the improved pancreatic lipid metabolism.

Pancreatic BF was impaired in obese patients with and without diabetes despite their larger pancreatic volume due to lipid accumulation. Based on the high relative BF to the pancreatic islets at both postabsorptive and absorptive state, it is suggestive that this decrease in pancreatic BF is at least partly due to the specific impairement in islet perfusion supporting previous studies in animal models of obesity and diabetes. In the cross-sectional data, impaired pancreatic/islet BF rate was associated with both β-cell glucose unresponsiveness and insulin secretory defect implying that inadequate islet BF attenuate both glucose and non-glucose insulin secretagogue delivery to the islets as well as insulin drainage from the islets. Surprisingly, however, six months after bariatric surgery pancreatic BF was further decreased in parallel with the surgery-induced increase in insulin sensitivity and thus lesser metabolic needs. Despite the groupwise decrease in pancreatic BF, those diabetic patients who had a good preservation in pancreatic BF had more favorable fasting glucose levels emphasizing the relevance of adequate pancreatic/islet perfusion on normal endocrine functions of pancreas. As no linear association between total pancreatic BF and insulin secretion during meal was observed, it is plausible that the relevance of pancreatic BF on glycemic homeostasis is more emphasized during the postabsorptive rather than during the absorptive state.

Meal ingestion is followed by a diffuse upregulation of splanchnic BF in both lean controls and obese patients with diabetes. In this physiological redistribution phenomenon, glucose, incretin hormones GIP and GLP-1, and neural factors have a significant contribution. Elevation in plasma glucose is associated with an increase in pancreatic BF whereas GIP increases small intestinal and decreases pancreatic BF. After bariatric surgery splanchnic vascular responses are largely enhanced and regulate intermediary metabolism by affecting nutrient absorption and hepatic and peripheral metabolism. While rapid small intestinal nutrient exposure may partly explain these post-surgical vascular responses, it is likely that the preponed glucose appearance and GIP-to-GLP-1 concentration ratio in the preportal circulation mainly determine the observed vascular outcomes within the splanchnic region after meal ingestion.

9 CONCLUSIONS

I. PET is a feasible method to quantitate pancreatic and intestinal GU, FA uptake, and BF. [^{18}F]FDG biodistribution is homogeneous within the pancreatic parenchyma whereas the majority of gut wall [^{18}F]FDG is preferentially accumulated in the mucosa.

II. Obesity impairs pancreatic GU and BF, and enhances pancreatic FA uptake and steatosis. These outcomes are irrespective of the diabetes status. High rate of pancreatic steatosis associates with lower insulin levels.

III. Bariatric surgery decreases pancreatic FA uptake and steatosis, and the decrease in latter correlates with increased insulin levels suggesting that reversal of pancreatic fat metabolism contributes to the beneficial metabolic effects of bariatric surgery.

IV. Insulin stimulates duodenal and jejunal GU in healthy individuals, whereas in glucose-tolerant obese subjects insulin does not elicit measurable increase in small intestinal GU suggesting obesity-induced intestinal insulin resistance.

V. Mixed-meal ingestion increases pancreatic and jejunal BF and unchanges duodenal BF. Of these responses, glucose affects pancreatic BF and GIP affects jejunal BF, respectively. In contrast, infusion of exogenous GLP-1 decreases pancreatic and unalters duodenal and jejunal BF, alluding it's lesser role in the regulation of splanchnic redistribution of BF after a meal.

VI. Bariatric surgery leads to marked increases in pancreatic and jejunal BF responses at postprandial state. In addition, duodenal BF is enhanced in VSG-treated but not RYGB-treated subjects. Bariatric surgery does not alter splanchnic BF responses elicited by the infusion of exogenous GIP.

ACKNOWLEDGEMENTS

This study was conducted within the Finnish Centre of Excellence in Molecular Imaging in Cardiovascular and Metabolic Research, and was carried out in Turku PET Centre, University of Turku, Turku, Finland, during the years 2010-2016.

I am deeply grateful to my supervisors professor Pirjo Nuutila, docent Patricia Iozzo and docent Jarna Hannukainen for all the guidance and kind support through these years. I have been honored to work with Pirjo Nuutila, one of the international leaders in the field of metabolic imaging, to deepen my knowledge and unravel scientific discoveries. Her constant enthusiasm, immense experience and respectful attitude has encouraged me to continue a career in the academia and also strengthened my clinical specialization to internal medicine, endocrinology and diabetology. I have always enjoyed our meetings and appreciated her feedback and criticism towards my work. Thank you Pirjo for everything; without you this work would have not been possible. I owe my sincere thanks to Patricia Iozzo, who has substantially contributed to this work and helped me to evolve as a researcher. Patricia, I have always admired your profound knowledge in isotopic methodology and metabolism, and hope that I manage to reach this point in future. Jarna Hannukainen is acknowledged for all her help in the practical issues, especially in my early years.

I am grateful to professor emeritus Jorma Viikari and professor Markus Juonala for granting me a permission to conduct this work at the Institute of Clinical Medicine, University of Turku. Professor Juhani Knuuti, a director of Turku PET Centre, is acknowledged for providing outstanding facilities and resources. Docent Veikko Koivisto and docent Kirsi Timonen are thanked for their constructive and insightful comments to my thesis which helped to improve this work. Vice dean Risto Huupponen and professor Jussi Pihlajamäki are acknowledged for their contribution in the supervisory committee of this thesis.

I have had an opportunity to meet exceptionally bright and like-minded individuals, some which I consider as my closest friends. In particular, Henry Karlsson and Jetro Tuulari are thanked for all the moments I have been privileged to share with, both in Finland and abroad in conferences. You have made these years as one of the best period in my life and I hope that our friendship continues now that all three of us have reached the “post-doc era”.

I want to express my gratitude to professor Leif Groop for establishing a successful collaboration between researchers of Universities of Lund and Turku. Professor Nils Wierup and research engineer Andreas Lindqvist are acknowledged for their collaboration and valuable (and not to mention, fun) moments we have shared.

This work would have not been possible without the help of the personnel of Turku PET Centre and University of Turku. Research nurse Mia Koutu, secretary Mirja Jyrkinen, radiographers Minna Aatsinki, Anne-Mari Jokinen, Hannele

Lehtinen, Johanna Pasanen and Tiina Santakivi, and laboratory nurses Hanna Liukko-Sipi, Heidi Partanen, Emilia Puhakka, Eija Salo, Sanna Suominen and Tiina Tuominen are thanked for making the data collection a smooth and enjoyable process. Marita Kailajärvi is thanked for her administrative contribution. Rami Mikkola and Marko Tättäläinen are acknowledged for their help in the IT issues, and Timo Laitinen, Sauli Piirola and Harri Merisaari for providing an easy-to-use Carimas-software for data analysis. Physicists Virva Saunavaara, Mika Teräs, Jarmo Teuho and Tuula Tolvanen offered invaluable help in technical issues. A special thanks go to Nobu Kudomi, Vesa Oikonen and Hannu Sipilä for helping in the modelling of the data. Ville Aalto, Saija Hurme and Irina Lisinen are acknowledged for the statistical help.

I want to thank my fellow researchers of Turku PET Centre, especially Kati Alakurtti, Robert Badeau, Marco Bucci, Prince Dadson, Laura Ekblad, Joonas Eskelinen, Miikka Honka, Ville Huovinen, Aino Hyypiä, Heidi Immonen, Tamiko Ishizu, Jarkko Johansson, Juho Joutsa, Kari Kalliokoski, Jukka Koffert, Kalle Koskensalo, Minna Lahesmaa, Linda Landini, Kirsi Mikkola, Kumail Motiani, Jaakko Mäkinen, Lauri Nummenmaa, Tam Pham, Juho Raiko, Eero Rissanen, Tiina Saanijoki, Miikka Tarkia, Lauri Tuominen, Kirsi Virtanen and Mueez Y Din for building a scientific athmosphere where I have had an opportunity to engage into innumerable inspiring conversations and happy moments. Moreover, co-authors of the original communications Veronica Fagerholm, Saila Kauhanen, Riitta Parkkola, Anne Roivainen, Paulina Salminen, Antti Saraste, Christoffer Stark and Minna Soinio are acknowledged. Especially I would like to express my gratitude to Andrea Mari for his invaluable contribution in the preparation of the manuscripts but also for discussions that have refined my view of science in general. Endocrinologists Hannu Järveläinen, Niina Matikainen and Milla Rosengård-Bärlund, and internist Sanna Kaye are acknowledged for their companionship in conferences and seminars.

I am greatful to chief physicians Terhi Holmström, Tami Siren, Mika Kallio and Pauli Sallinen for enabling my clinical work on flexible basis in health centres of Eura and Harjavalta. A special thanks go to exceptionally-skilled diabetes nurses Katja Virtanen and Päivi Tuominen with whom I have had an opportunity to increase the well-being of diabetic patients of the Satakunta region.

I have been fortunate to have the best people surround me. Olli Haataja, Taisto Lalli, Otto Meskanen, Eemeli Myllymäki and Vesa Pönkkä are thanked for their unconditional friendship that extends from the pre-school era and is still going strong. Ilkka Ketonen and Kimmo Lehtimäki are also acknowledged. My friends from the medical school, namely Joel Brander, Antti Haapasaari, Samuel Holm, Tomi Laitinen, Martti Merikari, Niko Nousiainen, Jussi Räisänen, Valtteri Uusitalo, Jussi Vatanen, Henri Viitanen, Olli Vuorio and Lauri Vähämurto are thanked for all the unforgettable and fun experiences during the years.

Above all, I am deeply indebted to my parents Anu and Risto, who have provided me and my sisters a loving and secure environment to grow, evolve, and lead an independent life. You have always encouraged me in all my personal choices and never stopped showing interest towards my clinical and scientific work. There are no words to express my gratitude. I have been particularly happy to see my two beloved sisters, Heidi and Laura, to find their place in the world and be a part of my life. Finally, I want to express my sincere love to Anni for being there during the good days but also at times when work seemed overwhelming.

This work was financially supported by the Academy of Finland and Sigrid Jusélius Foundation, and grants from Diabetes Research Foundation, Emil Aaltonen Foundation, Finnish Cultural Foundation, Finnish Medical Foundation, Jalmari and Rauha Ahokas Foundation, Maud Kuistila Foundation, Orion Research Foundation, The Gastroenterological Research Foundation, Turku University Foundation, Valto Takala Foundation and Varsinais-Suomi Regional Fund.

Turku, November 2016

Henri Honka

REFERENCES

Abraham M.A., Lam T.K. 2016 Glucagon action in the brain. Diabetologia 57:1367-1371.

Ahotupa M., Marniemi J., Lehtimaki T., Talvinen K., Raitakari O.T., Vasankari T., Viikari J., Luoma J., Yla-Herttuala S. 1998 Baseline diene conjugation in LDL lipids as a direct measure of in vivo LDL oxidation. Clin Biochem 31:257-261.

Ait-Omar A., Monteiro-Sepulveda M., Poitou C., Le Gall M., Cotillard A., Gilet J., Garbin K., Houllier A., Chateau D., Lacombe A., Veyrie N., Hugol D., Tordjman J., Magnan C., Serradas P., Clement K., Leturque A., Brot-Laroche E. 2011 GLUT2 accumulation in enterocyte apical and intracellular membranes: A study in morbidly obese human subjects and ob/ob and high fat-fed mice. Diabetes 60:2598-2607.

Almandoz J.P., Singh E., Howell L.A., Grothe K., Vlazny D.T., Smailovic A., Irving B.A., Nelson R.H., Miles J.M. 2013 Spillover of fatty acids during dietary fat storage in type 2 diabetes: Relationship to body fat depots and effects of weight loss. Diabetes 62:1897-1903.

Attali M., Stetsyuk V., Basmaciogullari A., Aiello V., Zanta-Boussif M.A., Duvillie B., Scharfmann R. 2007 Control of beta-cell differentiation by the pancreatic mesenchyme. Diabetes 56:1248-1258.

Backhed F., Ding H., Wang T., Hooper L.V., Koh G.Y., Nagy A., Semenkovich C.F., Gordon J.I. 2004 The gut microbiota as an environmental factor that regulates fat storage. Proc Natl Acad Sci U S A 101:15718-15723.

Ban K., Noyan-Ashraf M.H., Hoefer J., Bolz S.S., Drucker D.J., Husain M. 2008 Cardioprotective and vasodilatory actions of glucagon-like peptide 1 receptor are mediated through both glucagon-like peptide 1 receptor-dependent and -independent pathways. Circulation 117:2340-2350.

Bajaj M., Pratipanawatr T., Berria R., Pratipanawatr W., Kashyap S., Cusi K., Mandarino L., DeFronzo R.A. 2002 Free fatty acids reduce splanchnic and peripheral glucose uptake in patients with type 2 diabetes. Diabetes 51:3043-3048.

Baron A.D., Laakso M., Brechtel G., Hoit B., Watt C., Edelman S.V. 1990 Reduced postprandial skeletal muscle blood flow contributes to glucose intolerance in human obesity. J Clin Endocrinol Metab 70:1525-1533.

Baron A.D. 1994 Hemodynamic actions of insulin. Am J Physiol 267:E187-202.

Barrett E.J., Ferrannini E., Gusberg R., Bevilacqua S., DeFronzo R.A. 1985 Hepatic and extrahepatic splanchnic glucose metabolism in the postabsorptive and glucose fed dog. Metabolism 34:410-420.

Bazin R., Lavau M. 1982 Effects of high-fat diet on glucose metabolism in isolated pancreatic acini of rats. Am J Physiol 243:G448-54.

Begovatz P., Koliaki C., Weber K., Strassburger K., Nowotny B., Nowotny P., Mussig K., Bunke J., Pacini G., Szendrodi J., Roden M. 2015 Pancreatic adipose tissue infiltration, parenchymal steatosis and beta cell function in humans. Diabetologia 58:1646-1655.

Benjamin M.A., McKay D.M., Yang P.C., Cameron H., Perdue M.H. 2000 Glucagon-like peptide-2 enhances intestinal epithelial barrier function of both transcellular and paracellular pathways in the mouse. Gut 47:112-119.

Benoit S.C., Air E.L., Coolen L.M., Strauss R., Jackman A., Clegg D.J., Seeley R.J., Woods S.C. 2002 The catabolic action of insulin in the brain is mediated by melanocortins. J Neurosci 22:9048-9052.

Bergman R.N. 1977 Integrated control of hepatic glucose metabolism. Fed Proc 36:265-270.

Blair J.B., Cimbala M.A., Foster J.L., Morgan R.A. 1976 Hepatic pyruvate kinase. regulation by glucagon, cyclic adenosine 3'-5'-monophosphate, and insulin in the perfused rat liver. J Biol Chem 251:3756-3762.

Bojsen-Moller K.N., Dirksen C., Jorgensen N.B., Jacobsen S.H., Serup A.K., Albers P.H., Hansen D.L., Worm D., Naver L., Kristiansen V.B., Wojtaszewski J.F., Kiens B., Holst J.J., Richter E.A., Madsbad S. 2014 Early enhancements of hepatic and later of peripheral insulin sensitivity combined with increased postprandial insulin secretion contribute to improved glycemic control after roux-en-Y gastric bypass. Diabetes 63:1725-1737.

Bonner-Weir S., Orci L. 1982 New perspectives on the microvasculature of the islets of langerhans in the rat. Diabetes 31:883-889.

Bonner C., Kerr-Conte J., Gmyr V., Queniat G., Moerman E., Thevenet J., Beaucamps C., Delalleau N., Popescu I., Malaisse W.J., Sener A., Deprez B., Abderrahmani A., Staels B., Pattou F. 2015 Inhibition of the glucose transporter SGLT2 with dapagliflozin in pancreatic alpha cells triggers glucagon secretion. Nat Med 21:512-517.

Borra R.J., Salo S., Dean K., Lautamaki R., Nuutila P., Komu M., Parkkola R. 2009 Nonalcoholic fatty liver disease: Rapid evaluation of liver fat content with in-phase and out-of-phase MR imaging. Radiology 250:130-136.

Bouchard C. 1994 Genetics of obesity. CRC Press: Boca Raton.

Braghetto I., Davanzo C., Korn O., Csendes A., Valladares H., Herrera E., Gonzalez P., Papapietro K. 2009 Scintigraphic evaluation of gastric emptying in obese patients submitted to sleeve gastrectomy compared to normal subjects. Obes Surg 19:1515-1521.

Breen D.M., Rasmussen B.A., Kokorovic A., Wang R., Cheung G.W., Lam T.K. 2012 Jejunal nutrient sensing is required for duodenal-jejunal bypass surgery to rapidly lower glucose concentrations in uncontrolled diabetes. Nat Med 18:950-955.

Brissova M., Shostak A., Shiota M., Wiebe P.O., Poffenberger G., Kantz J., Chen Z., Carr C., Jerome W.G., Chen J., Baldwin H.S., Nicholson W., Bader D.M., Jetton T., Gannon M., Powers A.C. 2006 Pancreatic islet production of vascular endothelial growth factor--a is essential for islet vascularization, revascularization, and function. Diabetes 55:2974-2985.

Brun P., Castagliuolo I., Di Leo V., Buda A., Pinzani M., Palu G., Martines D. 2007 Increased intestinal permeability in obese mice: New evidence in the pathogenesis of nonalcoholic steatohepatitis. Am J Physiol Gastrointest Liver Physiol 292:G518-25.

Burcelin R., Dolci W., Thorens B. 2000 Glucose sensing by the hepatoportal sensor is GLUT2-dependent: In vivo analysis in GLUT2-null mice. Diabetes 49:1643-1648.

Byrne M.M., Sturis J., Sobel R.J., Polonsky K.S. 1996 Elevated plasma glucose 2 h postchallenge predicts defects in beta-cell function. Am J Physiol 270:E572-9.

Cahill G.F. Jr, Earle A.S., Zottu S. 1957 In vivo effects of glucagon on hepatic glycogen, phosphorylase and glucose-6-phosphatase. Endocrinology 60:265-269.

Cahill G.F. Jr 1976 Starvation in man. Clin Endocrinol Metab 5:397-415.

Cani P.D., Amar J., Iglesias M.A., Poggi M., Knauf C., Bastelica D., Neyrinck A.M., Fava F., Tuohy K.M., Chabo C., Waget A., Delmee E., Cousin B., Sulpice T., Chamontin B., Ferrieres J., Tanti J.F., Gibson G.R., Casteilla L., Delzenne N.M., Alessi M.C., Burcelin R. 2007 Metabolic endotoxemia initiates obesity and insulin resistance. Diabetes 56:1761-1772.

Carlsson P.O., Andersson A., Jansson L. 1996 Pancreatic islet blood flow in normal and obese-hyperglycemic (ob/ob) mice. Am J Physiol 271:E990-5.

Carlsson P.O., Iwase M., Jansson L. 1999 Stimulation of intestinal glucoreceptors in rats increases pancreatic islet blood flow through vagal mechanisms. Am J Physiol 276:R233-6.

Carlsson P.O., Olsson R., Kallskog O., Bodin B., Andersson A., Jansson L. 2002 Glucose-induced islet blood flow increase in rats: Interaction between nervous and metabolic mediators. Am J Physiol Endocrinol Metab 283:E457-64.

Carlsson P.O., Jansson L. 2015 Disruption of insulin receptor signaling in endothelial cells shows the central role of an intact islet blood flow for in vivo beta-cell function. Diabetes 64:700-702.

Carpentier A., Mittelman S.D., Lamarche B., Bergman R.N., Giacca A., Lewis G.F. 1999 Acute enhancement of insulin secretion by FFA in humans is lost with prolonged FFA elevation. Am J Physiol 276:E1055-66.

Cersosimo E., Gastaldelli A., Cervera A., Wajcberg E., Sriwijilkamol A., Fernandez M., Zuo P., Petz R., Triplitt C., Musi N., DeFronzo R.A. 2011 Effect of exenatide on splanchnic and peripheral glucose metabolism in type 2 diabetic subjects. J Clin Endocrinol Metab 96:1763-1770.

Chambers A.P., Smith E.P., Begg D.P., Grayson B.E., Sisley S., Greer T., Sorrell J., Lemmen L., LaSance K., Woods S.C., Seeley R.J., D'Alessio D.A., Sandoval D.A. 2014 Regulation of gastric emptying rate and its role in nutrient-induced GLP-1 secretion in rats after vertical sleeve gastrectomy. Am J Physiol Endocrinol Metab 306:E424-32.

Champe P.C., Harvey R.A. 2008 Biochemistry, 4th Edition. Lippincott Williams & Wilkins.

Chan J.M., Rimm E.B., Colditz G.A., Stampfer M.J., Willett W.C. 1994 Obesity, fat distribution, and weight gain as risk factors for clinical diabetes in men. Diabetes Care 17:961-969.

Chang J., Rayner C.K., Jones K.L., Horowitz M. 2010 Diabetic gastroparesis and its impact on glycemia. Endocrinol Metab Clin North Am 39:745-762.

Chen S., Ogawa A., Ohneda M., Unger R.H., Foster D.W., McGarry J.D. 1994

More direct evidence for a malonyl-CoA-carnitine palmitoyltransferase I interaction as a key event in pancreatic beta-cell signaling. Diabetes 43:878-883

Chou C.C., Burns T.D., Hsieh C.P., Dabney J.M. 1972 Mechanisms of local vasodilation with hypertonic glucose in the jejunum. Surgery 71:380-387.

Chou C.C., Coatney R.W. 1994 Nutrient-induced changes in intestinal blood flow in the dog. Br Vet J 150:423-437.

Chou C.C., Nyhof R.A., Kvietys P.R., Sit S.P., Gallavan R.H. 1985 Regulation of jejunal blood flow and oxygenation during glucose and oleic acid absorption. Am J Physiol. 249:G691-701.

Christensen M., Vedtofte L., Holst J.J., Vilsboll T., Knop F.K. 2011 Glucose-dependent insulinotropic polypeptide: A bifunctional glucose-dependent regulator of glucagon and insulin secretion in humans. Diabetes 60:3103-3109.

Cohade C., Osman M., Pannu H.K., Wahl R.L. 2003 Uptake in supraclavicular area fat ("USA-fat"): Description on 18F-FDG PET/CT. J Nucl Med 44:170-176.

Consoli A., Nurjhan N., Capani F., Gerich J. 1989 Predominant role of gluconeogenesis in increased hepatic glucose production in NIDDM. Diabetes 38:550-557.

Corbett S.W., Keesey R.E. 1982 Energy balance of rats with lateral hypothalamic lesions. Am J Physiol 242:E273-9.

Croset M., Rajas F., Zitoun C., Hurot J.M., Montano S., Mithieux G. 2001 Rat small intestine is an insulin-sensitive gluconeogenic organ. Diabetes 50:740-746.

Currie C.J., Poole C.D., Evans M., Peters J.R., Morgan C.L. 2013 Mortality and other important diabetes-related outcomes with insulin vs other antihyperglycemic therapies in type 2 diabetes. J Clin Endocrinol Metab 98:668-677.

Dadson P., Landini L., Helmiö M., Hannukainen J.C., Immonen H., Honka M.J., Bucci M., Savisto N., Soinio M., Salminen P., Parkkola R., Pihlajamaki J., Iozzo P., Ferrannini E., Nuutila P. 2016 Effect of bariatric surgery on adipose tissue glucose metabolism in different depots in patients with or without type 2 diabetes. Diabetes Care. 39:292-299.

Dai C., Brissova M., Reinert R.B., Nyman L., Liu E.H., Thompson C., Shostak A., Shiota M., Takahashi T., Powers A.C. 2013 Pancreatic islet vasculature adapts to insulin resistance through dilation and not angiogenesis. Diabetes 62:4144-4153.

DeFronzo R.A., Ferrannini E., Hendler R., Wahren J., Felig P. 1978 Influence of hyperinsulinemia, hyperglycemia, and the route of glucose administration on splanchnic glucose exchange. Proc Natl Acad Sci U S A 75:5173-5177.

DeFronzo R.A., Tobin J.D., Andres R. 1979 Glucose clamp technique: A method for quantifying insulin secretion and resistance. Am J Physiol 237:E214-23.

DeFronzo R.A., Ferrannini E., Hendler R., Felig P., Wahren J. 1983 Regulation of splanchnic and peripheral glucose uptake by insulin and hyperglycemia in man. Diabetes 32:35-45.

DeFronzo R.A., Gunnarsson R., Bjorkman O., Olsson M., Wahren J. 1985 Effects of insulin on peripheral and splanchnic glucose metabolism in

noninsulin-dependent (type II) diabetes mellitus. J Clin Invest 76:149-155.

DeFronzo R.A. 1987 Use of the splanchnic/hepatic balance technique in the study of glucose metabolism. Baillieres Clin Endocrinol Metab 1:837-862.

DeFronzo R.A., Ferrannini E., Simonson D.C. 1989 Fasting hyperglycemia in non-insulin-dependent diabetes mellitus: Contributions of excessive hepatic glucose production and impaired tissue glucose uptake. Metabolism 38:387-395.

DeFronzo R.A., Bonadonna R.C., Ferrannini E. 1992 Pathogenesis of NIDDM. A balanced overview. Diabetes Care 15:318-368.

DeGrado T.R., Wang S., Holden J.E., Nickles R.J., Taylor M., Stone C.K. 2000 Synthesis and preliminary evaluation of (18)F-labeled 4-thia palmitate as a PET tracer of myocardial fatty acid oxidation. Nucl Med Biol 27:221-231.

Deng S., Vatamaniuk M., Huang X., Doliba N., Lian M.M., Frank A., Velidedeoglu E., Desai N.M., Koeberlein B., Wolf B., Barker C.F., Naji A., Matschinsky F.M., Markmann J.F. 2004 Structural and functional abnormalities in the islets isolated from type 2 diabetic subjects. Diabetes 53:624-632.

Del Prato S., Matsuda M., Simonson D.C., Groop L.C., Sheehan P., Leonetti F., Bonadonna R.C., DeFronzo R.A. 1997 Studies on the mass action effect of glucose in NIDDM and IDDM: Evidence for glucose resistance. Diabetologia 40:687-697.

Delzenne N.M., Neyrinck A.M., Backhed F., Cani P.D. 2011 Targeting gut microbiota in obesity: Effects of prebiotics and probiotics. Nat Rev Endocrinol 7:639-646.

Diabeteksen ehkäisyn ja hoidon kehittämisohjelma Dehko 2000-2010, loppuraportti.

Dunaway G.A. 1983 A review of animal phosphofructokinase isozymes with an emphasis on their physiological role. Mol Cell Biochem 52:75-91.

Dupre J., Ross S.A., Watson D., Brown J.C. 1973 Stimulation of insulin secretion by gastric inhibitory polypeptide in man. J Clin Endocrinol Metab 37:826-828.

Eaton R.P., Allen R.C., Schade D.S., Erickson K.M., Standefer J. 1980 Prehepatic insulin production in man: Kinetic analysis using peripheral connecting peptide behavior. J Clin Endocrinol Metab 51:520-528.

Eaton R.P., Allen R.C., Schade D.S. 1983 Hepatic removal of insulin in normal man: Dose response to endogenous insulin secretion. J Clin Endocrinol Metab 56:1294-1300.

Ebeling P., Koistinen H.A., Koivisto V.A. 1998 Insulin-independent glucose transport regulates insulin sensitivity. FEBS Lett 436:301-303.

Edfalk S., Steneberg P., Edlund H. 2008 Gpr40 is expressed in enteroendocrine cells and mediates free fatty acid stimulation of incretin secretion. Diabetes 57:2280-2287.

Eriksson J.G., Sandboge S., Salonen M.K., Kajantie E., Osmond C. 2014 Long-term consequences of maternal overweight in pregnancy on offspring later health: Findings from the helsinki birth cohort study. Ann Med 46:434-438.

Fantuzzi G. 2005 Adipose tissue, adipokines, and inflammation. J Allergy Clin Immunol 115:911-9.

Fara J.W., Salazar A.M. 1978 Gastric inhibitory polypeptide increases mesenteric blood flow. Proc Soc Exp Biol Med 158:446-448.

Ferrannini E., Barrett E.J., Bevilacqua S., DeFronzo R.A. 1983 Effect of fatty acids on glucose production and utilization in man. J Clin Invest 72:1737-1747.

Ferrannini E., Simonson D.C., Katz L.D., Reichard G,Jr., Bevilacqua S., Barrett E.J., Olsson M., DeFronzo R.A. 1988 The disposal of an oral glucose load in patients with non-insulin-dependent diabetes. Metabolism 37:79-85.

Ferrannini E. 1998 Insulin resistance versus insulin deficiency in non-insulin-dependent diabetes mellitus: Problems and prospects. Endocr Rev 19:477-490.

Ferrannini E., Muscelli E., Frascerra S., Baldi S., Mari A., Heise T., Broedl U.C., Woerle H.J. 2014 Metabolic response to sodium-glucose cotransporter 2 inhibition in type 2 diabetic patients. J Clin Invest 124:499-508.

Field J.B. 1973 Extraction of insulin by liver. Annu Rev Med 24:309-314.

Fogelholm M., Kukkonen-Harjula K. 2000 Does physical activity prevent weight gain--a systematic review. Obes Rev 1:95-111.

Fowler M.J. 2008 Microvascular and macrovascular complications of diabetes. Clin Diab 26:77-82.

Franz M.J., Boucher J.L., Rutten-Ramos S., VanWormer J.J. 2015 Lifestyle weight-loss intervention outcomes in overweight and obese adults with type 2 diabetes: A systematic review and meta-analysis of randomized clinical trials. J Acad Nutr Diet.

Freidenberg G.R., Reichart D., Olefsky J.M., Henry R.R. 1988 Reversibility of defective adipocyte insulin receptor kinase activity in non-insulin-dependent diabetes mellitus. effect of weight loss. J Clin Invest 82:1398-1406.

Friedewald W.T., Levy R.I., Fredrickson D.S. 1972 Estimation of the concentration of low-density lipoprotein cholesterol in plasma, without use of the preparative ultracentrifuge. Clin Chem 18:499-502.

Gaborit B., Abdesselam I., Kober F., Jacquier A., Ronsin O., Emungania O., Lesavre N., Alessi M.C., Martin J.C., Bernard M., Dutour A. 2015 Ectopic fat storage in the pancreas using 1H-MRS: Importance of diabetic status and modulation with bariatric surgery-induced weight loss. Int J Obes (Lond) 39:480-487.

Ganong W.F. 2005 Review of Medical Physiology, 22th Edition. The McGraw-Hill Companies.

Garcia M.J., McNamara P.M., Gordon T., Kannel W.B. 1974 Morbidity and mortality in diabetics in the framingham population. sixteen year follow-up study. Diabetes 23:105-111.

Gentilcore D., Hausken T., Meyer J.H., Chapman I.M., Horowitz M., Jones K.L. 2008 Effects of intraduodenal glucose, fat, and protein on blood pressure, heart rate, and splanchnic blood flow in healthy older subjects. Am J Clin Nutr 87:156-161.

Gentilcore D., Nair N.S., Vanis L., Rayner C.K., Meyer J.H., Hausken T., Horowitz M., Jones K.L. 2009 Comparative effects of oral and

intraduodenal glucose on blood pressure, heart rate, and splanchnic blood flow in healthy older subjects. Am J Physiol Regul Integr Comp Physiol 297:R716-22.

Germano G., Chen B.C., Huang S.C., Gambhir S.S., Hoffman E.J., Phelps M.E. 1992 Use of the abdominal aorta for arterial input function determination in hepatic and renal PET studies. J Nucl Med 33:613-620.

Giacco F., Brownlee M. 2010 Oxidative stress and diabetic complications. Circ Res 107:1058-1070.

Gontier E., Fourme E., Wartski M., Blondet C., Bonardel G., Le Stanc E., Mantzarides M., Foehrenbach H., Pecking A.P., Alberini J.L. 2008 High and typical 18F-FDG bowel uptake in patients treated with metformin. Eur J Nucl Med Mol Imaging 35:95-99.

Golay A., DeFronzo R.A., Ferrannini E., Simonson D.C., Thorin D., Acheson K., Thiebaud D., Curchod B., Jequier E., Felber J.P. 1988 Oxidative and non-oxidative glucose metabolism in non-obese type 2 (non-insulin-dependent) diabetic patients. Diabetologia 31:585-591.

Gray H., Carter H.V. 2009 Gray's Anatomy, 40th Edition. Elsevier

Gribble F.M. 2012 The gut endocrine system as a coordinator of postprandial nutrient homoeostasis. Proc Nutr Soc 71:456-462.

Grodsky G.M. 1972 A threshold distribution hypothesis for packet storage of insulin and its mathematical modeling. J Clin Invest 51:2047-2059.

Groop L.C., Saloranta C., Shank M., Bonadonna R.C., Ferrannini E., DeFronzo R.A. 1991 The role of free fatty acid metabolism in the pathogenesis of insulin resistance in obesity and noninsulin-dependent diabetes mellitus. J Clin Endocrinol Metab 72:96-107.

Guiducci L., Gronroos T., Jarvisalo M.J., Kiss J., Viljanen A., Naum A.G., Viljanen T., Savunen T., Knuuti J., Ferrannini E., Salvadori P.A., Nuutila P., Iozzo P. 2007 Biodistribution of the fatty acid analogue 18F-FTHA: Plasma and tissue partitioning between lipid pools during fasting and hyperinsulinemia. J Nucl Med 48:455-462.

Guiducci L., Liistro T., Burchielli S., Panetta D., Bonora D., Di Cecco P., Bucci M., Moehrs S., Del Guerra A., Salvadori P.A., Iozzo P. 2011 Contribution of organ blood flow, intrinsic tissue clearance and glycaemia to the regulation of glucose use in obese and type 2 diabetic rats: A PET study. Nutr Metab Cardiovasc Dis 21:726-732.

Gutierrez Repiso C., Garcia Serrano S., Rodriguez Pacheco F., Garcia Arnes J., Valdes S., Soriguer F., Moreno Ruiz F.J., Rodriguez Canete A., Alcain Martinez G., Vazquez Pedreno L., Garcia Fuentes E. 2015 The expression of genes involved in in testinal gluconeogenesis is altered in morbidly obese subjects with higher insulin resistance. 51st Annual Meeting, European Association for the Study of Diabetes.

Haaparanta M., Paul R., Gronroos T., Bergman J., Kamarainen E.L., Solin O. 2003 Microdialysis and 2-[18F]fluoro-2-deoxy-D-glucose (FDG): A study on insulin action on FDG transport, uptake and metabolism in rat muscle, liver and adipose tissue. Life Sci 73:1437-1451.

Hamada Y., Kashima H., Hayashi N. 2014 The number of chews and meal duration affect diet-induced

thermogenesis and splanchnic circulation. Obesity (Silver Spring) 22:E62-9.

Haffner S.M., Lehto S., Ronnemaa T., Pyorala K., Laakso M. 1998 Mortality from coronary heart disease in subjects with type 2 diabetes and in nondiabetic subjects with and without prior myocardial infarction. N Engl J Med 339:229-234.

Hamacher K., Coenen H.H., Stocklin G. 1986 Efficient stereospecific synthesis of no-carrier-added 2-[18F]-fluoro-2-deoxy-D-glucose using aminopolyether supported nucleophilic substitution. J Nucl Med 27:235-238.

Hannukainen J.C., Borra R., Linderborg K., Kallio H., Kiss J., Lepomaki V., Kalliokoski K.K., Kujala U.M., Kaprio J., Heinonen O.J., Komu M., Parkkola R., Ahotupa M., Lehtimaki T., Huupponen R., Iozzo P., Nuutila P. 2011 Liver and pancreatic fat content and metabolism in healthy monozygotic twins with discordant physical activity. J Hepatol 54:545-552.

Hashimoto S., Kubota N., Sato H., Sasaki M., Takamoto I., Kubota T., Nakaya K., Noda M., Ueki K., Kadowaki T. 2015 Insulin receptor substrate-2 (Irs2) in endothelial cells plays a crucial role in insulin secretion. Diabetes 64:876-886.

Hattori Y., Jojima T., Tomizawa A., Satoh H., Hattori S., Kasai K., Hayashi T. 2010 A glucagon-like peptide-1 (GLP-1) analogue, liraglutide, upregulates nitric oxide production and exerts anti-inflammatory action in endothelial cells. Diabetologia 53:2256-2263.

Hattori Y., Jojima T., Tomizawa A., Satoh H., Hattori S., Kasai K., Hayashi T. 2012 Retraction note: A glucagon-like peptide-1 (GLP-1) analogue, liraglutide, upregulates nitric oxide production and exerts anti-inflammatory action in endothelial cells. Diabetologia 55:533.

Hayes M.T., Foo J., Besic V., Tychinskaya Y., Stubbs R.S. 2011 Is intestinal gluconeogenesis a key factor in the early changes in glucose homeostasis following gastric bypass? Obes Surg 21:759-762.

Helliwell P.A., Kellett G.L. 2002 The active and passive components of glucose absorption in rat jejunum under low and high perfusion stress. J Physiol 544:579-589.

Helmiö M., Victorzon M., Ovaska J., Leivonen M., Juuti A., Jaser N., Peromaa P., Tolonen P., Hurme S., Salminen P. 2012 SLEEVEPASS: A randomized prospective multicenter study comparing laparoscopic sleeve gastrectomy and gastric bypass in the treatment of morbid obesity: Preliminary results. Surg Endosc 26:2521-2526.

Heni M., Machann J., Staiger H., Schwenzer N.F., Peter A., Schick F., Claussen C.D., Stefan N., Haring H.U., Fritsche A. 2010 Pancreatic fat is negatively associated with insulin secretion in individuals with impaired fasting glucose and/or impaired glucose tolerance: A nuclear magnetic resonance study. Diabetes Metab Res Rev 26:200-205.

Heymann E., Mentlein R. 1978 Liver dipeptidyl aminopeptidase IV hydrolyzes substance P. FEBS Lett 91:360-364.

Higa M., Zhou Y.T., Ravazzola M., Baetens D., Orci L., Unger R.H. 1999 Troglitazone prevents mitochondrial alterations, beta cell destruction, and diabetes in obese prediabetic rats. Proc Natl Acad Sci U S A 96:11513-11518.

Hoang D.T., Matsunari H., Nagaya M., Nagashima H., Millis J.M., Witkowski P., Periwal V., Hara M., Jo J. 2014 A conserved rule for pancreatic islet organization. PLoS One 9:e110384.

Holman R.R. 1998 Assessing the potential for alpha-glucosidase inhibitors in prediabetic states. Diabetes Res Clin Pract 40 Suppl:S21-5.

Holst J.J., Vilsboll T., Deacon C.F. 2009 The incretin system and its role in type 2 diabetes mellitus. Mol Cell Endocrinol 297:127-136.

Hopsu-Havu V.K., Glenner G.G. 1966 A new dipeptide naphthylamidase hydrolyzing glycyl-prolyl-beta-naphthylamide. Histochemie 7:197-201.

Hyder A., Zenhom M., Klapper M., Herrmann J., Schrezenmeir J. 2010 Expression of fatty acid binding proteins 3 and 5 genes in rat pancreatic islets and INS-1E cells: Regulation by fatty acids and glucose. Islets 2:174-184.

Immonen H., Hannukainen J.C., Iozzo P., Soinio M., Salminen P., Saunavaara V., Borra R., Parkkola R., Mari A., Lehtimaki T., Pham T., Laine J., Karja V., Pihlajamaki J., Nelimarkka L., Nuutila P. 2014 Effect of bariatric surgery on liver glucose metabolism in morbidly obese diabetic and non-diabetic patients. J Hepatol 60:377-383.

Immonen H., Hannukainen J.C., Kudomi N., Parkkola R., Saunavaara V., Iozzo P., Nuutila P. 2014 Effect of bariatric surgery in hepatic fatty acid uptake and blood flow. Diabetologia 57:S76.

Ionut V., Castro A.V., Woolcott O.O., Stefanovski D., Iyer M.S., Broussard J.L., Burch M., Elazary R., Kolka C.M., Mkrtchyan H., Bediako I.A., Bergman R.N. 2014 Hepatic portal vein denervation impairs oral glucose tolerance but not exenatide's effect on glycemia. Am J Physiol Endocrinol Metab 307:E644-52.

Iozzo P., Hallsten K., Oikonen V., Virtanen K.A., Kemppainen J., Solin O., Ferrannini E., Knuuti J., Nuutila P. 2003 Insulin-mediated hepatic glucose uptake is impaired in type 2 diabetes: Evidence for a relationship with glycemic control. J Clin Endocrinol Metab 88:2055-2060.

Iozzo P., Geisler F., Oikonen V., Maki M., Takala T., Solin O., Ferrannini E., Knuuti J., Nuutila P., 18F-FDG PET Study 2003 Insulin stimulates liver glucose uptake in humans: An 18F-FDG PET study. J Nucl Med 44:682-689.

Iozzo P., Lautamaki R., Geisler F., Virtanen K.A., Oikonen V., Haaparanta M., Yki-Jarvinen H., Ferrannini E., Knuuti J., Nuutila P. 2004 Non-esterified fatty acids impair insulin-mediated glucose uptake and disposition in the liver. Diabetologia 47:1149-1156.

Iozzo P., Gastaldelli A., Jarvisalo M.J., Kiss J., Borra R., Buzzigoli E., Viljanen A., Naum G., Viljanen T., Oikonen V., Knuuti J., Savunen T., Salvadori P.A., Ferrannini E., Nuutila P. 2006 18F-FDG assessment of glucose disposal and production rates during fasting and insulin stimulation: A validation study. J Nucl Med 47:1016-1022.

Iozzo P., Jarvisalo M.J., Kiss J., Borra R., Naum G.A., Viljanen A., Viljanen T., Gastaldelli A., Buzzigoli E., Guiducci L., Barsotti E., Savunen T., Knuuti J., Haaparanta-Solin M., Ferrannini E., Nuutila P. 2007 Quantification of liver glucose metabolism by positron emission tomography: Validation study in pigs. Gastroenterology 132:531-542.

Iozzo P., Bucci M., Roivainen A., Nagren K., Jarvisalo M.J., Kiss J., Guiducci L., Fielding B., Naum A.G., Borra R., Virtanen K., Savunen T., Salvadori P.A., Ferrannini E., Knuuti J., Nuutila P. 2010 Fatty acid metabolism in the liver, measured by positron emission tomography, is increased in obese individuals. Gastroenterology 139:846-56, 856.e1-6.

Ishida T., Chap Z., Chou J., Lewis R., Hartley C., Entman M., Field J.B. 1983 Differential effects of oral, peripheral intravenous, and intraportal glucose on hepatic glucose uptake and insulin and glucagon extraction in conscious dogs. J Clin Invest 72:590-601.

Ishizu K., Nishizawa S., Yonekura Y., Sadato N., Magata Y., Tamaki N., Tsuchida T., Okazawa H., Miyatake S., Ishikawa M. 1994 Effects of hyperglycemia on FDG uptake in human brain and glioma. J Nucl Med 35:1104-1109.

Iwasaki K., Harada N., Sasaki K., Yamane S., Iida K., Suzuki K., Hamasaki A., Nasteska D., Shibue K., Joo E., Harada T., Hashimoto T., Asakawa Y., Hirasawa A., Inagaki N. 2015 Free fatty acid receptor GPR120 is highly expressed in enteroendocrine K cells of the upper small intestine and has a critical role in GIP secretion after fat ingestion. Endocrinology 156:837-846.

Iwase M., Tashiro K., Uchizono Y., Goto D., Yoshinari M. 2001 Pancreatic islet blood flow in conscious rats during hyperglycemia and hypoglycemia. Am J Physiol Regul Integr Comp Physiol 280:R1601-5.

Jarvala T., Raitala T., Rissanen P. 2010 Diabeteksen kustannukset Suomessa 1998-2007. Kansallinen diabetesohjelma Dehko.

Jackness C., Karmally W., Febres G., Conwell I.M., Ahmed L., Bessler M., McMahon D.J., Korner J. 2013 Very low-calorie diet mimics the early beneficial effect of roux-en-Y gastric bypass on insulin sensitivity and beta-cell function in type 2 diabetic patients. Diabetes 62:3027-3032.

Jansson L. 1994 The regulation of pancreatic islet blood flow. Diabetes Metab Rev 10:407-416.

Jansson L., Andersson A., Bodin B., Kallskog O. 2007 Pancreatic islet blood flow during euglycaemic, hyperinsulinaemic clamp in anaesthetized rats. Acta Physiol (Oxf) 189:319-324.

Jenkins J.S., Lowe R.D., Titterington E. 1964 Effect of adrenocortical hormones on release of free fatty acids and uptake of glucose in human peripheral tissues. Clin Sci 26:421-427.

Kahleova H., Belinova L., Malinska H., Oliyarnyk O., Trnovska J., Skop V., Kazdova L., Dezortova M., Hajek M., Tura A., Hill M., Pelikanova T. 2014 Eating two larger meals a day (breakfast and lunch) is more effective than six smaller meals in a reduced-energy regimen for patients with type 2 diabetes: A randomised crossover study. Diabetologia 57:1552-1560.

Kahn C.R., King G.L., Moses A.C., Weir G.C., Jacobson A.M., Smith R.J. 2005 Joslin's Diabetes Mellitus, 14th Edition. Lippincott Williams & Wilkins.

Kalant N. 1956 The effect of glucagon on metabolism of glycine-1-C14. Arch Biochem Biophys 65:469-474.

Kaneto H., Nakatani Y., Kawamori D., Miyatsuka T., Matsuoka T.A., Matsuhisa M., Yamasaki Y. 2005 Role of oxidative stress, endoplasmic reticulum stress, and c-jun N-terminal kinase in pancreatic beta-cell dysfunction and insulin resistance. Int J Biochem Cell Biol 37:1595-1608.

Karlsson H.K., Tuominen L., Tuulari J.J., Hirvonen J., Parkkola R., Helin S., Salminen P., Nuutila P., Nummenmaa L. 2015 Obesity is associated with decreased μ-opioid but unaltered dopamine D2 receptor availability in the brain. J Neurosci 35:3959-3965.

Kashyap S., Belfort R., Gastaldelli A., Pratipanawatr T., Berria R., Pratipanawatr W., Bajaj M., Mandarino L., DeFronzo R., Cusi K. 2003 A sustained increase in plasma free fatty acids impairs insulin secretion in nondiabetic subjects genetically predisposed to develop type 2 diabetes. Diabetes 52:2461-2474.

Kauhanen S., Rinta-Kiikka I., Kemppainen J., Gronroos J., Kajander S., Seppanen M., Alanen K., Gullichsen R., Nuutila P., Ovaska J. 2015 Accuracy of 18F-FDG PET/CT, multidetector CT, and MR imaging in the diagnosis of pancreatic cysts: A prospective single-center study. J Nucl Med 56:1163-1168.

Kawamitsu H., Kaji Y., Ohara T., Sugimura K. 2003 Feasibility of quantitative intrahepatic lipid imaging applied to the magnetic resonance dual gradient echo sequence. Magn Reson Med Sci 2:47-50.

Kelley D.E., Williams K.V., Price J.C., Goodpaster B. 1999 Determination of the lumped constant for [18F] fluorodeoxyglucose in human skeletal muscle. J Nucl Med 40:1798-1804.

Kelly T., Yang W., Chen C.S., Reynolds K., He J. 2008 Global burden of obesity in 2005 and projections to 2030. Int J Obes (Lond) 32:1431-1437.

Kemppainen J., Fujimoto T., Kalliokoski K.K., Viljanen T., Nuutila P., Knuuti J. 2002 Myocardial and skeletal muscle glucose uptake during exercise in humans. J Physiol 542:403-412.

Kety S.S., Schmidt C.F. 1946 Measurement of cerebral blood flow and cerebral oxygen consumption in man. Fed Proc 5:264.

Kiens B., Lithell H., Mikines K.J., Richter E.A. 1989 Effects of insulin and exercise on muscle lipoprotein lipase activity in man and its relation to insulin action. J Clin Invest 84:1124-1129.

Kim Y.W., Moon J.S., Seo Y.J., Park S.Y., Kim J.Y., Yoon J.S., Lee I.K., Lee H.W., Won K.C. 2012 Inhibition of fatty acid translocase cluster determinant 36 (CD36), stimulated by hyperglycemia, prevents glucotoxicity in INS-1 cells. Biochem Biophys Res Commun 420:462-466.

Kim S.Y., Kim H., Cho J.Y., Lim S., Cha K., Lee K.H., Kim Y.H., Kim J.H., Yoon Y.S., Han H.S., Kang H.S. 2014 Quantitative assessment of pancreatic fat by using unenhanced CT: Pathologic correlation and clinical implications. Radiology 271:104-112.

Kiss J., Naum A., Kudomi N., Knuuti J., Iozzo P., Savunen T., Nuutila P. 2009 Non-invasive diagnosis of acute mesenteric ischaemia using PET. Eur J Nucl Med Mol Imaging 36:1338-1345.

Koffert J., Honka H., Hannukainen J.C., Immonen H., Kauhanen S., Oikonen V., Tolvanen T., Iozzo P., Nuutila P. 2015 Intestinal fatty acid utilization after

bariatric surgery – cure for peripheral insulin resistance? WMIC Annual Congress, World Molecular Imaging Society.

Kogire M., Inoue K., Sumi S., Doi R., Takaori K., Yun M., Fujii N., Yajima H., Tobe T. 1988 Effects of synthetic human gastric inhibitory polypeptide on splanchnic circulation in dogs. Gastroenterology 95:1636-1640.

Kolterman O.G., Gray R.S., Griffin J., Burstein P., Insel J., Scarlett J.A., Olefsky J.M. 1981 Receptor and postreceptor defects contribute to the insulin resistance in noninsulin-dependent diabetes mellitus. J Clin Invest 68:957-969.

Komar G., Kauhanen S., Liukko K., Seppanen M., Kajander S., Ovaska J., Nuutila P., Minn H. 2009 Decreased blood flow with increased metabolic activity: A novel sign of pancreatic tumor aggressiveness. Clin Cancer Res 15:5511-5517.

Koska J., Sands M., Burciu C., D'Souza K.M., Raravikar K., Liu J., Truran S., Franco D.A., Schwartz E.A., Schwenke D.C., D'Alessio D., Migrino R.Q., Reaven P.D. 2015 Exenatide protects against glucose- and lipid-induced endothelial dysfunction: evidence for direct vasodilation effect of GLP-1 receptor agonists in humans. Diabetes 64:2624-2635.

Krebs H.A. 1972 Some aspects of the regulation of fuel supply in omnivorous animals. Adv Enzyme Regul 10:397-420.

Kreymann B., Williams G., Ghatei M.A., Bloom S.R. 1987 Glucagon-like peptide-1 7-36: A physiological incretin in man. Lancet 2:1300-1304.

Kudomi N., Slimani L., Jarvisalo M.J., Kiss J., Lautamaki R., Naum G.A., Savunen T., Knuuti J., Iida H., Nuutila P., Iozzo P. 2008 Non-invasive estimation of hepatic blood perfusion from H2 15O PET images using tissue-derived arterial and portal input functions. Eur J Nucl Med Mol Imaging 35:1899-1911.

Kusminski C.M., McTernan P.G., Kumar S. 2005 Role of resistin in obesity, insulin resistance and type II diabetes. Clin Sci (Lond) 109:243-256.

Kusminski C.M,. Shetty S., Orci. L., Unger R.H., Scherer P.E. 2009 Diabetes and apoptosis: Lipotoxicity. Apoptosis 14:1484-1495.

Kvietys P.R., Gallavan R.H., Chou C.C. 1980 Contribution of bile to postprandial intestinal hyperemia. Am J Physiol 238:G284-8.

Kvietys P.R., McLendon J.M., Granger D.N. 1981 Postprandial intestinal hyperemia: role of bile salts in the ileum. Am J Physiol 241:G469-77.

Labbe S.M., Croteau E., Grenier-Larouche T., Frisch F., Ouellet R., Langlois R., Guerin B., Turcotte E.E., Carpentier A.C. 2011 Normal postprandial nonesterified fatty acid uptake in muscles despite increased circulating fatty acids in type 2 diabetes. Diabetes 60:408-415.

Labbe S.M., Grenier-Larouche T., Noll C., Phoenix S., Guerin B., Turcotte E.E., Carpentier A.C. 2012 Increased myocardial uptake of dietary fatty acids linked to cardiac dysfunction in glucose-intolerant humans. Diabetes 61:2701-2710.

Laferrere B., Teixeira J., McGinty J., Tran H., Egger J.R., Colarusso A.,

Kovack B., Bawa B., Koshy N., Lee H., Yapp K., Olivan B. 2008 Effect of weight loss by gastric bypass surgery versus hypocaloric diet on glucose and incretin levels in patients with type 2 diabetes. J Clin Endocrinol Metab 93:2479-2485.

Lammertsma A.A., Brooks D.J., Frackowiak R.S., Beaney R.P., Herold S., Heather J.D., Palmer A.J., Jones T. 1987 Measurement of glucose utilisation with [18F]2-fluoro-2-deoxy-D-glucose: A comparison of different analytical methods. J Cereb Blood Flow Metab 7:161-172.

Landsberg L., Young J.B. 1984 The role of the sympathoadrenal system in modulating energy expenditure. Clin Endocrinol Metab 13:475-499.

Lau J., Svensson J., Grapensparr L., Johansson A., Carlsson P.O. 2012 Superior beta cell proliferation, function and gene expression in a subpopulation of rat islets identified by high blood perfusion. Diabetologia 55:1390-1399.

le Roux C.W., Bueter M. 2014 The physiology of altered eating behaviour after Roux-en-Y gastric bypass. Exp Physiol 99:1128-1132.

Leibel R.L., Hirsch J. 1984 Diminished energy requirements in reduced-obese patients. Metabolism 33:164-170.

Leibel R.L., Rosenbaum M., Hirsch J. 1995 Changes in energy expenditure resulting from altered body weight. N Engl J Med 332:621-628.

Ley R.E., Turnbaugh P.J., Klein S., Gordon J.I. 2006 Microbial ecology: Human gut microbes associated with obesity. Nature 444:1022-1023.

Li X., Zhang L., Meshinchi S., Dias-Leme C., Raffin D., Johnson J.D., Treutelaar M.K., Burant C.F. 2006 Islet microvasculature in islet hyperplasia and failure in a model of type 2 diabetes. Diabetes 55:2965-2973.

Liang Y., Bonner-Weir S., Wu Y.J., Berdanier C.D., Berner D.K., Efrat S., Matschinsky F.M. 1994 In situ glucose uptake and glucokinase activity of pancreatic islets in diabetic and obese rodents. J Clin Invest 93:2473-2481.

Lim G.E., Brubaker P.L. 2006 Glucagon-like peptide 1 secretion by the L cell. The view from within. Diabetes 55:S70-S77.

Lim S, Bae J.H., Chun E.J., Kim H., Kim S.Y., Kim K.M., Choi S.H., Park K.S., Florez J.C., Jang H.C. 2014 Differences in pancreatic volume, fat content, and fat density measured by multidetector-row computed tomography according to the duration of diabetes. Acta Diabetol 51:739-748.

Lindqvist A., Spegel P., Ekelund M., Garcia Vaz E., Pierzynowski S., Gomez M.F., Mulder H., Hedenbro J., Groop L., Wierup N. 2014 Gastric bypass improves beta-cell function and increases beta-cell mass in a porcine model. Diabetes 63:1665-1671.

Lillioja S., Mott D.M., Howard B.V., Bennett P.H., Yki-Jarvinen H., Freymond D., Nyomba B.L., Zurlo F., Swinburn B., Bogardus C. 1988 Impaired glucose tolerance as a disorder of insulin action. longitudinal and cross-sectional studies in pima indians. N Engl J Med 318:1217-1225.

Liu J.J., Lee T., DeFronzo R.A. 2012 Why do SGLT2 inhibitors inhibit only 30-50% of renal glucose reabsorption in humans? Diabetes 61:2199-2204.

Lu W.J., Yang Q., Sun W., Woods S.C., D'Alessio D., Tso P. 2008 Using the

lymph fistula rat model to study the potentiation of GIP secretion by the ingestion of fat and glucose. Am J Physiol Gastrointest Liver Physiol 294:G1130-8.

Lyssenko V., Eliasson L., Kotova O., Pilgaard K., Wierup N., Salehi A., Wendt A., Jonsson A., De Marinis Y.Z., Berglund L.M., Taneera J., Balhuizen A., Hansson O., Osmark P., Duner P., Brons C., Stancakova A., Kuusisto J., Bugliani M., Saxena R., Ahlqvist E., Kieffer T.J., Tuomi T., Isomaa B., Melander O., Sonestedt E., Orho-Melander M., Nilsson P., Bonetti S., Bonadonna R., Miccoli R., Delprato S., Marchetti P., Madsbad S., Poulsen P., Vaag A., Laakso M., Gomez M.F., Groop L. 2011 Pleiotropic effects of GIP on islet function involve osteopontin. Diabetes 60:2424-2433.

Madison L.L., Uger R.H., Rencz K. 1960 The physiologic significance of secretion of insulin into portal circulation: II. effect of rate of administration of glucagon-free insulin on magnitude of peripheral and hepatic actions. Metabolism 9:97-108.

Mannucci E., Ognibene A., Cremasco F., Bardini G., Mencucci A., Pierazzuoli E., Ciani S., Messeri G., Rotella C.M. 2001 Effect of metformin on glucagon-like peptide 1 (GLP-1) and leptin levels in obese nondiabetic subjects. Diabetes Care 24:489-494.

Marathe C.S., Rayner C.K., Jones K.L., Horowitz M. 2013 Relationships between gastric emptying, postprandial glycemia, and incretin hormones. Diabetes Care 36:1396-1405.

Marathe C.S., Rayner C.K., Bound M., Checklin H., Standfield S., Wishart J., Lange K., Jones K.L., Horowitz M. 2014 Small intestinal glucose exposure determines the magnitude of the incretin effect in health and type 2 diabetes. Diabetes 63:2668-2675.

Mari A., Pacini G., Murphy E., Ludvik B., Nolan J.J. 2001 A model-based method for assessing insulin sensitivity from the oral glucose tolerance test. Diabetes Care 24:539-548.

Mari A., Tura A., Gastaldelli A., Ferrannini E. 2002 Assessing insulin secretion by modeling in multiple-meal tests: Role of potentiation. Diabetes 51 Suppl 1:S221-6.

Mari A., Ferrannini E. 2008 Beta-cell function assessment from modelling of oral tests: An effective approach. Diabetes Obes Metab 10 Suppl 4:77-87.

Mari A., Tura A., Natali A., Laville M., Laakso M., Gabriel R., Beck-Nielsen H., Ferrannini E., RISC Investigators 2010 Impaired beta cell glucose sensitivity rather than inadequate compensation for insulin resistance is the dominant defect in glucose intolerance. Diabetologia 53:749-756.

Marso S.P., Daniels G.H., Brown-Frandsen K., et al. 2016 Liraglutide and Cardiovascular Outcomes in Type 2 Diabetes. N Engl J Med 375:311-322.

Mason E.E., Ito C. 1967 Gastric bypass in obesity. Surg Clin North Am 47:1345-1351.

Matheson P.J., Wilson M.A., Garrison R.N. 2000 Regulation of intestinal blood flow. J Surg Res 93:182-196.

Matschinsky F., Liang Y., Kesavan P., Wang L., Froguel P., Velho G., Cohen D., Permutt M.A., Tanizawa Y., Jetton T.L. 1993 Glucokinase as pancreatic beta cell glucose sensor and diabetes gene. J Clin Invest 92:2092-2098.

Matthews D.R., Hosker J.P., Rudenski A.S., Naylor B.A., Treacher D.F., Turner R.C. 1985 Homeostasis model assessment: Insulin resistance and beta-cell function from fasting plasma glucose and insulin concentrations in man. Diabetologia 28:412-419.

Meier J.J., Hucking K., Holst J.J., Deacon C.F., Schmiegel W.H., Nauck M.A. 2001 Reduced insulinotropic effect of gastric inhibitory polypeptide in first-degree relatives of patients with type 2 diabetes. Diabetes 50:2497-2504.

Meier J.J., Gallwitz B., Kask B., Deacon C.F., Holst J.J., Schmidt W.E., Nauck M.A. 2004 Stimulation of insulin secretion by intravenous bolus injection and continuous infusion of gastric inhibitory polypeptide in patients with type 2 diabetes and healthy control subjects. Diabetes 53 Suppl 3:S220-4.

Meier J.J., Veldhuis J.D., Butler P.C. 2005 Pulsatile insulin secretion dictates systemic insulin delivery by regulating hepatic insulin extraction in humans. Diabetes 54:1649-1656.

Miles J.M., Wooldridge D., Grellner W.J., Windsor S., Isley W.L., Klein S., Harris W.S. 2003 Nocturnal and postprandial free fatty acid kinetics in normal and type 2 diabetic subjects: Effects of insulin sensitization therapy. Diabetes 52:675-681.

Mingrone G., Castagneto-Gissey L. 2009 Mechanisms of early improvement/resolution of type 2 diabetes after bariatric surgery. Diabetes Metab 35:518-523.

Mithieux G. 2001 New data and concepts on glutamine and glucose metabolism in the gut. Curr Opin Clin Nutr Metab Care 4:267-271.

Mithieux G., Bady I., Gautier A., Croset M., Rajas F., Zitoun C. 2004 Induction of control genes in intestinal gluconeogenesis is sequential during fasting and maximal in diabetes. Am J Physiol Endocrinol Metab 286:E370-5.

Mithieux G., Gautier-Stein A., Rajas F., Zitoun C. 2006 Contribution of intestine and kidney to glucose fluxes in different nutritional states in rat. Comp Biochem Physiol B Biochem Mol Biol 143:195-200.

Mithieux G. 2014 Metabolic effects of portal vein sensing. Diabetes Obes Metab 16 Suppl 1:56-60.

Miyawaki K., Yamada Y., Ban N., Ihara Y., Tsukiyama K., Zhou H., Fujimoto S., Oku A., Tsuda K., Toyokuni S., Hiai H., Mizunoya W., Fushiki T., Holst J.J., Makino M., Tashita A., Kobara Y., Tsubamoto Y., Jinnouchi T., Jomori T., Seino Y. 2002 Inhibition of gastric inhibitory polypeptide signaling prevents obesity. Nat Med 8:738-742.

Moneta G.L., Taylor D.C., Helton W.S., Mulholland M.W., Strandness D.E.,Jr. 1988 Duplex ultrasound measurement of postprandial intestinal blood flow: Effect of meal composition. Gastroenterology 95:1294-1301.

Montague W., Taylor K.W. 1968 Regulation of insulin secretion by short chain fatty acids. Nature 217:853.

Muscelli E., Mari A., Casolaro A., Camastra S., Seghieri G., Gastaldelli A., Holst J.J., Ferrannini E. 2008 Separate impact of obesity and glucose tolerance on the incretin effect in normal subjects and type 2 diabetic patients. Diabetes 57:1340-1348.

Nannipieri M., Baldi S., Mari A., Colligiani D., Guarino D., Camastra S.,

Barsotti E., Berta R., Moriconi D., Bellini R., Anselmino M., Ferrannini E. 2013 Roux-en-Y gastric bypass and sleeve gastrectomy: Mechanisms of diabetes remission and role of gut hormones. J Clin Endocrinol Metab 98:4391-4399.

Nauck M.A., Homberger E., Siegel E.G., Allen R.C., Eaton R.P., Ebert R., Creutzfeldt W. 1986 Incretin effects of increasing glucose loads in man calculated from venous insulin and C-peptide responses. J Clin Endocrinol Metab 63:492-498.

Nauck M., Stockmann F., Ebert R., Creutzfeldt W. 1986 Reduced incretin effect in type 2 (non-insulin-dependent) diabetes. Diabetologia 29:46-52.

Nauck M.A., Bartels E., Orskov C., Ebert R., Creutzfeldt W. 1993 Additive insulinotropic effects of exogenous synthetic human gastric inhibitory polypeptide and glucagon-like peptide-1-(7-36) amide infused at near-physiological insulinotropic hormone and glucose concentrations. J Clin Endocrinol Metab 76:912-917.

Nauck M.A., Heimesaat M.M., Orskov C., Holst J.J., Ebert R., Creutzfeldt W. 1993 Preserved incretin activity of glucagon-like peptide 1 [7-36 amide] but not of synthetic human gastric inhibitory polypeptide in patients with type-2 diabetes mellitus. J Clin Invest 91:301-307.

Nauck M.A., Niedereichholz U., Ettler R., Holst J.J., Orskov C., Ritzel R., Schmiegel W.H. 1997 Glucagon-like peptide 1 inhibition of gastric emptying outweighs its insulinotropic effects in healthy humans. Am J Physiol 273:E981-8.

Nouspikel T., Iynedjian P.B. 1992 Insulin signalling and regulation of glucokinase gene expression in cultured hepatocytes. Eur J Biochem 210:365-373.

Nuutila P., Koivisto V.A., Knuuti J., Ruotsalainen U., Teras M., Haaparanta M., Bergman J., Solin O., Voipio-Pulkki L.M., Wegelius U. 1992 Glucose-free fatty acid cycle operates in human heart and skeletal muscle in vivo. J Clin Invest 89:1767-1774.

Nyholm B., Walker M., Gravholt C.H., Shearing P.A., Sturis J., Alberti K.G., Holst J.J., Schmitz O. 1999 Twenty-four-hour insulin secretion rates, circulating concentrations of fuel substrates and gut incretin hormones in healthy offspring of type II (non-insulin-dependent) diabetic parents: Evidence of several aberrations. Diabetologia 42:1314-1323.

Nyman L.R., Ford E., Powers A.C., Piston D.W. 2010 Glucose-dependent blood flow dynamics in murine pancreatic islets in vivo. Am J Physiol Endocrinol Metab 298:E807-14.

Okahara M., Mori H., Kiyosue H., Yamada Y., Sagara Y., Matsumoto S. 2010 Arterial supply to the pancreas; variations and cross-sectional anatomy. Abdom Imaging 35:134-142.

Oliva M.R., Mortele K.J., Segatto E., Glickman J.N., Erturk S.M., Ros P.R., Silverman S.G. 2006 Computed tomography features of nonalcoholic steatohepatitis with histopathologic correlation. J Comput Assist Tomogr 30:37-43.

Oliveira A.L., Azevedo D.C., Bredella M.A., Stanley T.L., Torriani M. 2015 Visceral and subcutaneous adipose tissue FDG uptake by PET/CT in metabolically

healthy obese subjects. Obesity (Silver Spring) 23:286-289.

Olsen T.S. 1978 Lipomatosis of the pancreas in autopsy material and its relation to age and overweight. Acta Pathol Microbiol Scand A 86A:367-373.

Olsson R., Carlsson P.O. 2011 A low-oxygenated subpopulation of pancreatic islets constitutes a functional reserve of endocrine cells. Diabetes 60:2068-2075.

Ost A., Lempradl A., Casas E., Weigert M., Tiko T., Deniz M., Pantano L., Boenisch U., Itskov P.M., Stoeckius M., Ruf M., Rajewsky N., Reuter G., Iovino N., Ribeiro C., Alenius M., Heyne S., Vavouri T., Pospisilik J.A. 2014 Paternal diet defines offspring chromatin state and intergenerational obesity. Cell 159:1352-1364.

Owen O.E., Morgan A.P., Kemp H.G., Sullivan J.M., Herrera M.G., Cahill G.F. Jr 1967 Brain metabolism during fasting. J Clin Invest 46:1589-1595.

Paolisso G., Gambardella A., Amato L., Tortoriello R., D'Amore A., Varricchio M., D'Onofrio F. 1995 Opposite effects of short- and long-term fatty acid infusion on insulin secretion in healthy subjects. Diabetologia 38:1295-1299.

Patel S.R., Hakim D., Mason J., Hakim N. 2013 The duodenal-jejunal bypass sleeve (EndoBarrier gastrointestinal liner) for weight loss and treatment of type 2 diabetes. Surg Obes Relat Dis 9:482-484.

Patlak C.S., Blasberg R.G. 1985 Graphical evaluation of blood-to-brain transfer constants from multiple-time uptake data. generalizations. J Cereb Blood Flow Metab 5:584-590.

Pendyala S., Walker J.M., Holt P.R. 2012 A high-fat diet is associated with endotoxemia that originates from the gut. Gastroenterology 142:1100-1101.e2.

Perley M.J., Kipnis D.M. 1967 Plasma insulin responses to oral and intravenous glucose: Studies in normal and diabetic sujbjects. J Clin Invest 46:1954-1962.

Phelps M.E., Huang S.C., Hoffman E.J., Selin C., Sokoloff L., Kuhl D.E. 1979 Tomographic measurement of local cerebral glucose metabolic rate in humans with (F-18)2-fluoro-2-deoxy-D-glucose: Validation of method. Ann Neurol 6:371-388.

Phillips C.M. 2013 Metabolically healthy obesity: Definitions, determinants and clinical implications. Rev Endocr Metab Disord 14:219-227.

Phillips L.K., Deane A.M., Jones K.L., Rayner C.K., Horowitz M. 2015 Gastric emptying and glycaemia in health and diabetes mellitus. Nat Rev Endocrinol 11:112-128.

Pickup J.C., Mattock M.B., Chusney G.D., Burt D. 1997 NIDDM as a disease of the innate immune system: Association of acute-phase reactants and interleukin-6 with metabolic syndrome X. Diabetologia 40:1286-1292.

Pilo A., Ferrannini E., Björkman O. 1981 Analysis of glucose production and disappearance rates following an oral glucose load in normal subjects: A double tracer approach. Cobelli C., Bergman R.N. (eds): Carbohydrate Metabolism. London, Wiley.

Pi-Sunyer X., Astrup A., Fujioka K., Greenway F., Halpern A., Krempf M., Lau D.C., le Roux C.W., Violante Ortiz R., Jensen C.B., Wilding J.P., SCALE Obesity and Prediabetes NN8022-1839 Study Group. 2015 A randomized, controlled trial of 3.0 mg of liraglutide in

weight management. N Engl J Med 373:11-22.

Polonsky K., Jaspan J., Emmanouel D., Holmes K., Moossa A.R. 1983 Differences in the hepatic and renal extraction of insulin and glucagon in the dog: Evidence for saturability of insulin metabolism. Acta Endocrinol (Copenh) 102:420-427.

Prasad R.B., Groop L. 2015 Genetics of type 2 diabetes – pitfalls and possibilities. Genes 6:87-123.

Prattala R., Sippola R., Lahti-Koski M., Laaksonen M.T., Makinen T., Roos E. 2012 Twenty-five year trends in body mass index by education and income in finland. BMC Public Health 12:936-2458-12-936.

Rabot S., Membrez M., Bruneau A., Gerard P., Harach T., Moser M., Raymond F., Mansourian R., Chou C.J. 2010 Germ-free C57BL/6J mice are resistant to high-fat-diet-induced insulin resistance and have altered cholesterol metabolism. FASEB J 24:4948-4959.

Rajas F, Bruni N, Montano S, Zitoun C, Mithieux G 1999 The glucose-6 phosphatase gene is expressed in human and rat small intestine: Regulation of expression in fasted and diabetic rats. Gastroenterology 117:132-139.

Randle P.J., Garland P.B., Hales C.N., Newsholme E.A. 1963 The glucose fatty-acid cycle. its role in insulin sensitivity and the metabolic disturbances of diabetes mellitus. Lancet 1:785-789.

Rayner C.K., Samsom M., Jones K.L., Horowitz M. 2001 Relationships of upper gastrointestinal motor and sensory function with glycemic control. Diabetes Care 24:371-381.

Rebelos E., Seghieri M., Natali A., Balkau B., Golay A., Piatti P.M., Lalic N.M., Laakso M., Mari A., Ferrannini E. 2015 Influence of endogenous NEFA on beta cell function in humans. Diabetologia 58:2344-2351.

Rees D.D., Palmer R.M., Hodson H.F., Moncada S. 1989 A specific inhibitor of nitric oxide formation from L-arginine attenuates endothelium-dependent relaxation. Br J Pharmacol 96:418-424.

Reinert R.B., Brissova M., Shostak A., Pan F.C., Poffenberger G., Cai Q., Hundemer G.L., Kantz J., Thompson C.S., Dai C., McGuinness O.P., Powers A.C. 2013 Vascular endothelial growth factor-a and islet vascularization are necessary in developing, but not adult, pancreatic islets. Diabetes 62:4154-4164.

Rena G., Pearson E.R., Sakamoto K. 2013 Molecular mechanism of action of metformin: Old or new insights? Diabetologia 56:1898-1906.

Revers R.R., Fink R., Griffin J., Olefsky J.M., Kolterman O.G. 1984 Influence of hyperglycemia on insulin's in vivo effects in type II diabetes. J Clin Invest 73:664-672.

Rothman D.L., Magnusson I., Katz L.D., Shulman R.G., Shulman G.I. 1991 Quantitation of hepatic glycogenolysis and gluconeogenesis in fasting humans with 13C NMR. Science 254:573-576.

Russek M. 1963 Participation of hepatic glucoreceptors in the control of intake of food. Nature 197:79-80.

Saad M.F., Knowler W.C., Pettitt D.J., Nelson R.G., Mott D.M., Bennett P.H. 1989 Sequential changes in serum insulin concentration during development of non-insulin-dependent diabetes. Lancet 1:1356-1359.

Saeidi N., Meoli L., Nestoridi E., Gupta N.K., Kvas S., Kucharczyk J., Bonab A.A., Fischman A.J., Yarmush M.L., Stylopoulos N. 2013 Reprogramming of intestinal glucose metabolism and glycemic control in rats after gastric bypass. Science 341:406-410.

Saisho Y., Butler A.E., Meier J.J., Monchamp T., Allen-Auerbach M., Rizza R.A., Butler P.C. 2007 Pancreas volumes in humans from birth to age one hundred taking into account sex, obesity, and presence of type-2 diabetes. Clin Anat 20:933-942.

Sattar N., Gill J.M. 2014 Type 2 diabetes as a disease of ectopic fat? BMC Med 12:123-014-0123-4.

Schirra J., Sturm K., Leicht P., Arnold R., Goke B., Katschinski M. 1998 Exendin(9-39)amide is an antagonist of glucagon-like peptide-1(7-36)amide in humans. J Clin Invest 101:1421-1430.

Schwenzer N.F., Machann J., Martirosian P., Stefan N., Schraml C., Fritsche A., Claussen C.D., Schick F. 2008 Quantification of pancreatic lipomatosis and liver steatosis by MRI: Comparison of in/opposed-phase and spectral-spatial excitation techniques. Invest Radiol 43:330-337.

Sellayah D, Cagampang FR, Cox RD 2014 On the evolutionary origins of obesity: A new hypothesis. Endocrinology 155:1573-1588.

Shulman G.I., Rothman D.L., Jue T., Stein P., DeFronzo R.A., Shulman R.G. 1990 Quantitation of muscle glycogen synthesis in normal subjects and subjects with non-insulin-dependent diabetes by 13C nuclear magnetic resonance spectroscopy. N Engl J Med 322:223-228.

Shulman G.I. 2014 Ectopic fat in insulin resistance, dyslipidemia, and cardiometabolic disease. N Engl J Med 371:1131-1141.

Sjostrom L., Rissanen A., Andersen T., Boldrin M., Golay A., Koppeschaar H.P., Krempf M. 1998 Randomised placebo-controlled trial of orlistat for weight loss and prevention of weight regain in obese patients. european multicentre orlistat study group. Lancet 352:167-172.

Sjostrom L., Narbro K., Sjostrom C.D., Karason K., Larsson B., Wedel H., Lystig T., Sullivan M., Bouchard C., Carlsson B., Bengtsson C., Dahlgren S., Gummesson A., Jacobson P., Karlsson J., Lindroos A.K., Lonroth H., Naslund I., Olbers T., Stenlof K., Torgerson J., Agren G., Carlsson L.M., Swedish Obese Subjects Study 2007 Effects of bariatric surgery on mortality in swedish obese subjects. N Engl J Med 357:741-752.

Sjostrom L., Lindroos A.K., Peltonen M., Torgerson J., Bouchard C., Carlsson B., Dahlgren S., Larsson B., Narbro K., Sjostrom C.D., Sullivan M., Wedel H., Swedish Obese Subjects Study Scientific Group 2004 Lifestyle, diabetes, and cardiovascular risk factors 10 years after bariatric surgery. N Engl J Med 351:2683-2693.

Slimani L., Kudomi N., Oikonen V., Jarvisalo M., Kiss J., Naum A., Borra R., Viljanen A., Sipila H., Ferrannini E., Savunen T., Nuutila P., Iozzo P. 2008 Quantification of liver perfusion with [(15)O]H(2)O-PET and its relationship with glucose metabolism and substrate levels. J Hepatol 48:974-982.

Snyder W.S., Nasset E.S., Karhausen L.R., Howells G.P., Tipton I.H. 1975 Report of the task group on reference man. Pergamon Press: Oxford.

Sokoloff L., Reivich M., Kennedy C., Des Rosiers M.H., Patlak C.S., Pettigrew K.D., Sakurada O., Shinohara M. 1977 The [14C]deoxyglucose method for the measurement of local cerebral glucose utilization: Theory, procedure, and normal values in the conscious and anesthetized albino rat. J Neurochem 28:897-916.

Solomon T.P., Knudsen S.H., Karstoft K., Winding K., Holst J.J., Pedersen B.K. 2012 Examining the effects of hyperglycemia on pancreatic endocrine function in humans: Evidence for in vivo glucotoxicity. J Clin Endocrinol Metab 97:4682-4691.

Someya N., Endo M.Y., Fukuba Y., Hayashi N. 2008 Blood flow responses in celiac and superior mesenteric arteries in the initial phase of digestion. Am J Physiol Regul Integr Comp Physiol 294:R1790-6.

Soskin S., Levine R. 1952 Carbohydrate metabolism. Chicago: University of Chicago Press.

Srikanthan P., Horwich T.B., Tseng C.H. 2016 Relation of muscle mass and fat mass to cardiovascular disease mortality. Am J Cardiol 117:1355-1360.

Stahl A., Evans J.G., Pattel S., Hirsch D., Lodish H.F. 2002 Insulin causes fatty acid transport protein translocation and enhanced fatty acid uptake in adipocytes. Dev Cell 2:477-488.

Steinberg D.M., Shafrir E., Vaughan M. 1959 Direct effect of glucagon on release of unesterified fatty acids (UFA) from adipose tissue. Clin Res 7:250.

Sutherland E.W., De Duve C. 1948 Origin and distribution of the hyperglycemic-glycogenolytic factor of the pancreas. J Biol Chem 175:663-674.

Svensson A.M., Efendic S., Ostenson C.G., Jansson L. 1997 Gastric inhibitory polypeptide and splanchnic blood perfusion: augmentation of the islet blood flow increase in hyperglycemic rats. Peptides 18:1055-1059.

Svensson A.M., Ostenson C.G., Efendic S., Jansson L. 2007 Effects of glucagon-like peptide-1-(7-36)-amide on pancreatic islet and intestinal blood perfusion in Wistar rats and diabetic GK rats. Clin Sci (Lond) 112:345-351.

Tahrani A.A., Barnett A.H., Bailey C.J. 2013 SGLT inhibitors in management of diabetes. Lancet Diabetes Endocrinol 1:140-151.

Takala T.O., Nuutila P., Pulkki K., Oikonen V., Gronroos T., Savunen T., Vahasilta T., Luotolahti M., Kallajoki M., Bergman J., Forsback S., Knuuti J. 2002 14(R,S)-[18F]fluoro-6-thia-heptadecanoic acid as a tracer of free fatty acid uptake and oxidation in myocardium and skeletal muscle. Eur J Nucl Med Mol Imaging 29:1617-1622.

Tam C.S., Redman L.M., Greenway F., LeBlanc K.A., Haussmann M.G., Ravussin E. 2016 Energy metabolic adaptation and cardiometabolic improvements one year after gastric bypass, sleeve gastrectomy and gastric band. J Clin Endocrinol Metab jc20161814.

Teras M., Tolvanen T., Johansson J.J., Williams J.J., Knuuti J. 2007 Performance of the new generation of whole-body PET/CT scanners: Discovery STE and discovery VCT. Eur J Nucl Med Mol Imaging 34:1683-1692.

Thiebaud D., DeFronzo R.A., Jacot E., Golay A., Acheson K., Maeder E., Jequier E., Felber J.P. 1982 Effect of long chain triglyceride infusion on

glucose metabolism in man. Metabolism 31:1128-1136.

Thomas D.E., Elliott E.J., Naughton G.A. 2006 Exercise for type 2 diabetes mellitus. Cochrane Database Syst Rev (3):CD002968

Thorogood A., Mottillo S., Shimony A., Filion K.B., Joseph L., Genest J., Pilote L., Poirier P., Schiffrin E.L., Eisenberg M.J. 2011 Isolated aerobic exercise and weight loss: A systematic review and meta-analysis of randomized controlled trials. Am J Med 124:747-755.

Tilg H., Moschen A.R. 2006 Adipocytokines: Mediators linking adipose tissue, inflammation and immunity. Nat Rev Immunol 6:772-783.

Tobin V., Le Gall M., Fioramonti X., Stolarczyk E., Blazquez A.G., Klein C., Prigent M., Serradas P., Cuif M.H., Magnan C., Leturque A., Brot-Laroche E. 2008 Insulin internalizes GLUT2 in the enterocytes of healthy but not insulin-resistant mice. Diabetes 57:555-562.

Toschi E., Camastra S., Sironi A.M., Masoni A., Gastaldelli A., Mari A., Ferrannini E., Natali A. 2002 Effect of acute hyperglycemia on insulin secretion in humans. Diabetes 51 Suppl 1:S130-3.

Trahair L.G., Horowitz M., Stevens J.E., Feinle-Bisset C., Standfield S., Piscitelli D., Rayner C.K., Deane A.M., Jones K.L. 2015 Effects of exogenous glucagon-like peptide-1 on blood pressure, heart rate, gastric emptying, mesenteric blood flow and glycaemic responses to oral glucose in older individuals with normal glucose tolerance or type 2 diabetes. Diabetologia 58:1769-1778.

Troy S., Soty M., Ribeiro L., Laval L., Migrenne S., Fioramonti X., Pillot B., Fauveau V., Aubert R., Viollet B., Foretz M., Leclerc J., Duchampt A., Zitoun C., Thorens B., Magnan C., Mithieux G., Andreelli F. 2008 Intestinal gluconeogenesis is a key factor for early metabolic changes after gastric bypass but not after gastric lap-band in mice. Cell Metab 8:201-211.

Tura A., Muscelli E., Gastaldelli A., Ferrannini E., Mari A. 2014 Altered pattern of the incretin effect as assessed by modelling in individuals with glucose tolerance ranging from normal to diabetic. Diabetologia 57:1199-1203.

Turnbaugh P.J., Ley R.E., Mahowald M.A., Magrini V., Mardis E.R., Gordon J.I. 2006 An obesity-associated gut microbiome with increased capacity for energy harvest. Nature 444:1027-1031.

Turner RC., Holman R.R. 1995 Lessons from UK prospective diabetes study. Diabetes Res Clin Pract 28 Suppl:S151-7.

Tushuizen M.E., Bunck M.C., Pouwels P.J., Bontemps S., van Waesberghe J.H., Schindhelm R.K., Mari A., Heine R.J., Diamant M. 2007 Pancreatic fat content and beta-cell function in men with and without type 2 diabetes. Diabetes Care 30:2916-2921.

U.K. prospective diabetes study 16. overview of 6 years' therapy of type II diabetes: A progressive disease. U.K. prospective diabetes study group. 1995 Diabetes 44:1249-1258.

Unger R.H., Orci L. 2010 Paracrinology of islets and the paracrinopathy of diabetes. Proc Natl Acad Sci U S A 107:16009-16012.

Utriainen T., Malmstrom R., Makimattila S., Yki-Jarvinen H. 1995 Methodological aspects, dose-response characteristics

and causes of interindividual variation in insulin stimulation of limb blood flow in normal subjects. Diabetologia 38:555-564.

Vaag A.A., Holst J.J., Volund A., Beck-Nielsen H.B. 1996 Gut incretin hormones in identical twins discordant for non-insulin-dependent diabetes mellitus (NIDDM)--evidence for decreased glucagon-like peptide 1 secretion during oral glucose ingestion in NIDDM twins. Eur J Endocrinol 135:425-432.

van Cauter E., Mestrez F., Sturis J., Polonsky K.S. 1992 Estimation of insulin secretion rates from C-peptide levels. comparison of individual and standard kinetic parameters for C-peptide clearance. Diabetes 41:368-377.

van der Zijl N.J., Goossens G.H., Moors C.C., van Raalte D.H., Muskiet M.H., Pouwels P.J., Blaak E.E., Diamant M. 2011 Ectopic fat storage in the pancreas, liver, and abdominal fat depots: Impact on beta-cell function in individuals with impaired glucose metabolism. J Clin Endocrinol Metab 96:459-467.

Vella A., Shah P., Basu R., Basu A., Camilleri M., Schwenk W.F., Rizza R.A. 2001 Type I diabetes mellitus does not alter initial splanchnic glucose extraction or hepatic UDP-glucose flux during enteral glucose administration. Diabetologia 44:729-737.

Vella A., Rizza R.A. 2009 Application of isotopic techniques using constant specific activity or enrichment to the study of carbohydrate metabolism. Diabetes 58:2168-2174.

Vella A. 2013 Does caloric restriction alone explain the effects of roux-en-Y gastric bypass on glucose metabolism? not by a long limb. Diabetes 62:3017-3018.

Vilsboll T., Krarup T., Madsbad S., Holst J.J. 2003 Both GLP-1 and GIP are insulinotropic at basal and postprandial glucose levels and contribute nearly equally to the incretin effect of a meal in healthy subjects. Regul Pept 114:115-121.

Vilsboll T., Knop F.K., Krarup T., Johansen A., Madsbad S., Larsen S., Hansen T., Pedersen O., Holst J.J. 2003 The pathophysiology of diabetes involves a defective amplification of the late-phase insulin response to glucose by glucose-dependent insulinotropic polypeptide-regardless of etiology and phenotype. J Clin Endocrinol Metab 88:4897-4903.

Virtanen K.A., Lonnroth P., Parkkola R., Peltoniemi P., Asola M., Viljanen T., Tolvanen T., Knuuti J., Ronnemaa T., Huupponen R., Nuutila P. 2002 Glucose uptake and perfusion in subcutaneous and visceral adipose tissue during insulin stimulation in nonobese and obese humans. J Clin Endocrinol Metab 87:3902-3910.

Virtanen K.A., Lidell M.E., Orava J., Heglind M., Westergren R., Niemi T., Taittonen M., Laine J., Savisto N.J., Enerback S., Nuutila P. 2009 Functional brown adipose tissue in healthy adults. N Engl J Med 360:1518-1525.

Virtanen S., Aro E., Keskinen P., Lindström J., Rautavirta M., Ventola A., Virtanen L. 2008 Diabeetikon ruokavaliosuositus.

Voight B.F., Scott L.J., Steinthorsdottir V., Morris A.P., Dina C., Welch R.P., Zeggini E., et al. MAGIC investigators, GIANT Consortium 2010 Twelve type 2 diabetes susceptibility loci identified

through large-scale association analysis. Nat Genet 42:579-589.

Vosselman M.J., Brans B., van der Lans A.A., Wierts R., van Baak M.A., Mottaghy F.M., Schrauwen P., van Marken Lichtenbelt W.D. 2013 Brown adipose tissue activity after a high-calorie meal in humans. Am J Clin Nutr 98:57-64.

Wadden T.A. 1993 Treatment of obesity by moderate and severe caloric restriction: results of clinical research trials. Ann Intern Med 229:688-693.

Wallin T., Ma Z., Ogata H., Jorgensen I.H., Iezzi M., Wang H., Wollheim C.B., Bjorklund A. 2010 Facilitation of fatty acid uptake by CD36 in insulin-producing cells reduces fatty-acid-induced insulin secretion and glucose regulation of fatty acid oxidation. Biochim Biophys Acta 1801:191-197.

Wang X., Misawa R., Zielinski M.C., Cowen P., Jo J., Periwal V., Ricordi C., Khan A., Szust J., Shen J., Millis J.M., Witkowski P., Hara M. 2013 Regional differences in islet distribution in the human pancreas--preferential beta-cell loss in the head region in patients with type 2 diabetes. PLoS One 8:e67454.

Ward W.K., Bolgiano D.C., McKnight B., Halter J.B., Porte D.Jr. 1984 Diminished B cell secretory capacity in patients with noninsulin-dependent diabetes mellitus. J Clin Invest 74:1318-1328.

Waterhouse C., Keilson J. 1969 Cori cycle activity in man. J Clin Invest 48:2359-2366.

Weyer C., Bogardus C., Mott D.M., Pratley R.E. 1999 The natural history of insulin secretory dysfunction and insulin resistance in the pathogenesis of type 2 diabetes mellitus. J Clin Invest 104:787-794.

White M.F., Yenush L. 1998 The IRS-signaling system: A network of docking proteins that mediate insulin and cytokine action. Curr Top Microbiol Immunol 228:179-208.

Wicklow B.A., Griffith A.T., Dumontet J.N., Venugopal N., Ryner L.N., McGavock J.M. 2015 Pancreatic lipid content is not associated with beta cell dysfunction in youth-onset type 2 diabetes. Can J Diabetes 39:398-404.

Wu L., Olverling A., Huang Z., Jansson L., Chao H., Gao X., Sjoholm A. 2012 GLP-1, exendin-4 and C-peptide regulate pancreatic islet microcirculation, insulin secretion and glucose tolerance in rats. Clin Sci (Lond) 122:375-384.

Wysham C.H., MacConell L.A., Maggs D.G., Zhou M., Griffin P.S., Trautmann M.E. 2015 Five-year efficacy and safety data of exenatide once weekly: Long-term results from the DURATION-1 randomized clinical trial. Mayo Clin Proc 90:356-365.

Xu G., Stoffers D.A., Habener J.F., Bonner-Weir S. 1999 Exendin-4 stimulates both beta-cell replication and neogenesis, resulting in increased beta-cell mass and improved glucose tolerance in diabetic rats. Diabetes 48:2270-2276.

Yabe D., Seino Y. 2011 Two incretin hormones GLP-1 and GIP: Comparison of their actions in insulin secretion and beta cell preservation. Prog Biophys Mol Biol 107:248-256.

Yamauchi T., Kamon J., Ito Y., Tsuchida A., Yokomizo T., Kita S., Sugiyama T., Miyagishi M., Hara K., Tsunoda M., Murakami K., Ohteki T., Uchida S.,

Takekawa S., Waki H., Tsuno N.H., Shibata Y., Terauchi Y., Froguel P., Tobe K., Koyasu S., Taira K., Kitamura T., Shimizu T., Nagai R., Kadowaki T. Yki-Jarvinen H., Helve E., Koivisto V.A. 1987 Hyperglycemia decreases glucose uptake in type I diabetes. Diabetes 36:892-896

Yki-Jarvinen H., Utriainen T. 1998 Insulin-induced vasodilatation: Physiology or pharmacology? Diabetologia 41:369-379.

Zaidi H., Ojha N., Morich M., Griesmer J., Hu Z., Maniawski P., Ratib O., Izquierdo-Garcia D., Fayad Z.A., Shao L. 2011 Design and performance evaluation of a whole-body ingenuity TF PET-MRI system. Phys Med Biol 56:3091-3106.

Zhong Q., Bollag R.J., Dransfield D.T., Gasalla-Herraiz J., Ding K.H., Min L., Isales C.M. 2000 Glucose-dependent insulinotropic peptide signaling pathways in endothelial cells. Peptides 21:1427-1432.

2003 Cloning of adiponectin receptors that mediate antidiabetic metabolic effects. Nature 423:762-769.

Zhou J., Wang X., Pineyro M.A., Egan J.M. 1999 Glucagon-like peptide 1 and exendin-4 convert pancreatic AR42J cells into glucagon- and insulin-producing cells. Diabetes 48:2358-2366.

Zierath J.R., He L., Guma A., Odegoard Wahlstrom E., Klip A., Wallberg-Henriksson H. 1996 Insulin action on glucose transport and plasma membrane GLUT4 content in skeletal muscle from patients with NIDDM. Diabetologia 39:1180-1189.

Zinman B., Wanner C., Lachin J.M., Fitchett D., Bluhmki E., Hantel S., Mattheus M., Devins T., Johansen O.E., Woerle H.J., Broedl U.C., Inzucchi S.E., EMPA-REG OUTCOME Investigators 2015 Empagliflozin, cardiovascular outcomes, and mortality in type 2 diabetes. N Eng J Med 373:2117-2128.